MAY 3 1929

U. S. DEPARTMENT OF COMMERCE

BUREAU OF STANDARDS JOURNAL OF RESEARCH

Vol. 2 APRIL, 1929 No. 4

CONTENTS

RP. No.	TITLE	Page
50	Apparatus for thermomagnetic analysis	659
51	The analysis of fluorspar	671
52	An interference method for the determination of axial and oblique aberrations	685
53	Determination of molecular weights in the vapor state from vapor pressure and evaporation data	703
54	The sulphoaluminates of calcium	715
55	An analysis of the arc and spark spectra of yttrium (Yt I and Yt II)	733
56	The precise measurement of X-ray dosage	771
57	Note on an electrical conductance method for determining liquefaction temperatures	787
58	Calibration of sixty-five 35-yellow Lovibond glasses	793
59	The compressive and transverse strength of brick	821

BUREAU OF STANDARDS JOURNAL OF RESEARCH

PARTIAL CONTENTS OF VOLUME 1

Price of bound volume, $2.75

August, 1928 (Vol. 1, No. 2)

RP6. Some measurements of the transmission of ultra-violet radiation through various kinds of fabrics. Price 5 cents.

RP7. Tinting strength of pigments. Price 5 cents.

RP8. Wave-length measurements in the arc and spark spectra of hafnium. Price 5 cents.

RP9. Tests of the effect of brackets in reinforced concrete rigid frames. Price 25 cents.

RP10. Accelerated laboratory corrosion test methods for zinc-coated steel. Price 35 cents.

September, 1928 (Vol. 1, No. 3)

RP11. Standard solar wave lengths (3592-7148A). Price 5 cents.

RP12. Wave lengths and Zeeman effects in yttrium spectra. Price 10 cents.

RP13. Wear and mechanical properties of railroad bearing bronzes at different temperatures. Price 35 cents.

RP14. Steel for casehardening—normal and abnormal steel. Price 35 cents.

RP15. Strain markings in mild steel under tension. Price 15 cents.

October, 1928 (Vol. 1, No. 4)

RP16. Methods for the derivation and expansion of formulas for the mutual inductance of coaxial circles and for the inductance of single-layer solenoids. Price 10 cents.

RP17. Effect of clearance and displacement of attracted disk and also of a certain arrangement of conducting hoops upon the constant of an electrometer. Price 5 cents.

RP18. Mutual inductance of any two circles. Price 5 cents.

RP19. Receiving sets for aircraft beacon and telephony. Price 15 cents.

RP20. Sensitization of photographic emulsions by colloidal materials. Price 10 cents.

Research papers are available as separates for purchase from the Superintendent of Documents United States Government Printing Office, Washington, D. C.

[Continued on page 3 of cover]

U. S. DEPARTMENT OF COMMERCE
BUREAU OF STANDARDS

BUREAU OF STANDARDS JOURNAL OF RESEARCH

April, 1929
Vol. 2, No. 4

UNITED STATES
GOVERNMENT PRINTING OFFICE
WASHINGTON : 1929

For a partial list of previous research papers appearing in Volumes 1 and 2, BUREAU OF STANDARDS JOURNAL OF RESEARCH, see pages 2, 3, and 4 of the cover

SOLD ONLY BY THE SUPERINTENDENT OF DOCUMENTS
U. S. GOVERNMENT PRINTING OFFICE
WASHINGTON, D. C.
AT
$2.75 PER YEAR ON SUBSCRIPTION

APPARATUS FOR THERMOMAGNETIC ANALYSIS

By Raymond L. Sanford

ABSTRACT

Thermomagnetic analysis consists in the study of magnetic effects occurring in a material during heating or cooling, with special reference to their interpretation in terms of structural changes or transformations. It is most conveniently carried out by means of a magnetometer of suitable type. The present paper describes thermomagnetic analysis apparatus set up at the Bureau of Standards and gives typical results obtained by its use.

CONTENTS

	Page
I. Introduction	659
II. General arrangement	660
III. The magnetometer	661
IV. Coils and furnace	665
V. Experimental procedure	666
VI. Typical results	667

I. INTRODUCTION

The magnetic properties of ferromagnetic materials depend not only upon previous thermal history but also upon the existing temperature. Even such relatively small variations of temperature as may occur within the atmospheric range bring about easily measurable changes in magnetic properties which can not be neglected [1] in work of high accuracy. Temperature changes of greater magnitude may produce alterations in the structure of the material accompanied by corresponding changes in magnetic properties. Observations of magnetic changes which occur during heating or cooling, when properly interpreted, therefore, are useful in the study of the constitution of ferromagnetic materials and the effect upon it of various treatments. The study of magnetic effects occurring during heating or cooling with special references to their interpretation in terms of structural changes or transformations is termed "thermomagnetic analysis."

Honda and his associates [2] have found the methods of thermomagnetic analysis very valuable for the study of iron and steel and have even extended them to the study of paramagnetic materials.

[1] Sanford B. S. Sci. Paper No. 245; 1915. Spooner, Phys. Rev., 27, p. 183; 1926.
[2] Many papers in Sci. Rep. Tohoku Univ., Sendai.; 1912, et seq.

Other investigators[3] have also employed thermomagnetic analysis to a certain extent, but thus far little use of this method of investigation has been made in the United States.

Much attention has been given in recent years to the relationships which exist between the magnetic properties of materials and their composition and structure. If sufficiently definite relationships are established and various experimental difficulties overcome, magnetic properties can be made the basis of nondestructive testing methods of great value. The term magnetic analysis has been adopted to distinguish magnetic testing of this type from that carried out solely for the purpose of determining the magnetic characteristics as such. Thermomagnetic analysis when properly developed should take its place as an important phase of the more general subject of magnetic analysis.

The apparatus described in the present paper was designed for the purpose of applying the methods of thermomagnetic analysis to the study of the structure of iron and steel as affected primarily by heat treatment. The problem was originally undertaken several years ago by Dr. C. Nusbaum, who carried out a considerable amount of work in connection with the design and construction of the apparatus. Unfortunately, it was necessary to interrupt the work in favor of more urgent problems and, consequently, he was unable to carry it to completion. The work has recently been taken up again. The apparatus has been somewhat simplified and modified so as to meet the difficult experimental conditions under which it is necessary to work, but the main features follow, in general, the original design.

No especial originality is claimed for the method or equipment, but, in view of the peculiar difficulties encountered in attempting to use this type of apparatus in a location where there are so many magnetic disturbances as are found at the Bureau of Standards, it was thought that a description would be of some interest

II. GENERAL ARRANGEMENT

There are two ways in which thermomagnetic analysis may be carried out. The specimen may be held at a series of fixed temperatures and complete magnetization curves determined for each temperature, or a fixed value of magnetizing force may be applied and the changes in magnetization noted as the temperature is gradually raised or lowered. Each of these methods has its own particular advantages and disadvantages. For the present purpose the second method seems to be preferable because by its use it is possible to make continuous observations of the magnetic changes and to note not only their magnitude, but also the rate at which they progress

[3] Curie (Mme.), Bull. de la Soc. d'Encouragement, **3**, p. 36; 1898. Morris, Phil. Mag., **44**, p. 213; 1897. Terry, Phys. Rev., **28**, p. 393; 1909. Smith, Phil. Trans. Roy. Soc. London, **215**, p. 177; 1915. Dejean, Annal. de Phys., 9 ser., **18**, p. 171; 1922.

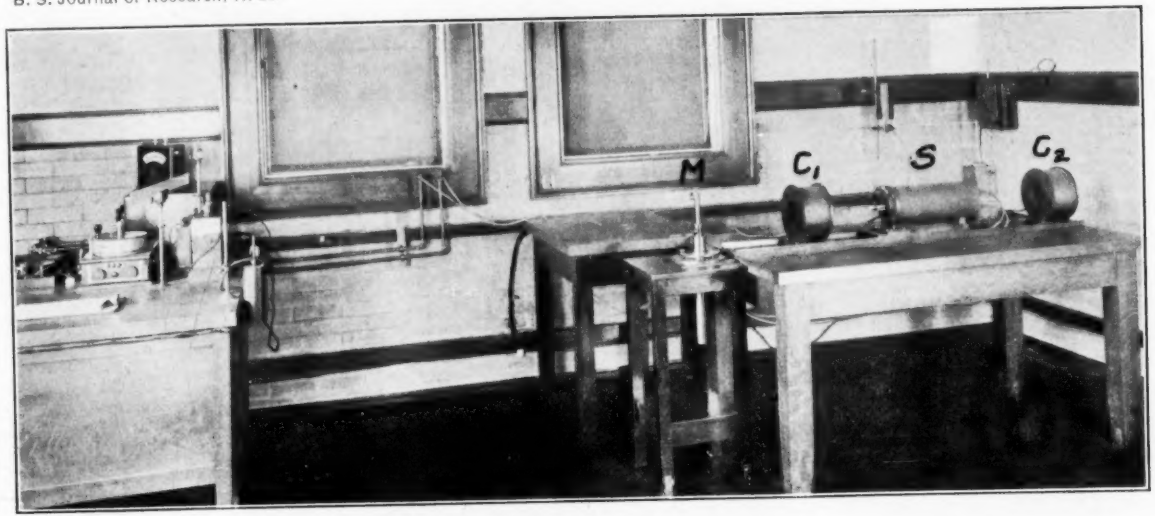

FIG. 1.—*Thermomagnetic analysis apparatus*

(*M* represents the magnetometer, *S* the magnetizing solenoid, and C_1 and C_2 the compensating coils. The axis of the coils is in an east-west direction)

with change in temperature. It is also possible to study the effect of rate of heating or cooling on the observed transformations.

For the continuous observation of relatively slow changes in magnetization such as occur during heating or cooling, the magnetometer is particularly suitable. With this method the magnetization is indicated by the deflection of a suspended magnetic needle placed in a definite position with respect to the test specimen. The direct action of the magnetizing solenoid is neutralized by suitable compensating coils. The sensitivity of a single needle magnetometer is determined not only by the strength of the needle, but also by the torsional strength of the suspension and the intensity of the earth's magnetic field. In the magnetic laboratory of the Bureau of Standards the field is continually varying both in direction and magnitude, due to outside disturbances from electrical machinery, elevators, and the like. Consequently, the use of a single needle is not practicable, and an astatic system must be used.

Figure 1 is a photograph of the apparatus which consists essentially of a magnetizing solenoid S, compensating coils C_1 and C_2, and the astatic magnetometer M. Within the solenoid S is mounted an electric furnace. On a separate table are mounted rheostats for controlling the magnetizing current, an autotransformer for controlling the heating current, a potentiometer for temperature measurement, and lamps and scales for reading the potentiometer and magnetometer deflections. The coils are arranged with their axes in an east-west direction, and the magnetometer is east of the coils. The furnace is water jacketed and a platinum, platinum-rhodium thermocouple is used in the temperature measurements.

III. THE MAGNETOMETER

The construction of the magnetometer system is shown in Figure 2. The moving system is suspended by means of a quartz fiber from the threaded brass rod, R, which extends through the torsion head of the instrument. Vertical adjustment is provided by means of a nut on the head. A tangent screw is also provided for fine adjustment of the zero. The quartz fiber suspension Q is approximately 8 cm long and 0.04 mm in diameter, and is attached to the rod with shellac. For the sake of convenience in making the necessary adjustments, the suspended system is in two parts connected by small hooks made of flat wire so as to prevent relative twisting of the two parts. The upper part of the system carries a plane mirror, M, 1 cm in diameter and a mica damping vane, V, as shown. The image of a lamp filament is focused on a ground glass scale by means of a lens of 2 m focal distance mounted in the case of the instrument. The mica vane hangs in a damping chamber and provides practically critical damping.

In the lower system the magnetic needles are mounted in short brass tubes as shown. A brass rod 1 mm in diameter extends between the needles, and the distance can be varied by changing the length of the rod. The usual distance is approximately 25 cm. As the distance rod is held by friction in tubular projections, the magnets can easily be oriented with respect to each other. This type of magnet system was chosen because, since there is a vertical gradient in the horizontal intensity of the magnetic field, it is desirable to be able to adjust the magnetic moments of the needles separately. The needles, 1 cm long and 3 mm in diameter, are made of special magnet steel containing about 15 per cent cobalt. This type of steel, when properly heat treated, has a coercive force from two to three times as great as that of the ordinary 5 per cent tungsten steel and for this reason is especially adapted for short, thick magnets. The magnetic moment of the needles has not been determined, but comparative tests indicate that the strength is about three times as great as could be obtained with the same weight of steel of the ordinary type. With an astatic system, the sensitivity depends directly upon the strength of the needles, so the stronger needles constitute a distinct advantage. The total weight of the suspended system is about 6 g. The outer case of the magnetometer is made of sections of brass tubing which are removable so that the various parts of the suspended system are easily accessible.

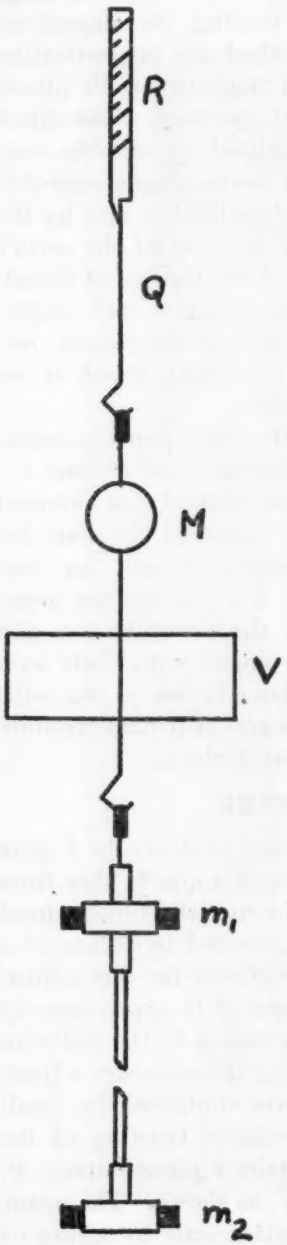

FIG. 2.—*Magnetometer moving system*

In setting up and attempting to use the apparatus two difficulties were encountered which may be of interest to mention. As first set up the zero was found to drift badly. For several days the reading was brought back to zero each day by adjusting the torsion head, but the zero continually drifted in the same direction, sometimes as much as 5 cm in a day. Various parts of the apparatus were investigated in an attempt to locate the reason for this behavior, which

was finally traced to the supporting rod R. It was found that, apparently due to the relief of internal stresses, the rod was continually twisting. The trouble was eliminated by annealing the rod at 500° C. The second difficulty was a tendency for the shellac to yield gradually, thus lowering the system and altering the sensitivity and compensation. This difficulty was obviated by heating the shellac to slightly above 100° C. and holding it at this temperature overnight after application to the rod and suspension hook but previous to attaching the quartz fiber. One suspension mounted in this way has now been in use several months without signs of yielding.

On account of the variability of the field in which the magnetometer is located, its behavior depends largely upon the care with which the relative strengths and orientation of the needles are adjusted. Not only is the field variable, but also there is a vertical gradient in horizontal intensity. The gradient amounts to a variation in field strength of about 0.3 per cent per cm of vertical distance. It is necessary, therefore, in order to make the resultant torque zero, to adjust the strength of the needles so as to be inversely proportional to the respective strengths of the field in which they hang. This adjustment can be made only approximately, because the ratio of the field strengths at the two positions is constantly changing. The wandering of the zero due to this cause is a function of the variation in this ratio.

While it is essential to have the relative strengths of the needles properly adjusted, it is even more necessary to have their magnetic axes parallel. If there is an angle between the two axes, there is a resultant magnetic moment nearly at right angles to the needles, and any variation in the strength of the earth's field causes a wandering of the zero. In addition to this, if the magnetizing and compensating coils are adjusted to give no torque at the zero position, the compensation does not remain good if the system is deflected. The reason for this can be shown as follows:

Let

T_1 = torque of upper needle,
T_2 = torque of lower needle,
θ = angle between axis of coils and upper needle,
α = angle between axes of the needles,
$\theta+\alpha$ = angle between axis of coils and lower needle.

then

$$T_1 = k_1 \sin \theta \tag{1}$$

$$T_2 = k_2 \sin (\theta+\alpha) \tag{2}$$

where k_1 and k_2 are constants. When the system is compensated

$$T_1 = T_2$$

or

$$k_1 \sin \theta = k_2 \sin (\theta+\alpha) \tag{3}$$

This condition can hold good for more than one θ only when $\alpha=0$. In other words, in order for the compensation to remain good when the needles are deflected by the magnetic field of the specimen, the magnetic axes of the needles must be parallel to each other.

The adjustment of the magnetometer system is carried out as follows:

1. The magnet system is replaced by an equivalent nonmagnetic weight, and the torsion head is adjusted so as to bring the reading to zero. This adjustment is not subsequently altered.

2. The upper hook of the magnet system, which is held by friction, is then oriented so as to bring the needles approximately perpendicular to the earth's field when suspended, and the relative strengths of the needles are adjusted so that, when the system is suspended, the reading is zero, thus indicating that there is no resultant torque. This is most conveniently done by reducing the strength of the stronger needle by subjecting it to the influence of a powerful permanent magnet.

3. Next, the lower needle is removed and the hook so oriented as to bring the reading to zero when the system is suspended. In this position there is no torque on the suspension, as the needle is oriented in the direction of the earth's magnetic field.

4. The lower needle is then replaced and so oriented with aspect to the upper needle that when the system is again hung on the suspension the reading is zero, thus indicating that the torque due to each needle is completely balanced by that of the other. The system is then in proper adjustment.

In locations where there is considerable magnetic disturbance due to stray fields it is desirable to make the final adjustment at a time when the disturbances are a minimum, which is generally some time in the neighborhood of 3 a. m. The adjustment of the system as at present constructed is rather tedious because there is no provision for twisting the various elements with respect to each other by known small amounts. It is possible that considerable improvement could be made in this respect, though it would be objectionable to increase the weight of the system.

As stated earlier, the behavior of the magnetometer is largely a function of the care with which the initial adjustments are made. On account of the nature of the variations in the magnetic field it is not possible to eliminate entirely the wandering of the zero. It has been possible, however, so to adjust the system that when the sensitivity is such as to give a maximum deflection of 20 cm the wandering is not over 1 mm. The feasibility of improving this performance to any appreciable extent is rather doubtful.

IV. COILS AND FURNACE

The magnetizing solenoid consists of 16 layers of No. 12 double cotton covered copper wire wound on a brass form 36 cm in length. For convenience a tap was brought out from every fourth layer. The total number of turns is 2,364, and the field at the center calculated on the basis of a coil of infinite length and the same number of turns per cm would be 83.1 times the current in amperes. In order to accommodate the furnace, however, the inside diameter has to be rather large, about 8 cm, so that the actual value is nearly 5 per cent less. The magnetizing field in gilberts per cm at the center of the solenoid as calculated and checked experimentally is 79.2 times the current in amperes and for a distance of 12 cm at the center does not vary by more than 2 per cent.

The compensating coils are wound on brass forms 10 cm long of approximately the same inside diameter as the main magnetizing coil and have 22 layers of No. 12 double cotton covered wire. It was at first intended to locate one compensating coil on the opposite side of the magnetometer from the magnetizing coil, but as finally set up it was found more convenient to have it on the same side. Consequently, since this coil must be quite near the magnetometer, only the outside layer of the winding is actually used.

The three coils are mounted on bases which slide on bronze tracks permanently secured to the table. The coils were carefully oriented so as to be coaxial, as any angle between the axis of the magnetizing and compensating coil would give a component of field in the direction of the magnetometer needles. If this condition exists, the sensitivity varies with the current in the coils (the Erhardt effect).[4]

The furnace consists of a bifilar winding of platinum strip wound on an alundum tube approximately 2 cm in diameter. This winding is noninductive to such a degree that with 5 amperes d. c. flowing there is no appreciable effect on the magnetometer. To prevent short circuiting, the winding is held in place on the tube by means of alundum cement.

Alternating current for heating is provided by an autotransformer with which the supply voltage can be regulated in steps of 0.1 volt. This arrangement gives exceptionally good control of rate heating or cooling. The temperature in the furnace is uniform to within 3° C. over a length of approximately 12 cm at the middle.

Surrounding the furnace is a brass water jacket to which water is brought by means of brass pipe and rubber tubing. The cooling is very effective, no rise in temperature being observed in the magnetizing winding even with the furnace operating at 1,000° C.

[4] Gray and Rogs, An Improved Form of Magnetometer, Proc. Roy. Soc. Edinburgh, **29**, p. 182; 1908–9.

The specimens are supported within the furnace by means of a glazed porcelain tube 1 cm in inside diameter and 50 cm long. Arrangements can easily be made for heating in a vacuum or in a gaseous atmosphere.

Temperatures are measured by means of a Pt, Pt-10 per cent Rh thermocouple, and a Leeds & Northrup type K potentiometer. The cold junctions are maintained at 0° C. by means of an ice box in the usual way.

V. EXPERIMENTAL PROCEDURE

Observations are ordinarily made in the following way: First, the magnetizing coil is set at the required distance from the magnetometer, and, with no specimen in the coil, the compensating coils are adjusted so as to exactly neutralize the effect of the magnetizing coil. The final adjustment is made by moving the coil C_2. The sample and thermocouple are then inserted and the reading of the magnetometer noted when the magnetizing current has been set to the proper value. After starting the circulation of the cooling water the heating current is turned on and adjusted to such a value as to give the desired heating rate. The potentiometer is then set for the first temperature at which an observation is to be taken and the reading of the magnetometer is noted when the given temperature is reached. The potentiometer is then set for the next temperature and so on.

The results obtained depend somewhat upon the form of specimen and in particular upon the ratio of length to diameter. For a cylindrical specimen in a uniform magnetic field the effective magnetizing force is less than the impressed force.

$$H = H' - NI \tag{7}$$

where

H = the effective magnetizing force,
H' = the impressed magnetizing force,
N = the demagnetizing factor, and
I = the intensity of magnetization.

The factor N varies with the dimensional ratio. Since the intensity of magnetization depends upon the susceptibility of the material and the susceptibility varies with temperature, it is obvious that, as the test proceeds, the effective magnetizing force also varies. For specimens having a small ratio of length to diameter there is a tendency for the effect of a change in susceptibility to be neutralized by the resulting change in the value of the effective magnetizing force. Under these conditions the effect of structural changes may appear to be so small as to go unnoticed.

In view of the fact that other apparatus in use in the laboratory for testing small samples is adapted for specimens 6 mm in diameter, this was chosen as the standard diameter for this test. In order to have as uniform temperature conditions as possible it is advisable to use the shortest specimen which will give satisfactory results. By experiment it was found that the specimens should be at least 8 cm long, and preferably 10 cm. Accordingly, the specimens are usually 6 mm in diameter and 10 cm long with a small hole drilled axially in one end for insertion of the thermocouple.

It is desirable to work with the distance from the specimen to the magnetometer as great as possible, for under this condition the compensation is most easily adjusted and maintained.

It is generally not necessary to know the exact value of magnetization of the specimen, as the significant data are the temperatures at which definite changes in magnetization occur. These are shown by the form of the curve obtained by plotting magnetization, represented by magnetometer deflection, against the corresponding temperature. However, when calibration is desired, it can most easily be accomplished by means of a specimen of known magnetic properties. This procedure has been found preferable to the use of a standard coil on account of the short distance between the magnetometer needles and the finite length of the specimen.

VI. TYPICAL RESULTS

In Figures 3 to 7, inclusive, are shown typical results obtained with the apparatus. Figure 3 represents the magnetic behavior of pure iron when heated above the transformation temperature. For the magnetizing force used, 200 gilberts per cm, there is no appreciable drop in magnetization until a temperature of approximately 725° C. is reached. From then on the drop is rapid to about 775° C. The approach to the zero value is more gradual and it is usually very difficult to determine the exact temperature at which magnetization completely disappears. This is characteristic of all ferromagnetic materials.

Nickel, as indicated in Figure 4, shows somewhat different characteristics in that the magnetization begins to drop immediately upon the start of heating. The magnetic transformation temperature of nickel is much lower than that of iron. Magnetization is practically completely lost for the sample of Figure 4 at a temperature of approximately 330° C. The applied magnetizing force was 240 gilberts per cm.

When a material is made up of two or more magnetically distinct constituents having different magnetic transformation temperatures, their presence may be detected by means of the resulting breaks in

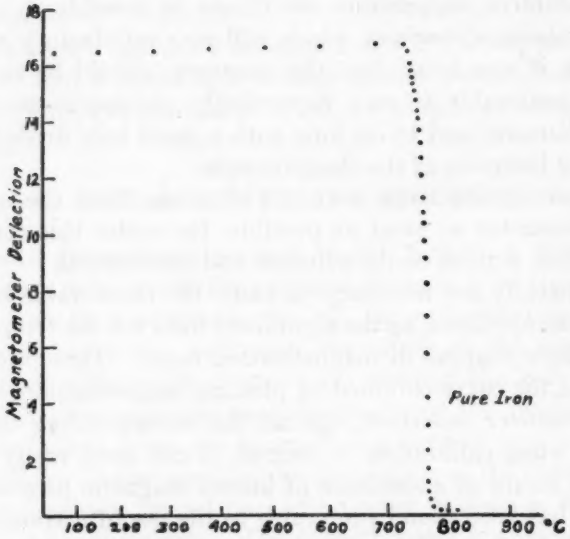

FIG. 3.—*Heating curve for pure iron*
Applied magnetizing force, 200 gilberts per cm

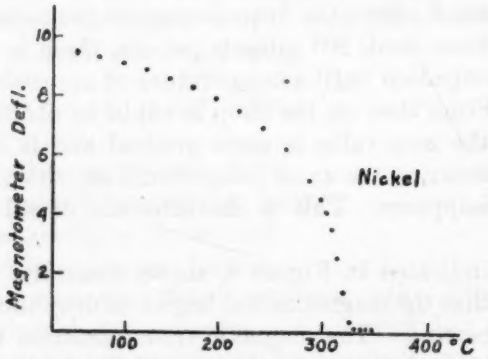

FIG. 4.—*Heating curve for commercially pure nickel*
Applied magnetizing force, 240 gilberts per cm

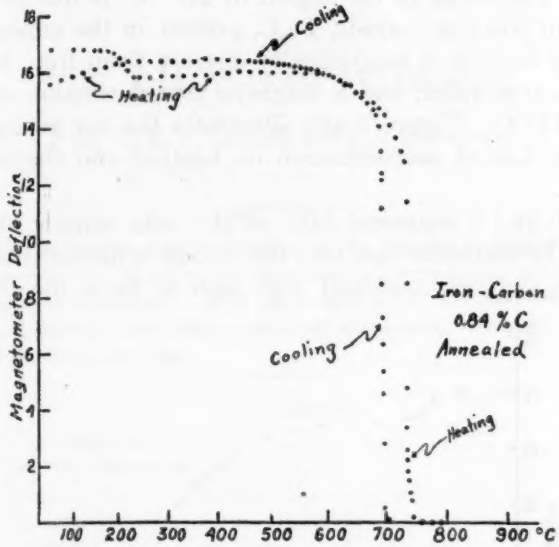

FIG. 5.—*Heating and cooling curves for annealed iron-carbon alloy of eutectoid composition*
Applied magnetizing forces, 200 gilberts per cm

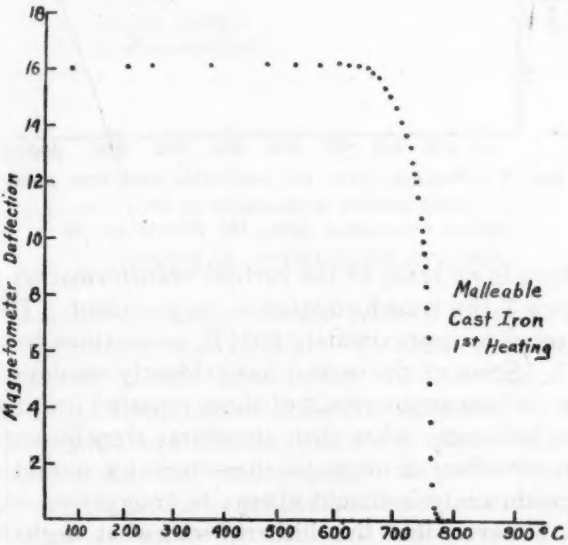

FIG. 6.—*Heating curve for malleable cast iron*
Applied magnetizing force, 160 gilberts per cm

the magnetization-temperature curve. One such instance is shown in Figure 5. The break in the region of 215° C. is due to the transformation of the iron carbide, Fe_3C, present in the annealed carbon alloy. Iron carbide is magnetically distinct from iron, has a much lower saturation value, and a magnetic transformation temperature of about 215° C. Figure 5 also illustrates the lag generally found between the loss of magnetization on heating and the recovery on cooling.

Figures 6 and 7 represent runs on the same sample of malleable cast iron. In malleable cast iron the carbon is normally in the form of graphite and not combined with iron to form the carbide. In

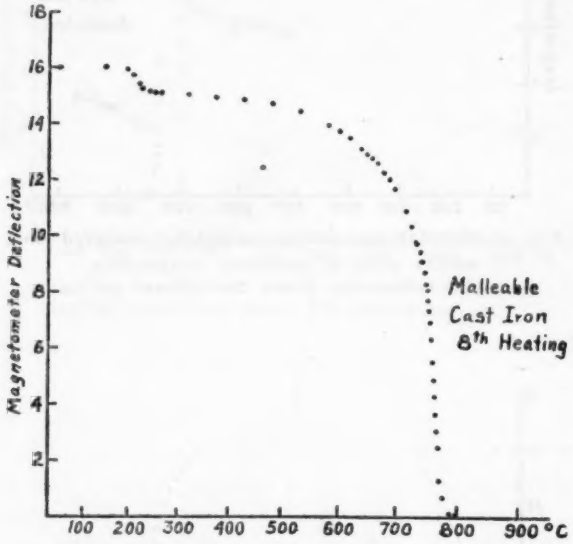

FIG. 7.—*Heating curve for malleable cast iron previously heated seven times to 800° C.*
Applied magnetizing force, 160 gilberts per cm

Figure 6 there is no trace of the carbide transformation at 215° C., but in Figure 7 the transformation is very evident. The specimen had been heated to approximately 800° C. seven times before the run of Figure 7. Some of the carbon has evidently combined with iron to form the carbide as the result of these repeated heatings.

There are influences other than structural transformations which may lead to variations in magnetic characteristics, so that the data of thermomagnetic analysis should always be interpreted with caution. It appears, however, that this hitherto somewhat neglected method should be capable of yielding significant and valuable results.

WASHINGTON, October 1, 1928.

THE ANALYSIS OF FLUORSPAR

By G. E. F. Lundell and J. I. Hoffman

ABSTRACT

In connection with the standardization of the Bureau of Standards standard sample of fluorspar No. 79, old methods of analysis were tested and modified, and new methods were developed. This paper sets forth the procedures that have been found desirable for the determination of carbonates, silica, calcium fluoride, sulphur, barium, lead, and zinc.

CONTENTS

	Page
I. General considerations	671
1. Calcium carbonate	671
2. Silica	672
3. Calcium fluoride	673
4. Sulphur	675
II. Methods of analysis	676
1. Fineness of the sample	676
2. Drying	676
3. Carbonates	676
4. Silica	677
5. Calcium fluoride	677
(*a*) Umpire method	677
(*b*) Routine method	679
6. Sulphur	680
7. Barium	681
8. Lead	681
9. Zinc	682
10. Other constituents	682
III. Acknowledgment	682

I. GENERAL CONSIDERATIONS

The determinations that are usually made in fluorspar are those of calcium fluoride, silica, and sulphur. To these may be added calcium carbonate or carbon dioxide, lead sulphide, zinc sulphide, the oxides of iron and aluminum, and barium sulphate, which are occasionally determined, and alkalies, magnesia, titania, zirconia, phosphorus pentoxide and other minor constituents, which are sometimes present and would have to be determined in a complete analysis.

1. CALCIUM CARBONATE

The correct determination of calcium that is present as carbonate in fluorspar is difficult, because it is impossible to dissolve the carbonate without at the same time dissolving some calcium fluoride.

The amount of the latter which dissolves varies with conditions, such as the amount of calcium introduced into solution through solution of the carbonate, or of fluorine through the solution of other soluble fluorides.

If fluorspar is digested with a 10 to 20 per cent solution of acetic acid, practically all of the calcium and magnesium carbonates are dissolved, together with more or less calcium fluoride, iron, aluminum, lead, and possibly zinc. Most of the methods now in use call for such a treatment, followed by more or less elaborate separations and the precipitation of the calcium as oxalate. The latter is then ignited to oxide or titrated with permanganate. Even if these methods should yield consistent results, they entirely ignore other carbonates, such as those of lead, magnesium, iron, and the like, which, if present, must also be regarded as impurities in fluorspar. It would seem more satisfactory, therefore, to determine carbon dioxide directly by treating with acid and catching the gas in a weighed absorbent and to report the carbon dioxide so found as "Total carbonates as $CaCO_3$." Such a determination is not only much more rapid than present procedures but gives more significant and consistent results as well.

If organic matter is known to be absent, it is satisfactory for all ordinary purposes to determine carbon dioxide by heating the sample in the furnace used for determining carbon in steel, if the usual provisions for removing compounds of sulphur are made.[1] This procedure is described in the Methods of the Chemists of the United States Steel Corporation for the Sampling and Analysis of Fluxes, Cinders, and Refractories.

2. SILICA

Most of the methods used for determining silica in fluorspar are modifications of that described by Bidtel.[2] In such methods the calcium carbonate is removed by extracting with acetic acid. Sulphides are oxidized by roasting with mercuric oxide or by digesting with a solution containing potassium bromide and bromine. The sulphates so formed are usually removed by digesting with ammonium acetate, ammonium citrate, or other solvents and then filtering. Finally the residue is ignited and weighed, and silica is determined by treating with hydrofluoric acid, evaporating to dryness, igniting, and again weighing.

In the absence of appreciable quantities of lead and zinc, fairly accurate results for silica can be obtained by leaching the fluorspar with dilute acetic acid, igniting, weighing, treating with hydrofluoric acid, and again igniting and weighing. Lead or zinc sulphides cause serious errors in such a method, for on ignition these are gradually

[1] W. F. Muehlberg, of the Newburgh Steel Works, Cleveland, Ohio, obtained satisfactory results by applying this method to the analysis of the Bureau of Standards standard sample of fluorspar No. 79.

[2] J. Ind. Eng. Chem., 4, p. 201; 1912; 6, p. 265; 1914.

oxidized to sulphates. According to Hofman and Wanjukow,[3] lead sulphate begins to decompose at about 637° C., while zinc sulphate begins to decompose at about 702° C. The uncertainty as to the oxidation or partial decomposition of these substances necessitates as complete oxidation or removal of them as possible.

Treatment with glacial acetic acid containing 20 per cent of liquid bromine was found to be more efficacious than the potassium bromide-bromine treatment in oxidizing zinc sulphide, but less satisfactory in oxidizing lead sulphide. Both constituents were satisfactorily oxidized by first treating with a solution of bromine in glacial acetic acid and then with a solution of potassium bromide and bromine. Treatment with mercuric oxide was not tried, because mercury vapors are objectionable. In any case the sulphates that are formed can be satisfactorily removed by treatment with ammonium acetate.

Lead and zinc sulphides not removed by the preliminary treatments are oxidized to sulphates during the ignition of the siliceous residue. This should therefore be ignited at temperatures just below 650° C., preferably in a muffle furnace, and the final ignition should not be unduly prolonged.

In spite of the fact that the method to be described and similar methods give fairly consistent results, it is not to be supposed that such results of necessity represent the actual silica content. Some silicates may remain unattacked by the hydrofluoric acid treatment, and changes occurring between the first and second ignitions may cause errors, either positive or negative.

3. CALCIUM FLUORIDE

A direct determination of fluorine is rarely, if ever, attempted in analyses involving the sale of fluorspar. The usual custom is to report the percentage of calcium fluoride as calculated from a determination of the calcium that remains after a preliminary treatment which is intended to remove calcium that is not present as the fluoride. Bidtel's method [4] or some modification of it is widely used for the determination. In such methods calcium carbonate is first extracted with dilute acetic acid and the silica next volatized by means of hydrofluoric acid. These treatments leave lead and zinc, which must also be removed. This is accomplished by oxidizing the sulphides to sulphates and then extracting with a solution of ammonium citrate or ammonium acetate containing ammonium citrate.[5] After the lead and zinc are extracted, together with more or less iron and other constituents, the residue is ignited and converted to sulphate by treatment with sulphuric acid. The sulphate is then weighed and

[3] Trans. Am. Inst. Mining Eng., **43**, p. 523; 1912; Chem. and Met. Eng., **10**, p. 172; 1912.

[4] See footnote 2.

[5] Some chemists remove the lead, zinc, iron, and the like by precipitating with ammonium sulphide.

the percentage of calcium fluoride calculated on the assumption that only calcium sulphate is present, or else it is dissolved, the calcium precipitated as the oxalate, and ignited to the oxide or titrated with permanganate. In either case the CaO so found is calculated to calcium fluoride. In some methods the residue left after the extraction of lead, zinc, iron, and the like with ammonium citrate-ammonium acetate is dried, ignited, and weighed as CaF_2.

In the umpire method to be described calcium carbonate is removed by digesting the sample on the steam bath with a 10 per cent solution of acetic acid and filtering. Sulphides are then decomposed and removed by usual procedures before determining the calcium that is present as the fluoride. In the routine method calcium carbonate and the sulphides are removed at the same time by treating the sample in turn with a solution of bromine in acetic acid, then with a solution of potassium bromide and bromine, and finally with a solution of ammonium acetate.

In any method for the determination of calcium fluoride the following facts should be considered:

(*a*) Practically all of the calcium carbonate and calcium sulphate in fluorspar can be removed by digesting with 10 to 20 per cent acetic acid and filtering. Glacial, or 50 per cent, acetic acid is not so effective as the more dilute acid. Ignited calcium sulphate is but slowly attacked by dilute acetic acid. Both hydrated and anhydrous calcium sulphate readily dissolve in dilute acetic acid containing a small quantity of ammonium acetate.

(*b*) Tests show that from 2 to 2.5 mg of calcium fluoride is dissolved when pure calcium fluoride is treated with dilute acetic acid as will be described in the "umpire method." However, if as much as 5 per cent of calcium carbonate is present, the amount of calcium fluoride dissolved in the same treatment is only about 1 mg, the decrease in solubility probably being caused by the common ion effect of the calcium. When pure calcium fluoride is treated as prescribed in the "routine method" from 6 to 7 mg is dissolved. In the presence of calcium carbonate the solubility falls to about 5 mg. As calcium carbonate is present in all commercial fluorspar, a correction of 1 mg is recommended in the umpire method and 5 mg in the routine method.

(*c*) Any method that is based on extraction with dilute acetic acid will be in error if insoluble compounds of calcium, other than calcium fluoride, are present. For example, if calcium silicate were present, it would remain with the calcium fluoride and would be counted as the latter. Fortunately, there is apparently little to be feared from this source.

(*d*) The oxidation of sulphides by roasting is not to be recommended, because there is some loss of fluorine, probably the result of the dis-

placement of fluorine by the sulphur dioxide or trioxide that is formed. If the roasted sample is subsequently treated with dilute acetic acid, calcium equivalent to the quantity of fluorine lost will be dissolved, and the results for calcium fluoride will be low. In the routine method sulphides are converted to sulphuric acid, and this exerts a solvent action on the calcium fluoride. Ordinarily this is not serious, but there is a tendency toward low results by the routine method if sulphur is high.

(*e*) Any lead or zinc that escapes extraction in the treatment with the solution of bromine in acetic acid, the solution of potassium bromide and bromine, and the solution of ammonium acetate as described in the "routine method" causes a positive error in the result for calcium fluoride. The error is small, as a rule, for most of the lead and zinc is extracted and what remains is but partially precipitated when the calcium is precipitated as oxalate.

(*f*) Calcium fluoride can be decomposed by fuming with either sulphuric or perchloric acid. Perchloric acid is advantageous because the products are soluble, and the perchlorates do not "creep" over the rim of the crucible as badly as do the sulphates. All or nearly all of 1 g of calcium fluoride can be converted to the perchlorate by evaporating to dryness twice with 3 to 5 ml portions of perchloric acid in a platinum crucible. A third evaporation with perchloric acid after transferring the solution from the crucible to a beaker is advisable, because any fluorine still left in the solution will cause low results, especially in the routine method. The perchloric acid may be evaporated rather rapidly, but the residue in the crucible should not be heated too strongly when it is just approaching dryness, because of possible mechanical loss. Perchloric acid is not hazardous unless in contact with strong reducing material at temperatures above 100° C. If organic matter is present, heat with perchloric acid at 100° C., add nitric acid dropwise until reaction ceases, and then heat until the perchloric acid volatilizes.

4. SULPHUR

Sulphur in fluorspar is usually determined by fusing the sample with an oxidizing flux, extracting the melt with water, and finally precipitating and weighing as barium sulphate. Melts obtained with potassium carbonate and potassium nitrate dissolve more rapidly than those obtained with sodium carbonate and sodium nitrate and lead to equally accurate results.

Unless great care is exercised in fusing fluorspar, the very fluid melt will overflow or "creep" over the top and adhere to the outside surface of the crucible. There is little danger of loss, but if a gas flame is used this alkaline film on the outside of the crucible or cover may absorb a considerable quantity of sulphur. Positive errors from this source were found to be as high as 0.04 per cent of sulphur.

The use of an electric furnace in making the fusion is to be recommended, because with proper care there is little chance of contaminating the melt with sulphur from outside sources.

Alcohol or petroleum ether flames may be used as a source of heat, but alcohol flames are somewhat difficult to control, and not all petroleum ether is free from sulphur.

Fluorine accompanies sulphur in the water extract of the melt, and most of it must be removed before barium sulphate is precipitated, lest barium fluoride also be thrown down. Most of the fluorine can be removed by evaporating the water extract twice with an excess of hydrochloric acid, and interference by that which remains in solution can be avoided by using only a slight excess of barium chloride in the precipitation of the sulphate.

II. METHODS OF ANALYSIS

1. FINENESS OF THE SAMPLE

The sample should be ground to pass a No. 80 sieve. Coarser material has a tendency to decrepitate on ignition.

2. DRYING

Fluorspar offers little difficulty in drying or weighing the sample. A sample dried for one hour at 105 to 110° C. is satisfactory.

3. CARBONATES

Determine CO_2 by evolving it with dilute HCl (1:1) [6] and absorbing it in ascarite. Less attack on the flask results if H_3BO_3 is also used. If desired, the CO_2 may be absorbed in $Ba(OH)_2$ and determined by titration. Report as "total carbonates as $CaCO_3$."

The apparatus used by the authors consists of a flask fitted with a small reflux condenser which is followed by bulbs or tubes containing (1) H_2SO_4, (2) pumice impregnated with anhydrous $CuSO_4$,[7] (3) "dehydrite" ($Mg(ClO_4)_2 \cdot 3H_2O$), (4) a weighed tube containing ascarite and "dehydrite," and (5) a protecting tube containing "dehydrite." All connections are made by simple mercury seals. P_2O_5 may be used instead of "dehydrite." Dilute HCl (1:1) containing 1 g of H_3BO_3 per 100 ml was used in the evolution of the CO_2.

A determination of CO_2 by heating the sample in a combustion tube would include organic carbon and possibly a little SiF_4.

---

[6] Prepared by mixing 50 ml of the concentrated acid with 50 ml of water. This system of designating dilute acid is used throughout the paper. For example, dilute HCl (5 : 95) denotes a solution containing 5 ml of the concentrated acid and 95 ml of water. If no dilution is specified, the concentrated reagent is intended.

[7] Prepared by saturating pumice with a solution of $CuSO_4$, drying and heating at 150 to 160° C. for four to five hours.

4. SILICA

Transfer a 1.000 g sample to a 50 ml beaker, add 3 ml of acetic acid-bromine mixture,[8] cover the beaker, and digest on the steam bath for 10 minutes. Next add 10 ml of water and 10 ml of potassium bromide-bromine mixture [9] and digest for 40 minutes. Finally add 5 ml of a 50 per cent solution of $NH_4C_2H_3O_2$ and digest for 10 minutes. Add a little paper pulp and filter on a paper of close texture. Wash with 30 to 40 ml of hot water, ignite in platinum at approximately 650° C., cool in a desiccator, and weigh. Treat with about 3 ml of HF, break up the lumps or cakes with a platinum rod, and evaporate to dryness. Repeat the treatment with HF, ignite at approximately 650° C. for about five minutes, cool, and weigh. The difference between the two weights is to be regarded as silica. Owing to the possible retention of some lead and zinc, the temperature of ignition should be rather closely controlled. This can be conveniently done in a muffle furnace.

By this method the authors obtained an average of 1.89 per cent of silica in the Bureau of Standards fluorspar No. 79. Eight of the cooperating analysts obtained an average of 1.87 per cent, the extreme results being 1.74 and 1.95 per cent. By the use of a method in which the fluorine was removed before the determination of silica, an average of 1.77 per cent was obtained by the authors.

5. CALCIUM FLUORIDE

(*a*) UMPIRE METHOD.—Transfer 0.5000 g of the sample (dried at 105 to 110° C.) to a 30 ml platinum crucible, add 15 ml of 10 per cent $HC_2H_3O_2$ and digest on the steam bath for one-half hour, stirring with a small glass rod at 5-minute intervals. Filter through a 7 cm filter paper of close texture and thoroughly wash the crucible and paper with small portions of hot water, using about 35 ml in all. Transfer the paper and precipitate to the crucible, dry, and ignite at a dull red heat.

Treat the residue in the crucible with about 3 ml of HF and evaporate to dryness. Add 1 to 2 ml of H_2SO_4 and evaporate to dryness under the hood. Cool, wash down the inside of the crucible with 1 ml more of H_2SO_4 (in order to catch any undecomposed particles of calcium fluoride), and again evaporate to dryness. Two or three evaporations with 3 to 4 ml of a 60 to 70 per cent solution of $HClO_4$ may be substituted for the evaporation with H_2SO_4. Cool the

[8] Add 20 ml of liquid bromine to 80 ml of glacial $HC_2H_3O_2$ and mix thoroughly. If liquid bromine comes in contact with the skin, painful burns will result which can be checked and relieved by quickly immersing and thoroughly rubbing the wound in carbon tetrachloride, and then allowing it to dry. The evaporation of the tetrachloride carries with it the free bromine.

[9] A 20 per cent solution of KBr saturated with Br_2. Transfer 500 g of Br to a liter bottle, add 700 ml of a 20 per cent solution of KBr, and cautiously shake. When the solution is exhausted, more of the 20 per cent solution of KBr may be added.

crucible and immerse it in a beaker containing 150 ml of dilute HCl (5:95). Warm gently and remove the platinum crucible, being sure to cleanse it from adhering particles of $CaSO_4$.

Boil the contents of the beaker for 10 minutes, and if any insoluble matter remains, filter, wash, and ignite the residue in platinum.[10]

Pass H_2S into the clear filtrate for a few minutes and then make the solution ammoniacal. Continue the current of gas for 10 minutes and allow the precipitate to settle for 20 to 30 minutes. Filter and wash with $NH_4Cl-(NH_4)_2S$ solution.[11]

Neutralize the filtrate and washings with HCl, add 20 ml of the acid in excess, and boil for two to three minutes to expel most of the H_2S. Add KBr–Br_2 solution [12] until the solution remains yellow, boil until the finely divided sulphur has been oxidized, and continue the boiling until the bromine has been expelled. Filter if sulphur or sulphides are not removed by the treatment with bromine. Precipitate the calcium in the filtrate in a volume of about 200 ml by adding 2 g of $(NH_4)_2C_2O_4.H_2O$ and then NH_4OH slowly and with stirring until the solution is slightly ammoniacal. Heat on the steam bath for one-half to one hour, stirring occasionally, cool to room temperature, and filter on a paper of close texture. Wash with a cold 0.1 per cent solution of $(NH_4)_2C_2O_4H_2O$, ignite to constant weight, and calculate the CaO to CaF_2 (factor = 1.392). The determination may be finished by titrating the calcium oxalate with a standard solution of $KMnO_4$. In this case filter through a platinum or asbestos pad, finally wash the CaC_2O_4 with three or four 10 ml portions of cold water, and titrate as usual. To the CaF_2 found should be added 0.20 per cent to allow for the fluoride dissolved by the $HC_2H_3O_2$ and this result then corrected in accordance with the results obtained in a blank carried through all steps of the determination.

It is believed that analyses made by this method should be accurate to ± 0.25 per cent.

The use of platinum crucibles for the initial digestion with $HC_2H_3O_2$ obviates the quantitative transfer of the residue to the paper, and this saves time and keeps the volume of the washing solution at a minimum. Digestion can, however, be carried out in small glass beakers. A small rod just a little longer than the depth of the crucible is very convenient to use in stirring the solution during the digestion and to

[10] This residue may consist of $BaSO_4$, $PbSO_4$, or undecomposed CaF_2. Owing to the small size of the sample originally taken, it is not advisable to determine lead and barium at this point. The residue should be treated, however, with a few drops of HF and H_2SO_4, heated until these are expelled, digested with 1 to 2 ml of HCl on the steam bath, and the solution added to the main solution for the determination of calcium. If the original material contains much barium, more or less $BaSO_4$ separates, but this is of no consequence.

[11] Prepared by passing a moderate stream of H_2S for five minutes through a solution containing 5 ml of NH_4OH and 10 g of NH_4Cl per liter.

[12] A 20 per cent solution of KBr saturated with Br_2. See method for silica. The addition of KBr-Br_2 solution soon after acidification is more efficacious in removing sulphur than it would be if the boiling were continued until sulphur coagulated and the KBr–Br_2 then added.

pour against as the solution is transferred from the crucible to the paper.

After the treatment with $HC_2H_3O_2$, particles of the residue adhere to the surface of the crucible near the rim. These should be brushed to the bottom of the crucible with a piece of moist filter paper.

Sulphur is removed before calcium is precipitated, because sulphite or sulphate is formed when calcium oxalate containing sulphur is ignited, and in large precipitates these can not be entirely decomposed even by strong ignition. Results would consequently be high. Removal of sulphur is not needed if titration is to follow.

The results given under the umpire method in Table 1 are averages of closely agreeing analyses made by the authors. By the use of the method, 12 chemists who cooperated in the analysis of Bureau of Standards sample of fluorspar No. 79 obtained an average of 94.88 per cent of CaF_2 with variations from 94.72 to 95.27.

(*b*) ROUTINE METHOD.—Add 3 to 5 ml of 60 to 70 per cent $HClO_4$ to the residue obtained in the determination of silica as already described and evaporate to dryness in a radiator or over an asbestos gauze. Repeat the evaporation with $HClO_4$, cool, add 3 to 5 ml of dilute HCl (5:95), warm slightly, and transfer the solution and any residue to a beaker. Add 3 to 5 ml of $HClO_4$, again evaporate to dryness, cool, and take up the residue in 100 ml of dilute HCl (5:95). The solution at this point should be clear unless the original material contains much barium and sulphur. $BaSO_4$, if present, does not interfere. Transfer the solution to a 250 ml graduated flask, make up to volume, mix well, and pipette a 100-ml portion into a 400-ml beaker. Heat the solution nearly to boiling, add NH_4OH until methyl red just turns yellow, and then a solution of $H_2C_2O_4$ (10 g of $H_2C_2O_4.2H_2O$ per 100 ml of water) dropwise until the red color reappears. Now add 10 ml of the $H_2C_2O_4$ solution and 50 ml of a saturated solution (about 4 per cent) of $(NH_4)_2C_2O_4.H_2O$. Digest on the steam bath for one-half to one hour, cool to room temperature, filter through a platinum or asbestos pad in a perforated crucible, wash the beaker and precipitate a few times with cold water.[13] Return the crucible and precipitate to the beaker in which the precipitation was performed, add 100 ml of dilute H_2SO_4 (5:95), heat nearly to boiling, and titrate with 0.2 *N* $KMnO_4$. Multiply the number of ml required by 2.5 and then by the titer of the solution. (1 ml of 0.2*N* $KMnO_4$ = 0.00781 g of CaF_2.) To the result should be added 0.0050 g of calcium fluoride to correct for that dissolved during the treatment with acetic acid and the solution of potassium bromide and bromine.

This method should be used for routine analyses only. The results should be accurate to ± 0.5 per cent, although in most cases

[13] Filtration can be made through paper if desired. In this case, the washed precipitate should be sluiced into the beaker and the paper added just before the end point is obtained.

the accuracy is better than this, as is indicated in Table 1. By the routine method five of the cooperating analysts obtained an average of 94.8 per cent, with variations from 94.7 to 95.1.

TABLE 1.—*Results for CaF_2 obtained by the use of the recommended methods*

Material	CaF_2 indicated		
	Umpire method		Routine method
	Gravimetric, weighing as CaO	Volumetric, titration with $KMnO_4$	
	Per cent	*Per cent*	*Per cent*
1. B. S. fluorspar No. 79	94.96	94.91	94.81
2. Bethlehem Steel Co.s tandard "Q" (recommended value 85.25 per cent)	85.18	85.0	84.88
3. Pure CaF_2 to which was added $CaCO_3$, PbS, ZnS to make 6 per cent of each	99.94	----------	99.57

6. SULPHUR

Mix 1.000 g of the sample in a platinum crucible with 10 g of K_2CO_3 and 0.5 g of KNO_3, place the covered crucible in the muffle of an electric furnace, and heat until the mass is completely fused and the melt is quiet. An alcohol or petroleum ether flame may be used if an electric muffle is not available. When fusion is complete, gently rotate the crucible so that the cooling melt will solidify in a layer on the walls. Place the cooled melt in a beaker containing 150 ml of warm water, digest on the steam bath and stir occasionally.

When the melt is disintegrated, filter and wash the residue thoroughly with small portions of hot water. Acidify the filtrate with HCl and add 20 to 25 ml of HCl in excess. Evaporate to dryness, wash down the inside of the beaker, again add 20 to 25 ml of HCl, and evaporate to dryness. Dissolve the salts in 100 ml of dilute HCl (2:98), filter, wash with hot water, and add 5 ml of a 5 per cent solution of $BaCl_2 \cdot 2\ H_2O$ to the filtrate, which should have a volume of approximately 150 ml. Boil for 10 to 15 minutes, allow to stand for four hours or preferably overnight, filter, wash with hot water, ignite, and weigh as $BaSO_4$. A blank on the reagents should be carried through all steps of the method.

In analyses made by the authors an average value of 0.132 per cent as compared with the certificate value 0.14 was obtained for the Bureau of Standards standard fluorspar No. 79, and 0.28 per cent as compared with a recommended value of 0.27 per cent for a standard sample of fluorspar prepared by the chemists of the Bethlehem Steel Co.[14]

[14] Sample furnished by W. E. Steiner, chief chemist of the Bethlehem Steel Co., Cambria plant, Johnstown, Pa.

7. BARIUM

Transfer 5.00 g of sample to a platinum dish and digest on the steam bath for 10 minutes with 10 ml of HF. Then add 5 ml of HNO_3 and 25 ml of 60 to 70 per cent $HClO_4$ and evaporate to dryness. Again add 25 ml of $HClO_4$ and evaporate to dryness. Repeat the addition of $HClO_4$ and again evaporate. Take up the dry mass in 50 ml of dilute HCl (1:9) and heat to boiling. If a residue remains, filter, wash with warm water, ignite at as low a temperature as possible, and treat with 5 to 10 ml of HF and 5 to 10 drops of H_2SO_4. Expel the acids at a low temperature, fuse with about 1 g of Na_2CO_3, and extract the melt with water. Filter, wash the paper and residue with hot water, dissolve the residue in HCl, avoiding more than a few drops in excess, and add the clear solution to the main one. Dilute the combined solutions to 200 ml, heat nearly to boiling, and add dropwise and with stirring 4 ml of dilute H_2SO_4 (1:3). Boil for 15 minutes and digest on the steam bath for three to four hours. Do not allow the solution to cool below 40° to 50° C., because of the tendency of $CaSO_4$ to separate. If a precipitate forms, filter, wash with hot dilute HCl (1:99), and then with cold water. Ignite the precipitate and weigh as $BaSO_4$.

If lead is present in appreciable amount, the $BaSO_4$ may be contaminated by $PbSO_4$. To correct for this, add 5 ml of a 20 per cent solution of $NH_4C_2H_3O_2$ to the weighed precipitate, digest on the steam bath for 30 minutes, filter, and wash with hot water. Add a few drops of HCl to the filtrate, treat with H_2S, and if any PbS forms, remove it by filtration, cautiously ignite it at a dull red heat, treat with a few drops of HNO_3 and H_2SO_4, and again ignite at a dull red heat. Subtract the weight of $PbSO_4$ here found from that of the mixed sulphates and calculate the percentage of BaO or $BaSO_4$. A corresponding correction should also be made in the subsequent determination of lead.

8. LEAD

Pass H_2S for a few minutes into the filtrate obtained in the barium determination and then render the solution slightly ammoniacal. Continue the current of H_2S for 10 minutes and allow the solution to stand at the side of the steam bath for 30 minutes. Filter, wash a few times with NH_4Cl–$(NH_4)_2S$ solution, and discard the filtrate. Dissolve the precipitate in 25 ml of hot dilute HNO_3 (1:2), dilute the solution, and repeat the precipitation and washing in order to eliminate all calcium which might otherwise be precipitated with the lead. Dissolve the precipitate in HNO_3 as before, add 3 ml of H_2SO_4, and evaporate until dense fumes of the acid appear. Cool, dilute with water to 50 ml, and allow to stand for three hours or over night. Filter, wash a few times with cold dilute H_2SO_4 (1:20), ignite the precipitate very cautiously to dull redness (preferably in

a muffle or radiator), and weigh as $PbSO_4$. If the sulphate was caught on paper instead of asbestos, the ignited residue should be treated with HNO_3 and H_2SO_4 before the final ignition.

The filtrate from the $PbSO_4$ may contain a trace of lead. To recover this and to free the solution from platinum before zinc is determined, adjust the acidity by neutralizing with NH_4OH and then adding 2 ml of H_2SO_4 per 100 ml of solution. Treat with H_2S, and if a precipitate forms, filter, wash, and cautiously ignite the residue at a low temperature. Treat with a few drops of H_2SO_4 and HNO_3, again ignite at a very dull red heat, and weigh. Add 5 ml of a 20 per cent solution of $NH_4C_2H_3O_2$, allow to stand on the steam bath for 30 minutes, filter, ignite in the same crucible, and again weigh. The difference between the two weights represents $PbSO_4$ which should be added to that already obtained. This correction is usually so small that it need not be made except in very accurate work. The treatment with H_2S in acid solution, however, should be made to remove the trace of lead and the varying amounts of platinum which may be present. Otherwise these would subsequently contaminate the zinc.

9. ZINC

After having removed lead and platinum, boil the filtrate to remove H_2S, add methyl orange, carefully neutralize the solution, and then add enough H_2SO_4 to make the solution 0.01 *N*. If iron or aluminum are present in large amounts, they must be removed before the acidity is adjusted, for otherwise they will be precipitated in part. Pass a stream of H_2S through the cool solution for 30 minutes, allow to stand for one hour, filter on a paper of close texture, and wash with cold water. Ignite at a low temperature until the carbon of the paper is gone and then at a dull red. Weigh as ZnO.

10. OTHER CONSTITUENTS

The oxides of iron and aluminum may be determined by the usual procedures after fluorine has been volatilized by fuming with H_2SO_4 or $HClO_4$. Alkalies may be determined by the J. Lawrence Smith method.

III. ACKNOWLEDGMENT

The authors hereby wish to express their appreciation of the interest that was shown and the helpful suggestions that were made by the following chemists who cooperated in the analysis of the Bureau of Standards standard sample of fluorspar No. 79: S. B. Benzing, chief chemist, Lebanon Plant, Bethlehem Steel Co.; W. D. Brown, chief chemist, Duquesne works, Carnegie Steel Co.; H. E. Campbell, chief chemist, Clairton works, Carnegie Steel Co.; L. P. Chase, chief chemist, South works, Illinois Steel Co.; J. L. Harvey,

chief chemist, Homestead works, Carnegie Steel Co.; K. D. Jacob, associate chemist, Bureau of Chemistry and Soils, United States Department of Agriculture; F. G. Kelly, chief chemist, Tennessee Coal, Iron & Railroad Co.; W. F. Lantz, chief chemist, Bethlehem plant, Bethlehem Steel Co.; W. F. Muehlberg, chief chemist, Newburgh Steel Works; C. E. Nesbitt, chief chemist, Edgar Thomson works, Carnegie Steel Co.; N. M. Randall, chief chemist, Maryland plant, Bethlehem Steel Co.; W. E. Steiner, chief chemist, Cambria plant, Bethlehem Steel Co.; George P. Vanier, chief chemist, Steelton plant, Bethlehem Steel Co.; and Frederick Wynkoop, Booth, Garrett & Blair.

WASHINGTON, November 6, 1928.

AN INTERFERENCE METHOD FOR THE DETERMINATION OF AXIAL AND OBLIQUE ABERRATIONS

By A. H. Bennett

ABSTRACT

An interference method for the determination of the axial and oblique monochromatic aberrations of a lens system is described. Equations necessary in the design of the apparatus, and for the computation of the results are given. The simplicity of the apparatus, especially the use of but one auxiliary reflecting surface, lessens the probability of large instrumental errors. The aberrations of three astronomical objectives are investigated, and the results are expressed in the form of phase contours.

CONTENTS

	Page
I. Introduction	685
II. Description of method	687
1. Theory	687
2. Apparatus	688
3. Experimental procedure	691
(*a*) Adjustment of apparatus	691
(*b*) Making the exposures	691
(*c*) Measurement of the plates	692
(*d*) Computation of results	692
(*e*) Method of expressing results	694
III. Results	695
1. Objective of 155 mm diameter and 1,800 mm focal length	695
2. Objective of 145 mm diameter and 2,900 mm focal length	697
3. Objective of 300 mm diameter and 3,940 mm focal length	699
IV. Summary and conclusions	701

I. INTRODUCTION

In a paper on a modification of the Hartmann [1] test, based on interference, Gardner and Bennett [2] have described a method for the determination of the spherical aberration of a lens system. The following brief review of its essential characteristics is given, since the method described in this paper is a development along similar lines of procedure.

If the small apertures used in isolating the rays in the Hartmann method are correctly spaced and of suitable diameter, interference

[1] Hartmann, Zeits. f. Instrumentenk., **24**, p. 1; 1904.

[2] I. C. Gardner and A. H. Bennett, J. Opt. Soc. Am. and Rev. Sci. Inst., **11**, pp. 441–452; 1925. Also Trans. by H. Kessler, Zeits. f. Instrumentenk., **47**, pp. 197–204; 1927, and Geiger and Scheel's Handb. d. Phys., **18**, pp. 810–811.

28486°—29——1

fringes are formed between adjacent extra-focal images of these apertures. Advantage is taken of the displacement of the fringes caused by differential aberration between adjacent apertures. By adding these differential aberrations, determined by a measurement of the displacement of the fringes, the total phase aberration is found. This method combines many of the desirable features of several prior methods. It requires no more elaborate apparatus than that used in the original Hartmann method. High precision is obtainable because the measurements are made on narrow interference fringes rather than on the conventional extra and infra focal shadowgraph disks, which are always of larger diameter than is desirable. In this respect the method is similar to that devised by Merland.[3] As in the interference methods of Twyman,[4] Waetzman and Bratke,[5] Michelson,[6] and Cotton,[7] the magnitudes of the aberrations are expressed as phase differences rather than as geometrical aberrations.

In the present paper the Gardner-Bennett method outlined above has been extended to apply to a wave front proceeding from an object point, either on the axis or at some distance from the center of the field. Measurements can be made along any desired number of meridians, and the aberration can be determined at a sufficient number of points to enable a contour map to be drawn showing the form of the entire wave surface which emerges from the lens. These contours are similar in many respects to the Twyman[8] interferograms.

The applications of the method herein described have been restricted to the measurement of the monochromatic aberrations of telescope objectives. In view of the small magnitudes of the aberrations present in a well-designed and constructed astronomical telescope objective, the application of the method to such a lens should serve to demonstrate the suitability of the procedure when applied to microscope or photographic objectives or other types of lenses. A further reason for selecting telescope objectives was the need of information concerning the amounts of axial and oblique aberration of three astronomical objectives of 5½ to 12 inches diameter and having focal lengths from 6 to 12 feet, which are a part of the laboratory equipment of the optical instrument section of the Bureau of Standards. The results of the measurements described in this paper are of interest beyond their indications concerning the adaptability of the objectives to their special purposes because they also show particular effects arising from certain characteristics of design, materials, and construction.

---

[3] A. Merland, Rev. d'Opt., **3**, pp. 401–413; 1924.
[4] F. Twyman, Phil. Mag. (6), **35**, p. 49; 1918.
[5] Bratke and Waetzman, Ann. d Phys., 72, **7**, pp. 501–515; 1923.
[6] A. Michelson, Astrophys. J., **47**, pp. 283–288; 1918.
[7] A. Cotton, Physics, **1**, pp. 274–283; 1921.
[8] See footnote 4.

II. DESCRIPTION OF METHOD

1. THEORY

If a series of equidistant slits of equal width are placed within or beyond the focal point of a lens, the relation between slit width and distances between centers can be made such that the separation of the geometric bundles of rays at some position along their course will permit the first diffraction bands from any pair of adjacent slits to overlap. Over the region of overlapping a group of sharp fringes[9] is visible provided the source of light is of small dimensions. It was shown in the previously mentioned paper that when the grating is placed within the focus the position of the central fringe in each group is dependent on the shape of the portion of the emergent wave front included between the two corresponding adjacent slits. That the same condition obtains when the series of slits is placed beyond the focal point can be shown in a similar manner, as follows:

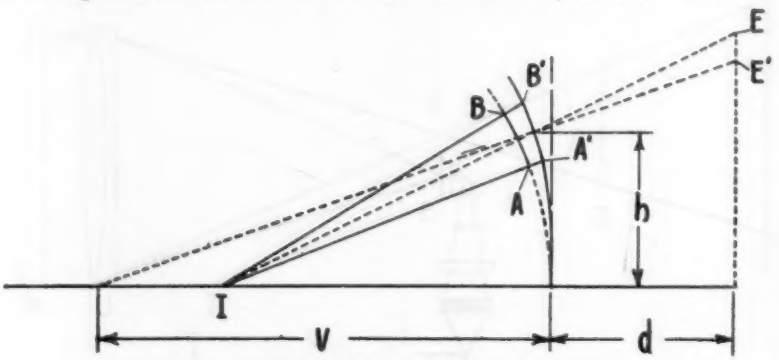

FIG. 1.—*Sketch illustrating theory of method*

In Figure 1 let I be the focus through which the waves are assumed to pass, proceeding from left to right, before they are transmitted by the diaphragm. A and B are the portions of a spherical wave front, with its center at I, which are transmitted through two adjacent apertures. A' and B' represent the corresponding portions of the actual wave front distorted by the presence of aberrations. The problem at hand is to find the difference in phase between the distorted and ideal wave fronts in passing through I, the selected focus. In the case illustrated the marginal portions at A' or B' have been accelerated with respect to the axial portion which is tangent to the ideal spherical wave front. The phase acceleration on arrival at I is measured by the radial distance between the two wave fronts. Portions of the spherical wave front passing through the two adjacent apertures would interfere and form a central fringe at E on the radius passing midway between A and B. The actual

[9] R. W. Wood, Physical Optics, p. 190.

fringes are formed between adjacent extra-focal images of these apertures. Advantage is taken of the displacement of the fringes caused by differential aberration between adjacent apertures. By adding these differential aberrations, determined by a measurement of the displacement of the fringes, the total phase aberration is found. This method combines many of the desirable features of several prior methods. It requires no more elaborate apparatus than that used in the original Hartmann method. High precision is obtainable because the measurements are made on narrow interference fringes rather than on the conventional extra and infra focal shadowgraph disks, which are always of larger diameter than is desirable. In this respect the method is similar to that devised by Merland.[3] As in the interference methods of Twyman,[4] Waetzman and Bratke,[5] Michelson,[6] and Cotton,[7] the magnitudes of the aberrations are expressed as phase differences rather than as geometrical aberrations.

In the present paper the Gardner-Bennett method outlined above has been extended to apply to a wave front proceeding from an object point, either on the axis or at some distance from the center of the field. Measurements can be made along any desired number of meridians, and the aberration can be determined at a sufficient number of points to enable a contour map to be drawn showing the form of the entire wave surface which emerges from the lens. These contours are similar in many respects to the Twyman[8] interferograms.

The applications of the method herein described have been restricted to the measurement of the monochromatic aberrations of telescope objectives. In view of the small magnitudes of the aberrations present in a well-designed and constructed astronomical telescope objective, the application of the method to such a lens should serve to demonstrate the suitability of the procedure when applied to microscope or photographic objectives or other types of lenses. A further reason for selecting telescope objectives was the need of information concerning the amounts of axial and oblique aberration of three astronomical objectives of 5½ to 12 inches diameter and having focal lengths from 6 to 12 feet, which are a part of the laboratory equipment of the optical instrument section of the Bureau of Standards. The results of the measurements described in this paper are of interest beyond their indications concerning the adaptability of the objectives to their special purposes because they also show particular effects arising from certain characteristics of design, materials, and construction.

---

[3] A. Merland, Rev. d'Opt., **3**, pp. 401–413; 1924.
[4] F. Twyman, Phil. Mag. (6), **35**, p. 49; 1918.
[5] Bratke and Waetzman, Ann. d Phys., 72, **7**, pp. 501–515; 1923.
[6] A. Michelson, Astrophys. J., **47**, pp. 283–288; 1918.
[7] A. Cotton, Physica, **1**, pp. 274–283; 1921.
[8] See footnote 4.

II. DESCRIPTION OF METHOD

1. THEORY

If a series of equidistant slits of equal width are placed within or beyond the focal point of a lens, the relation between slit width and distances between centers can be made such that the separation of the geometric bundles of rays at some position along their course will permit the first diffraction bands from any pair of adjacent slits to overlap. Over the region of overlapping a group of sharp fringes[9] is visible provided the source of light is of small dimensions. It was shown in the previously mentioned paper that when the grating is placed within the focus the position of the central fringe in each group is dependent on the shape of the portion of the emergent wave front included between the two corresponding adjacent slits. That the same condition obtains when the series of slits is placed beyond the focal point can be shown in a similar manner, as follows:

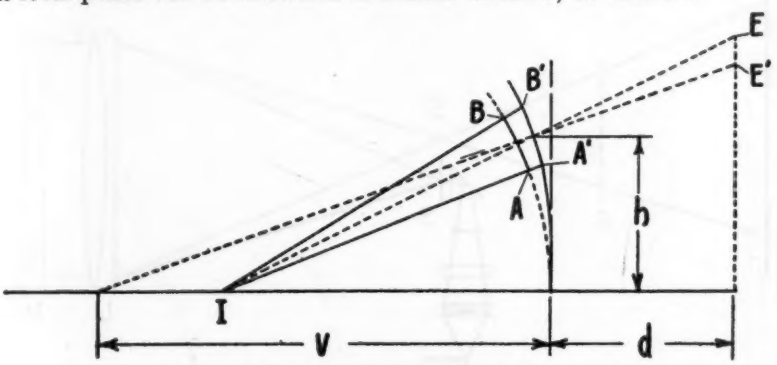

FIG. 1.—*Sketch illustrating theory of method*

In Figure 1 let I be the focus through which the waves are assumed to pass, proceeding from left to right, before they are transmitted by the diaphragm. A and B are the portions of a spherical wave front, with its center at I, which are transmitted through two adjacent apertures. A' and B' represent the corresponding portions of the actual wave front distorted by the presence of aberrations. The problem at hand is to find the difference in phase between the distorted and ideal wave fronts in passing through I, the selected focus. In the case illustrated the marginal portions at A' or B' have been accelerated with respect to the axial portion which is tangent to the ideal spherical wave front. The phase acceleration on arrival at I is measured by the radial distance between the two wave fronts. Portions of the spherical wave front passing through the two adjacent apertures would interfere and form a central fringe at E on the radius passing midway between A and B. The actual

[9] R. W. Wood, Physical Optics, p. 190.

distorted wave front likewise forms a central fringe at E', which is on the perpendicular bisector of the chord $A'\,B'$. The phase difference for points A' and B' on the actual wave front on arrival at I is

$$\frac{A\,A'-B\,B'}{\lambda}$$

Using w to represent the distance between two adjacent fringes in a group on the plane at $E\,E'$, the quantity $\frac{E\,E'}{w}$ is likewise the phase difference at the focus I in wave lengths between the portions of the wave transmitted by the two adjacent apertures.
Hence

$$\frac{A\,A'-B\,B'}{\lambda}=\frac{E\,E'}{w} \tag{1}$$

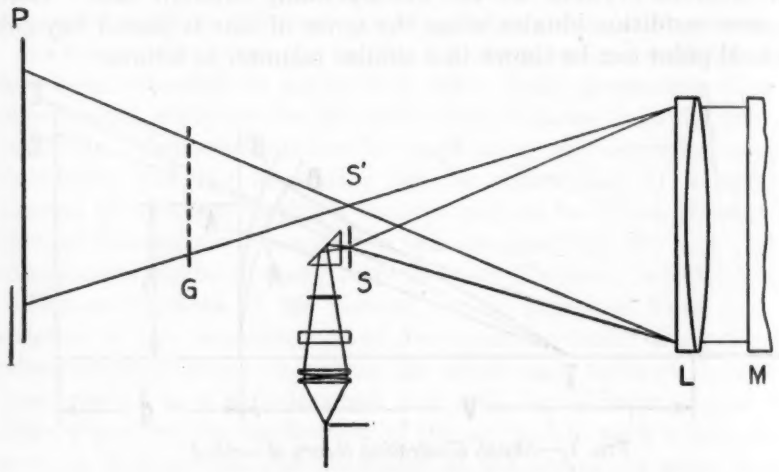

FIG. 2.—*Diagram of apparatus*

The phase difference between an axial point on the wave front and a point at any height can be found by adding the consecutive values of $\frac{E\,E'}{w}$ for each pair of apertures.

2. APPARATUS

A diagram (not to scale) of the apparatus is shown in Figure 2. Light from a carbon arc, after passing through a water cell and a Wratten No. 73 "monochromatic" filter having its maximum transmission at about 580 mμ, is focused through a total reflecting prism on the small hole S, of which the diameter is approximately 0.1 mm. This artificial star is placed about 2 mm to one side of the axis of the telescope objective L, under test. The mirror M is a front silvered glass flat, whose diameter should be as large as that of the lens. After reflection at M the light is focused at S'. For the determination of the axial aberration the entire system was aligned on a very

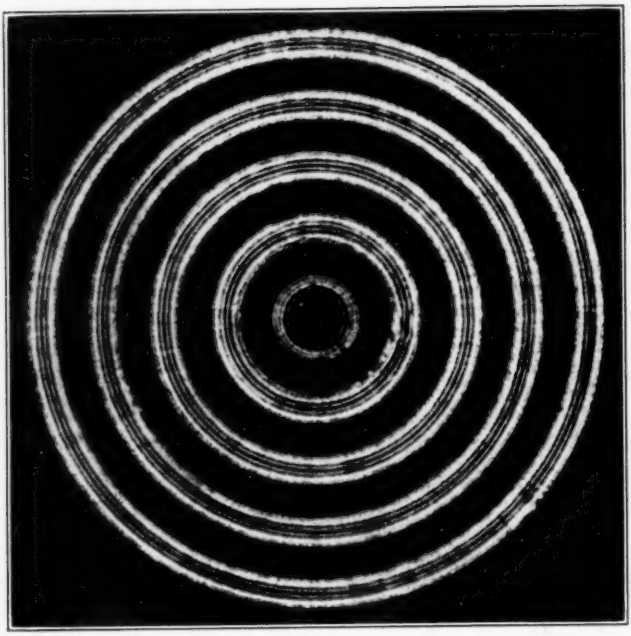

FIG. 4.—*Interference fringes*

This illustration is an enlarged negative of only the central portion of an entire fringe system.

rigid optical bench so that the "point" source S and its image S' were symmetrically placed with respect to the axis of the lens. For the oblique measurements the source S was kept in the position indicated, and the mirror M was tilted to throw the image S' at the desired oblique position off the axis.

At G is a circular grating, a reproduction of which is shown approximately full size in Figure 3. This grating consists of equispaced, concentric slits in a silver film chemically deposited on glass. The distance between the centers of slits was 1.33 mm, and the slits were 0.30 mm wide. These dimensions were selected in accordance with the relationships expressed in the equations of the next paragraph. The surfaces of the glass plate were flat to about 0.1 λ and parallel to about 1.5 seconds although, as will be shown later, compensation was made for the errors introduced by the glass plate. The fringes formed by the interference of light from consecutive slits are recorded on the photographic plate at P (fig. 2). Several of these fringes are illustrated in Figure 4, which is a negative. In order to avoid fogging the plate by scattered light, the entire apparatus, with the exception of the arc lamp, water cell, and filter, was inclosed.

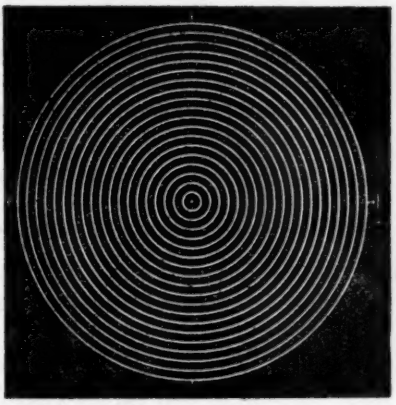

FIG. 3.—*Circular grating (full size)*

In the design of the diaphragm for use with this method the correct dimensions must be found if satisfactory fringes are to be obtained on the photographic plate. The fringe system is formed at the overlapping of the first diffraction bands from each pair of adjacent slits. The angle subtended at the diaphragm by the first diffraction band is λ/s, where s is the slit width. At the diaphragm the angular subtense of consecutive minima in the interference system is λ/e, where e is the distance between centers of the slits. Then, if each interference group is to consist of n fringes

$$e = ns \tag{2}$$

In making the measurements of the fringes there should be at least three fringes in a group, since it is necessary to determine the distance between consecutive fringes. It has been found, however, that it is necessary to measure only a few of these values, since they remain practically constant over the photographic plate, provided proper care is used in obtaining uniform spacing of the concentric slits on the diaphragm. In equation (2) it is well to set $n = 5$ if three fringes are to be used because of the low intensity of the extreme fringes.

The distance between adjacent fringes is

$$w=\frac{\lambda}{e}d \tag{3}$$

where d is the distance from diaphragm to photographic plate. For overlapping of the first diffraction bands the distance between geometric, extra-focal images must be

$$e'=\frac{3\lambda d}{s}=3wn \tag{4}$$

The distance between diaphragm and intersection of the ray with the axis is

$$V=\frac{ad}{b-a} \tag{5}$$

where a is the distance between the axis and the slit in the diaphragm, and b is the corresponding distance on the photographic plate. If F is the ratio of focal length to aperture of the lens under test and m is the number of central fringes corresponding to the semiaperture, then

$$V=2Fme \tag{6}$$

By combining the above equations (2) to (6) it is found that:

$$e=\frac{6Fmn\lambda w}{w+2Fm\lambda} \tag{7}$$

$$d=\frac{6Fmnw^2}{w+2Fm\lambda} \tag{8}$$

$$b=me' \tag{9}$$

and

$$V=\frac{12F^2m^2n\,\lambda\,w}{w+2Fm\lambda} \tag{10}$$

In designing the apparatus, desired values are assigned to w, the fringe width; s, the slit width; n, the number of fringes in a group; and m, the number of central fringes corresponding to the semiaperture.[10] Then, substituting these values in equations (7), (8), and (10), respectively, e, the distance between centers of slits; d, the distance from focal point to diaphragm; and V, the distance from diaphragm to photographic plate, are computed. The necessary size of the photographic plate is found from equation (9).

Some difficulty was experienced at first in accurately ruling the concentric slits in the silvered surface of the diaphragm (fig. 3). The

[10] As will be shown, this number, m, is the number of points on the graph of phase difference plotted against semiaperture.

final method of construction was as follows: The silvered disk of glass was mounted horizontally on the table of a spectrometer with the silvered surface uppermost. The silvered surface was adjusted normal to the axis of rotation of the conical bearing supporting the table. In order to accomplish this adjustment, an autocollimating telescope was mounted vertically above the surface, and the leveling screws on the spectrometer table were adjusted until the autocollimated image of the reticule of the telescope remained stationary when the table bearing the disk was rotated. After removal of the telescope a micrometer screw, to which was attached a finely pointed German silver stylus, was mounted in a horizontal position above the silvered surface. The correct movement of the stylus was determined by means of the micrometer head, which could be read to 0.001 mm. It was necessary to make a preliminary determination of the width of the cut produced by the stylus, after which, during the process of cutting, it was possible by means of the micrometer screw to move the stylus horizontally by the correct amount to engrave slits of the desired width, having the predetermined distance between centers.

3. EXPERIMENTAL PROCEDURE

(*a*) ADJUSTMENT OF APPARATUS.—As shown in Figure 2, autocollimation was used in the measurements of the phase errors. The axial aberration was first determined by having the source and its image practically on the axis. In measuring the oblique aberration, since the source was kept on the axis, it was necessary to subtract the axial aberration from the measured quantity which consisted of the sum of the true oblique and axial aberrations. Hence, it was necessary to align the apparatus accurately on an optical bench. The location of the axis of the lens under test (fig. 2) was determined by the use of the principle that, if a luminous object is placed on the axis, the object and its images formed by reflection from the surfaces of the lens all lie in a straight line. After the axis was located the mirror M (fig. 2) was adjusted by tilting until its reflecting surface was normal to the axis. With the autocollimating mirror normal to the axis, the object and image become symmetrically placed with respect to the axis. The artificial star S (fig. 2) was adjusted laterally and longitudinally until it was about 4 mm from its image S' in a plane approximately normal to the axis. The diaphragm containing the circular slits and the plate-holding device were constructed as a camera unit. By means of proper adjustment of this camera for height and leveling the diaphragm is made concentric with the cone of rays emerging from the star image. When this condition obtains, the extra-focal images are complete circles.

(*b*) MAKING THE EXPOSURES.—In order to avoid errors arising from tilt of the photographic plate, and from spherical aberration of

the plane parallel plate upon which the concentric slits are ruled, or from irregularities of surfaces and index of refraction of this plate, two photographs were made for each determination of aberration. The first exposure was made with the apparatus adjusted as has just been described. A second exposure was made on another plate with the star image S' replaced by a small aperture about 0.1 mm in diameter. This artificial star was placed in the position previously occupied by the image with the aid of an auxiliary microscope provided with a right-angled objective prism. The same illuminating system was utilized to illuminate this comparison star as was used for the star S (fig. 2). The set of fringes obtained with the pinhole directly represents the ideal condition, since the emerging wave fronts are spherical. The fringes on the first plate are found to be displaced relatively to those on the second. These relative displacements arise principally from the aberration of the test lens. It is necessary, however, to eliminate similar effects resulting from the difference in position of star image and pinhole and the errors of the autocollimating reflecting surface. The method of eliminating these errors is treated later in (*d*) Computation of results.

(*c*) Measurement of the Plates.—In measuring the fringes the object is to determine the distance from the center of the system to the consecutive fringes. It is difficult to have the exact center registered on the photograph. On the first trial a small aperture was placed at the center of the slit system in the diaphragm, but this produced an unsatisfactory center on the photographic plate because of overexposure and halation, as very long exposures are required to show the fainter fringes. The method finally adopted was as follows: A very small hole was made in the emulsion near the center of the finished plate. The positions of the central fringes in each group were measured with respect to this arbitrary point. The average of the readings along each of six diameters was found, and the differences between the average readings and the readings for the arbitrary point were plotted against the azimuths of the diameters. From the maximum displacement along the resulting sine curve and the corresponding azimuth it was possible to locate the true center of the fringe system with reference to the arbitrary center and make proper correction to the readings for the location of the fringes.

(*d*) Computation of Results.—Let the distances from the axis to the fringes on the plate exposed with the test lens in position be a_1, a_2, a_3 . . . . . , and let c_1, c_2, c_3, ... represent the corresponding distances on the plate taken with light emerging directly from the comparison star. Then, a_1-c_1, a_2-c_2 . . . . . represent the displacements arising from aberration and, in addition, errors of the reflecting surface and errors of adjustment of the source of the

reference wave front. If w is the distance between two adjacent fringes,

$$\frac{a_1-c_1}{w},\ \frac{a_2-c_2}{w},\ \ldots\ .\ \frac{a_n-c_n}{w}$$

are the differences in phase between points on the actual wave front corresponding to the respective adjacent apertures in the diaphragm.

Hence, $\sum_1^n \frac{a_n-c_n}{w}=$ the difference in phase, at the nth aperture, between the wave front emerging from the test lens and the spherical reference wave front emerging from the pinhole. As has been pointed out, the reference wave front may have its center displaced laterally or longitudinally from the position of best focus; that is, position of smallest phase residuals, although the error is small by reason of the method used in setting the pinhole to occupy the position of the image. Any error in placing the pinhole may give rise to a tilting and a change in center of the reference wave front. Hence, in computing the results it will generally be necessary to refer the actual wave front to several reference wave fronts having their centers at various positions along the axis (for axial measurements) or the chief ray (for oblique measurements) by which means the effects of a change of focus on the phase residuals are determined. In addition, the reference wave front is tilted until greatest symmetry of phase residuals appears over the entire wave front under investigation. These corrections are made empirically in the following manner.

If $y_1, y_2 \ldots\ldots y_n$ represent the distances from the center of the diaphragm to the respective concentric slits, the effect of a tilt of the reference wave front on the phase difference for different apertures can be expressed as

$$\eta_t = K\ y_1 \sin\psi,\ K\ y_2 \sin\psi,\ \ldots\ldots\ldots \text{ etc.} \qquad (11)$$

where K is a constant for all zones of the wave front; that is, all values of y, and ψ is the azimuth of the meridian of the wave front measured from the axis of tilt. The value of K, which is the angle of tilt, and the azimuth of the axis of tilt which furnish the most symmetrical distribution of the phase residuals about the axis are found empirically.

The effect of a change in curvature of the reference wave front on the phase residuals for any aperture is expressed by

$$\eta_t = C\ y_1^2,\ C\ y_2^2,\ \ldots\ldots\ldots \text{ etc.} \qquad (12)$$

where C is a constant for all values of y and is made of such value as to reduce the total phase residuals of the lens to a minimum. The

phase residuals between the actual and ideal wave fronts can now be written [11]

$$\eta = \sum_{1}^{n} \frac{a_n - c_n}{w} + K \sin \psi \; y_n + C \; y_n^2 \tag{13}$$

where a is the distance from center to fringes on the plate taken with actual wave front, c the corresponding distance on plate taken with the reference wave front, y the distance from center to slit in diaphragm, and K and C the constants of equations (11) and (12).

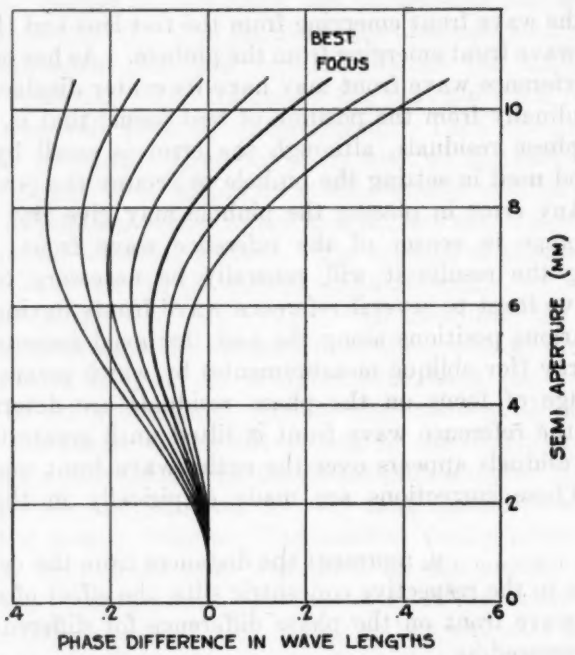

FIG. 5.—*Graphs showing variation in phase differences with change of focus*

In computing the graph marked "best focus" the value of C (equation (13)), which gives smallest phase differences, was used

(*e*) METHOD OF EXPRESSING RESULTS.—The values of η, the phase differences, are plotted against corresponding values of y, the semiapertures of the diaphragm. The latter are closely proportional to the corresponding semiapertures of the objective under test. Figure 5 illustrates a family of such graphs for a single meridian of the wave front. Here various values of the constant C, equation (13), have been applied in order that the phase difference at the best focus can be determined. Such graphs are obtained for each meridian

[11] In equation (13) it should be noted that, by the use of autocollimation, the actual wave front has twice the aberration produced by the lens as it is ordinarily used with incident light in the case of axial imagery. For oblique imagery the axial aberration is also included in the expression for η, the phase difference.

of the wave front measured. From these a set of contours, showing lines of equal phase difference over the entire wave surface can be easily drawn. In most of the examples given meridians at intervals of 30° were measured. As a rule, meridians 30° apart will be sufficient to enable one to gain information concerning the entire wave front, although in cases of irregularity of surfaces of the test lens or lack of homogeneity of the glass it may be desirable to select meridians at smaller intervals.

III. RESULTS

The monochromatic aberrations of three telescope objectives were investigated by the method described. Phase contours,[12] represent-

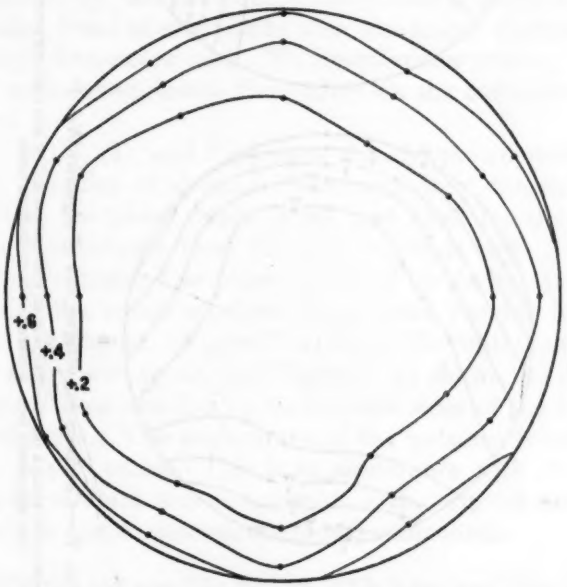

FIG. 6.—*Phase contours for best axial focus of objective No. 1*

ing the axial and oblique aberrations, were drawn. In all cases the center of the map is taken as the position of zero phase difference, and the numerical values of the contours are indicative of the phase difference expressed in wave lengths ($\lambda = 580$ mμ).

1. OBJECTIVE OF 155 mm DIAMETER AND 1,800 mm FOCAL LENGTH (NO. 1)

The contours of Figure 6 show the axial aberration at the best axial focus. The contours are drawn at intervals of 0.2λ. This lens shows a departure of 0.6λ at the edge. However, if the lens is

[12] The characteristic forms of phase contours corresponding to the various geometrical aberrations have been discussed by F. Twyman, Trans. Opt. Soc., London, **22**, pp. 182–185; 1920–21; and also by G. C. Steward, Camb. Phil. Soc. Proc., **24**, pp. 166–170; January, 1928.

FIG. 7.—*Contours for oblique foci of objective No. 1*

These contours represent conditions at three successive foci along a bundle of rays at an obliquity of 2.5°, a and c are contours corresponding to positions near the two astigmatic foci. *b* corresponds to the best focus

stopped to about two-thirds of its diameter the Rayleigh tolerance of 0.25λ is not exceeded. The small irregularities in the contours are probably the effects of lack of homogeneity of the glass or errors arising from slight deformation of surfaces. In the apparatus as previously described for testing this lens the mirror M (fig. 2) was tested for flatness by the interferometry section of the Bureau of Standards. The surface was found to be slightly spherical with a sagitta of about 0.1λ. The sphericity of this optical flat does not enter as a correction factor in the results because it simply necessitates a slight amount of refocusing, which is the equivalent of changing the factor C in equation (13). The extremely small aberration produced by this reflecting surface itself is neglected, since it is of a smaller order of magnitude than the actual aberration of the telescope objective under test. No irregularities greater than 0.01λ in the flat were found, hence their effect on the contours could also be neglected.

Figures 7 (*a*), 7 (*b*), and 7 (*c*) show the oblique aberration of this lens for an obliquity of about 2.5° to one side of the axis. Figure 7 (*b*) indicates the phase errors at the best focus for this obliquity. At this angular distance from the axis, which is large for a lens of this type, the definition is seriously impaired by the presence of astigmatism and coma which produce phase errors ranging from +5 to −5 whole wave lengths. Figure 7 (*a*) shows the contours corresponding to one astigmatic focus, and Figure 7 (*c*) shows the other astigmatic focus. These two foci lie on opposite sides of the most nearly symmetrical focus. The asymmetry of the patterns is indicative of a large amount of coma. This is in accordance with the fact that the correction of coma was not sought in the original design of the objective which has an equiconvex crown component.

2. OBJECTIVE OF 145 mm DIAMETER AND 2,900 mm FOCAL LENGTH (NO. 2)

The axial aberration of the above lens is shown in Figure 8. In general, the aberration of the best axial focus does not exceed +0.2 λ, but there are small regions in the lens in which the error reaches a value of −0.2 λ, as shown in the left side of the figure. A consideration of the graphs of phase difference plotted against semiapertures which were made preliminary to the contours showed that these two areas of negative phase difference are not joined. It is believed that these regions represent an actual variation on optical path arising from irregularity of surface or heterogeniety of the glass or, perhaps, a combination of the two.

The oblique aberration at an angular distance of 10 minutes from the axis and at the best oblique focus is shown in Figure 9. The aberration varies from +0.2 λ (over a small portion of the figure)

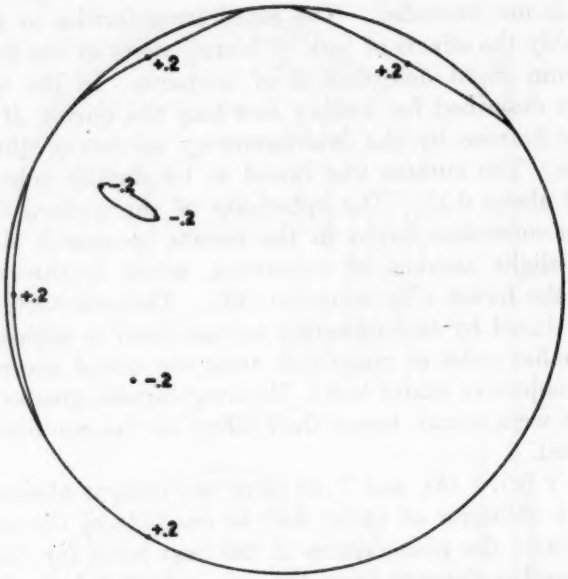

FIG. 8.—*Phase contours for best axial focus of objective No. 2*

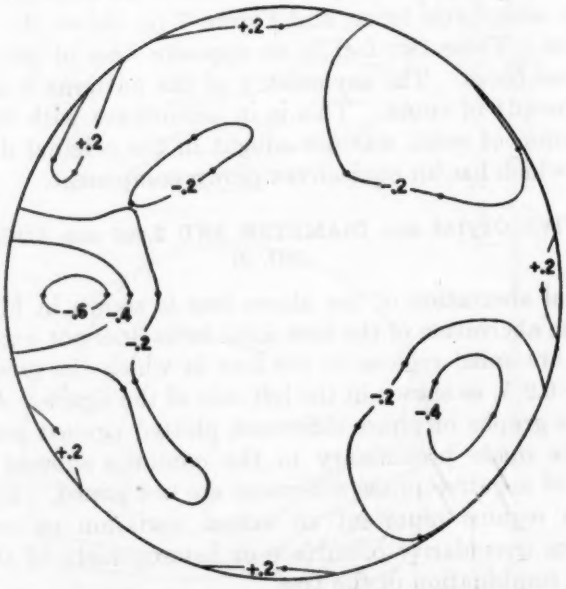

FIG. 9.—*Phase contours for best oblique focus of objective No. 2. (Obliquity 10′)*

to $-0.6\ \lambda$. At this angle the contours show an asymmetry which indicates a radial flare in the image, since the lens is considered to be tilted about a vertical axis. With this objective the same flat was used as with the one previously discussed, and likewise it was not necessary to correct the results for errors introduced by the flat.

3. OBJECTIVE OF 300 mm DIAMETER AND 3,940 mm FOCAL LENGTH (NO. 3)

This objective is an achromatic doublet, corrected for spherical aberration and coma. Although the largest flat available was used for autocollimation, unfortunately it was not of sufficient size to cover the entire aperture of the objective. The aperture covered by the flat was 258 mm in diameter, and the contours of this lens represent conditions over this aperture. The flat was found to be convex but did not sufficiently approach a true sphere, so that the departures from sphericity could be neglected. The flat was measured by the interferometry section of the Bureau of Standards, and the departures from flatness were found to be expressible by the equation

$$y = -719.7\times10^{-7}\,x^2 + 2.239\times10^{-9}\,x^4 - 2.809\times10^{-13}\,x^6 \qquad (14)$$

where y is the departure from flatness expressed in half-wave lengths ($\lambda = 0.5876\mu$), and x is the distance from the center of the flat in millimeters. The flat impresses twice its sagitta on the wave front after reflection; hence, the error in phase arising from the flat is

$$\eta_{\text{flat}} = -719.7\times10^{-7}\,x^2 + 2.239\times10^{-9}\,x^4 - 2.809\times10^{-13}\,x^6 \qquad (15)$$

where η_{flat} is expressed in whole wave lengths. For the axial measurements, η in equation (13) represents twice the phase aberration of the lens combined with the aberration of the flat, η_{flat}, and the latter is used as a correcting value. In making the oblique measurements, η, equation (13), is a combination of the axial aberration, the aberration produced by the flat, and the oblique aberration. Since the first two aberrations are known, the latter is found simply by subtraction.

A point of interest in connection with the lens is that, in testing the lens visually during its construction, the autocollimated image of an artificial star was examined by racking the eyepiece in and out of the focus. Presumably the same flat was used during these constructional tests as was used in the present investigation, and it is found that this objective contains errors which are neutralized to a certain extent by the errors of the flat. This is illustrated by Figures 10(*a*) and 10(*b*). Figure 10(*a*) shows the axial aberration at the best focus of the lens when the flat is considered perfect; while, if correction is made for the errors of the flat and the best focus again found, the contours of Figure 10(*b*) are obtained, indicating an

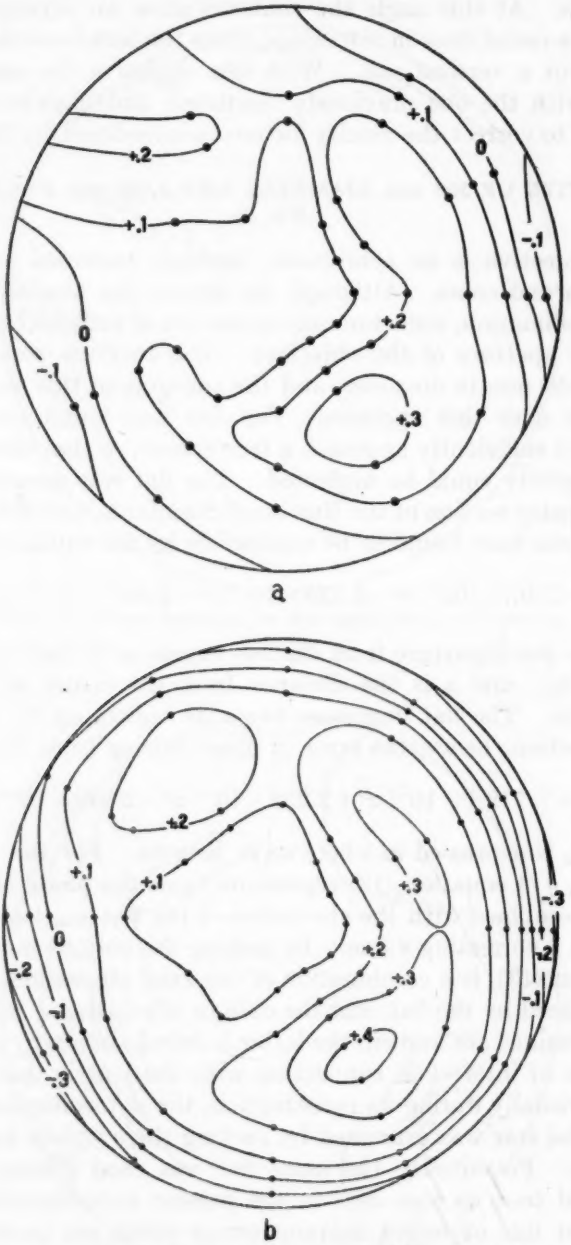

FIG. 10.—*Phase contours for best axial focus of objective No. 3*

a, Combined errors of lens and flat. b, Errors of lens only, with correction made for errors introduced by flat. This illustration indicates that the errors of lens and flat tend to neutralize each other

increase of positive phase aberration (overcorrection) near the center and at the edge an increase of the negative aberration (undercorrection). This indicates the importance of using accurate flats in testing lenses during the process of construction.

The diagram (fig. 10(*b*)), also shows the presence of a number of irregularities, from which it is to be concluded that an improvement in the performance of this objective could be effected by local and zonal retouching of the surface.

The best oblique focus, at an angular distance of 1° from the axis, is represented by Figure 11. The asymmetry from top to bottom of the figure is radial from the axis of the lens and represents a small amount of residual coma.

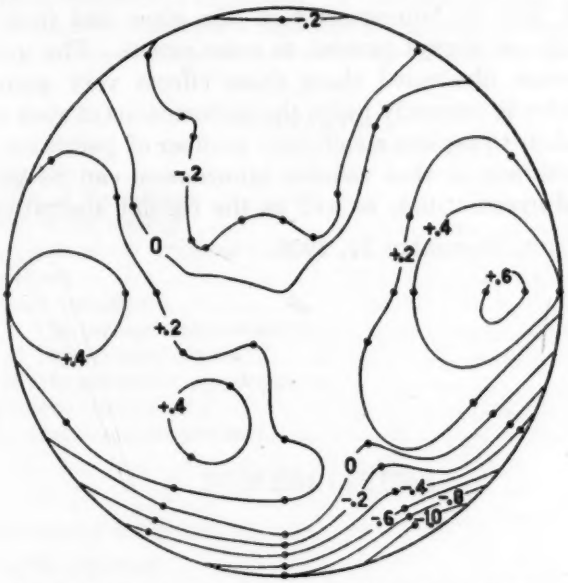

FIG. 11.—*Phase contours for best oblique focus of objective No. 3. (Obliquity 1°)*

IV. SUMMARY AND CONCLUSIONS

A method for measuring the axial and oblique aberrations of a lens system is described. This method, which is based on interference, determines the aberrations directly in terms of the difference of phase between the various positions of the emergent wave front in passing through any point on the axis or chief ray. By a simple computation such a point may be selected which will produce minimum phase residuals, representing the point of best imagery. The expression of the aberrations directly in terms of phase differences enables one to compare them with the Rayleigh tolerance.

The method requires only simple apparatus, but its accuracy is of the order of the geometric method of Hartmann.

Examples of the application of the method to the measurement of the monochromatic aberrations of three telescope objectives are presented. These examples show the performance of the lens as compared with the Rayleigh tolerance. The characteristic effects of the axial aberration; that is, spherical aberration; and also of the oblique aberrations, coma, and astigmatism; on the emergent wave front are illustrated.

The procedure is an accurate method, utilizing simple apparatus, for the determination of the small amounts of aberration present in astronomical objectives. It should be pointed out that even in a well-designed astronomical objective the "technical" aberrations, arising from lack of homogeneity of the glass and from errors in workmanship, are always present to some extent. The irregularities of the contours illustrated show these effects very pronouncedly. Hence, in order to correctly judge the performance of such a lens care should be taken to explore a sufficient number of points on the emergent wave surface so that reliable information can be gained concerning local irregularities, as well as the regular aberrations.

WASHINGTON, November 21, 1928.

DETERMINATION OF MOLECULAR WEIGHTS IN THE VAPOR STATE FROM VAPOR PRESSURE AND EVAPORATION DATA

By Edward W. Washburn

ABSTRACT

If one determines at the same temperature the vapor pressure of a substance and the amount of it required to saturate, by aspiration, a measured volume of an indifferent gas, the molecular weight of the substance in the gaseous state is calculable. By employing a reference substance of known molecular weight the measurement of the volume of aspirated gas is unnecessary and the quantities measured have small temperature coefficients. A precision discussion of the method is given. It should be capable of a high degree of accuracy in many cases and is applicable at much lower temperatures than are the methods commonly employed.

CONTENTS

	Page
I. Nomenclature	703
II. Principle of the method	703
III. History of the method	704
IV. Description of the reference method	705
V. Derivations	707
VI. Precision discussion	708
1. The pressure measurements	708
2. Temperature control	709
3. The saturation measurements	710
VII. Illustrative example	711
VIII. Effect of atmospheric pressure	713

I. NOMENCLATURE

M, Molecular weight.
p, Vapor pressure.
B, Barometric pressure.
ΔP, Manometric pressure difference.
m, Mass in grams.
v, Volume.
R, Gas constant.
T, Temperature, ° K.
t, Temperature, ° C.
$\delta_x M$, Variation in M caused by a variation δx in any variable x.

II. PRINCIPLE OF THE METHOD

None of the methods commonly employed for determining the molecular weights of substances in the vapor state are applicable at temperatures at which the vapor pressure of the substance is small.

A method which is based upon determining, at the same temperature, the vapor pressure of the substance and the amount of it required to saturate, by aspiration, a known volume of an indifferent gas is applicable at low vapor pressures and offers possibilities of a degree of precision equal to or better than that attainable with the more commonly used methods. The method should be applicable even at temperatures at which the vapor pressure is not more than 0.1 mm Hg, if the temperature is within the working range of one of the types of sensitive low-pressure manometers.[1] The purpose of the present paper is to discuss the precision aspects of the method.

III. HISTORY OF THE METHOD

According to Wrewsky,[2] the method was first proposed and used by Horstmann.[3] More recently Wrewsky [2] has employed the method for investigating the dissociation of formic and acetic acids in the vapor state.

In the form in which the method was employed by these investigators, the molecular weight, M, is calculated from the perfect gas law

$$M=\frac{mRT}{pv}$$

where p is the vapor pressure and m the number of grams of the substance present in v liters of the saturated gas.

When used in this form, however, the method has two objectionable features.

1. A given percentage error in v produces the same percentage error in M, consequently in precision work v has to be very accurately determined. This may be done either by measuring the volume of the indifferent gas [4] or by absorbing and weighing the indifferent gas after condensing out of it the substance under investigation;[5] for example, CO_2 by absorption, H_2 by combustion and absorption of the H_2O, O_2 (or the O_2 content of air) by absorption with hot copper, etc. The accurate determination of v is therefore possible.

2. The second objectionable feature of the method arises from the large temperature coefficient of p, which necessitates very close regulation of temperature during both the vapor pressure determination and the frequently prolonged saturation determination.

The required precision in temperature control can be computed as follows:

---

[1] For example, the Rayleigh tilting manometer sensitive to 0.0005 mm Hg up to $p=5$ mm. Rayleigh, Phil. Trans., **196**, p. 205: 1901; Scheel and Heuse, Z. Instrumentenk., **29**, p. 344; 1909.

[2] Wrewsky, Z. physik. Chem., **133**, p. 363; 1928.

[3] Horstmann, Ber. Deutsch. Chem. Ges, **3**, p. 78; 1870; **11**, p. 1287; 1878.

[4] Compare Wrewsky, Z. physik. Chem., **133**, pp. 360, 366, Table 4; 1928.

[5] See footnote 3.

It is obvious from the above equation that a fractional error, $\frac{\delta p}{p}$, in p will produce an equal fractional error, $\frac{\delta M}{M}$, in M. From the Clausius-Clapeyron equation

$$\frac{\delta_T M}{M}=\frac{\delta_T p}{p}=\frac{L}{RT^2}\delta T$$

where L is the latent heat of vaporization per mole.

It is obvious, therefore, that the two bath temperatures must be identical and constant within

$$\delta T=\frac{RT^2}{L}\,\frac{\delta_T M}{M}\text{ degrees}$$

if the fractional error in M arising from the temperature difference or fluctuation is not to exceed $\frac{\delta_T M}{M}$.

Illustrative example: Suppose the substance whose molecular weight is to be determined belongs to the class of liquids for which Trouton's ratio has the value

$$\frac{L}{T_B}=22$$

at the normal boiling point, T_B °K.

Combining this with the above equation gives

$$\delta T=\frac{T}{11T_B}\times T\times\frac{\delta_T M}{M}.$$

If now we assume that the error in M arising from the uncertainty $\delta T°$ in T is not to exceed $\frac{\delta_T M}{M}=0.001=0.1$ per cent and, if further, $\frac{T}{T_B}$ has the value $\frac{3}{5}$ and T the value 300° K., we find the limiting condition

$$\delta T\gtrless 0.016°\text{ C.}$$

Temperature control within this limit is difficult but possible. The necessity for such close regulation of temperature can, however, be avoided by employing a reference substance of known molecular weight, thus making the method practically independent of temperature fluctuations and at the same time eliminating the measurement of the volume of gas aspirated in the saturation determination.

IV. DESCRIPTION OF THE REFERENCE METHOD

This method is carried out as follows:

1. Place the substance, the molecular weight of which is to be determined, in a tube connected to a mercury manometer and evacuate until all air and other dissolved gases are removed.

2. Immerse the manometer in a bath and make an approximate determination of two points on the vapor pressure curve (for example, at $p=1$ mm and $p=10$ mm).

3. From available vapor pressure and boiling point data select a reference substance, the vapor pressure of which in the same temperature region is as near as possible to that of the substance under investigation and the molecular weight of which in the vapor state is known. Let the difference in the two vapor pressures, D_p, equal p_1-p_2, where D_p is a positive quantity. The two substances are now identified by the subscripts 1 and 2.

4. Determine in accordance with the following relations the temperature, t, at which the measurements are to be made. (These relations are derived below, p. 708.)

$$p_1 < \frac{\delta D_p}{\frac{\delta_{Dp} M}{M}}$$

$$p_2 < \frac{\delta p_2}{1+\left(\frac{\delta p_2}{p_1 \frac{\delta_{p_1} M}{M}}\right)\frac{\delta_{p_1} M}{M}}$$

where δD_p and δp_2 are the unavoidable errors in measuring D_p and p_2, and $\frac{\delta M}{M}$ the corresponding allowable fractional errors in M arising therefrom.

5. By means of a differential manometer and a manometer immersed in the same well-stirred bath, determine D_p and p_2 at the temperature t.

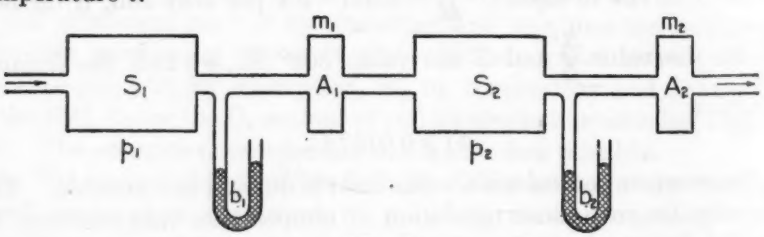

FIG. 1

S_1, S_2, saturators for saturating the gas stream with substances 1 and 2 whose vapor pressures are p_1 and p_2

A_1, A_2, condensers or absorbers for condensing substances 1 and 2, the condensates weighing m_1 and m_2 grams, respectively

b_1, b_2, open-arm manometers indicating the slight pressure differences ΔP_1 and ΔP_2 respectively

6. By means of two similar saturators immersed close together in a well-stirred bath, saturate a gas stream successively with the vapors of 1 and 2 and determine the mass, m, of each substance evaporated (for example, by the arrangement shown diagrammatically

in fig. 1). If these two masses are to be obtained by the weighing of condensers or absorbers of like size and shape, the operation of weighing should be conducted so as to give as accurately as possible the difference, $m_1 - m_2$. This could be conveniently accomplished by one weighing with the absorbers or condensers on opposite pans of the balance followed by a direct, and usually less accurate, weighing of one of the absorbers or condensers.

Accurate temperature control is not necessary in either experiment (5 and 6), but uniformity of temperature in the bath is essential in both cases.[6]

From the above data the molecular weight of either substance can be calculated, if that of the other is known.

The general technic of both of the operations involved is well established. Consequently, an experimental test of the method is not required. The special technic will depend upon the natures of the substances employed.

V. DERIVATIONS

$$M = \frac{mRT}{pv} \tag{1}$$

$$\frac{M_1}{M_2} = \frac{m_1 p_2 v_2}{m_2 p_1 v_1} \tag{2}$$

$$\frac{v_1}{v_2} = \frac{B - p_2 - \Delta P_2}{B - p_1 - \Delta P_1} \tag{3}$$

$$D_p = p_1 - p_2 \text{ and } \frac{p_1}{p_2} = 1 + \frac{D_p}{p_2} = 1 + R_p \tag{4}$$

$$\frac{v_1}{v_2} = 1 + \frac{\Delta P_1 - \Delta P_2 + D_p}{B - p_2 - D_p - \Delta P_1} = 1 + R_v \tag{5}$$

where R_v is small in comparison with unity. ΔP_1 and ΔP_2 can usually be made negligibly small.

$$m_1 - m_2 = D_m \tag{6}$$

$$\frac{m_1}{m_2} = 1 + \frac{D_m}{m_2} = 1 + R_m \tag{7}$$

Combining equations (2), (4), (5), and (7) gives finally

$$\frac{M_1}{M_2} = \frac{(1 + R_m)}{(1 + R_p)\ (1 + R_v)} \tag{8}$$

from which either M_1 or M_2 may be calculated in terms of quantities which are not sensitive to temperature.[7]

---

[6] See below, p. 709.

[7] Compare the similar equation for determining vapor pressure differences, J. Am. Chem. Soc., **37**, p. 311; 1915.

If the two substances employed are solid and (or) not soluble in each other at the temperature of the experiment, and if they do not react chemically with each other or interfere with the rapid attainment of vaporization equilibrium, and if, further, their mixture can be conveniently analyzed, then only one saturator and one absorber need be employed and R_v becomes equal to zero.

VI. PRECISION DISCUSSION

Inspection of equation (5) shows that errors in D_p and p_2 will produce in the factor $1+R_v$ an effect which is entirely negligible in comparison with that produced in the factor $1+R_p$ by these same errors. Consequently, since at most only two significant figures are required in a precision factor, R_v may, for purposes of precision computations, be taken as equal to zero; that is, $v_1=v_2=v$. On differentiation of equation (8) we obtain

$$\frac{\delta_{R_x} M}{M}=\frac{\delta R_x}{1+R_x} \tag{9}$$

in which M is either M_1 or M_2 and x is either m or p.

1. THE PRESSURE MEASUREMENTS

Putting

$$x=p \tag{10}$$

and combining with equation (4) gives

$$\frac{\delta M}{M}=\frac{p_2}{p_1}\delta\left(\frac{D_p}{p_2}\right) \tag{11}$$

For D_p as the variable this becomes

$$\frac{\delta_{D_p} M}{M}=\frac{\delta D_p}{p_1} \tag{12}$$

and for p_2

$$\frac{\delta_{p_2} M}{M}=\frac{D_p \delta p_2}{p_1 p_2}=\frac{(p_1-p_2)\delta p_2}{p_1 p_2} \tag{13}$$

Solutions of these equations determine minimum values for p_1 and p_2 as follows:

In each of these equations let $\frac{\delta M}{M}$ represent the maximum allowable fractional error in M_1. Then

$$p_1 \leqslant \frac{\delta D_p}{\frac{\delta_{D_p} M}{M}} \tag{14}$$

and

$$p_2 \leqslant \frac{\delta p_2}{\left(1+\frac{\delta p_2}{p_1 \frac{\delta_{p_2} M}{M}}\right)\frac{\delta_{p_2} M}{M}} \tag{15}$$

The minimum value which p_2 can have obviously occurs when p_1 has the value given by equation (14). If the errors in D_p and p_2 produce equal errors in M (that is, $\delta_{D_p} M = \delta_{p_2} M = \delta M$; principle of equal effects), then equations (14) and (15) give

$$p_2 \ll \frac{\delta p_2}{\left(1+\frac{\delta p_2}{\delta D_p}\right)\frac{\delta M}{M}} \tag{16}$$

which is the smallest value p_2 can have under these conditions.

From equation (15) it is obvious that the largest minimum value for p_2 will occur when $\dfrac{\delta p_2}{p_1 \dfrac{\delta_{p_1} M}{M}}$ is negligible in comparison with unity and will be

$$p_2 \ll \delta p_2 \Big/ \frac{\delta_{p_1} M}{M} \tag{17}$$

2. TEMPERATURE CONTROL

The required precision in temperature control can be computed as follows:

From equation (9)

$$\frac{\delta_T M}{M} = \frac{\delta_T R_p}{1+R_p} = \delta_T \log (1+R_p) = \delta_T \log \frac{p_1}{p_2} = \delta_T \log p_1 - \delta_T \log p_2$$

From the Clausius-Clapeyron equation

$$\delta_T \log p_1 - \delta_T \log p_2 = \frac{L_1 - L_2}{RT^2}\delta T$$

Hence

$$\frac{\delta_T M}{M} = \frac{\Delta L}{RT^2}\delta T$$

The preliminary measurements (see p. 706) will ordinarily yield the necessary data for computing $\dfrac{\delta_T M}{M}$ in any specific case. It is obviously zero when ΔL is zero, that is, when the two vapor-pressure curves have the same slope at the temperature of the experiments.

Illustrative example: Suppose that both substances belong to the class of liquids for which Trouton's ratio has the value

$$\frac{L}{T_B} = 22$$

and that they differ in boiling point by Δt_B. It follows that $\Delta L = 22\Delta t_B$ and if we assume that ΔL is independent of T, we have

$$\frac{\delta_T M}{M} = \frac{22\Delta t_B}{RT^2}\delta T$$

For example, if $\Delta t_B = 10°$ C. and $T = 300°$ K. and if we impose the condition that $\frac{\delta_T M}{M}$ is not to exceed $0.001 = 0.1$ per cent, this gives

$$\delta T > 0.8° \text{ C.}$$

which may be compared with the analogous case when no reference substance is employed (see above, p. 709).

3. THE SATURATION MEASUREMENTS

Putting $x = m$ in equation (9) and proceeding as in 1 above we obtain an analogous set of relations as follows:

$$\frac{\delta_{Dm} M}{M} = \frac{\delta D_m}{m_1} \tag{18}$$

and

$$\frac{\delta_{m_2} M}{M} = \frac{D_m}{m_1}\frac{\delta m_2}{m_2} = \frac{(m_1 - m_2)\,\delta m_2}{m_1 m_2} \tag{19}$$

$$m_1 < \frac{\delta D_m}{\frac{\delta_{Dm} M}{M}} \tag{20}$$

$$m_2 < \frac{\delta m_2}{\left(1 + \frac{\delta m_2}{m_1 \frac{\delta_{m_2} M}{M}}\right)\frac{\delta_{m_2} M}{M}} \tag{21}$$

By combining relations (20) and (21) with equation (1) and solving for v, we obtain an expression giving a minimum value for v as follows:

$$v < \frac{RT}{M_1 p_1}\frac{\delta D_m}{\delta_{Dm} M/M} < \left(\frac{RT}{M_2 p_2} - \frac{RT}{M_1 p_1}\right)\frac{\delta m_2}{\delta_{m_2} M/M} \tag{22}$$

which may also be written

$$v < \frac{RT\left(\frac{M_2}{M_1}\right)}{p_1 M_2}\frac{\delta D_m}{\delta_{Dm} M/M} < \left(\frac{RT}{p_2 M_2} - \frac{RT\left(\frac{M_2}{M_1}\right)}{p_1 M_2}\right)\frac{\delta m_2}{\delta_{m_2} M/M} \tag{23}$$

For equal effects the second expression in (23) takes precedence over the first for all values of $\frac{M_2}{M_1}$ up to

$$\frac{M_2}{M_1} = \left(\frac{\delta m_2}{\delta D_m + \delta m_2}\right)\frac{p_1}{p_2} \tag{24}$$

or for the common case where $\delta D_m = \delta m_2$, the second expression will take precedence up to

$$\frac{M_2}{M_1} = \frac{1}{2}\frac{p_1}{p_2} \tag{25}$$

VII. ILLUSTRATIVE EXAMPLE

Suppose the substance whose molecular weight is to be determined has at 27° C. a vapor pressure of 10 mm and let us select naphthalene as the reference substance. Its vapor pressure at 27° is 9.57 mm. We have then

$$p_2 = 9.57 \text{ mm}$$
$$D_p = 0.430 \text{ mm}$$
$$M_2 = 128.06$$
$$M_1 = ?$$

Let us further assume that the permissible error in M_1 arising from the error in each measured factor is

$$\frac{\delta M_1}{M_1} = 0.001 = 0.1 \text{ per cent.}$$

From equation (12) we find the allowable error in D_p to be

$$\delta D_p = p_1 \frac{\delta M}{M} = 10.0 \times 0.001 = 0.01 \text{ mm}$$

Suppose that δD_m and δm_2 be taken as 0.0002 g each.

From relation (22) we find the minimum value for v to be

$$v_{\text{min.}} = \frac{0.08207 \times 300 \times 0.0002 \times 760}{10 \times 128.06 \times 0.001 \times M_1/M_2} = 2.92 \frac{M_2}{M_1} \text{ liters} \qquad (26)$$

or

$$= 3.05 - 2.92 \frac{M_2}{M_1} \text{ liters} \qquad (27)$$

The values of $v_{\text{min.}}$ as given by equations 26 (v_1) and 27 (v_2), respectively, are shown in the following table:

TABLE 1.—*Values of* $v_{\text{min.}}$ *for* $\delta D_m = \delta m_2 = 0.0002$ *g*

M_1/M_1	$\delta D_m = 0.0002$ g v_1	$\delta m_2 = 0.0002$ g v_2
0	0	3.05
.1	.292	2.66
$0.522 = \frac{1}{2}\frac{p_1}{p_2}$	1.53	1.53
1.0	2.92	.13
$1.045 = \frac{p_1}{p_2}$	3.05	0
$2.090 = \frac{2p_1}{p_2}$	6.10	3.05
5	14.6	11.6
10	29.2	26.9
100	292	289

Taking any value, v, larger than $v_{\text{min.}}$, we have (equation (1)) $m_2=0.65\ v$ g.

The allowable errors in p_2 and m_2 then become (equations (13) and (19)).

$$\delta p_2=\frac{p_2 p_1}{D_p}\frac{\delta M_1}{M_1}=\frac{9.57\times 10}{0.43}\times 0.001=0.22 \text{ mm}$$

$$\delta m_2=\frac{m_2 m_1}{D_m}\frac{\delta M_1}{M_1}=\frac{v M_2 \frac{\delta M_1}{M_1}}{RT\left(\frac{1}{p_2}-\frac{M_2}{M_1}\times\frac{1}{p_1}\right)}=\frac{0.0068\ v\times 0.001}{\frac{1}{9.57}-\frac{1}{10}\frac{M_2}{M_1}}$$

TABLE 2.—*Values of* δm_2 *for* $M_2=126$, $\frac{\delta m_2 M}{M}=0.001$, $p_2=9.57$ *and* $p_1=10$ *mm Hg*

$\frac{M_2}{M_1}$	δm_2 in milligrams		
	For $v=v$	For $v=10$	For $v=30$
0.0	$0.065\ v$	0.65	2.0
.1	$.072\ v$	.72	2.2
.5	$.127\ v$	1.27	3.8
1.0	$1.5\ v$	15	45
$1.045\left(=\frac{p_1}{p_2}\right)$	∞	∞	∞
1.1	$.123\ v$	1.23	3.7
2	$.0712\ v$	.71	2.1
$2.090\left(=\frac{2p_1}{p_2}\right)$	$.065\ v$	.65	2.0
5	$.0172\ v$	.17	.5
10	$.0076\ v$	.076	.2

Suppose now that as a result of this preliminary survey we decide to impose the condition that $\delta D_m < 0.002$ g, since it will be much easier to attain this moderate degree of accuracy. Suppose further that a preliminary determination has yielded the information that $\frac{M_2}{M_1}$ = about 0.5. Equation (26) now gives $v_{\text{min.}}$ = about 15 liters. This value for v will, according to Table 2, require an accuracy in m_2 given by "δm_2 need not be less than 0.0018 g." It will suffice therefore if $v < 15$ liters. As regards the accuracy required in D_p and p_2, the values computed above are not difficult of attainment. Our final conclusions might therefore be somewhat as follows:

For $\frac{M_2}{M_1}$ = about 0.5; $p_1=10$ mm, $p_2=9.57$ mm, $D_p=0.430$ mm, $M_2=128.06$, and $v=15$ liters, the allowable errors in the measured quantities are

For p_2, 0.2 mm

For D_p, 0.01 mm

For m_2, 0.0018 g

For D_m, 0.002 g

The final precision in M will be

$$100\frac{\delta M}{M}=100\sqrt{4\times(0.001)^2}=0.2 \text{ per cent}$$

and the largest possible error in M will be

$$100\left(\frac{\delta M}{M}\right)_{\text{max.}}=0.4 \text{ per cent}$$

VIII. EFFECT OF ATMOSPHERIC PRESSURE

In the equations given above it has been tacitly assumed that D_p and p_2 as measured by the manometers are identical with the values which prevail during the saturation determination. This is not strictly true, since both values are functions of the external pressure and, in the case of liquids, are also functions of the solubilities of the gas used in the saturation measurements. In exact work small corrections may, therefore, be necessary to allow for these two effects. These corrections may be computed as follows:[8]

1. The pressure correction.

Increase the measured value of p_2 by Δp_2

$$\Delta p_2=\frac{p_2V_2}{RT}(B-\Delta P_2-p_2)$$

where V is the molal volume of the substance at $T°$ K. and in the state (liquid or solid) in which it exists at $T°$ and B mm.

Similarly *increase* the measured value of D_p by ΔD_p

$$\Delta D_p=(\text{approx.})\frac{B}{RT}[V_1D_p+p_2(V_1-V_2)]$$

2. The gas-solubility correction (for liquids only).

Decrease the measured value of p_2 by $\Delta' p_2$

$$\Delta' p_2=\frac{p_2V_2\ (B-\Delta P_2-p_2)}{RT}\left(1-\frac{1}{S_2}\right)$$

where S is the solubility of the gas in the liquid; that is, S = the ratio of the concentrations of the gas in the two phases, gas/liq.

Similarly *decrease* the measured value of D_p by

$$\Delta' D_p=\frac{p_1V_1(B-\Delta P_1-p_1)}{RT}\left(1-\frac{1}{S_1}\right)-\frac{p_2V_2(B-\Delta P_2-p_2)}{RT}\left(1-\frac{1}{S_2}\right)$$

In practically all cases the algebraic sum of these two corrections will be negligible.

WASHINGTON, August 7, 1928.

[8] Compare Washburn, Science, 51, p. 49; 1925.

THE SULPHOALUMINATES OF CALCIUM

By William Lerch, F. W. Ashton, and R. H. Bogue

ABSTRACT

Two calcium sulphoaluminates have been prepared and their compositions and optical characteristics determined. One of these, having the composition $3CaO.Al_2O_3.3CaSO_4.31H_2O$, is relatively stable in aqueous solutions but is decomposed by solutions of magnesium salts and of carbonates. The other, having the composition $3CaO.Al_2O_3.CaSO_4.12H_2O$, is relatively unstable except in high concentration of hydroxyl ion. It is readily converted to the high sulphate form in aqueous solutions but is decomposed by magnesium salts and carbonates. In sulphate solutions the high sulphate form may be produced, but in the presence of a slight excess of magnesium salts or carbonates neither of the sulphoaluminates can continue to exist. In these cases the less soluble magnesium hydroxide and calcium carbonate, respectively, are formed.

CONTENTS

	Page
I. Introduction	715
II. Review of the literature	716
III. Experimental procedure	718
1. The high sulphate calcium sulphoaluminate	718
2. The low sulphate calcium sulphoaluminate	722
3. Calcium sulphosilicoaluminate	724
IV. Conditions of stability in salt solutions	725
V. Relative stability with calcium chloraluminate	729
VI. Summary	729

I. INTRODUCTION

Among the products formed by the action of sulphate waters on Portland cement there has been observed, under some conditions, a calcium sulphoaluminate. This has been ascribed by some investigators to be responsible for certain expansion effects observed at times in concrete which is exposed to sea water and to alkali soil waters. The exact nature of this compound and its conditions of formation and stability have not been adequately treated, however.

The present investigation is concerned with the formation, properties, and conditions of equilibrium of such compounds as may be obtained by the interaction of CaO, Al_2O_3, and SO_3 in aqueous solutions with especial reference to the conditions under which these compounds may be formed in concrete. In addition to the above, attempts were made to obtain a compound of lime, alumina, silica, and sulphate.

31400°—29——1

II. REVIEW OF THE LITERATURE

Candlot[1] appears to have been the first to establish the formation of a definite compound by the interaction of an aqueous solution of calcium aluminate with calcium sulphate. He mixed saturated solutions of a calcium aluminate and calcium sulphate and observed the formation of small crystalline spherulites 2 to 3 mm. in diameter. The addition of a saturated solution of calcium hydroxide caused a more abundant precipitation of the crystals, as they seem to be less soluble in calcium hydroxide solutions. From analysis of a sample of these crystals Candlot ascribed to them the composition $3CaO.Al_2O_3.2.5CaSO_4.59H_2O$. He described the crystals as being only slightly soluble in water and insoluble in alcohol and in lime-water containing more than 0.2 g. CaO per liter.

Because of the widespread interest in the action of sulphate waters on concrete the identification of a calcium sulphoaluminate immediately attracted the attention of cement chemists. Michaelis[2] prepared the compound by the reaction of a solution of aluminum sulphate with limewater. The crystals resembled bacilli in size and shape and so were called by him "cement bacilli." Michaelis described the crystals as broad, needle-shaped prisms belonging to the tetragonal system, some with and some without truncated ends.

From analysis of a sample dried to constant weight over sulphuric acid he derived the formula $3CaO.Al_2O_3.3CaSO_4.30H_2O$. Although this formula is not identical to that given by Candlot to the sulphoaluminate, yet from the descriptions given it seems probable that the two preparations were indeed the same compound. The formula of Michaelis for the anhydrous material, $3CaO.Al_2O_3.3CaSO_4$, has been confirmed by Deval,[3] Poirson,[4] Klein and Phillips,[5] Kühl and Albert,[6] Lafuma,[7] and McIntire and Shaw.[8] There is, however, a difference of opinion on the number of combined molecules of water, due probably to different methods of procedure in the preparation and drying of the samples.

Some authors have believed that they obtained still other calcium sulphoaluminates. Klinkenberg[9] claimed to have obtained three definite compounds by adding to a sintered mixture of "dicalcium aluminate" 1, 2, and 3 equivalents of gypsum and allowing the

[1] Bull. soc. encour. ind. nat., p. 682; 1890.
[2] Tonind. Ztg., **16**, p. 105; 1892.
[3] Bull. soc. encour. ind. nat. (5th ser.), Pt. I, **5**, 49; 1900.
[4] Zentr. hydraul. Zement, **1**, p. 151; 1910 C. A., **5**, p. 1328; 1911.
[5] B. S. Tech. Paper, No. 43; 1914.
[6] Zement, **12**, p. 279; 1923.
[7] Ciment, **30**, p. 175; 1925.
[8] Soil Science, **19**, p. 125; 1925.
[9] Dinglers polytech. J., **249**, p. 89, 1894; J. Soc. Chem. Ind., **14**, p. 365; 1895.

reactions to proceed for six months. He has assigned to them the formulas:

$$2CaO.Al_2O_3.CaSO_4.12.49H_2O$$
$$2CaO.Al_2O_3.2CaSO_4.18.25H_2O$$
$$2CaO.Al_2O_3.3CaSO_4.19.55H_2O$$

However, there is no evidence given that the products were definite chemical compounds and not mixtures.

On determining the quantity of water fixed by mixtures of "dicalcium aluminate" and calcium sulphate in variable proportions, Schott [10] thought he demonstrated the existence of the compound

$$2CaO.Al_2O_3.2CaSO_4.18H_2O$$

Rebuffat [11] criticized the work and conclusions of Schott and claimed to have produced two calcium sulphoaluminates. To one of these he gave the formula $3CaO.Al_2O_3.3CaSO_4.10H_2O$. This, he said, is formed when a solution of calcium sulphate is mixed with an aqueous solution of any calcium aluminate, or when either tricalcium aluminate or "dicalcium aluminate" in the solid form is shaken with a solution of calcium sulphate. The second calcium sulphoaluminate, to which he gave the formula $CaO.Al_2O_3.CaSO_4.10H_2O$, was said to be formed when the solid monocalcium aluminate was shaken with calcium sulphate solution.

In a later paper, from a study of his own work and that of Candlot, Deval, and others Rebuffat [12] concludes that the formula for the first calcium sulphoaluminate should be $3CaO.Al_2O_3.2.5CaSO_4.7H_2O$. This, he says, is formed from any calcium aluminate and calcium sulphate in the presence of calcium hydroxide.

Klein and Phillips,[13] however, found that monocalcium aluminate, 5-3 calcium aluminate, and tricalcium aluminate all react with calcium sulphate to give the same calcium sulphoaluminate. They give the formula for the compound as $3CaO.Al_2O_3.3CaSO_4.xH_2O$, the value of x varying with the method of drying. The crystals are described as long, slender needles showing very low interference colors and a biaxial, positive interference figure, with a large optic axial angle. Elongation was negative and extinction parallel. Refractive indices were less than 1.48. Twinning was not noted, but occasional irregular intergrowths were observed. The ends of the needles were said to be flat and perpendicular to the long axis of the needles.

---

[10] Tonind. Ztg., **18**, p. 819; 1894.
[11] Rend. accad. sci. (Napoli), **35**, No. 11, p. 280; 1896.
[12] Gazz. chim. ital., **32**, No. 2, p. 158; 1902.
[13] See footnote 5.

Shelton [14] has reported that all the calcium aluminates react with magnesium sulphate when present in dilute solution (less than 0.1 M) or with sodium sulphate in all concentrations to form the same calcium sulphoaluminate. In higher concentrations of magnesium sulphate than 0.1 M the only crystalline product was gypsum. The calcium sulphoaluminate is said by Shelton to occur usually as fine needles but sometimes as coarse prisms, frequently with short needles growing parallel to each other from opposite ends of a prism. Optical properties were determined on the coarse prisms, after separating them from the solution, washing with water and drying in a desiccator until just dry, usually less than an hour. The optical character was reported to be positive and optic angle large, but the interference figure was indistinct. Elongation was negative and refractive indices were $\gamma = 1.463 \pm 0.003$, $\alpha = 1.461 \pm 0.003$.

Deval [15] attempted to show, by a rather indirect method, that the amount of calcium sulphate fixed by a cement may greatly exceed that required to convert all of the alumina to calcium sulphoaluminate. Lafuma [16] has reported similar results and has suggested the formation of a calcium sulphosilicoaluminate.

III. EXPERIMENTAL PROCEDURE

In the course of experimentation it was observed that there were two sulphoaluminates of calcium characterized by different chemical composition, optical properties, and crystal form. To avoid confusion, the two are treated separately below. In addition to these, the formation of a more complex compound, reported by Lafuma [16] as a calcium sulphosilicoaluminate, has been investigated.

1. THE HIGH SULPHATE CALCIUM SULPHOALUMINATE

Several methods were employed in the preparation of this calcium sulphoaluminate. By far the most important of these was by the interaction of calcium sulphate and calcium aluminate. This method was essentially the same as had been recommended by Candlot [17] and later by Klein and Phillips.[18] A calcium aluminate solution was prepared by adding 20 g of the 5–3 calcium aluminate to 1 liter of water and shaking for one hour. The solution was filtered off and 200 ml of saturated calcium sulphate solution added. Under these conditions the crystals formed very slowly, but the addition of 200 ml of a saturated solution of calcium hydroxide greatly increased the rate of crystallization. After one week the crystalline phase consisted of very fine needles.

[14] Ind. Eng. Chem., 17, p. 1267; 1925.
[15] Bull. soc. encour. ind. nat., 101, Pt. II, pp. 96 and 784; 1901; J. Soc. Chem. Ind., 21, p. 971; 1902.
[16] See footnote 7, p. 716.
[17] See footnote 1, p. 716.
[18] See footnote 5, p. 716.

The chemical analyses of a number of these preparations showed them to be somewhat variable in composition. In some cases the ratio of CaO, Al_2O_3, and SO_3 was found to be represented by the composition $3CaO.Al_2O_3.2.5CaSO_4.aq$, and in other cases the $CaSO_4$ content was somewhat higher. In no one of these preparations was there sufficient $CaSO_4$ present to give the composition $3CaO.Al_2O_3.3CaSO_4.aq$.

Preparations were then made by using a larger quantity of calcium hydroxide and calcium sulphate. Five hundred and 750 ml, respectively, of the calcium aluminate solution were added to 1,500 ml of a solution saturated with calcium hydroxide and calcium sulphate. The preparations were allowed a week to approach equilibrium. The precipitates were then filtered off, washed with alcohol and ether to remove the excess water and dried to constant weight in air. The analysis of these crystals is given in Table 1.

TABLE 1.—*Analysis of high sulphate calcium sulphoaluminate*

	1,500 ml $Ca(OH)_2$+$CaSO_4$ solution			
	No. 1, 500 ml calcium aluminate solution		No. 2, 750 ml calcium aluminate solution	
	Per cent composition	Molecular composition	Per cent composition	Molecular composition
Al_2O_3	8.24	1.00	8.21	1.00
CaO	27.20	6.01	27.15	6.02
SO_3	19.30	2.99	19.20	2.98
H_2O by difference	45.26	31.10	45.44	31.30

On calculating these analyses to molecular composition the compound is found to have a composition which may be represented by the formula:

$$3CaO.Al_2O_3.3CaSO_4.31H_2O$$

The composition of the crystalline phases obtained by the above methods of preparation is thus seen to vary and appears to be determined by the concentration of calcium sulphate present in the mother liquor. In the presence of low concentrations of calcium sulphate the crystalline phase is found to have a composition which approaches the formula $3CaO.Al_2O_3.2.5CaSO_4.aq$, but in the presence of higher concentrations of calcium sulphate as given in Table 1 the composition becomes

$$3CaO.Al_2O_3.3CaSO_4.31H_2O.$$

Two possible explanations may be advanced for this variation in composition: (1) That the actual composition of the crystalline phase is $3CaO.Al_2O_3.2.5CaSO_4.aq$, and that the crystals adsorb calcium

sulphate from the solution; (2) that the composition of the crystalline phase is $3CaO.Al_2O_3.3CaSO_4.aq$, but that in the presence of low concentrations of calcium sulphate this compound forms an equilibrium mixture with $3CaO.Al_2O_3.aq$.

If the adsorption theory were correct, the amount of calcium sulphate adsorbed would vary with the calcium sulphate concentration of the solution and would reach a maximum value only when the solution was saturated with calcium sulphate. The results reported in Table 1 indicate a uniformity of composition in the two preparations, even though the calcium sulphate concentration of the mother liquor in preparation No. 1 was considerably greater than in preparation No. 2. These results support the belief that the lower values for the SO_3/Al_2O_3 ratio obtained in some of the preparations is due to an equilibrium between the compounds $3CaO.Al_2O_3.3CaSO_4.aq$ and $3CaO.Al_2O_3.aq$. On increasing the concentration of calcium sulphate in the mother liquor the amount of $3CaO.Al_2O_3.aq$. in solution decreases and eventually disappears.

The size of the crystals appears to vary through a wide range, dependent on the concentration of the reacting solutions. In the presence of high concentrations of calcium sulphate and calcium hydroxide, as in the samples prepared for the chemical analysis, the crystals are submicroscopic. In other samples prepared by the interaction of solutions of the calcium aluminates with less concentrated solutions of calcium sulphate and calcium hydroxide the needle like crystals were present as shown in Figure 1. These were about 0.002 to 0.003 mm wide and 0.15 to 0.25 mm long. In some solutions which had been allowed to stand in the laboratory several months a few of the crystals attained a length of 1 cm or more.

In order to obtain crystals of larger cross section for optical examination, two modifications of the above procedure were employed. In one of these the crystals were allowed to grow by slow diffusion in a gel.[19] The calcium aluminate solution was incorporated into a 5 per cent agar gel and the gel then placed in a solution saturated with calcium sulphate and calcium hydroxide. After about two months the crystals of calcium sulphoaluminate had grown to much greater dimensions than were ordinarily obtained by the other methods. Some of these were about 0.06 mm long and 0.03 to 0.04 mm on cross section.

By another procedure 90 per cent $3CaO.5Al_2O_3$ and 10 per cent calcium sulphate were mixed and a few grains placed on a glass slide with a drop of water. A cover glass was sealed on to prevent evaporation. Large crystals appeared in about a week, one of which is shown in Figure 2. The photomicrograph with higher magnification shows beautifully the hexagonal cross section of the crystal.

[19] Performed by L. T. Brownmiller.

FIGURE 1.—*Calcium sulphoaluminate needles. High sulphate form. Analyzer out.* × *200*

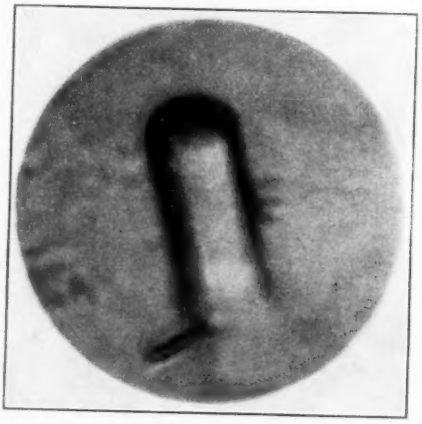

FIGURE 2.—*Crystal of calcium sulphoaluminate (high sulphate form) showing hexagonal prismatic habit. No nicols.* × *1,290*

FIGURE 3.—*Calcium sulphoaluminate spherulite from an old briquette. High sulphate form. Reflected light.* × 75

FIGURE 4.—*A mixture of calcium sulphoaluminates. Crossed nicols.* × 130

The needles are the high sulphate form. The star shaped aggregates are the low sulphate

These larger crystals were used for the optical determinations. The crystals show parallel extinction and negative elongation and appear isotropic when seen on end. The refractive indices for sodium light obtained by the immersion method were $\omega_D = 1.464 \pm 0.002$ $\epsilon_D = 1.458 \pm 0.002$, birefraction 0.006. The interference figure is uniaxial negative.

A spherulite of the high sulphate form of calcium sulphoaluminate from an old mortar briquette is shown in Figure 3. The crystals sometimes occur in this spherulitic structure.

Upon dehydration of the sulphoaluminate crystals at 110° C. the water content dropped to an equivalent of $7H_2O$ and remained constant. This loss of water was accompanied by a longitudinal cracking or splitting of the crystals and a change in optical properties. The mean refractive index rose to about 1.50, and the character of elongation changed from negative to positive. On placing the dehydrated crystals in an atmosphere saturated with water vapor the character of elongation again changed and the mean refractive index dropped. The final value is close to 1.45, somewhat higher than the index of the original crystals.

The specific gravity of the compound $3CaO.Al_2O_3.3CaSO_4.31H_2O$ determined in absolute alcohol was found to be 1.48 at 20° C.

Three other methods were used for the preparation of the calcium sulphoaluminate crystals. The interaction of aluminum sulphate with saturated limewater (3 g added to 1 liter) gave first a flocculent precipitate characteristic of aluminum hydroxide. This gradually changed in appearance and assumed the more crystalline character of the calcium sulphoaluminate. After three months a microscopic examination showed it to consist almost entirely of the latter.

Another sample was prepared by the action of a solution containing calcium hydroxide and calcium sulphate on precipitated aluminum hydroxide. In this case the action was very slow, but after a month the residue was shown microscopically to contain a large amount of calcium sulphoaluminate.

Still another method consisted in the addition of sodium sulphate solutions (20 ml of 0.5, 1.0, 2.5, and 5.0 per cent) to 1 g each of the four anhydrous calcium aluminates (3:5, 1:1, 5:3, 3:1). The aluminates each reacted with these solutions to produce a large increase in the volume of the solid phase. In the 2.5 and 5.0 per cent solutions this increase in volume was sufficient in three hours to produce a gel. In each case the material when examined under the microscope was found to contain large quantities of calcium sulphoaluminate, with the exception of the tricalcium aluminate in the 0.5 and 1.0 per cent solutions. Evidence obtained by determining the loss of SO_3 from a solution containing 5 g of tricalcium aluminate in 200 ml of 1 per cent sodium sulphate solution (a decrease from 0.5714 g per 100 ml in the

FIGURE 3.—*Calcium sulphoaluminate spherulite from an old briquette. High sulphate form. Reflected light.* × 75

FIGURE 4. *A mixture of calcium sulphoaluminates. Crossed nicols.* × 130

solution after six days of reaction) suggests that the formation of calcium sulphoaluminate from the tricalcium aluminate probably has occurred as in the other solutions but that the crystals are too small for positive identification.

A naturally occurring calcium sulphoaluminate, Ettringite, has been described by Dana [20] and Larsen.[21]

This is given the formula $6CaO.Al_2O_3.3SO_3.33H_2O$, but the actual analyses could equally well be represented by a somewhat lower SO_3 content. The system is given as hexagonal, the optical character as uniaxial negative, and the average refractive index as 1.49 with a birefraction ± 0.01. An examination in this laboratory of a sample of this mineral, obtained through the courtesy of the United States National Museum, gave $\omega_D = 1.489 \pm 0.003$ and $\epsilon_D = 1.475 \pm 0.003$ for white light. In other respects the sample was similar to that described by Dana and Larsen. Since the analyses of the Ettringite and of the artificial sulphoaluminate correspond so closely, and since the indices of the artificial material after heating and rehydration approach those obtained for the Ettringite, it seems probable that the two are essentially the same material.

Moses [22] describes a sample of Ettringite from Tombstone, Ariz., which he believes is slightly different from the one described by Lehman [23] and Dana. He gives the formula $10CaO.2Al_2O_3.5SO_3.54H_2O$ for this material and $10CaO.2Al_2O_3.5SO_3.22H_2O$ for the dried material. He describes the crystals but gives no optical measurements.

2. THE LOW SULPHATE CALCIUM SULPHOALUMINATE

In the preparation of the high sulphate form of calcium sulphoaluminate it had been observed that when the calcium hydroxide content of the aluminate solution was high the addition of calcium sulphate solution caused the almost immediate formation of a very fine-grained precipitate. On allowing this to stand in the mother liquor for a week or so the appearance of the precipitate changed completely. It then resembled the matted masses of long needles described above. This change in macroscopic character was so striking that further investigation of the fine-grained material was undertaken.

A sample of this material was prepared as follows: Two hundred milliliters of saturated limewater were added to 500 ml of a calcium aluminate solution prepared from the $5CaO.3Al_2O_3$. The precipitate which formed was filtered off and 200 ml of saturated calcium sulphate solution added to the clear filtrate. After two hours the precipitate which formed was separated by filtration. This residue did

[20] System of Mineralogy, New York, 6th ed., p. 976; 1911.
[21] U. S. Geol. Survey, Bull., p. 679; 1921.
[22] Am. J. Sci., 45, p. 489; 1893.
[23] Jahrb. Min., p. 273; 1847; C. F. Dana, loc. cit. No. 15.

FIGURE 5.—*Low sulphate calcium sulphoaluminate. Crossed nicols.* × *200*

FIGURE 6.—*Low sulphate calcium sulphoaluminate showing the platy form. Analyzer out.* × *200*

Note the star-shaped aggregates on several of the plates

not form a mat on the filter paper but was loose, light, and granular in character.

A chemical analysis was made of a portion of this material which had been washed with alcohol and ether and dried to constant weight in air. The results are given in Table 2.[24]

TABLE 2.—*Analysis of low sulphate calcium sulphoaluminate*

	Per cent composition	Molecular composition
Al_2O_3	16.06	1.00
CaO	35.30	4.01
SO_3	12.90	1.02
H_2O	35.80	12.20

This gives a molecular composition which may be represented by the formula

$$3CaO.Al_2O_3.CaSO_4.12H_2O$$

It is thus seen that there is an essential difference in composition between the two forms, the ratio of tricalcium aluminate to calcium sulphate in the first preparation being 1 to 3 and in this preparation being 1 to 1. Hence, the former is referred to as the high sulphate form; the latter as the low sulphate form.

Microscopic examination of this sulphoaluminate showed it to be very different from the long needles of the compound first described. The difference is brought out very clearly in Figure 4, which shows a photomicrograph with crossed nicols of a mixture of the two sulphoaluminates. Figure 5 shows the most common appearance of the low sulphate compound with crossed nicols, and Figure 6 is a photomicrograph with ordinary light of a sample showing the platy habit. The star-shaped or spherulitic birefracting masses seen in Figure 5 are groups of these plates joined together at an edge and standing more or less perpendicularly to the plane of the paper. They are often joined to a basal plate and then present the appearance seen in Figure 6. As may be seen in Figure 4, the crystals appear much smaller than the needles of the high sulphate calcium sulphoaluminate. In the usual preparations of the low sulphate calcium sulphoaluminate the length of the needles (edges of the plates) is seldom over 0.015 mm. and the thickness is about 0.002 mm. Occasionally a sample will consist of plates much larger than this, the largest measured having a diagonal length of nearly 0.14 mm.

The crystals of the low sulphate calcium sulphoaluminate belong to the hexagonal system and are uniaxial negative in character. Refractive indices are $\omega_D = 1.504 \pm 0.002$, $\epsilon_D = 1.488 \pm 0.002$. The

[24] Analysis performed by the chemistry division of the Bureau of Standards.

radiating needles (or edges of plates) seen in the star-shaped aggregates show parallel extinction and positive elongation. This sulphoaluminate is therefore easily distinguished by its optical and crystallographic properties from that first described. Its refractive indices are higher, its crystal habit platy instead of acicular, and the character of elongation is positive instead of negative. The specific gravity of this compound determined in absolute alcohol was found to be 1.95 at 20° C.

On dehydrating the low sulphate calcium sulphoaluminate to constant weight at 110° C. the water content was reduced to an equivalent of $6H_2O$. The crystals were so altered in size and form that satisfactory optical and crystallographic measurements were not obtainable. The refractive indices were somewhat variable and may indicate a decomposition as well as dehydration. The values obtained were $\alpha = 1.510–1.527$, $\gamma = 1.529–1.535$.

3. CALCIUM SULPHOSILICOALUMINATE

Lafuma [25] has given the results of some experiments which he believes indicate the formation of a calcium sulphosilicoaluminate. He prepared a special cement of the composition $17CaO + Al_2O_3 + 5SiO_2$, burned at 1,500° C., and mixed this with definite quantities of sulphuric acid, aluminum sulphate, water, and after a week, lime. This was left for five months and then the excess of calcium sulphate and lime extracted. The ratio of alumina to calcium sulphate in the residue was calculated to be 1 to 6.9, indicating to Lafuma an amount of calcium sulphate greatly in excess of that which could be combined with the alumina in the formation of a calcium sulphoaluminate, and suggesting to him the existence of a calcium sulphosilicoaluminate to which he assigned the formula

$$9CaO.4SiO_2.Al_2O_3.7CaSO_4.80H_2O.$$

A repetition of this experiment was performed in this laboratory because it is very important to establish definitely the products of hydrolysis and interaction with salts in the setting of cement or the disintegration of the set cement.

The final residue obtained was found to contain alumina and calcium sulphate in the ratio of about 1 to 3.5, which does not approach the ratio of 1 to 6.9 reported by Lafuma.

A microscopic examination of this residue showed that it contained several phases and was not a homogeneous material. Not all of the materials present were susceptible of microscopic identification, but there were found a large number of very small needles of the high

[25] See footnote 7, p. 716.

sulphate form of calcium sulphoaluminate. The presence of this calcium sulphoaluminate, and the ratio of alumina to calcium sulphate in these residues, seem to make very improbable the existence of the calcium sulphosilicoaluminate in these preparations.

IV. CONDITIONS OF STABILITY IN SALT SOLUTIONS

A study of the stability of the calcium sulphoaluminates in solutions of the various salts which are present in sea water and "alkali" soil waters is of especial importance as a means for determining the rôle played by these calcium sulphoaluminates when formed in concrete exposed to such waters. In studying these relations 0.5 g of each of the calcium sulphoaluminates was placed separately in 100 ml portions of the salt solutions to be studied and allowed to stand for a period of time varying from 10 to 60 days. The residues were then filtered off and examined under the microscope. The filtrates in some instances were analyzed for lime, alumina, and SO_3.

The results obtained with the high sulphate form of calcium sulphoaluminate are given in Table 3. The compound is found to be only slightly hydrolyzed in distilled water and is probably more stable in solutions of calcium sulphate and calcium hydroxide than in pure water. With sodium chloride and sodium sulphate there is a greater hydrolysis than in water.

With solutions of sodium carbonate and of magnesium sulphate the results were different. In these solutions the crystals of calcium sulphoaluminate were completely decomposed. In the magnesium sulphate solution, the residue consisted of crystals of gypsum and an amorphous material. The residue from the sodium carbonate solutions contained calcium carbonate as the only crystalline phase. The probable reactions may be represented in an incompleted form, as follows:

$$MgSO_4 + 3CaO.Al_2O_3.3CaSO_4.nH_2O \rightarrow CaSO_4 + Mg(OH)_2 + Al(OH)_3$$

$$Na_2CO_3 + 3CaO.Al_2O_3.3CaSO_4.nH_2O \rightarrow CaCO_3 + CaSO_4 + NaOH + Al(OH)_3$$

These are left unbalanced as an indication that they are not complete nor stoichiometric. Various other products will doubtless be present, as aluminates of calcium, magnesium, or sodium.

TABLE 3.—*High sulphate calcium sulphoaluminate placed in aqueous solutions for three weeks; residues then filtered off and examined under the microscope and solutions analyzed in some cases for CaO, Al_2O_3, and SO_3*

Solution used	In 100 ml of solution			Microscopic report	Remarks
	CaO	Al_2O_3	SO_3		
	g	*g*	*g*		
H_2O	0.0045	0.0012	0.0050	Contained the high sulphate needle-like crystals of calcium sulphoaluminate, unchanged.	Hydrolysis slight; condition of greatest stability.
0.17 per cent $Ca(OH)_2$ (saturated).	-------	None.	.0010		
3 per cent $CaCl_2$	-------	None.	(1)		
0.18 per cent $CaSO_4$ (saturated).	-------	None.	-------		
3 per cent NaOH	-------	-------	-------		
3 per cent NaCl	.0258	.0085	.0169	----do----	Hydrolysis pronounced.
30 per cent NaCl	.0268	.0097	.0205		
3 per cent $Na_2SO_4 \cdot 10H_2O$.	.0220	.0081	-------		
0.6 per cent $MgSO_4$	-------	-------	-------	No calcium sulphoaluminate present; gypsum crystals and amorphous material present.	Calcium sulphoaluminate does not exist in excess of these reagents.
1.2 per cent $MgSO_4$	-------	-------	-------		
3 per cent Na_2CO_3	-------	-------	-------	Calcium carbonate only crystalline phase present.	

[1] Small amount.

Blanks indicate "not determined."

The results obtained on placing the low sulphate form of calcium sulphoaluminate in the various solutions are given in Table 4. In water and in solutions of calcium sulphate, sodium sulphate, calcium chloride, and sodium chloride there is a tendency for this compound to change to the high sulphate form of calcium sulphoaluminate. This conversion proceeds less rapidly in a saturated solution of calcium hydroxide than in water and does not take place at all in a 3 per cent solution of sodium hydroxide. It would seem, therefore, that a high hydroxyl-ion concentration is one of the factors determining the stability of the low sulphate form of calcium sulphoaluminate. These results are to be expected on the basis of a consideration of the hydrolytic reactions involved. Thus, we may write the probable reactions, in aqueous solution, in the incompleted form

$$3CaO.Al_2O_3.CaSO_4.nH_2O + CaSO_4 \rightleftarrows 3CaO.Al_2O_3.3CaSO_4.nH_2O$$

and

$$3CaO.Al_2O_3.CaSO_4.nH_2O + H_2O \rightleftarrows 3CaO.Al_2O_3.3CaSO_4.nH_2O + Ca(OH)_2 + Al(OH)_3$$

An application of the mass law to these hypothetical reactions would indicate that the direction of the reaction would be thrown to the right by the addition of sulphates or calcium salts and to the left by the addition of hydroxyl-ion or aluminum salts.

TABLE 4.—*Low sulphate calcium sulphoaluminate placed in aqueous solutions for varying periods; residue filtered off and examined under the microscope*

Solution used	Time of contact	Microscopic and chemical report	Remarks
	Days		
H_2O	10	Consisted largely of the high sulphate calcium sulphoaluminate with some of original material; solution contained CaO, Al_2O_3, and trace of SO_3.	Changes rapidly to high sulphate form.
0.18 per cent $CaSO_4$ (Sat.).	10	Consisted entirely of long needles of high sulphate form.	
10 per cent Na_2SO_4. $10H_2O$.	10	Consisted largely of high sulphate form, some amorphous material; solution contained CaO, SO_3, and trace of Al_2O_3.	
3 per cent $CaCl_2$	10	Contained both high and low sulphate forms; no calcium chloraluminate present; solution free of SO_3 and Al_2O_3.	
10 per cent NaCl	10	Mostly the high sulphate form present; solution contained CaO, Al_2O_3, and SO_3.	
0.17 per cent $Ca(OH)_2$ (Sat.).	10	Almost entirely the low sulphate form with some needles of high sulphate sulphoaluminate.	Changes slowly to high sulphate form.
	40	About equal amounts of the two forms present.	
3 per cent NaOH	30	Only low sulphate form present	Condition of stability for low sulphate form.
	60		
0.6 per cent $MgSO_4$	30	Some gypsum, amorphous material	Decomposed by these solutions.
1.2 per cent $MgSO_4$	30	Gypsum and amorphous material	
3 per cent Na_2CO_3	30	Calcium carbonate only crystal phase present.	

This compound, like the high sulphate calcium sulphoaluminate, is decomposed by solutions of magnesium sulphate and sodium carbonate when these salts are present in excess.

It appears from these experiments that only the high sulphate form of calcium sulphoaluminate can be stable under the usual conditions in which a calcium sulphoaluminate may be formed in concrete. Even if a little of a low sulphate form were produced it would be converted more or less rapidly to the high sulphate form.

Chlorides and sulphates of sodium, calcium, and magnesium are the principal constituents present in sea water and "alkali" soil waters. It has been found that sodium sulphate and calcium sulphate solutions of any concentration react with all of the calcium aluminates to form calcium sulphoaluminate. In the case of calcium sulphate solution, no other reactions appear to take place. With sodium sulphate, however, there seems to be a preliminary reaction of the calcium aluminate and sodium sulphate to form calcium sulphate and sodium aluminate

$$3Na_2SO_4 + 3CaO.Al_2O_3 + 2H_2O \rightleftarrows 3CaSO_4 + Na_2O.Al_2O_3 + 4NaOH$$

The calcium sulphate thus formed reacts with the calcium aluminate which remains to form calcium sulphoaluminate, and the sodium aluminate hydrolyzes to sodium hydroxide and aluminum hydroxide

$$nCaSO_4 + 3CaO.Al_2O_3.nH_2O \rightleftarrows 3CaO.Al_2O_3.3CaSO_4.nH_2O$$

$$Na_2O.Al_2O_3 + nH_2O \rightleftarrows 2NaOH + 2Al(OH)_3$$

Since the calcium sulphoaluminate is stable in the presence of calcium sulphate, sodium sulphate, and sodium hydroxide solutions it will not be subsequently destroyed by the presence of these substances.

Still other reactions appear with magnesium sulphate solutions. Here, again, there is doubtless a preliminary reaction between magnesium sulphate and the calcium aluminate

$$3MgSO_4 + 3CaO.Al_2O_3 + nH_2O \rightarrow 3CaSO_4 + 2Al(OH)_3 + 3Mg(OH)_2$$

The products formed are calcium sulphate, aluminum hydroxide, and magnesium hydroxide, the latter being an amorphous, colloidal substance, highly insoluble in neutral or alkaline solutions. Due to the insolubility of the magnesium hydroxide, this preliminary reaction proceeds until practically all of the available magnesium sulphate has been used. It is only after the available magnesium sulphate has been almost completely precipitated in this first reaction that the calcium sulphoaluminate can be formed by the reaction of calcium sulphate with any remaining calcium aluminate.

This viewpoint was confirmed by the following experiments:

(*a*) Eight one-hundredths of a gram of tricalcium aluminate was added to 5 ml of 0.6 per cent (0.05 M) magnesium sulphate solution. A large quantity of calcium sulphoaluminate was formed, but no gypsum crystallized out. In this case the lime present was in excess of the amount required to precipitate all of the magnesia.

(*b*) Eight one-hundredths of a gram of tricalcium aluminate was added to 5 ml of 4.8 per cent (0.4 M) magnesium sulphate solution. No calcium sulphoaluminate was formed, but a large number of gypsum crystals were present. In this case the magnesium sulphate was present in excess.

(*c*) Five-tenths of a gram of tricalcium aluminate was added to 5 ml of 4.8 per cent magnesium sulphate solution. In this case both gypsum and calcium sulphoaluminate crystallized out. This amount of tricalcium aluminate gives an excess of lime, and in this case so much gypsum was formed that, even after the formation of the calcium sulphoaluminate, some crystals of gypsum remained in the solid phase.

With the other calcium aluminates it was necessary to vary the amount of the compound added to the magnesium sulphate solution because of the differences in lime content of these compounds. However, in each case it could be shown that the formation of calcium sulphoaluminate was dependent on the ratio of the lime content of the calcium aluminate to magnesium sulphate and not entirely on the original concentration of magnesium sulphate, as had been suggested by Shelton.[26]

[26] See footnote 13, p. 717.

V. RELATIVE STABILITY WITH CALCIUM CHLORALUMINATE

Friedel [27] demonstrated the existence of a calcium chloraluminate, a double salt containing tricalcium aluminate and calcium chloride. Since chlorides and sulphates generally occur together in sea water and "alkali" ground waters, it seemed desirable to examine the relative stability of this calcium chloraluminate and calcium sulphoaluminate. To do this three experiments were performed.

(*a*) Two hundred milliliters of a 2.0 per cent solution of calcium chloride and 200 ml of a saturated calcium sulphate solution were added to 500 ml of a calcium aluminate solution. This mixture contained initially approximately the same concentrations of sulphate and chloride ions. After a week the precipitate which had formed was found by microscopic examination to consist entirely of the high sulphate calcium sulphoaluminate. No calcium chloraluminate could be found. Qualitative examinations of the precipitate indicated the presence of a large amount of lime, alumina, and sulphate but only a trace of chloride.

(*b*) Some calcium chloraluminate was prepared by adding 200 ml of 2.0 per cent calcium chloride solution to 500 ml of calcium aluminate solution. After standing for a day a precipitate had formed which was identified by optical examination as calcium chloraluminate. About 0.5 g of this precipitate was allowed to remain in 200 ml of saturated calcium sulphate solution for three weeks. The precipitate was then found to be composed entirely of the high sulphate calcium sulphoaluminate.

(*c*) About 0.5 g of calcium chloraluminate was placed in 600 ml of a solution containing 0.6 per cent calcium chloride, 0.6 per cent calcium sulphate, and 0.6 per cent calcium hydroxide. After three weeks it was found that the calcium chloraluminate had been converted completely to the high sulphate calcium sulphoaluminate.

Thus, it seems that the product formed by the reaction of the calcium aluminates with solutions containing both chlorides and sulphates will be the high sulphate calcium sulphoaluminate. The calcium chloraluminate will not be formed until all or practically all of the available sulphate has been combined as the calcium sulphoaluminate.

VI. SUMMARY

From a review of the literature it appears that the formation of one calcium sulphoaluminate had been definitely established. The results of different workers show slight variations in the sulphate content and wide variations in the amount of water of crystallization of the compound, but, due to the similarity in optical properties,

[27] Bull. soc. franc. mineral., **26**, p. 121; 1903.

there is little doubt that the compounds described by these different workers are the same. The composition of the compound as reported had varied from $3CaO.Al_2O_3.2.5CaSO_4.aq$ to $3CaO.Al_2O_3.3CaSO_4.aq$.

Samples have been prepared in this laboratory by several methods, but that which has given most satisfactory results consists in the interaction of solutions of calcium sulphate and calcium aluminate, preferably with added calcium hydroxide. An analysis of the pure material indicates a composition which may be expressed by the formula $3CaO.Al_2O_3.3CaSO_4.31H_2O$. In the presence of dilute solutions of calcium sulphate, precipitates have been obtained which contain less than 3 mols of calcium sulphate to 1 mol of tricalcium aluminate. The ratio in some cases was of such a value that the composition of the precipitate could be expressed by the formula $3CaO.Al_2O_3.2.5CaSO_4.aq$. This ratio appears to vary with the concentration of the calcium sulphate in solution and indicates an equilibrium mixture of $3CaO.Al_2O_3.3CaSO_4.aq$ and $3CaO.Al_2O_3.aq$. As the concentration of calcium sulphate increases the amount of the hydrated calcium aluminate decreases and eventually disappears. This would explain the difference in composition assigned to this compound by different writers.

Microscopic examinations of some of the larger crystals have shown them to be long needle-like hexagonal crystals of refractive indices $\omega_D 1.464 \pm 0.002$, $\epsilon_D 1.458 \pm 0.002$, uniaxial negative in character and showing negative elongation. The specific gravity of this compound was found to be 1.48 at 20° C.

The existence of a new calcium sulphoaluminate, $3CaO.Al_2O_3.CaSO_4.12H_2O$, has been demonstrated. This compound has a lower sulphate content than the other form and may be distinguished by its higher indices of refraction $\omega_D = 1.504 \pm 0.002$, $\epsilon_D = 1.488 \pm 0.002$, and by a platy crystal habit, distinctly different from that of the high sulphate compound. In general, it may be said that this compound is unstable. Under conditions commonly encountered in concrete it is converted to the more stable form with the higher calcium sulphate content. This transformation is retarded by increasing hydroxyl-ion concentration, being slow in saturated calcium hydroxide solutions and apparently entirely prevented by a 3 per cent solution of sodium hydroxide. The specific gravity of this compound is 1.95 at 20° C.

The high sulphate calcium sulphoaluminate has been found to be slightly dissociated in water. This dissociation is somewhat repressed by solutions of calcium hydroxide and calcium sulphate and slightly increased by solutions of sodium chloride and sodium sulphate, but in all of these solvents the amount of lime, alumina, or sulphate going into solution is far less than the amount which will go into solution from a calcium aluminate or from calcium sulphate.

When carbonates are present, the lime liberated by hydrolysis of the calcium sulphoaluminates appears to be converted to the more insoluble compound, calcium carbonate. One product of the reaction being thus removed from solution, the hydrolysis proceeds until all of the calcium sulphoaluminate is decomposed, provided there is a sufficient amount of carbonate solution present. If a magnesium salt is present, the hydroxyl ions of the $Ca(OH)_2$ are removed by precipitation of magnesium hydroxide. Thus, it is apparent that in the presence of only a slight excess of soluble carbonates or magnesium salts the calcium sulphoaluminates will be entirely destroyed.

It has been shown that, when both sulphate and chloride solutions are present, the high sulphate calcium sulphoaluminate will be formed to the exclusion of calcium chloraluminate if there is sufficient calcium sulphate present to convert all of the calcium aluminate to calcium sulphoaluminate.

A tabulation of the formulas which have been reported for the calcium sulphoaluminates is given in Table 5, and a comparison of optical and crystallographic data is given in Table 6.

TABLE 5.—*Formulas reported for the calcium sulphoaluminates*

Authority	Date	Formula	Remarks
Lehman	1847	$6CaO.Al_2O_3.3SO_3.33H_2O$	The mineral Ettringite.
Candlot	1890	$3CaO.Al_2O_3.2.5CaSO_4.59H_2O$	Crystalline spherulites.
Michaelis	1892	$3CaO.Al_2O_3.3CaSO_4.30H_2O$	Broad, needle-shaped prisms.
Moses	1893	$10CaO.2Al_2O_3.5SO_3.54H_2O$	The mineral Ettringite.
Klinkenberg	1894	$2CaO.Al_2O_3.CaSO_4.12.49H_2O$	
Do	1894	$2CaO.Al_2O_3.2CaSO_4.18.25H_2O$	
Do	1894	$2CaO.Al_2O_3.3CaSO_4.19.55H_2O$	
Schott	1894	$2CaO.Al_2O_3.2CaSO_4.18H_2O$	
Rebuffat	1896	$3CaO.Al_2O_3.3CaSO_4.10H_2O$	This compound refuted in 1902.
Do	1896	$CaO.Al_2O_3.CaSO_4.10H_2O$	
Deval	1900	$3CaO.Al_2O_3.3CaSO_4.nH_2O$	
Rebuffat	1902	$3CaO.Al_2O_3.2.5CaSO_4.7H_2O$	
Poirson	1910	$3CaO.Al_2O_3.3CaSO_4.nH_2O$	
Klein and Phillips	1914	$3CaO.Al_2O_3.3CaSO_4.nH_2O$	Long, slender needles.
Kühl and Lafuma	1923	$3CaO.Al_2O_3.3CaSO_4.nH_2O$	
McIntire and Shaw	1925	$3CaO.Al_2O_3.3CaSO_4.nH_2O$	
Lerch, Ashton, and Bogue	1929	$3CaO.Al_2O_3.3CaSO_4.31H_2O$	Fine needle-like crystals.
Do	1929	$3CaO.Al_2O_3.CaSO_4.12H_2O$	Star-shaped spherulites.

TABLE 6.—*Comparison of crystal data on the calcium sulphoaluminates*

	Klein and Phillips	Shelton	Lerch, Ashton, and Bogue	
			High sulphate form	Low sulphate form
Formula	$3CaO.Al_2O_3.3CaSO_4.aq.$	Not given	$3CaO.Al_2O_3.3CaSO_4.31H_2O$.	$3CaO.Al_2O_3.CaSO_4.12H_2O$.
Habit	Long, slender needles often in spherulitic form.	Long needles and coarse prisms.	Long needles often in spherulitic form.	Hexagonal plates often in star-shaped groups of 4 to 8 plates.
Optical character.	Biaxial positive; large optic axial angle.	Biaxial positive	Uniaxial negative	Uniaxial negative.
Extinction	Parallel	Parallel	Parallel	Parallel.
Elongation	Negative	Negative	Negative	Positive.
Refractive indices.	Less than 1.48	α 1.461±0.003 γ 1.463± .003	ω_D=1.464±0.002 ϵ_D=1.458± .002	ω_D=1.504±0.002. ϵ_D=1.488± .002.
Birefraction	Low	0.002	0.006	0.016.

WASHINGTON, October 12, 1928.

AN ANALYSIS OF THE ARC AND SPARK SPECTRA OF YTTRIUM (Yt I AND Yt II)

By William F. Meggers and Henry Norris Russell

ABSTRACT

All the available data (wave-length measurements and intensity estimates, temperature classes, Zeeman effects) on yttrium lines have been correlated and interpretated in an analysis of the arc and spark spectra. The total number of lines classified is 448 in the Yt I spectrum, 223 in the Yt II spectrum, and 10 in the Yt III spectrum.

Series-forming terms have been identified in each of the spectra, and from these the ionization potentials of 6.5 volts for the neutral Yt atom, 12.3 volts for the Yt^{+} atom, and 20.6 volts for the Yt^{++} atom have been deduced.

Yttrium is a chemical analogue of scandium, and the corresponding spectra are now seen to be strikingly similar. A ^2D term (from a d electron) represents the lowest energy (normal state) of both Sc III and Yt III, and another ^2D (from the s^2d configuration) describes the normal state of Sc I and of Yt I. The configurations which do not contain a d-electron are much lower in Yt II than in Sc II; a consequence of the fact that the s and p states in Yt III are lower compared with the d state than in Sc III. This results in $^1S_0$ (s^2) as the normal state for Yt II, while it is ^3D (sd) for Sc II.

The analyses of Yt I and Yt II spectra are supported by measurements of Zeeman effects, which are interpreted with the aid of Landé's theory of Zeeman effects and multiplet structure. All details of the three spectra, Yt I, Yt II, and Yt III, are in accord with Hund's correlation of spectral terms with electron configurations.

CONTENTS

		Page
I.	Introduction	733
II.	The spectrum of doubly ionized yttrium (Yt III)	735
III.	The spectrum of singly ionized yttrium (Yt II)	737
IV.	The spectrum of neutral yttrium (Yt I)	745
V.	Theoretical interpretation of the spark spectra and comparison with scandium	759
VI.	A note on Sc II	761
VII.	Interpretation of the terms of Yt I	762
VIII.	Ionization potentials of yttrium atoms	767
IX.	Yttrium in the sun	768

I. INTRODUCTION

Last year the authors[1] published an analysis of the arc and spark spectra of scandium (Sc, Z=21), the lightest element exhibiting a spectrum of the type characteristic of the heavier metals in which

[1] Russell and Meggers, B. S. Sci. Paper, No. 558, 22, p. 329; 1927.

the lines are very numerous, multiplets are abundant, and series are inconspicuous. Yttrium (Yt, Z=39) is a chemical analogue of scandium; it occupies a corresponding position in the second long period of elements, and, since it has the same number and type of outer electrons, its spectral structures may be expected to resemble those of scandium. Such resemblances between homologous spectra are often very close (as for Ca and Sr, which immediately precede Sc and Yt). In other instances, however, there are minor but significant differences (mainly in the relative levels of the terms) which may prove of importance in the refinement of present atomic theories.

In the present paper the authors give the results of an extensive analysis of yttrium spectra in much the same manner as their results for scandium; the summary of recent theory and, except for a slight variation, the notation given in the earlier publication apply also to the present case.

The first regularities in yttrium spectra were found in 1914 by Popow,[2] who measured the Zeeman effects of certain lines and recognized two "compound triplets" of six lines each. These cover the intervals 3179–3242 A and 4199–4423 A; both are of the type ^3D–^3P and arise from ionized yttrium atoms. A larger number of lines with wave-number differences of 205, 405, and 1,847 cm^{-1} was listed by Paulson[3] in 1915. These differences express the separations of four low-energy levels in the Yt II spectrum now identified as a^3D_1, a^3D_2, a^3D_3, a^1D_2. Additional multiplets belonging to the Yt II spectrum, and the first regularities among arc lines (compound doublets in the Yt I spectrum) were published by Meggers[4] in 1924, and new observations of Zeeman effects enabled Meggers and Moore[5] to find the principal quartet-system multiplets in Yt I. Further extensions of the analyses of both spectra were published in 1926 by Meggers and Kiess,[6] who found singlet terms in Yt II and also intercombinations between the singlet and triplet terms of Yt II and between the doublet and quartet terms of Yt I.

The lowest terms then found were a doublet-D in Yt I and a triplet-D term in Yt II (resembling the normal terms of scandium). The complete analysis shows that the former corresponds to the normal state of neutral yttrium, while the normal state of the ionized atom is given by a singlet-S term about 0.1 volt lower in the energy diagram than ^3D. For the higher homologue, lanthanum, the normal states appear to correspond to ^2D for La I and to $^2F'$ for La II. These differences find a simple explanation on Hund's theory[7] of spectral structure.

---

[2] Popow, Ann. d. Physik, **45**, p. 163; 1914.
[3] Paulson, Astrophys. J., **41**, p. 72; 1915.
[4] Meggers, J., Wash. Acad. Sci., **14**, p. 427; 1924.
[5] Meggers and Moore, J., Wash. Acad. Sci., **15**, p. 207; 1925.
[6] Meggers and Kiess, J., Opt. Soc. Am., **12**, p. 417; 1926.
[7] Hund, Linienspektren und periodisches system der Elemente, Julius Springer, Berlin; 1927.

The preliminary classifications of yttrium lines were seriously handicapped by the lack of descriptive data. Although tables of wave lengths and intensity estimates in arc and spark spectra have been published by many observers, the lists, individually and collectively, still left much to be desired in the way of completeness and consistency. For these reasons the arc and spark spectra of yttrium were recently remeasured by one of us.[8] Many new lines were recorded in the infra-red where an interval of nearly 2000 A was added to the arc spectrum, and a critical differentiation of lines belonging, respectively, to the Yt I, Yt II, and Yt III spectra resulted from a comparison of line intensities in arc and spark sources. In addition to these new wave-length determinations the Zeeman effects for 220 lines were measured by one of us,[9] and the excellent separation of 451 yttrium lines into classes corresponding to their development with furnace temperatures has been recently published by King and Carter.[10] These new data have made it relatively easy to classify almost all the lines ascribed to yttrium atoms, to specify without ambiguity practically all of the spectral terms, and correlate them with electron configurations. It has been possible to establish and identify many high (third set) terms in both the Yt I and the Yt II spectra. In both spectra certain of these higher terms have been identified as the second members of series, the extrapolation of which lead to ionization potentials of 6.5 volts for neutral Yt atoms and 12.3 volts for Yt^+ atoms. The total number of classified lines in the various spectra is as follows: 448 in the Yt I spectrum, 223 in the Yt II spectrum, and 10 in the Yt III spectrum.

The detailed results will be presented, first, for Yt III, then for Yt II, and finally for Yt I, thus proceeding from the relatively simple (alkali) case of 1 valence electron to the 2-electron spectrum and lastly to the complex spectrum arising from the increased transition possibilities with the full complement of 3 electrons.

II. THE SPECTRUM OF DOUBLY IONIZED YTTRIUM (Yt III)

Yttrium belongs to the second long period in which electron orbits of the types $5s$, $5p$, and $4d$ are successively added to the completed krypton shell. In doubly ionized yttrium only one valency electron remains; in the normal state this electron is in a $4d$ orbit, which produces a ^2D term. The next lowest state corresponds to the $5s$ orbit, and higher states arise from $5p$, $6s$, $5d$, and $4f$ orbits. These terms and their combinations were published in 1926 by Bowen and Millikan,[11] who gave 165,289 as the term value for $^2D_2$. The terms

[8] Meggers, B. S. Jour. Research, **1** (RP12), p. 319; September, 1928.
[9] Meggers, B. S. Jour. Research, **1** (RP12), p. 319; September, 1928.
[10] King and Carter, Astrophys. J., **65**, p. 86; 1927.
[11] Bowen and Millikan, Phys. Rev., **28**, p. 923; 1926.

measured upward from the lowest energy level are shown in Table 1 and the combinations in Table 2.

The lines of doubly ionized yttrium are characterized by an enormous intensity difference in spark and arc. Whereas the estimated intensities of these lines in the spark spectrum range from 20 to 200 only the four strongest lines involving the low ^2D and ^2S terms have been observed in the 220-volt arc spectrum; these are 2367.25 (3), 2414.68 (5), 2817.03 (5), and 2945.92 (4).

The series limit 165,289 in the Yt III spectrum corresponds to an ionization potential of 20.4 volts for the Yt^{++} atom.

TABLE 1.—*Terms in the Yt III spectrum*

Configuration	Terms	Levels	
4*d*	4^3D_2	0.0	724.8
	4^3D_3	724.8	
5*s*	5^3S_1	7,466.2	
5*p*	5^3P_1	41,401.2	1553.5
	5^3P_2	42,954.7	
6*s*	6^3S_1	86,713.9	
5*d*	5^3D_2	88,378.8	198.3
	5^3D_3	88,577.1	
4*f*	4^3F_3	101,090.0	

Table 2 gives the known lines of this spectrum. No additions have been made in the present paper, but the wave-length measurements and intensity estimates are new except for the first two lines.

TABLE 2.—*Classified lines of Yt III*

λ	Intensity	ν (vac)	Terms
[1] 989.21	1	101,090.8	4^3D_2–4^3F_3
[1] 996.37	2	100,364.3	4^3D_3–4^3F_3
2,127.99	100	46,977.8	5^3P_1–5^3D_3
2,191.22	200	45,622.4	5^3P_2–5^3D_3
2,200.80	50	45,423.8	5^3P_2–5^3D_2
2,206.22	30	45,312.2	5^3P_1–6^3S_1
2,284.5	100	43,759.7	5^3P_2–6^3S_1
2,327.30	20	42,955.0	4^3D_2–5^3P_2
2,367.25	200	42,230.2	4^3D_3–5^3P_2
2,414.68	100	41,400.8	4^3D_2–5^3P_1
2,817.03	200	35,488.2	5^3S_1–5^3P_2
2,945.92	150	33,935.4	5^3S_1–5^3P_1

[1] Quoted from Bowen and Millikan, Phys. Rev., 28, p. 923; 1926.

Of the remaining groups which might be anticipated in this spectrum 4D–6S should lie near 1000 A, 6S–6P and 5D–4F near 8000 A, and 5D–6P beyond 9000 A. In the visible region the combinations 6P–6D, 6P–7S and 5D–5F may be anticipated—the first two a little short of 5600 A and the last near 3800 A—but all of these are probably very faint. Further extension of the spectrum is therefore likely to be difficult.

III. THE SPECTRUM OF SINGLY IONIZED YTTRIUM (Yt II)

In addition to the relatively small number of lines characteristic of Yt^{++} the spark spectrum of yttrium shows about 230 lines which are associated with Yt^{+}. Comparison of arc and spark spectrograms readily identifies most of these lines and divides them roughly into two classes. The strongest lines arise from combinations of low energy states with the next higher or middle set; they are generated with almost equal intensity in a 6-ampere, 220-volt arc and in a high-voltage condensed discharge and have nearly the same appearance in both sources. The second class of lines is very much enhanced upon passing from the arc to the spark. In the latter source, they are often decidedly hazy and shaded toward longer wave lengths. In the arc they are faint, and many do not appear at all in this source. The majority of these lines lie in the ultra-violet region; practically all of them have been identified as combinations between the second or middle set of terms and a higher or third set. Their hazy and unsymmetrical character suggests that, as in other spectra, these high terms correspond to larger electron "orbits" and are thus especially susceptible to Stark- and "pressure" effects. In scandium such lines were recognized by their strong enchancement at the negative electrode of the arc.[12]

In general, the structure of the Yt II spectrum parallels that of Sc II. Most of the strong lines represent combinations between $^3P'$, ^3D, $^3F'$ terms of low energy and a triad ^3P, $^3D'$, ^3F lying between 24,000 and 30,000 cm^{-1} higher. Two outstanding lines, 3327.89 (150 III E) and 4374.94 (300 III E), were described as singlet combinations by Meggers and Kiess,[13] who also called attention to two prominent unclassified lines, 3496.08 (150 III E) and 3633.13 (300 III E), suspected of involving singlet terms. The first two of these arise from a ^1D term, analogous to one in Sc II. The other two were at first puzzling, but it was later found that they arise from a ^1S term which lies 840.18 cm^{-1} below a^3D and defines the normal state of the ionized yttrium atom.

The singlet combination $a^1D_2 - z^1P_1$, 4127.57 (2), is abnormally faint in Yt II. In Sc II it is considerably stronger, though still the faintest in the triad to which it belongs.

The terms which have been identified in the Yt II spectrum are listed in Table 3. The term values are measured upward from the lowest known energy level, a^1S_0, which is undoubtedly the lowest in the ionized atom. Term symbols, relative values of the levels, separations of the sublevels of polyfold terms, and combinations with other terms are given in successive columns.

[12] Russell and Meggers, B. S. Sci. Papers No. 558, **22**, p. 331; 1927.
[13] Meggers and Kiess, J. Opt. Soc. Am., **12**, p. 425; 1926.

All the terms are confirmed by combinations with two or more levels, except b^1S_0 and b^1G_4, which depend on only a single line in each case. For the second of these the identification of the line, which is the strongest member of a "supermultiplet," is practically certain; for the first, it is probable, but not entirely assured.

TABLE 3.—*Relative terms in the Yt II spectrum*

Term	Level	Δν	Combinations	Term	Level	Δν	Combinations
a^1S_0	0.00		z^1P, y^1P, z^3P, y^3P, z^3D'.	y^1P_1	44,568.2		a^1S, a^1D, b^1D, f^1D, a^1P.
a^3D_1	840.18	204.91	z^3P, y^3P, z^3D', z^3F, z^1D', z^1F.	b^3D_1	54,955.6	76.4	z^3P, y^3P, z^3D', z^3F, z^1P, z^1D', z^1F?
a^3D_2	1,045.09	404.79		b^3D_2	55,032.0	613.4	
a^3D_3	1,449.88			b^3D_3	55,645.4		
a^1D_2	3,296.27		z^1P, y^1P, z^1D', z^1F, z^3P, y^3P, z^3D', z^3F.	c^1D_2	55,724.9		z^1P, z^1D', z^1F, y^1P, z^3D', z^3F.
$a^3F'_2$	8,003.12	324.80	y^3P, z^3D', z^3F, z^1P, z^1D', z^1F.	a^1S_1	58,261.7		z^3P, y^3P.
$a^3F'_3$	8,328.01	415.38		$a^1F'_3$	58,533.0		z^1D', z^1F, z^3P, y^3P?, z^3D', z^3F.
$a^3F'_4$	8,743.39			$b^3P'_0$	58,775.7	371.5	z^3P, y^3P, z^3D', z^3F?, z^1P, z^1D'.
$a^3P'_0$	13,883.47	134.86	y^3P, z^3D', z^1P, y^1P, z^1F.	$b^3P'_1$	59,147.2	522.4	
$a^3P'_1$	14,018.33	79.84		$b^3P'_2$	59,669.6		
$a^3P'_2$	14,098.17			a^3G_3	59,178.9	292.9	y^3P, z^3D', z^3F, z^1D'.
b^1D_2	14,832.91		z^1P, y^1P, z^1D', z^1F, y^3P, z^3D', z^3F.	a^3G_4	59,471.8	428.6	
a^1G_4	15,683.0		z^1F, z^3D'.	a^3G_5	59,900.4		
z^3P_0	23,445.10	331.16	a^3S, b^3S, b^3P', a^3D, b^3D, c^3D, d^3D, a^1S, a^1D, d^1D, a^1F'.	c^3D_1	58,719.7	226.9	z^3P, y^3P, z^3D', z^3F, z^1D', z^1F.
z^3P_1	23,776.26	870.92		c^3D_2	58,946.6	380.5	
z^3P_2	24,647.18			c^3D_3	59,327.1		
$z^1D'_2$	26,147.21		a^1P', a^1D, b^1D, c^1D, d^1D, e^1D, f^1D, a^1F', b^3F', a^3D, b^3D, c^3D, d^3D', a^3F', b^3F', a^3G.	b^1S_0	59,615.8?		$z'P$?
				$a^1P'_1$	59,715.4		z^1P, z^1D', z^3D', z^3F.
				d^1D_2	60,535.1		z^1P, z^1D', z^1F, z^3P, z^3F.
z^1P_1	27,516.71		a^1S, b^1S?, c^1S, a^1P', a^1D, b^1D, c^1D, d^1D, e^1D, f^1D, a^1P', b^3P', a^3D, b^3D, a^3F', (b^3F'??).	b^3S_1	61,200.2		z^3P, y^3P.
				$b^3F'_2$	61,336.7	313.8	z^3D', z^3F, (z^1P??), z^1D'.
				$b^3F'_3$	61,650.5	283.6	
z^3F_2	27,226.97	305.25	b^3P'?, a^3D, b^3D, c^3D, a^3F', b^3F', a^3G, a^1P', a^1D, b^1D, c^1D, d^1D, e^1D, a^1F'.	$b^3F'_4$	61,934.1		
z^3F_3	27,532.22	862.09		c^1S_0	61,367.3		z^1P, z^3D'.
z^3F_4	28,394.31			c^1D_2	62,495.2		z^1P, z^1D', z^3D', z^3F.
$z^3D'_1$	28,595.25	134.80	a^3P', b^3P', c^3P', a^3D, b^3D, c^3D, a^3F', b^3F', a^3G, a^1S, c^1S, a^1P', a^1D, b^1D, c^1D, e^1D, a^1F', a^1G.	b^1G_4	63,350.0		z^1F.
$z^3D'_2$	28,730.05	484.02		$c^3P'_0$	64,102.9	159.8	y^3P, z^3D'.
$z^3D'_3$	29,214.07			$c^3P'_1$	64,262.7	334.4	
y^3P_0	32,048.82	75.31	a^3S, b^3S, a^3P', b^3P', c^3P', a^3D, b^3D, c^3D, d^3D, a^3F', a^3G, a^1S, a^1D, b^1D, c^1D, d^1D, a^1F'?	$c^3P'_2$	64,597.1		
y^3P_1	32,124.13	159.45		d^3D_1	65,131.5	57.2	z^3P, y^3P, z^1D'.
y^3P_2	32,283.58			d^3D_2	65,188.7	86.3	
z^1F_3	33,336.74		a^1D, b^1D, c^1D, d^1D, a^1F', a^1G, b^1G, a^3P', a^3D, b^3D?, c^3D, a^3F'.	d^3D_3	65,275.0		
				f^1D_3	70,223.2		z^1P, y^1P, z^1D'.

Diagrams of the terms and combinations are reproduced in Figures 1 and 2, in which black dots represent singlet terms and circles triplet terms. Full lines represent singlet-singlet combinations, and

triplet-triplet, and broken lines singlet-triplet combinations. The resemblance to the corresponding diagram [14] for Sc II is striking.

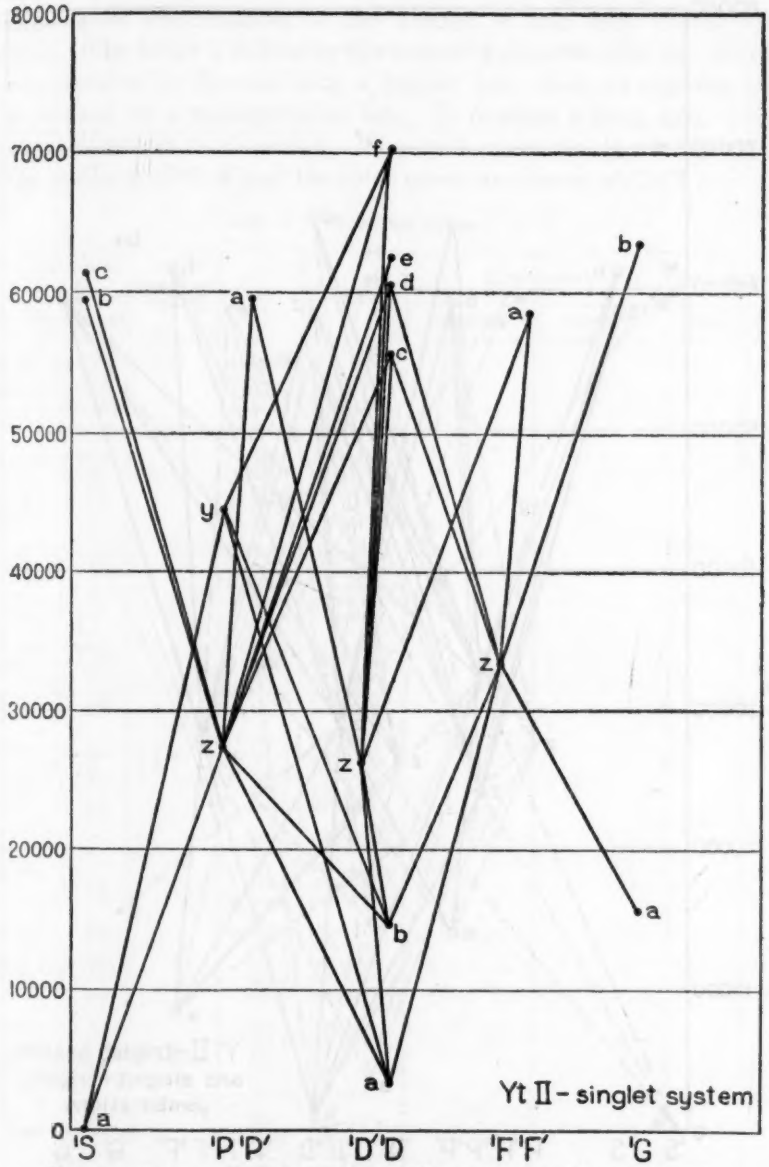

FIG. 1.—*Energy diagram for the Yt II spectrum singlet system only*
See Figure 2 for triplet system and singlet-triplet combinations

The complete data for all classified lines of ionized yttrium are given in Table 4, successive columns of which contain the wave

[14] Russell and Meggers, B. S. Sci. Papers No. 558, **22**, p. 334; 1927.

lengths, arc and spark intensities, arc intensities and furnace classes by King and Carter (loc. cit.), the vacuum wave numbers, the ob-

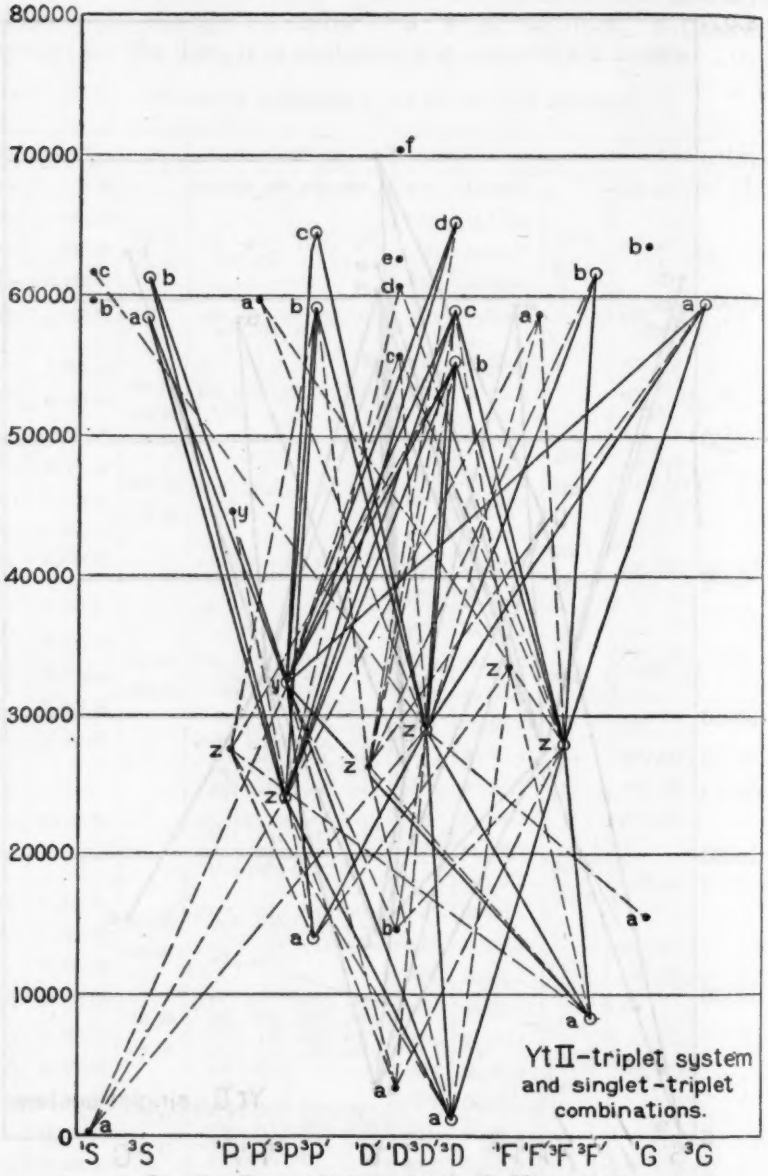

FIG. 2.—*Energy diagram for the Yt II spectrum*

Black dots represent singlet terms, circles triplet terms. Full lines represent triplet-triplet combinations, and broken lines singlet-triplet combinations. See Figure 1 for singlet system

served and theoretical Zeeman effects, and finally the intensities on Rowland's scale of those lines which appear in the spectra of the

sun's disk and of sun spots. The intensities and identifications of solar lines are taken from the Revision of Rowland's Table.[15] Those in the sun-spot spectrum have been newly assigned by one of us (HNR) from examination of the Mount Wilson map of the spot spectra. The letter b following the intensity denotes that the yttrium line is blended in the sun with a fainter line, while m signifies that it is masked by a stronger solar line. N denotes a hazy line; ? that the identification is doubtful. The spot spectrum is unobservable to the violet of 3900 A and the solar spectrum ceases at 2975 A.

TABLE 4.—*Classified lines of Yt II*

λ	Intensity M		Intensity Class K	ν	Terms	Zeeman effect		Solar intensity	
	Arc	Spark				Observed	Calculated	Disk	Spot
2,243.06	25	50		44,568.1	a^1S_0–y^1P_1				
2,268.14	—	2 h		44,075.3	$z^1D'_2$–f^1D_2				
2,340.8	1	10 h		42,707.3	z^1P_1–f^1D_2				
2,398.14	1	10 hl		41,686.3	z^3P_0–d^3D_1				
2,413.92	—	3 h		41,413.8	z^3P_1–d^3D_1				
17.4	1	5 h		354.2	z^3P_1–d^3D_1				
22.22	20	50		41,271.9	a^1D_2–y^1P_1				
60.62	2	20		40,627.9	z^3P_2–d^3D_2				
2,465.90	—	5 h		40,540.9	z^3P_2–d^3D_2				
2,564.3	—	1		38,985.3	$z^1D'_2$–d^3D_1				
2,734.98	—	4 h		36,552.5	z^3P_2–b^3S_1				
50.40	—	3 h		36,347.6	$z^1D'_2$–c^1D_2				
85.23	—	3		35,893.1	z^3P_1–$b^3P'_2$				
2,785.60	—	2		888.3	z^3P_2–d^1D_2				
2,800.11	—	4		702.4	z^3P_0–$b^3P'_1$				
13.61	—	4 h		531.1	$z^3D'_3$–$c^3P'_1$				
25.37	—	3 h		383.2	$z^3D'_3$–$c^3P'_2$				
26.38	1	5		370.6	z^3P_1–$b^3P'_1$				
34.57	—	5 h		268.4	z^3F_2–c^1D_2				
40.98	1	5 h		188.8	$z^1D'_2$–$b^3F'_3$				
42.5	—	1		170.0	z^3P_1–c^3D_2				
54.45	2	15	3 V E	35,022.8	z^3P_2–$b^3P'_2$				
56.32	1	6	1 V	34,999.8	z^3P_1–$b^3P'_0$				
58.06	1	4 h		978.5	z^1P_1–c^1D_2				
71.4	—	1 h		816.0	z^3P_0–a^3S_1				
97.70	1	5	1 V	500.0	z^3P_2–$b^3P'_1$				
2,898.93	1	3	tr V	485.4	z^3P_1–a^3S_1				
2,907.18	—	2		387.5	$z^1D'_2$–d^1D_2				
30.15	1	6 h		118.0	z^3F_3–$b^3F'_3$				
30.8	—	2 h		34,110.4	z^3F_2–$b^3F'_2$				
48.98	—	3 h		33,900.1	$z^3D'_1$–c^1D_2				
50.33	—	1 h		884.6	z^3P_2–$a^1F'_3$				
53.28	—	3 h		850.8	z^1P_1–c^1S_0				
56.04	1	5 h		819.2	z^1P_1–$b^3F'_2$				
57.39	—	2 h		803.8	z^3F_3–$b^3F'_2$				
74.02	1	5 h		614.7	z^3P_2–a^3S_1				
78.18	—	3 h		567.8	$z^1D'_2$–$a^1P'_1$				
80.7	2	20 hl	2 V E	539.4	z^3F_4–$b^3F'_4$				
2,982.20	—	2		522.5	$z^1D'_2$–$b^3P'_2$				
3,001.42	—	2		307.9	z^3F_2–d^1D_2				
06.0	1	2 hl		257.1	z^3F_4–$b^3F'_3$				
23.50	—	2 h		064.7	y^3P_1–d^3D_2				
26.5	2	10 hl		031.9	$z^1D'_2$–a^3G_3				
27.75	—	3		33,018.3	z^1P_1–d^1D_2				
30.2	1	4 h		32,991.5	y^3P_2–d^3D_3				
36.7	3	25 hl		920.9	$z^3D'_3$–$b^3F'_3$				
50.5	—	1 h		772.0	$z^3D'_1$–c^1S_0				
53.3	2	15 hl		742.0	$z^3D'_1$–$b^3F'_2$				
55.3	4	50 hl		720.5	$z^3D'_3$–$b^3F'_4$				
3,066.02	—	4 h		32,606.1	$z^3D'_2$–$b^3F'_2$				

[15] Papers of the Mount Wilson Observatory, **3**, Washington; 1928.

TABLE 4.—*Classified lines of Yt II*—Continued

λ	Intensity M		Intensity Class K	ν	Terms	Zeeman effect		Solar intensity	
	Arc	Spark				Observed	Calculated	Disk	Spot
3,069.26	—	5 h		32,571.7	$z^1D'_2$–c^3D_1				
77.14	—	4 h		488.3	z^3F_2–$a^1P'_1$				
78.64	—	4 h	2 V E	472.5	y^3P_1–$c^3P'_2$				
81.6	—	2 h		441.3	z^3F_2–$b^3P'_2$				
82.16	—	3 h		435.4	$z^3D'_2$–$b^3F'_3$				
86.9	5	30 hl	7 V	385.6	$z^1D'_2$–$a^1F'_3$				
93.76	1	10 h		313.8	y^3P_2–$c^3P'_2$				
3,095.88	3	5	25 V E	291.6	a^3D_3–z^1F_3			0m	
3,103.3	—	2 h		214.4	y^3P_0–$c^3P'_1$				
04.82	—	4 h		198.7	z^1P_1–$a^1P'_1$				
09.3	—	1		152.3	z^1P_1–$b^3P'_2$				
10.65	—	2 h		138.3	z^3F_2–$b^3P'_2$? y^3P_1–$c^3P'_1$				
12.05	2	4	18 V E	123.9	a^1S_0–y^3P_1			m	
14.45	—	10 h		32,099.1	z^3F_2–c^3D_3? z^1P_1–b^1S_0?				
26.16	—	4 h		31,978.9	y^3P_2–$c^3P'_1$ y^3P_1–$c^3P'_0$				
28.8	3	20 hl	5 V E	951.9	z^3F_2–a^3G_3				
30.0	5	40 hl	10 V E	939.7	z^3F_2–a^3G_4			−1Nm	
35.17	4	5	25 V E	887.0	a^3D_3–z^1F_3			−2	
44.37	—	2 h		793.7	z^3F_2–c^3D_3				
60.60	—	1 h		630.4	z^1P_1–$b^3P'_1$				
73.07	6	100 hl	10 V E	506.1	z^3F_4–a^3G_5	(0.00)—			
79.42	5	10	40 V E	443.2	a^3D_1–y^3P_2	(0.00)—	(**0.60**, 1.00) (0.50, 1.50, **2.50**)	m	
82.42	1	3 hl		413.6	z^3F_3–c^3D_2				
93.48	—	2 hl		304.8	z^3F_2–$a^1F'_3$				
95.62	25	50	100 III E	283.8	a^3D_1–y^3P_1	(0.95) 1.40	(1.00) 0.50, **1.50**	2 h	
3,198.5	—	2 h		255.6	z^3P_1–b^3D_2				
3,200.28	25	50	100 III E	238.3	a^3D_2–y^3P_2	(w) 1.26 B	(0.50) 1.33 B ur	2Nd m	
03.33	30	60	100 III E	208.5	a^3D_1–y^3P_0	(0.00) 0.46	(0.00) 0.50	1	
12.40	1	5 hl		120.4	$z^3D'_1$–$a^1P'_1$				
16.70	50	100	150 III E	31,078.8	a^3D_2–y^3P_1	(0.00) 0.98	(**0.08**) 1.00 A¹ur	1	
25.17	1	5 hl		30,997.2	z^3P_2–b^3D_3				
31.20	—	2 h		939.4	$z^1D'_2$–$b^3P'_2$				
32.00	—	3 h		931.7	z^3F_4–c^3D_3				
42.30	60	150	200 III E	833.4	a^3D_3–y^3P_2	(0.00) 1.18	(0.08) 1.17 A¹ur	1b	
80.91		? Ag	10 V E	470.6	$a^3P'_2$–y^3P_1				
82.51	—	2		455.7	$z^3D'_3$–$b^3P'_2$				
86.71	—	3 h		416.8	$z^3D'_2$–$b^3P'_1$				
3,293.9	—	3 h		350.4	$z^3D'_1$–c^3D_2?				
3,304.0	—	2 h		257.7	$z^3D'_3$–a^3G_4				
08.4	2	20 hl		217.4	$z^3D'_2$–c^3D_2				
12.5	—	4 hl		180.0	$z^3D'_1$–$b^3P'_0$				
18.6	1	4 hl		124.6	$z^3D'_2$–c^3D_1				
19.8	1	15 hl		113.7	$z^3D'_3$–c^3D_3				
27.89	50	100	150 III E	040.5	a^1D_2–z^1F_3	(0.00) 1.00	(0.00) 1.00	2	
30.9	2	20 hl	3 V E	30,013.3	z^1F_3–b^1G_4				
33.6	—	2 h		29,989.0	$z^3D'_2$–c^3D_1				
35.3	1	4 hl		964.7	$z^3D'_3$–a^3G_3				
62.00	4	30 hl	20 V E	735.7	b^1D_2–y^1P_1	(0.00) 1.10	(0.00) 1.00		
3,380.1	—	5 hl		576.5	$z^1D'_2$–c^1D_2				
3,409.9	1	4 hl		318.0	$z^3D'_2$–$a^1F'_3$				
29.4	—	3 h		29,151.3	y^3P_0–b^3S_1				
48.82	8	10	35 V E	28,987.1	a^1D_2–y^1P_1	(0.72) 1.20 Bw	(0.75) 1.25 B ur	0m	
57.1	1	4 hl		917.7	y^3P_2–b^3S_1				
61.0	2	20 hl	4 V ?	885.1	$z^1D'_2$–b^3D_2				
67.88	4	5	20 V E	827.8	a^1D_2–y^3P_1			−2 ?	
70.3	—	5 hl		807.7	$z^1D'_2$–b^3D_1				
3,496.08	40	80	150 III E	595.0	a^1S_0–$z^3D'_1$	(0.60) 0.62	(0.00) 0.50	0m	
3,508.0	2	8 hl		498.2	z^3F_3–c^1D_2				
44.0	1	3 hl		208.7	z^1P_1–c^1D_2				
3,549.02	50	100	150 III E	28,168.8	a^3D_2–$z^3D'_2$	(0.00) 1.52 A²	(**0.08**) 1.50 A² ur	2	

TABLE 4.—*Classified lines of Yt II*—Continued

λ	Intensity M		Intensity Class K	ν	Terms	Zeeman effect		Solar intensity	
	Arc	Spark				Observed	Calculated	Disk	Spot
3,556.1	1	5 hl		28,112.7	z^3F_3–b^3D_3				
3,584.53	60	100	150 III ? E	27,889.7	a^3D_1–$z^3D'_2$	(**0.00**, 0.60) 0.54, 1.15, **1.74**	(**0.00**, 0.67) 0.50, 1.17, **1.83**	2	
3,600.74	100	300	500 III E	764.2	a^3D_3–$z^3D'_3$	(0.00) 1.31	(0.00)? 1.33	3	
01.93	75	100	200 III E	755.0	a^3D_1–$z^3D'_1$	(0.00) 0.55	(0.00) 0.50	1	
05.4	2	10 hl		728.3	z^3F_2–b^3D_1				
11.06	100	200	400 III E	684.8	a^3D_2–$z^3D'_2$	(0.00) 1.16	(0.00) 1.17	2	
28.71	50	100	150 III E	550.2	a^3D_2–$z^3D'_1$	(**0.00**, 0.59) 0.58, 1.16, **1.72**	(**0.00**, 0.67) 0.50, 1.17, **1.83**	2	
33.13	100	200	300 III E	516.7	a^1S_0–z^1P_1	(0.00) 0.91	(0.00) 1.00	2	
35.4	3	20 hl		499.5	z^3F_3–b^3D_3			−1 ?	
43.4	1	3 hl		439.1	z^1P_1–b^3D_1				
50.45	—	2 h		386.1	y^3P_2–$b^3P'_2$				
64.62	100	150	200 III E	280.2	a^3D_3–$z^3D'_2$	(0.00) 1.50 A[3]	(0.08) 1.50 A[3] ur	2	
68.5	5	50 hl	3 V E	251.4	z^3F_4–b^3D_3			−1	
75.6	1	5 hl		198.7	z^1F_3–d^1D_2				
84.9	1	5 hl		130.1	$z^3D'_1$–c^1D_2				
89.2	—	2 h		098.5	y^3P_0–$b^3P'_1$				
3,696.6	3	25 hl		27,044.2	y^3P_2–c^3D_3				
3,703.3	1	5 hl		26,995.3	$z^3D'_2$–c^1D_2				
10.30	200	500	800 III E	944.4	a^3D_3–z^3F_4	(w) 1.15 A[1]	(0.06) 1.12 A[1] ur	3	
14.3	1	5 hl		915.3	$z^3D'_2$–b^3D_3				
17.0	1	7 hl		895.8	y^3P_2–a^3G_3				
21.4	3	4		864.0	y^3P_2–b^3P_1'				
27.0	2	20 hl		823.6	y^3P_1–c^3D_2				
47.55	30	40	20 III E	676.5	a^3D_1–z^1P_1	(0.44) 0.48, 0.94	(0.50) 0.50, 1.00	1	
58.9	1	3 hl		596.0	y^3P_1–c^3D_1				
74.33	150	300	200 III E	487.3	a^3D_2–z^3F_3	(0.00) 1.05	(0.04) 1.00 A[1] ur	3	
76.56	50	75	40 III E	471.6	a^3D_2–z^1P_1	(0.00) 1.31 A[3]	(0.04) 1.25 A[2] ur	1m	
82.3	5	50 hl		431.5	z^3D_2'–b^3D_3				
88.70	100	200	100 III E	386.8	a^3D_1–z^3F_2	(0.00) 0.82 A[3]	(0.04) 0.77 A[2] ur	2	
3,792.5	2	10 hl		360.4	z^3D_1'–b^3D_1				
3,800.9	2	15 hl		302.1	z^3D_2'–b^3D_2				
08.7	—	1 h		248.2	y^3P_2–a^1F_3'				
12.2	1	5 hl		225.5	z^3D_2'–b^3D_1				
13.8	—	2 hl		213.2	y^3P_0–a^3S_1				
18.34	40	60	20 III E	182.0	a^3D_2–z^3F_2	(0.36, **0.76**) 0.40, **0.79**, **1.20**, 1.57	(0.50, **1.00**) 0.17, **0.67**, **1.17**, 1.67	1	
24.8	1	5 hl		137.8	y^3P_1–a^3S_1				
32.89	50	100	30 III E	26,082.6	a^3D_2–z^3F_3	(0.66) 0.69, 0.90, **1.10**, **1.30**, 1.51, 1.72	(0.25, 0.50, **0.75**), 0.58, 0.83, **1.08**, **1.33**, 1.58, 1.84	m	
46.5	1	3 h		25,990.3	z^1F_3–c^3D_2				
48.2	?	8 hl		978.8	y^3P_2–a^3S_1				
72.3	?	5 hl		817.2	z^3D_3'–b^3D_2				
78.28	15	20	20 V ? E	777.3	a^1D_2–z^3F_2			2b	
3,896.8	1	10 hl		654.8	y^1P_1–f^1D_2				
3,930.66	15	15	10 V E	433.8	a^1D_2–z^1D_2'	(w) 1.06 B	(0.29) 1.08 B ur	0	
46.21	3	2		333.6	a^3F_2'–z^1F_3				
50.35	150	200	150 III E	307.1	a^3D_1–z^1D_2'	(**0.00**, 0.46) 0.45, 0.97, **1.49**	(**0.00**, 0.50) 0.50, 1.00, **1.50**	2	2
51.59	10	5	8 V E	299.1	a^1D_2–z^3D_1'	(w) 1.28 A[3]	(**0.00**, 0.50) 0.50, 1.00, **1.50**	0Nd	0
67.7	3	15 hl		196.4	z^1F_3–a^1F_3'				
82.59	100	150	100 III E	102.2	a^3D_2–z^1D_2'	(0.38) 1.03 B	(0.29) 1.08 B ur	3b	3b
3,997.43	1	1		25,009.1	a^3F_3'–z^1F_3				
4,064.99	2	2		24,593.4	a^3F_4'–z^1F_3				
4,124.91	20	15	20 III E	236.1	a^1D_2–z^3F_3	(0.00) 1.14	(0.04) 1.17 A[2] ur	0	0
27.57	2	2		24,220.5	a^1D_2–z^1P_1				
73.76	1	?		23,955.4	a^3F_3'–y^3P_2				
77.54	100	125	125 III E	930.8	a^1D_2–z^3F_2	(0.44) 0.90 B	(0.58) 0.84 B ur	3	3[1]m
4,199.27	10	5	8 V E	807.0	a^3D_1–z^3P_0	(0.00) 0.63, 1.51, **2.41**	(**0.00**, 1.00) 0.50, 1.50, **2.50**	−1	−1
4,204.69	20	10	20 V E	776.3	a^1S_0–z^3P_1	(0.00) 1.48		1	1
35.73	40	20	40 IV E	602.1	a^3D_2–z^3P_2			0	0
64.88	—	1 h		440.7	y^3P_2–c^1D_2				
4,279.3	2	5 hl		361.8	y^3P_2–b^3D_3				
4,309.62	70	50	125 III E	23,197.4	a^3D_3–z^3P_2	(w) 1.15 A[1]	(0.08) 1.17 A[1] ur	1b	1

TABLE 4.—*Classified lines of Yt II*—Continued

λ	Intensity M		Intensity Class K	ν	Terms	Zeeman effect		Solar intensity	
	Arc	Spark				Observed	Calculated	Disk	Spot
4,358.73	40	30	50 III E	22,936.0	a^3D_1–z^3P_1	(0.94) 0.48, **1.46**	(1.00) 0.50, 1.50	0m	1
64.01	2	?		908.3	y^3P_1–b^3D_2				
64.17	1	?		907.4	y^3P_0–b^3D_1				
74.94	200	300	300 III E	851.1	a^1D_2–z^1D_2'	(0.15) 0.95	(0.00) 1.00	2m	2
4,398.02	75	50	100 III E	731.1	a^3D_2–z^3P_1	{(**0.00**, 0.32) (**0.79**, 1.10, 1.41	{(**0.00**, 0.33) **0.83**, 1.17, 1.50	}1	1
4,422.59	50	40	80 III E	604.9	a^3D_1–z^3P_0	(0.00) 0.51	(0.00) 0.50	3m	m
4,465.4	—	10 hl		22,388.1	z^1F_3–c^1D_2				
4,607.94				21,695.6	z^1F_3–b^3D_2?				
4,682.32	30	20	20 V E	21,351.0	a^1D_2–z^3P_2	{(0.89) 0.52, (**0.95**, **1.40**, 1.84	{(0.50, **1.00**) 0.50, **1.00**, **1.50**, 2.00	}1 b	1 b
4,713.26	—	—	(1) H N R	21,210.8	a^3F_2'–z^3D_3'				
4,786.58	30	20	10 IV E	20,885.9	a^3F_3'–z^3D_3'	(0.65 w) 1.20 Bw	(0.63) 1.20 B ur	3 m	½ m
4,823.31	40	30	12 V E	726.9	a^3F_2'–z^3D_2'	{(0.46, **0.99**) 0.17, (**0.64**, **1.13**, 1.62	{(0.50, **1.00**) 0.17, **0.67**, **1.17**, 1.67	}−2	−3
54.87	100	150	70 V E	592.1	a^3F_3'–z^3D_1'	(0.00) 0.72	(0.04) 0.75 A² ur	1 b	1 b
81.44	2	2		480.0	a^1D_2–z^3P_1				
4,883.69	150	200	80 V E	470.6	a^3F_4'–z^3D_3'	(0.00) 1.11 A¹	(0.06) 1.12 A¹ ur	2	1
4,900.13	125	150	80 III E	401.9	a^3F_3'–z^3D_2'	(0.00) 0.97 A¹	(0.04) 1.00 A¹ ur	2	1
4,982.13	15	15 l	8 V E	20,066.2	a^3F_3'–z^3F_4	(w) 1.56 A³	(0.12) 1.50 A² ur	−2	
5,087.42	50	100 l	150 V E	19,650.9	a^3F_4'–z^3F_4	(0.00) 1.22	(0.00) 1.25	1	−1
5,119.12	10	20 l	15 V E	529.2	a^3F_3'–z^3F_3	{(**0.00**, 0.40) (1.39, **1.82**	{(**0.00**, 0.42, 0.83) (0.25, 0.67, 1.08, (1.50, **1.92**	}−1	
23.21	30	50 l	40 V E	513.6	a^3F_2'–z^3P_1	(0.00) 0.52 A¹	(0.08) 0.50 A¹ ur	0	−1
5,196.43	5	10 l	2 V E	238.6	a^3F_2'–z^1F_3				
5,200.42	40	60	60 V E	223.9	a^3F_3'–z^3F_3	(0.00) 0.72	(0.00) 0.67	0	0
05.73	50	80	80 V E	19,204.3	a^3F_3'–z^3F_3	(0.00) 1.07	(0.00) 1.08	0	0
5,289.82	4	5 l	4 V E	18,899.0	a^3F_3'–z^3F_2	(w) 1.73 A³	(0.21) 1.50 A² ur	−2	
5,320.78	2	4 l		789.0	a^3F_4'–z^3F_3			−2 N?	
5,402.78	20	50 l	20 V E	503.9	b^1D_2–z^1F_3	(0.00) 0.89	(0.00) 1.00	0	−1
73.40	10	20 l	10 V E	265.1	a^3P_1'–y^3P_2	(0.00) 1.48	(0.00) 1.50	−2	
80.75	10	15 l	8 V E	240.6	a^3P_0'–y^3P_1	(0.00) 1.48	(0.00) 1.50	−2	m
5,397.42	20	50	25 V E	185.3	a^3P_2'–y^3P_2	(0.00) 1.43	(0.00) 1.50	−3	m
5,509.91	30	30 l	40 V E	144.1	a^3F_2'–z^1D_2'	(0.45) 0.76 Bw	(0.58) 0.84 B ur	0 m	0 m
21.70	2	20	30 II +E	105.3	a^3P_1'–y^3P_1	(0.00) 1.46	(0.00) 1.50	−1 m	
44.61	15	10 l	25 III +E	030.5	a^3P_1'–y^3P_0	(0.00) 1.50	(0.00) 1.50	−2 m	−1m
5,546.02	8	10 l	3 V E	18,026.0	a^3P_2'–y^3P_1	(0.00) 1.46	(0.00) 1.50	−2	
5,610.36	1	2		17,819.2	a^3F_2'–z^1D_2'				
5,662.95	50	200	50 V E	653.8	a^1G_4–z^1F_3	(0.00) 0.98	(0.00) 1.00	1 m	2 m
5,728.91	10	10 l		450.5	b^1D_2–y^3P_2	(0.80) 1.27 Bw	(0.75) 1.25 B ur	−1 dm	
5,781.69	5	5 l	2 V E	17,291.2	b^1D_2–y^3P_1	{(**0.00**, 0.41) 0.73 A¹	{(**0.00**, 0.50) **0.50**, 1.00, 1.50		
6,613.74	25	20	15 V E	15,115.9	a^3P_2'–z^3D_3'	(0.00) 1.24 A¹	(0.08) 1.17 A¹ ur		
6,795.41	20	30	15 V E	14,711.8	{a^3P_1'–z^3D_2' a^3P_0'–z^3D_1'	}(—) 0.83	{(**0.00**, 0.33) **0.83**, 1.17, 1.50, (0.00) 0.50	}−2 d?	
6,832.49	3	4	1 V E	631.9	a^3P_2'–z^3D_2'			−3?	
58.25	3	5	1 V E	577.0	a^3P_1'–z^3D_1'				
6,896.00	5	10	3 V E	497.2	a^3P_2'–z^3D_1'	(—) 2.21	{(**0.00**, 1.00) (0.50, 1.50, **2.50**		
6,951.68	1	3	1 V E	14,381.1	b^1D_2–z^3D_2'				
7,193.74	1	1		13,897.2	b^1D_2–z^3D_3'				
7,264.19	7	10	8 IV E	762.5	b^1D_2–z^3D_1'				
7,332.97	1	2		633.3	a^3P_0'–z^1P_1				
7,388.46	1	1		530.9	a^1G_4–z^3D_3'				
7,406.23	1	2		498.4	a^3P_1'–z^1P_1				
7,450.32	5	5	5 III? E	13,418.6	a^3P_2'–z^1P_1				
7,881.90	20	10	10 V E	12,683.8	b^1D_2–z^3P_1				
8,066.20	3	?		12,394.0	b^1D_2–z^3F_2				
8,835.85	2	?		11,314.4	b^1D_2–z^1D_2'				

The term notation in Table 4 is in common use except for a minor variation in the term coefficients. The even terms have been denoted by the letters $a, b, c, \ldots\ldots, a$ being at the lowest level; the odd terms by $z, y, x \ldots\ldots, z$ being the lowest. This is the only departure from previous custom; it has been adopted on account of the danger of confusion in writing or printing between such combinations as a^4F'–b^4F and a^4F–b^4F'.

The symbols accompanying intensities and Zeeman effects are those generally understood; their meanings are completely defined in the paper describing the observations on yttrium spectra [16] except for *ur*, which appears with some of the theoretical Zeeman effects in the last column. This symbol indicates that the magnetic components are unresolved, and the theoretical separations of such fused groups of components are assumed to be increased or decreased by one-fourth the distance from the strongest to the weakest in Back's [17] A^1 and A^2 types, respectively. This rule was found by Russell [18] to fit the measurements of unresolved Zeeman effects in titanium spectra; it also holds remarkably well for the yttrium spectra presented in Tables 4 and 6. Some of the resolved patterns give evidence that there are slight deviations from the Landé g values, but a detailed discussion of these should be based on measurements of higher precision. Very few enhanced lines remain unclassified. Those with intensity greater than 2 in the spark are as follows:

λ	Intensity		ν
	Arc	Spark	
3,407.7	—	3h	29,336.9
4,734.52	—	5h	21,115.6
4,829.36	—	10h	20,700.9

The last two may possibly represent 6P–6D of Yt III, but unfortunately this can not be established at present. King and Carter (loc. cit.) published a line at 3,847.87 (15 IV? E) which is probably an error, since this line has never been recorded by other observers.

IV. THE SPECTRUM OF NEUTRAL YTTRIUM (Yt I)

The normal state of the neutral atom is represented by a doublet-D term with separation of 530 wave numbers. Transitions between this and higher terms account for most of the lines of Classes I and II which King and Carter (loc. cit.) have found to be strong in the furnace at low temperatures. No absorption data for these lines exist except in the solar spectrum, where many of them appear strengthened

[16] Meggers, B. S. Jour. Research, 1 (RP12), p. 319; September, 1928.
[17] Back, Zeitschr. f. Phys., 15, p. 212; 1923.
[18] Russell, Astrophys. J., 66, p. 308; 1927.

in the sun spots. A low quartet F′ term combining with a triad ^{4}D′, ^{4}F, ^{4}G′ accounts for a considerable number of strong lines of Classes II and III. The companion ^{4}P′ term gives several good multiplets. The remaining terms of the low-energy set which have been identified are ^{2}D, ^{2}F′, and ^{2}G. A ^{2}P term belonging to the middle set lies lower than any of these and a triad ^{4}P, ^{4}D′, ^{4}F somewhat higher. These combine with many high terms of the third set and greatly extend the list of classified lines. They also combine with the fundamental ^{2}D term to give important lines in the red and infra-red. The observations of Zeeman effects, which revealed intersystem combinations, were helpful in unraveling these tangles.

Table 5, which is arranged similarly to Table 3, gives the terms which have been identified in the arc spectrum of yttrium. A few isolated levels are denoted by 1, 2, 3, . . . ; these are probably portions of terms of which the remainder could not be identified. The subscripts denote the inner quantum number; for ease of printing and reading whole numbers a half unit larger than the true j values for levels of even multiplicities are used.

TABLE 5.—*Relative terms in the Yt I spectrum*

Term	Level	Δν	Combinations	Term	Level	Δν	Combinations
a^3D_2	0.0	530.5	z^3P, y^3P, z^3P, w^3P, z^3D', y^3D', z^3D', w^3D', v^3D', z^3F, y^3F, x^3F, w^3F, v^3F, z^3G', y^3G', z^3S', z^1P, y^1P, z^1D', y^1D', x^1D', z^1F, y^1F, z^1G'.	$z^3D'_2$	16,146.1	−80.1	b^3P', c^3P', a^3D, c^3D, d^3D, c^1P', a^1D, b^1D, d^1D, b^1F', c^1F', d^1F', a^1G, (3_4).
a^3D_3	530.5			$z^3D'_3$	16,066.0		
				$z^1D'_1$	16,435.8		
				$z^1D'_2$	16,597.3	161.5	c^1P', d^1P', a^1D, b^1D, c^1D, b^1F', c^1F', d^1F', f^1F', a^1G, b^3P', c^3P', a^3D, c^3D, (3_4).
z^3P_1	10,529.2	830.5	a^3S, b^3S, c^3S, b^3P', c^3P', a^3D, c^3D, d^3D, e^3D, b^1P', c^1P', a^1D, d^1D, $b^1F'?$, (1_3), $(2_{3,1})$.	$z^1D'_3$	16,816.6	219.3	
z^3P_2	11,359.7			$z^1D'_4$	17,116.3	299.7	
$a^4F'_2$	10,937.4	141.2	y^1P, y^1D', y^1F, z^1G', z^3D', w^3D', y^3F, z^3F, z^3G'.	a^3G_4	18,512.4	−13.2	z^3F, w^3F, v^3F, z^3G', y^3G', z^3H, y^1F.
$a^4F'_3$	11,078.6	199.4		a^3G_5	18,499.2		
$a^4F'_4$	11,278.0	254.1		z^1P_1	18,976.3	51.2	b^1P', c^1P', d^1P', a^1D, b^1D, d^1D, $b^3P'?$, a^3D, c^3D, e^3D.
$a^4F'_5$	11,532.1			z^1P_2	19,027.5	120.5	
z^4F_2	14,949.0	296.8	a^4D, b^4D, c^4D, d^4D, b^4F', c^4F', d^4F', a^4G, b^2P', c^2P', a^2D, c^2D, d^2D, (3_4).	z^1P_3	19,148.0		
z^4F_3	15,245.8	466.6		$a^3P'_1$	19,237.7	168.4	z^3S', z^3D', v^3D'.
z^4F_4	15,712.4	522.1		$a^3P'_2$	19,406.1		
z^4F_5	16,234.5			z^3F_2	21,528.6	386.8	a^3D, c^3D, d^3D, e^3D', d^1D, c^1F', $d^1F'?$, (1_4).
$a^4P'_1$	15,221.7	107.3	z^4S', y^4P, y^4D', z^4D', z^4G', w^2P, z^2D', w^2D', z^2F, z^2G', y^2G'.	z^3F_4	21,915.4		
$a^4P'_2$	15,329.0	147.7		$y^1D'_2$	24,131.2	615.4	a^3D, d^3D.
$a^4P'_3$	15,476.7			$y^1D'_3$	24,746.6		
$a^3F'_3$	15,326.8	537.6	z^1P, x^1D', w^1D', v^1D', z^1F, w^1F, z^1G', y^1G', z^1S', y^1P, y^1D', x^1D', $y^1F?$, z^1G'.	y^3F_3	24,518.8	380.7	a^3D, a^1F', (1_3).
$a^3F'_4$	15,864.4			y^3F_4	24,899.5		
b^3D_2	15,994.0	164.8	z^3P, w^3P, z^3D', w^3D', z^3F, w^3F, $v^3F?$, z^3G', y^3G', y^4P, y^4D', z^4D'.	y^3P_1	24,698.8	−218.2	b^3S, a^3D, d^3D, $(2_3, 1)$.
b^3D_3	16,158.8			y^3P_2	24,480.6		

TABLE 5.—*Relative terms in the Yt I spectrum*—Continued

Term	Level	Δν	Combinations	Term	Level	Δν	Combinations
z^4P_1	27,824.5	315.1	a^2D, b^2D. a^2F'.	$x^4D'_1$	35,816.7	319.0	a^4P', e^4P', a^2D, b^2D, a^2F'.
z^4P_2	28,139.6			$x^4D'_2$	36,135.7	−74.7	
$z^4G'_3$	28,694.0	294.9	a^4P', a^4F', d^4F', e^4F', a^2D, a^2F'.	$x^4D'_3$	36,061.0	300.3	
$z^4G'_4$	28,988.9	375.3		$x^4D'_4$	36,361.3		
$z^4G'_5$	29,364.2	456.2		d^2D_2	36,420.5	10.5	z^2P, y^2P, z^2D', y^2D', z^2F, z^4F.
$z^4G'_6$	29,820.4			d^2D_3	36,431.0		
$b^4F'_2$	29,272.0	148.3	z^4D', z^4F, $z^2P?$, z^2D'.	$w^2D'_2$	36,452.3	166.2	a^2D, b^2D, a^2F', a^4P', a^4F'.
$b^4F'_3$	29,420.3	193.3		$w^2D'_3$	36,618.5		
$b^4F'_4$	29,613.6	229.0		$z^4S'_2$	36,750.8		a^4P', a^2D, a^2F'.
$b^4F'_5$	29,842.6			y^4P_1	37,039.5	109.0	a^4P', e^4P', a^4F', a^2D, b^2D, a^2F'.
y^4F_2	31,508.4	171.6	a^4F', d^4F', e^4F', a^2D, $a^2F'?$, a^2G.	y^4P_2	37,148.5	327.5	
y^4F_3	31,680.0	229.2		y^4P_3	37,476.0		
y^4F_4	31,909.2	278.9		w^2P_1	37,279.3	−35.6	a^2D, b^2D, a^4P'.
y^4F_5	32,188.1			w^2P_2	37,243.7		
a^2S_1	31,671.6		z^2P.	w^2F_3	37,412.9	206.9	a^2D, b^2D, a^2F', a^2G.
$b^4P'_1$	31,977.5	113.5	z^4P, z^2P.	w^2F_4	37,619.8		
$b^4P'_2$	32,091.0	275.3		z^2H_3	37,588.2	379.0	a^2G.
$b^4P'_3$	32,366.3			z^2H_4	37,967.2		
a^4D_1	33,148.3	89.5	z^4P, z^4D', z^4F, z^2P, z^2D'.	b^4D_1	38,469.9	73.8	z^4P, z^4D', z^4F, z^2D'.
a^4D_2	33,237.8	173.7		b^4D_2	38,543.7	131.7	
a^4D_3	33,411.5	341.2		b^4D_3	38,675.4	190.2	
a^4D_4	33,752.7			b^4D_4	38,865.6		
$y^4D'_1$	33,215.4	49.9	a^4P', a^4F', a^2D, b^2D, a^2F'.	$y^2G'_4$	38,479.0	117.7	a^2D, b^2D, a^2F', a^2G, a^4P'.
$y^4D'_2$	33,265.3	92.3		$y^2G'_5$	38,590.7		
$y^4D'_3$	33,357.6	256.9		a^4G_3	38,635.6	126.4	z^4D' z^4F, z^2D'.
$y^4D'_4$	33,614.5			a^4G_4	38,762.0	187.3	
$z^2G'_4$	33,432.3	356.5	a^2D, b^2D, a^2F', a^2G, a^4P', a^4F'.	a^4G_5	38,949.3	273.7	
$z^2G'_5$	33,788.8			a^4G_6	39,223.0		
z^4F_3	33,608.2	421.6	a^2D, b^2D, a^2F', a^2G, a^4P', a^4F'.	$c^4F'_2$	39,446.3	118.7	z^4D', z^4F z^2D', z^2F.
z^4F_4	34,029.8			$c^4F'_3$	39,565.0	192.8	
$b^2P'_1$	33,613.2	229.1	z^2P, z^2D', $z^4P?$, z^4D', z^4F.	$c^4F'_4$	39,757.8	206.0	
$b^2P'_2$	33,842.3			$c^4F'_5$	39,963.8		
$z^2D'_2$	33,906.8	340.9	a^2P', a^2D, b^2D, a^2F', a^4P', a^4F'.	$d^4P'_1$	----------		
$z^2D'_3$	34,247.7			$d^4P'_2$	40,455.1	62.0	z^4P, z^4D'.
$c^4P'_1$	33,911.5	244.3	z^4P, z^4D', z^2P, z^2D'.	$d^4P'_3$	40,517.1		
$c^4P'_2$	34,155.8	365.4		$z^2D'_2$	40,636.3	36.1	a^2P', a^2D, a^2F'.
$c^4P'_3$	34,521.2			$z^2D'_3$	40,672.4		
c^2D_2	34,231.2	26.2	z^2P, z^2D', z^2F, z^4P, z^4D', z^4F.	e^2D_2	42,655.8	414.0	z^2P, $z^2F?$, z^4P.
c^2D_3	34,257.4			e^2D_3	43,069.8		
$z^2S'_1$	34,438.2		a^2P'.	b^2S_1	42,685.5		z^2P, y^2P.

TABLE 5.—*Relative terms in the Yt I spectrum*—Continued

Term	Level	Δν	Combinations	Term	Level	Δν	Combinations
z^2F_3	42,857.9	136.9	a^2D, b^2D?, a^2G.	d^4D_1	44,660.2	88.1	
z^2F_4	42,994.8			d^4D_2	44,748.3	260.0	z^4P, z^4F, z^2P, z^2D', z^2F.
$d^4F'_2$	43,095.7	241.8	z^4D', z^4F, y^4F, z^4G', z^2D', z^2F?.	d^4D_3	45,008.3	195.7	
$d^4F'_3$	43,337.5	366.9		d^4D_4	45,204.0		
$d^4F'_4$	43,704.4	486.1		$f^4F'_2$	44,742.6?	326.7?	
$d^4F'_5$	44,190.5			$f^4F'_3$	45,069.3	319.2	z^4D'.
c^2S_1	43,643.9		z^2P.	$f^4F'_4$	45,388.5	408.0	
$e^4F'_2$	----------			$f^4F'_5$	45,796.5		
$e^4F'_3$	44,053.0?	312.7?	y^4F, z^4G'.	$c^2P'_1$	45,947.5	46.5	z^2P, z^2D', z^4D', z^4F.
$e^4F'_4$	44,365.7	393.9		$c^2P'_2$	45,994.0		
$e^4F'_5$	44,759.6			$e^4P'_1$	----------		
c^4D_1	----------			$e^4P'_2$	----------		y^4P, x^4D'.
c^4D_2	----------		z^4D', z^4F.	$e^4P'_3$	50,254.0		
c^4D_3	44,655.0	267.1		1_3	37,074.1		z^2P, z^2F, y^2F.
c^4D_4	44,922.1			$2_{2,1}$	44,984.5		z^2P, y^2P.
				3_4	45,663.5		z^2D', z^4D', z^4F.

The terms and combinations are represented diagramatically in Figures 2 and 3, where black dots represent doublet terms and circles quartet terms. Full lines represent doublet-doublet combinations and quartet-quartet, and broken lines doublet-quartet combinations. These diagrams are again very similar to those for scandium.

In Table 6 complete details for all classified Yt arc lines are given in the same arrangement and with the same notation as in Table 4. Most of the lines are taken from Meggers's[19] paper, but it appears that the 220-volt arc employed for these measurements produced a large percentage of ionized atoms and on this account failed to generate the fainter arc lines with appreciable intensity. The list is therefore supplemented by faint lines from Eder's list (labeled E), some from Exner and Haschek's table (E and H), and a number which were found and measured by one of us (HNR) on the spectrograms made by King and Carter (loc. cit.). All of these are in good agreement with the combinations of well-established terms and may, therefore, be regarded as true arc lines of yttrium. The line 5556.43 A, classified as z^4F_3–a^4D_2, is abnormally strong in the furnace spectrum and is given by King and Carter as of Class IA. The arc line agrees both in intensity and position with the assigned place in the multiplet. If the furnace line is due to yttrium, it indicates the existence of a

[19] Meggers, B. S. Jour. Research, 1 (RP 12), p. 319; 1928.

rather low middle level which gives no other levels and for which no theoretical place can be found. It appears probable that it is due to some impurity.

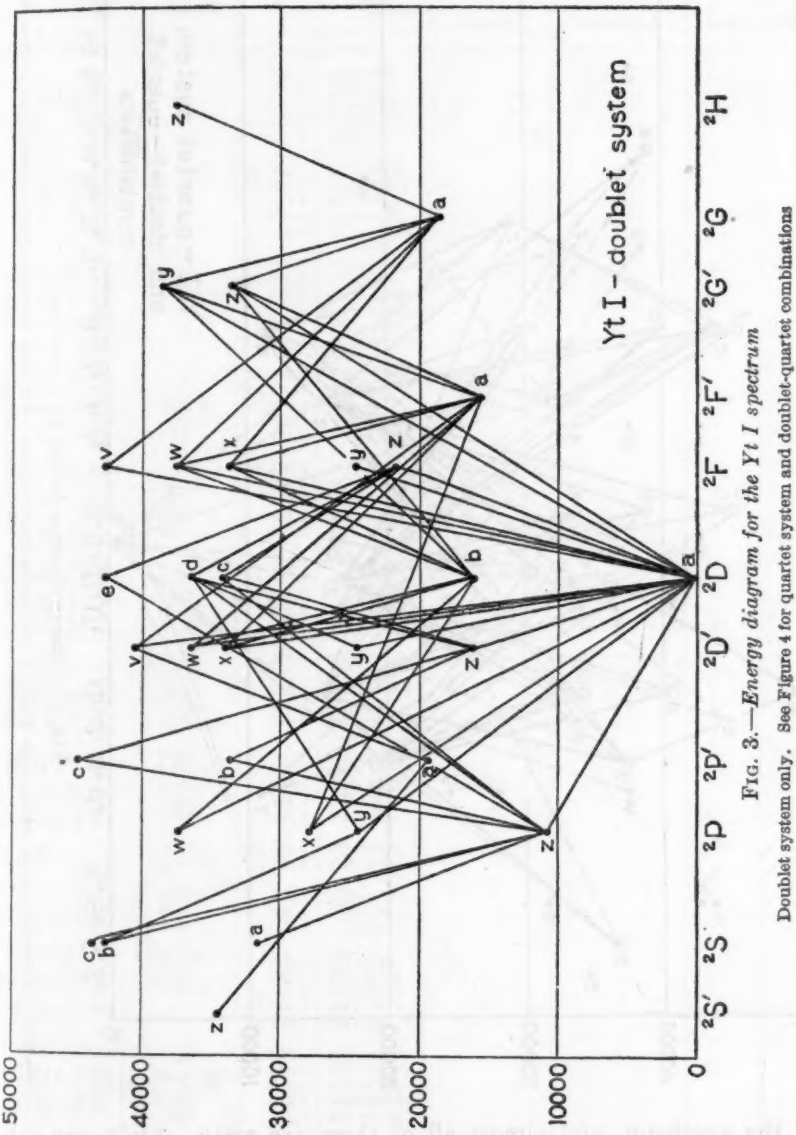

FIG. 3.—*Energy diagram for the Yt I spectrum*

Doublet system only. See Figure 4 for quartet system and doublet-quartet combinations

The discordance between observed and calculated Zeeman effects for 3 lines, 4484, 5424, and 5468 A, casts doubt upon the reliability of the observations in these 3 cases.

The stronger arc lines of yttrium which remain unclassified are listed in Table 7. They are not numerous considering the complexity

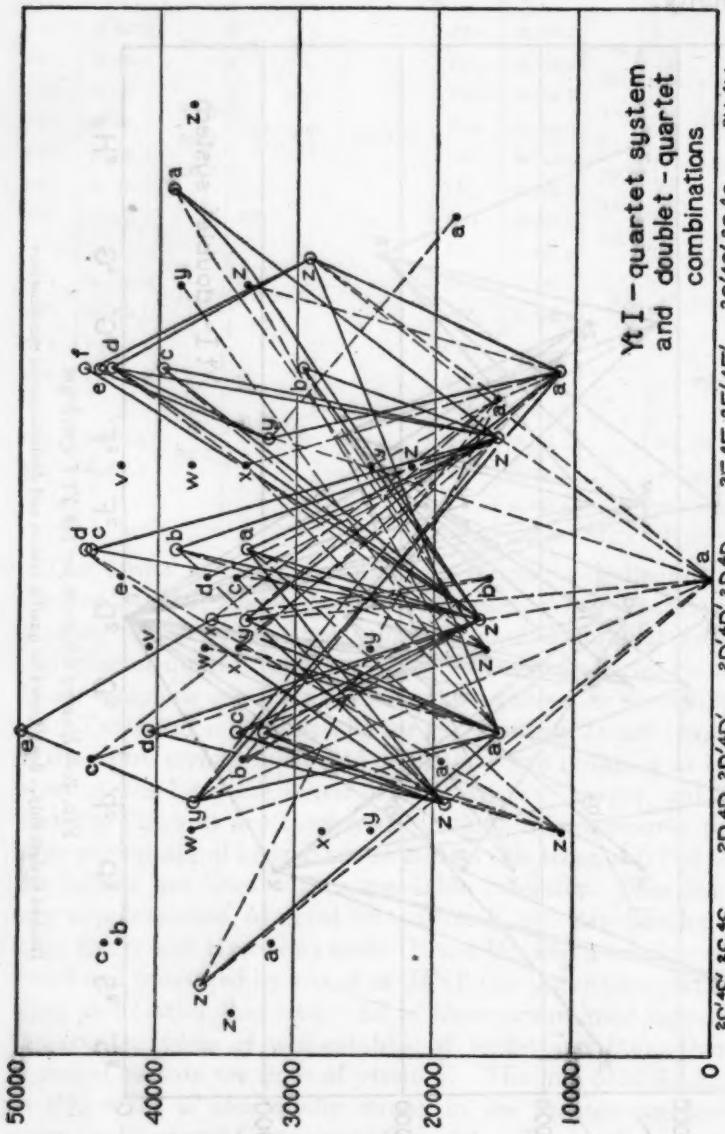

FIG. 4.—*Energy diagram for the Yt I spectrum*

Black dots represent doublet terms, as in Figure 3, and circles quartet terms. Full lines represent quartet-quartet and broken lines doublet-quartet combinations. See Figure 3 for doublet system

of the spectrum, and almost all of them are weak. Only one line (3587.75 A) reaches the intensity 20 on King's scale or 5 on Meggers's.

TABLE 6.—*Classified lines of Yt I*

λ	Intensity M	Intensity Class K	ν	Terms	Zeeman effect		Solar intensity	
					Observed	Calculated	Disk	Spot
2,332.58	(2 E)		42,857.8	a^3D_3–e^3F_3				
54.20	(3 E)		464.3	a^3D_3–e^3F_4				
2,361.81	(2 E)		42,327.5	a^3D_2–e^3F_2				
2,457.93	(½ E)		40,672.3	a^3D_2–$e^3D'_3$				
60.11	(1 E)		636.3	a^3D_2–$e^3D'_2$				
2,490.4	1		40,142.1	a^3D_2–$e^3D'_3$				
2,634.32	(1 E)		37,949.2	a^3D_3–$y^3G'_4$				
72.08	(1 E)		412.9	a^3D_3–e^3F_3				
81.65	(1 E)		279.4	a^3D_3–w^3P_1				
84.20	(½ E)		244.0	a^3D_3–y^4P_3				
2,695.40	(1 E)		37,089.2	a^3D_3–w^3F_4				
2,705.85	(1 E)		36,946.0	a^3D_3–y^4P_2				
23.00	(3 E)		713.3	a^3D_3–w^3P_2				
30.06	(1 E)		618.4	a^3D_2–$w^3D'_3$ a^3D_3–y^4P^3				
42.55	(3 E)		451.7	a^3D_2–$w^3D'_2$				
60.10	(3 E)		36,219.9	a^3D_3–$z^4S'_2$				
2,791.20	(1 E)		35,816.3	a^3D_2–$z^4D'_1$				
2,807.66	(1 E)	1 III A	606.4	a^3D_3–$z^4D'_2$				
13.64	(1 E)	8 III	531.1	a^3D_2–$z^4D'_3$				
18.87	(1 E)	3 IV	464.8	z^3P_1–$c^3P'_2$				
22.56	(1 E)	10 IV	35,418.4	z^3P_1–$c^3P'_1$				
86.49	(2 E)	15 III	34,634.0	z^3P_2–$c^3P'_2$				
2,890.40	(1 E)	3 IV	587.2	z^3P_2–$c^3P'_1$				
2,901.48	(1 E)	6 III	455.1	z^3P_1–$(2_{2,1})$				
09.05	3	20 II	247.7	a^3D_2–$z^4D'_3$				
29.00	(1 E)		34,131.4	z^3P_1–d^3D_1				
48.39	5	30 II	33,906.9	a^3D_3–$z^4D'_2$				
64.96	5	30 II	717.5	a^3D_3–$z^4D'_3$				
74.59	6	35 II	608.2	a^3D_2–z^4F_2				
84.25	10	50 II	499.5	a^3D_3–z^4F_4			−3?	
95.26	1	10 III	376.4	a^3D_2–$z^4D'_2$				
2,996.94	2	20 III	357.7	a^3D_2–$y^4D'_3$			−2m	
3,005.26	1	12 III	265.4	a^3D_3–$y^4D'_2$				
18.95	(2 E)	6? III	114.5	z^3P_1–c^3S_1				
21.74	2	15 II	083.9	a^3D_3–$y^4D'_4$				
22.28	2	12 II	33,077.9	a^3D_3–z^4F_3				
38.46	(1 E)	4 III A	32,901.9	a^3D_3–$z^4G'_4$				
45.36	4	20 II	827.3	a^3D_2–$y^4D'_3$				
3,096.57	(1 E)	3 III	284.5	z^3P_2–$c^3S'_2$				
3,108.86	(2 E)	5 III	156.8	z^3P_1–b^3S_1			0m	
11.80	1	15 III	32,126.5	z^3P_1–e^3D_2			2?m	
52.67	(2 E)	15 n III	31,710.0	z^3P_2–e^3D_3				
55.62	(1 E & H)	3 III A	680.4	a^3D_2–y^4F_3				
72.85	(1 E & H)	4 III A	508.3	a^3D_3–y^4F_3				
85.93	(1 E)	2 III A	379.0	a^3D_3–y^4F_4				
91.34	2	15 III	326.0	z^3P_2–b^3S_1				
3,194.37	(2 E)	6 III	296.3	z^3P_2–e^3D_3				
3,209.35	(2 E)	3 III A	31,150.0	a^3D_3–y^4F_3				
3,251.29	(2 E)		30,748.2	z^4F_3–$c^3P'_2$				
3,337.84	1		29,950.9	z^4F_3–(3_4)				
40.37	(3 E)	7 III	928.2	$z^3D'_3$–$c^3P'_2$				
54.57	(2 E)	10 d? III	801.5	$z^3D'_2$–$c^3P'_1$				
54.81	(1 E & H)		799.4	z^4F_2–d^4D_2				
58.94	(2 E)	5 III	762.8	z^4F_3–d^4D_3				
64.78	1	7 III	711.1	z^4F_2–d^4D_1				
77.72	(2 E)	6 III	597.3	$z^3D'_3$–(3_4)				
88.59	1	15 III	502.3	z^4F_3–d^4D_2				
89.81	(2 E & H)	5 IV?	491.7	z^4F_4–d^4D_4				
3,397.04	2	15 III	429.0	z^4F_3–(3_4)				
3,406.17	(1 E & H)		350.1	$z^4D'_2$–$c^3P'_1$				
12.47	2	12 III	295.9	z^4F_4–d^4D_3				
31.01	(2 E & H)	6 V	29,137.6	$z^3D'_3$–d^4D_4				
50.95	2	12 III	28,969.2	z^4F_3–d^4D_4				
54.17	(2 E & H)		942.2	z^4F_4–c^4D_3				
3,484.06	2	10 III	28,694.0	a^3D_3–$z^4G'_3$				

TABLE 6.—*Classified lines of Yt I*—Continued

λ	Intensity M	Intensity Class K	ν	Terms	Zeeman effect		Solar intensity	
					Observed	Calculated	Disk	Spot
3,484.89	2		28,687.1	z^4F_5–c^4D_4				
85.73	4	40 III	680.2	$z^4D'_4$–$f^4F'_5$	(0.00) 1.15	(0.12) 1.17 A¹ ur		
3,498.94	2	10n III	571.9	$z^4D'_3$–$f^4F'_4$				
3,501.95	2	2 IV	547.4	$z^4D'_4$–(3₄)			−2N?	
10.54	1	8 III	477.5	z^4F_4–$d^4F'_5$				
11.19	2	15 III	472.2	$z^4D'_2$–$f^4F'_3$				
12.89	3	20 III	458.5	z^4F_3–$d^4F'_4$ a^2D_2–$z^4G'_4$	(−) 1.50 A²	(0.20) 1.50 A² ur		
21.54	1	6 III	388.6	z^4F_2–$d^4F'_3$				
31.71	3		306.8	$z^4D'_1$–f^4F_2?				
36.03	1		272.2	$z^4D'_4$–$f^4F'_4$				
38.52	2		252.4	$z^4D'_2$–$f^4F'_3$				
51.80	2	8 III?	146.7	z^4F_2–$d^4F'_2$				
52.70	10	40 I	139.6	a^2D_2–x^2P_2	(0.80) 0.45, 1.00, 1.54	(0.27, **0.80**) 0.53, **1.06**, 1.60		
58.76	2	5 II	28,091.7	z^4F_3–$d^4F'_3$				
71.43	4	10 II	27,992.0	z^4F_4–$d^4F'_4$	(−) 1.22	(0.00) 1.24		
76.05	5	12 III	955.8	z^4F_5–$d^4F'_5$	(−) 1.30	(0.00) 1.33		
89.68	2	5? III?	849.7	z^4F_3–$d^4F'_2$				
91.09	1		838.8	$z^4D'_2$–c^4D_2				
92.92	25	200 II	824.6	a^2D_2–x^2P_1	(0.00) 0.84	(0.07) 0.73, **0.87**	0m	
3,595.27	1		806.4	$z^4D'_4$–c^4D_4				
3,618.78	1		625.8	z^4F_4–$d^4F'_3$				
20.95	50	400 II	609.3	a^2D_2–x^2P_2	(0.00) 1.10 A¹	(0.10) 1.10 A¹ ur	−1	
3,639.28	1		470.2	z^4F_3–$d^4F'_4$	(−) 1.39	(0.12) 1.50 A² ur	1m	
65.75	1		271.8	$z^4D'_3$–$d^4F'_3$				
3,692.53	3	8 III	27,074.0	$z^4D'_4$–$d^4F'_5$				
3,718.12	2	5 IV	26,887.7	$z^4D'_3$–$d^4F'_4$				
21.40	3		864.0	b^2D_2–v^2F_3?				
38.62	2	4 III	740.3	$z^4D'_2$–$d^4F'_2$				
49.89	2		659.9	$z^4D'_1$–$d^4F'_2$				
3,787.16	(2 E & H)		25,397.5	$a^4F'_3$–y^4P_3				
3,887.76	2		25,714.5	z^2P_2–(1₃)				
3,892.41	(2 E)		683.8	z^4P_1–d^4D_1				
3,900.27	(1 E)		632.0	z^4P_2–d^4D_1				
18.24	2	4 III	514.5	$a^4F'_4$–$w^2D'_2$				
3,987.49	2	4 III	25,071.4	z^2P_2–d^2D_3	(−) 1.00	(0.10) 1.10 A¹ ur		
4,029.84	2	3 IV	24,807.9	$a^2F'_4$–$v^2D'_3$	(−) 0.96	(0.06) 1.07 A¹ ur		
39.83	20	60 II	746.6	a^2D_2–$y^2D'_3$	(w) 1.40 A²	(0.30) 1.50 A² ur	−1m	0m
47.64	40	80 II	698.8	a^2D_2–y^2P_1	(0.00) 0.84	(0.07) 0.73, **0.87**	0N	1
77.38	100	300 II	518.7	a^2D_2–y^2F_3	(0.00) 1.00	(0.04) 0.90 A² ur	1Ndm	1m
80.93	2	5 III	497.3	z^4F_2–$c^4F'_2$				
81.22	3	9 II	495.6	a^2G_5–v^2F_4				
4,083.71	50	100 II	480.6	a^2D_2–y^2P_2	(0.76) 0.53, **1.01**, 1.51	(0.27, **0.80**) 0.53, **1.06**, 1.60	1 m	1 m
4,102.38	150	350 II	369.2	a^2D_2–y^2F_4	(0.00) 1.08	(0.06) 1.07 A¹ ur	0	2
4,106.39	3		345.4	a^2G_4–v^2F_3				
10.80	3	5 III	319.3	z^4F_3–$c^4F'_2$				
28.31	150	300 II	216.2	a^2D_2–$y^2D'_2$	(0.22) 1.15	(0.00) 1.20	−1	1
42.86	100	200 II	131.2	a^2D_2–$y^2D'_2$	(0.00) 0.82	(0.00) 0.80	−1	0
57.63	5	6 III	045.4	z^4F_4–$c^4F'_4$				
58.12	(2 E & H)		24,042.6	z^4P_2–c^2D_3				
67.52	50	100 II	23,988.4	a^2D_2–y^2F_3	(−, 0.51, **0.85**) 0.40, 0.74, **1.08**, 1.40, 1.73	(0.17, 0.51, **0.86**) 0.34, 0.69, **1.03**, 1.37, 1.72	1	1 m
74.14	30	100 II	950.3	a^2D_2–y^2P_2	(0.00) 1.10 A¹	(0.10) 1.10 A¹ ur	—	−1
4,191.28	1		852.4	z^4F_4–$c^4F'_3$				
4,213.01	(½ E)	6 IV	729.3	z^4F_5–$c^4F'_5$				
13.54	2	5 III?	726.4	z^4F_2–b^4D_2				
17.80	5	10 III	702.4	z^2P_1–c^2D_2	(−) 1.06	(0.07) 0.73, **0.87**,		
20.62	10	30 III	686.6	z^4F_3–a^4G_2	(w?) 1.03 B?	(0.13) 0.70 A² ur		
29.20	2	2 III	638.5	$z^4D'_3$–$d^4P'_3$				
31.30	(1 E & H)		626.8	z^2P_1–$c^4P'_2$				
32.54	2	1 III	619.9	z^4F_5–b^4D_4				
4,235.94	20	100 II	23,600.9	a^2D_2–$y^2D'_2$			m	m

TABLE 6.—*Classified lines of Yt I*—Continued

λ	Intensity M	Intensity Class K	ν	Terms	Zeeman effect		Solar intensity	
					Observed	Calculated	Disk	Spot
4,237.12	(1 E & H)		23,594.3	z^4F_2–b^4D_2				
49.87	1	1 III	523.5	z^4F_3–$c^4F'_4$				
50.36	1	1 III	520.8	z^2F_2–b^4D_1				
51.19	10	40 III	516.2	z^4F_2–a^4G_4	(0.00) 0.96	(0.04) 0.93 A^1 ur		
54.35	1		498.8	$z^2D'_2$–$c^4F'_3$				
66.89	1	1 III	429.7	z^4F_2–b^4D_2				
68.84	(1 E & H)		419.0	$z^2D'_2$–$c^4F'_3$				
72.12	2	2 III	401.0	$z^4D'_4$–$d^4P'_3$	(0.00) 1.14	(0.17) 1.21 A^1 ur		
74.18	1	1 III A	389.7	z^4F_2–a^4G_3				
75.50	1 (E & H)		382.5	z^2P_1–$c^4P'_1$				
88.20		(0 H N R)	313.3	z^2P_1–$b^2P'_2$				
91.04	2	2 III	297.8	z^4F_2–b^4D_2	(—) 0.85	(0.12) 0.90 A^1 ur		
4,292.79			288.3	z^2F_4–d^4D_4				
4,302.30	20	50 III	236.9	z^4F_4–a^4G_5	(0.52 w)1.04 A^2	(0.08) 1.05 A^1 ur	2 m	2 m
14.92		(1 H N R)	168.9	$a^4F'_3$–$x^2D'_2$				
16.30	2	3 III	161.5	z^2P_2–$c^4P'_3$				
17.87	1		153.1	z^4F_4–b^4D_4				
18.21	1		152.1	$a^2F'_3$–$y^2G'_4$				
30.78	5	10 III	084.1	z^2P_1–$b^2P'_1$	(0.00) 0.73	(0.00) 0.67		
37.30	2	2 III	049.4	z^4F_4–a^4G_4	(—) 1.13 B	(0.70) 1.11 B ur		
44.64	3	4 III	010.4	$z^4D'_1$–$c^4F'_2$	(—) 0.83 A^2	(0.20) 0.20, **0.60**		
46.14	1	1 III	23,002.5	$a^4P'_2$–$y^2G'_4$				
48.78	25	60 III	22,988.5	z^4F_2–a^4G_3	(0.00) 1.10	(0.09) 1.14 A^1 ur	−1 N?	m
52.33	2	5 III	969.8	$a^4F'_2$–$x^2D'_2$ / $a^4F'_4$–$x^2D'_3$	(—) 1.27	(0.04) 1.25 A^2 ur		
52.68	4	4 III	967.9	$z^4D'_2$–$c^4F'_3$	(—) 0.96	(0.12) 0.90 A^1 ur		
53.63	2		962.9	z^4F_4–b^4D_3				
57.73	6	10 III	941.3	$z^4D'_3$–$c^4F'_4$	(—) 0.98	(0.13) 1.07 A^1 ur	−2	
61.18	1		923.2	z^4F_4–a^4G_3				
66.03	5	10 III	897.7	z^2P_2–c^2D_3	(0.00) 1.18	(0.10) 1.10 A^1 ur		
70.97	1	1 III	871.8	z^2P_2–c^2D_2	(—) 0.98	(0.27, **0.80**) 0.53, **1.06**, 1.60		
75.61	3	8 III	847.6	$z^4D'_4$–$c^4F'_5$				
79.34	3	6 III	828.1	$a^4F'_3$–$x^2D'_2$	(—) 1.19 A^2	(0.16) 1.20 A^2 ur		
84.80	2		799.7	$z^2D'_3$–b^4D_4				
85.48	2	3 III	796.1	z^2P_2–$c^4P'_2$	(—) 1.36	(0.20, **0.60**) 1.13, **1.53**, 1.93		
94.01	2	3 III	751.9	$a^4F'_4$–x^2F_4	(—) 1.17 B	(0.12) 1.19 B ur		
94.67	2	2 III	748.5	$z^4D'_3$–$c^4F'_3$				
4,397.79	(2 E & H)	3 III	732.3	$a^2F'_4$–$y^2G'_5$				
4,401.13	2		715.1	z^4F_3–a^4G_3				
02.38	(1 E & H)		708.6	z^2P_1–a^4D_2				
04.85	3		695.9	$z^2D'_2$–a^4G_4				
09.71	1		670.9	$a^4F'_2$–x^2F_3				
15.37	2	3 III	641.8	$z^4D'_4$–$c^4F'_4$	(w) 1.23 B w	(0.52) 1.33 B ur		
17.44	2	2 III	631.2	z^4F_3–b^4D_4	(—) 1.22	(0.12) 1.16 A^1 ur		
21.74	1	1 IV	609.2	$z^2D'_2$–b^4D_3				
32.92	1	1 IV	552.2	z^2P_2–$c^4P'_1$				
36.13	1		535.8	$a^4F'_3$–$y^4D'_4$				
37.34	5	10 III	529.7	$a^4F'_3$–x^2F_3	(—) 0.90	(0.35) 0.94 B ur		
43.66	7	15 III	497.7	$a^4F'_3$–x^2F_4	(—) 1.70 A^2	(0.24) 1.66 A^2 ur		
45.31	3	3 IV	489.3	$z^2D'_2$–a^4G_3	(—) 0.62	(0.16) 0.40 A^1 ur		
46.63	8	15 III	482.6	z^2P_2–$b^4P'_2$	(0.00) 1.32	(0.00) 1.33	−2m	
59.01	1		420.2	$a^4P'_2$–$y^4D'_2$				
63.53	1 (E & H)		397.5	$z^2D'_2$–b^4D_2				
75.72	10	20 III	336.5	$a^4F'_4$–$y^4D'_4$	(0.50) 1.29 B w	(0.53) 1.33 B ur	−2N	
76.96	10	25 III	330.3	$a^4F'_4$–x^2F_3	(—) 1.66 A^2	(0.38) 1.72 A^2 ur		
77.45	10	25 III	327.9	$a^4F'_3$–$y^4D'_2$	(—) 0.00, 0.78, 1.54	(0.40, **1.20**) 0.00, **0.80**, 1.60	−1N	−1
78.99	1	2 IV	320.2	b^2D_3–$y^2G'_4$				
84.44	2	5 II?	293.1	$a^2F'_3$–w^2F_4?	(—) 1.06	(0.28) 1.50 A^2 ur		
87.28	8	20 III	279.0	$a^4F'_3$–$y^4D'_3$	(w) 1.20 B w	(0.69) 1.20 B ur	−1	−1
87.47	15	40 III	278.0	$a^4F'_3$–$y^4D'_1$	(—) 0.60	(0.20) 0.20, **0.60**	−1	−1
91.75	3	5 III	256.8	$a^4F'_3$–$z^4G'_3$				
4,492.42	3	4 III	253.5	z^2P_2–$b^2P'_1$	(—) 1.48	(0.33) 1.50 A^2 ur		
4,505.95	25	50 II	186.7	$a^4F'_3$–$y^4D'_3$	(0.00) 0.90	(0.12) 0.90 A^1 ur	−2?	−2
13.58	3	4 III	149.3	$a^2F'_3$–y^4P_2	(—) 1.24	(1.40) **1.23** B ur	−1?	0
14.02	5	8 III	147.0	$a^4P'_2$–y^4P_2	(—) 1.31	(0.10) 1.50 A^1 ur		
4,522.05	2	3 III	22,107.7	$z^4D'_1$–b^4D_2	(—) 1.79	(0.60) 0.60, **1.80**		

TABLE 6.—*Classified lines of Yt I*—Continued

λ	Intensity M	Intensity Class K	ν	Terms	Zeeman effect		Solar intensity	
					Observed	Calculated	Disk	Spot
4,527.25	40	80 II	22,082.3	$a^4F'_5$–$y^4D'_4$	(0.00) 1.15 A[1]	(0.12) 1.17 A[1] ur	m	m
27.80	30	50 II	079.6	$a^4F'_4$–$y^4D'_3$	(0.00) 1.05 A[1]	(0.12) 1.07 A[1] ur	m	m
28.10	2	3 III	078.1	$z^4D'_3$–b^4D_3				
33.50	1	1 IV	051.8	z^2P_2–a^4D_3				
34.09	3	3 III	049.0	$z^4D'_3$–b^4D_4				
36.31	1		038.2	$z^4D'_2$–a^4G_3				
37.16	2	2 III	034.0	$z^4D'_1$–b^4D_1				
39.60	1	1 III	22,022.2	$a^4P'_1$–w^2P_2				
44.31	6	10 III	21,999.4	$a^4P'_2$–y^4P_3				
54.46	2	2 III	950.4	$a^4P'_2$–w^2P_1				
55.30	2		946.3	$z^4D'_3$–b^4D_2				
59.37	7	10 III	926.7	$a^4P'_1$–y^4P_2	(−) **1.03, 2.04**	(0.47) **1.26**, 2.20	−3?	
61.8	2		915.0	$a^4P'_2$–w^2P_2				
64.94	2	2 IV?	900.0	$a^4F'_5$–$z^2G'_4$				
70.67	2	3n III	872.5	$z^4D'_2$–b^4D_1				
73.56	6	10 III	858.7	$z^4D'_3$–b^4D_3	(−) 1.20	(0.00) 1.38		
78.87	1	1 III	833.3	$z^4D'_4$–a^4G_5				
81.32	2	6 II A	821.7	$a^2F'_3$–y^4P_2				
81.77	1	3 III A	819.5	$a^4P'_2$–y^4P_2 / $z^4D'_3$–a^4G_3?				
82.16	1	2 III	817.7	$a^4P'_1$–y^4P_1				
4,596.55	10	12 III	749.4	$z^4D'_4$–b^4D_4	(−) 1.34	(0.00) 1.43	−1	−1
4,601.28	1	2 III	727.0	$z^4D'_3$–b^4D_2				
04.80	6	10 III	710.4	$a^4P'_2$–y^4P_1	(−) 1.26	(0.47) **1.26**, 2.20		
13.00	2	4 III	671.8	$a^4P'_2$–y^4P_2				
36.50	(1 E & H)	1 IV	562.0	z^2P_1–$b^4P'_2$				
43.69	50	150 I	528.6	a^2D_2–z^2F_3	(0.00) 0.89	(0.04) 0.90 A[2] ur	−IN	2
52.13	1		489.5	z^4P_2–$d^4P'_3$				
53.78	2	4 III	481.9	b^2D_2–y^4P_2				
54.47	(1 E & H)		478.7	z^4P_1–$d^4P'_2$				
56.03	(1 E & H)		471.5	z^4F_2–d^2D_2				
58.32	10	12 III	461.0	b^2D_3–w^2F_4	(0.00) 0.94	(0.06) 1.07 A[1] ur		
66.38	1	3 III	423.9	$a^2F'_3$–$z^4S'_2$				
66.84	2	3 III	421.8	$a^4P'_2$–$z^4S'_2$ / z^2F_3–$d^4F'_3$				
67.47	4	8 III	418.9	b^2D_2–w^2F_3	(−) 0.84	(0.07) 0.90 A[2] ur		
71.87	(1 E & H)		398.7	a^2P_1–$e^2D'_2$				
74.84	45	125 I	385.1	a^2D_3–z^2F_4	(0.00) 1.06	(0.06) 1.07 A[1] ur	−2	1
78.35	2	3 III	369.1	z^4P_2–$d^4P'_3$				
89.77	3	4 III	317.1	b^2D_3–y^4P_3				
91.97	(1 E)	1 III A	307.1	z^4P_2–$d^4P'_2$				
96.81	6	8 III	285.1	b^2D_2–w^2P_1	(0.00) 0.97	(0.07) 0.73, **0.87**		
4,699.24	(2 E)	1 III?	274.1	$a^4P'_2$–$z^4S'_2$				
4,701.00	1	2 III	266.2	$a^2P'_2$–$e^2D'_2$				
04.64	(1 E)		249.7	b^2D_2–w^2P_2				
08.84	1	3 III ?	230.7	$a^4P'_1$–$w^2D'_2$				
18.95	(1 E & H)		185.3	z^4F_2–d^2D_2				
25.84	2	3 III	154.4	z^2F_1–e^2D_2? / b^2D_2–y^4P_2				
28.52	10	20 III ?	142.4	z^2P_1–a^2S_1	(0.67) 1.29	(0.67) 1.33	m	
32.37	3	3 III ?	125.2	$a^2F'_3$–$w^2D'_2$				
41.40	5	8 III	084.9	b^2D_2–w^2P_2	(0.00) 1.04	(0.10) 1.10 A[1] ur		
52.79	10	12 III	034.4	$a^2F'_3$–$z^4D'_4$	(0.00) 1.90 A[2] w	(0.19+) 2.14 A[2] ur		
59.07	(1 E & H)		21,006.6	z^2P_2–$b^4P'_2$				
60.98	30	40 I	20,998.2	a^2D_2–z^2F_3	(0.50, **0.80**) / 0.40, 0.72, **1.04**, 1.36, 1.69	(0.47, 0.51, **0.86**) / 0.34, 0.69, **1.03**, 1.37, 1.72	—	0
62.99	1 (E & H)		989.4	b^2D_2–y^4P_2				
80.18	(1 E)	1 III	913.9	$a^4P'_1$–$z^4D'_2$				
81.04	10	10 III	910.1	$a^4F'_4$–y^4F_3	(0.00) 1.45 A[2]	(0.12) 1.50 A[2] ur	−3?	
86.89	10	10 III	884.6	$a^4P'_2$–$z^4D'_4$				
4,790.30	15	15 III	830.5	$a^4F'_5$–y^4F_4	(w) 1.52 A[2]	(0.20) 1.50 A[2] ur		
4,804.31	3	4 III	808.8	$a^2F'_3$–$z^4D'_2$				
04.81	5	6 III	806.7	$a^4P'_2$–$z^4D'_2$				
4,819.64	7	10 III	20,742.7	$a^4F'_5$–y^4F_5	(**0.31**, 0.95) / (0.64, 1.28, **1.93**	(**0.21**, 0.94) 0.09, 0.71, 1.34, **1.97**	−3?	

TABLE 6.—*Classified lines of Yt I*—Continued

λ	Intensity M	Intensity Class K	ν	Terms	Zeeman effect		Solar intensity	
					Observed	Calculated	Disk	Spot
4,821.62	1	2 IV	734.1	$a^3F'_3$–$z^4D'_3$				
22.12	6	8 III	732.0	$a^4P'_2$–$z^4D'_3$	(w) 0.90	(0.27) 1.10 A[1] ur		
39.14	2	3 III	659.3	$a^4P'_3$–$z^4D'_3$	(**0.34**, 0.96) –	(**0.20**, 0.60) 1.00, 1.40, 1.80, **2.20**		
39.87	60	60 II	656.0	$a^4F'_3$–y^4F_3	(0.00) 1.30	(0.00) 1.33	–2	–1
45.67	50	50 II	631.2	$a^4F'_4$–y^4F_4	(0.00) 1.20	(0.00) 1.24	m	m
52.69	40	50 II	601.4	$a^4F'_3$–y^4F_3	(0.00) 1.01	(0.00) 1.03	–	–2
54.26	1	4 III	594.6	$a^4P'_1$–$z^4D'_1$				
56.70	2	3 III	584.4	$a^4P'_2$–$z^4D'_2$	(w?) 1.28	(0.45) 1.48 B ur		
59.84	25	40 II	571.1	$a^4F'_2$–y^4F_2	(0.00) 0.40	(0.00) 0.40	m	m
79.64	(2 E)	4 III	487.6	$a^4P'_2$–$z^4D'_1$	(0.70) 2.28	(0.81) 0.81, **2.60**		
86.28	3	4 III	459.8	b^3D_3–$w^3D'_3$	(0.00) 1.24	(0.00) 1.20		
86.65	3	3 III	458.2	b^3D_2–$w^3D'_2$	(0.00) 0.84	(0.00) 0.80		
4,893.44	8	6 III A	429.8	$a^4F'_3$–y^4F_3	(**0.33**, 0.95) (0.70, 1.30, **1.90**)	(**0.31**, 0.94) 0.09, 0.71, 1.34, **1.97**		
06.11	8	6 III A	377.1	$a^4F'_5$–y^4F_4	(0.00) 1.50 A[2]	(0.12) 1.50 A[2] ur		
09.00	2	2 III	365.1	$z^2D'_3$–d^2D_3	(0.00) 1.18	(0.00) 1.20		
21.86	10	10 III A	311.8	z^2P_2–a^2S_1	(0.35) **0.95**, 1.66	(0.33) **1.00**, 1.67		
26.31	1	tr III A	293.5	b^3D_3–$w^3D'_3$				
28.22	2	1 III	285.6	$z^2D'_3$–d^2D_3; y^2P_1–$(2_{1,1})$				
30.94	3	2 III	274.5	$z^2D'_3$–d^2D_3	(0.00) 0.83	(0.00) 0.80		
48.54	1	tr IV	202.4	b^3D_3–$z^4D'_4$				
74.30	5	10 III?	097.7	a^2G_3–$y^2G'_3$	(0.00) 1.08	(0.00) 1.11		
4,977.54		(0 H N R)	20,084.7	a^2G_4–$y^2G'_3$				
5,003.67		(0 H N R)	19,979.8	a^2G_3–$y^2G'_4$				
06.96	6	10 IV	966.6	a^2G_4–$y^2G'_4$	(0.00) 0.87	(0.00) 0.89		
70.20	2	5 V	717.6	z^4P_2–b^4D_4				
5,088.18	1	3 V	647.9	z^2P_2–b^4D_3				
28.42	1		493.8	z^4P_1–b^4D_1				
5,135.20	4	25 III	468.0	a^2G_3–z^2H_4	(0.00) 1.02	(0.02) 1.04 A[1] ur		
5,228.56	2		120.4	a^2G_3–w^2F_4				
37.20		(0 H N R)	088.9	a^2G_3–z^2H_5				
40.80	4	15 IV	19,075.8	a^2G_4–z^2H_5	(0.00) 0.94	(0.02) 0.94 A[3] ur		
5,253.68	2		18,921.0	$a^2F'_3$–$z^2D'_3$				
5,325.84	1		771.2	$a^4P'_2$–$z^2D'_2$				
69.78		(1 IA H N R)	617.6	a^2D_2–z^4P_1				
75.87	1		596.5	z^4F_2–$b^2P'_2$				
80.62	5	15 III	580.1	$a^2F'_3$–$z^2D'_3$				
88.41	1		553.2	$a^4P'_3$–z^2F_4				
5,390.82	2		545.0	z^4F_4–c^2D_3				
5,417.02	2	3 IV?	455.2	$z^2D'_3$–$c^4P'_3$				
24.36	5	20 III	430.2	$a^4P'_3$–$z^2D'_2$	(**0.22**, 0.66) 1.78 A[2]	(**0.40**, 1.20) 0.40, 1.20, 2.00, **2.80**		
38.24	20	50 II	383.2	$a^2F'_4$–$z^2D'_3$	(0.00) 1.09 B?	(0.06) 1.07 A[1] ur		
66.46	50	300 II	288.3	$a^4F'_5$–$z^4G'_4$; z^4F_3–a^4D_2	(0.00) 1.10	(0.09) 1.16 A[1] ur	m	m
68.47	10	40 III	281.6	$a^2F'_3$–z^4F_3	(0.39) 1.04	(0.00) 0.86		
69.19	1		279.2	$a^4P'_2$–z^2F_3				
91.45	(3 E)	1 V	205.1	y^2P_2–b^2S_1				
93.16	5	15 III	199.4	z^4F_2–a^4D_1	(0.22) 0.62	(0.20) 0.20, **0.60**		
5,495.59	2	8 III	191.4	$z^2D'_3$–c^2D_3				
5,503.34	2	100{5 III 25 II	165.8	z^4F_2–a^4D_3				
03.47	10		165.4	$a^2F'_4$–z^4F_4	(0.00) 1.15	(0.00) 1.14		
13.66	5	20 II	131.8	$a^4P'_2$–z^2F_3	(0.65) –			
21.59	10	30 II+E	105.7	$a^2F'_3$–$z^2G'_4$			–1m	m
26.74	2	2 IV	088.8	b^3D_3–$z^2D'_2$				
27.54	40	250 II	086.2	$a^4F'_4$–$z^4G'_3$	(0.00) 1.03 A[1]	(0.08) 1.05 A[1] ur	–2d b	–1b
27.75		(10 H N R)	085.5	$z^2D'_2$–c^2D_2				
40.61	(1 E)		043.6	$a^4P'_1$–$y^4D'_2$				
41.64	2	3 III	040.2	z^4F_4–a^4D_4				
44.61	15	25 III+E	030.5	$a^2F'_3$–$y^4D'_3$			–2m	–1m
51.00	1		18,009.8	$z^2D'_2$–$c^4P'_1$				
56.43	5	20 I A	17,992.2	z^4F_2–a^4D_1	(0.00) 0.09	(0.12) 0.90 A[1] ur	–3	–2
6,367.75	5	15 II	17,955.6	$a^4P'_2$–$z^2G'_4$				

TABLE 6.—*Classified lines of Yt I*—Continued

λ	Intensity M	Intensity Class K	ν	Terms	Zeeman effect		Solar intensity	
					Observed	Calculated	Disk	Spot
5,577.43	10	30 II	17,924.5	$a^3F'_4$–$z^3G'_5$	(0.00) 1.06	(0.03) 1.06 A^1 ur		
81.08	2	3 IV	912.7	z^3P_2–$b^1F'_3$? / b^3D_3–$z^3D'_3$				
81.87	30	150 II	910.2	$a^4F'_3$–$z^4G'_4$	(0.00) 0.92	(0.03) 0.93 A^2 ur	m	m
90.96	2	2 IV	881.1	$a^4P'_3$–$y^4D'_3$				
5,594.12	2	2 IV	871.0	b^3D_3–z^3F_4				
5,603.26	(1 E)		841.8	z^3F_4–$c^1F'_4$				
06.33	10	20 II	832.0	$a^4F'_3$–$z^4G'_4$	(0.62) 1.20 B w	(0.59) 1.26 B ur		
19.98	1		788.7	$a^4P'_3$–$y^4D'_3$				
23.89	2		776.3	$z^3D'_3$–$b^3P'_2$				
30.14	20	100 II	756.6	$a^4F'_2$–$z^4G'_3$	(0.00) 0.71 A^2	(0.13) 0.70 A^2 ur	−2?	−1
32.24	2	3 I A	750.0	$a^2F'_4$–$y^4D'_4$				
32.89	1		748.0	b^3D_3–$z^3D'_3$				
44.69	10	20 II	710.9	$a^4F'_4$–$z^4G'_4$	(0.85) 1.10 B w	(0.71) 1.11 B ur		
46.68	1		704.6	$z^4D'_3$–$c^4P'_2$				
48.46	10	20 II	699.0	z^4F_4–a^4D_3	(0.00) 1.06	(0.13) 1.07 A^1 ur		
60.90	(1 E)		660.1	$z^4D'_2$–c^2D_3				
69.22	1	1 IV	634.2	$z^4D'_2$–c^2D_2				
75.28	5	15 II	615.4	$a^4F'_3$–$z^4G'_3$	(1.14) 0.82 B w	(1.14−) 0.80 B ur		
75.63	1	1 V	614.3	b^3D_2–z^3F^3				
5,693.63	2	2 II A	558.6	$z^4D'_2$–$c^4P'_2$				
5,706.74	15	30 II	518.3	z^4F_3–a^4D_4	(0.00) 1.12	(0.12) 1.17 A^1 ur		
14.91	1 h	3 n IV	493.2	$a^3F'_4$–$y^4D'_3$				
20.61	2	3 IV	475.8	$z^4D'_1$–$c^4P'_1$	(1.23) 1.32	(1.33) 1.33		
23.44	1	1 IV	467.2	$z^2D'_2$–$b^2P'_1$				
26.88		(1 H N R)	456.7	$a^4F'_5$–$z^4G'_4$				
32.09	2	3 II	440.8	z^4D'–c^2D_3	(−) 1.35	(0.35) 1.29 B ur		
40.22	1	1 III A	416.1	$a^4F'_4$–$z^4G'_3$				
43.86	6	15 III	405.1	$z^4D'_4$–$c^4P'_3$	(0.00) 1.28	(0.17) 1.22 A^1 ur		
63.58	1		345.5	$z^2D'_3$–a^4D_3				
65.65	5	12 III	339.3	$z^4D'_3$–$c^4P'_2$	(0.00) 1.18	(0.27) 1.10 A^1 ur		
73.94	2	4 IV	314.4	$z^4D'_2$–$c^4P'_1$	(0.62) 0.48	(0.73) **0, 47** 1.94		
87.71	1	1 IV	273.2	b^2D_3–$z^2G'_4$				
5,797.15	1	1 IV A	245.2	$z^4D'_2$–$b^2P'_2$				
5,812.66	2		199.1	b^2D_3–$y^4D'_3$				
21.88	3	4 III	171.8	z^2D_3–a^4D_2				
32.26	2	3 IV	141.3	$z^4D'_4$–c^2D_3				
71.82	2	2 IV	025.8	$z^4D'_2$–$b^2P'_2$				
5,879.96	2	3 IV	17,002.2	$z^2D'_2$–a^4D_1				
5,902.95	4	7 IV	16,936.0	$z^4D'_3$–a^4D_4	(−) 1.50	(0.06) 1.50 A^3 ur		
44.87	(2 E)		816.6	a^2D_2–$z^4D'_3$				
45.72	4	6 IV	814.2	$z^4D'_2$–a^4D_3	(0.00) 1.52 B?	(0.13) 1.50 A^2 ur		
50.02	3	5 IV	802.0	$z^4D'_1$–a^4D_2	(0.64)−	(0.60) 0.60, **1, 80**		
5,981.89	3		712.5	$z^4D'_1$–a^4D_1				
6,007.69	2		640.7	$z^4D'_2$–a^4D_2	(0.00) 1.24	(0.00) 1.20		
09.19	8	10? IV	636.6	$z^4D'_4$–a^4D_4	(0.00) 1.40	(0.00) 1.43		
23.41	4	20? I A	597.3	a^2D_2–$z^4D'_2$	{(−) 0.60, 0.98, 1.36	(0.20, **0, 60**) 0.60, **1, 00**, 1.40	—	0
24.30	1	? III	594.9	$z^4D'_3$–a^4D_3				
40.28	(1 E)		550.9	$z^4D'_2$–a^4D_1				
6,088.00	2		421.2	$z^4D'_3$–a^4D_3	(0.00) 1.52	(0.13) 1.50 A^2 ur		
6,135.05	2	? III	295.3	$z^4D'_4$–a^4D_3	(0.00) 1.50	(0.06) 1.50 A^2 ur		
38.44	5	15? I A	286.3	a^2D_2–$z^4D'_3$	(0.39) 1.28 B	(0.43−) 1.29 B ur	—	1b
6,191.73	50	100? I A	146.1	a^2D_2–$z^2D'_3$	(0.00) 0.78	(0.00) 0.80	—	4
6,222.59	10	50? I A	066.0	a^2D_2–$z^2D'_3$	{(**0, 19**, 0.58) 1.75 A^3	(**0, 20**, 0.60) 0.60, 1.00, 1.40, **1, 80**	—	1
6,230.83		(1 H N R)	16,044.8	$a^3F'_4$–y^4F_4				
6,402.02	10	50 I A	15,615.8	a^2D_2–$z^2D'_2$	{(**0, 21**, 0.60) 1.76 A^3	(**0, 20**, 0.60) 0.60, 1.00, 1.40, **1, 80**	—	1
35.02	100	500 I A	535.7	a^2D_2–$z^2D'_3$	(0.00) 1.16	(0.00) 1.20	−3	3
37.18	3	5 IV?	530.5	a^2G_3–z^2F_4				
52.49		(0 H N R)	493.6	z^4P_2–$c^4P'_2$				
6,493.78	1	4 V	395.1	$z^4G'_5$–$c^4F'_5$				
6,501.3	2		15,377.3	$z^4G'_4$–$c^4F'_4$				

TABLE 6.—*Classified lines of Yt I*—Continued

λ	Intensity M	Intensity Class K	ν	Terms	Zeeman effect		Solar intensity	
					Observed	Calculated	Disk	Spot
6,503.05		(0 H N R)	15,373.2	z^4P_3–$c^4P'_3$				
38.59	15	35 III	289.6	a^2G_5–$z^2G'_5$	(0.00) 1.12	(0.00) 1.11	−2m	−2m
44.19		(0 H N R)	276.5	a^2G_4–$z^2G'_5$				
57.40	10	30 I A	245.7	a^2D_2–z^4F_3	(0.00) 1.37 A^3	(0.11+) **1.37**− A^2 ur	−	−1
76.86	5	6 III	200.6	$a^2P'_1$–$z^2S'_1$	(−) 1.40	(0.67) 1.33		
6,584.89	2	5 II A	182.1	a^2D_3–z^4F_4				
6,595.04	1		158.7	z^2F_4–(1_5)				
6,616.59	(1 E)		109.4	z^4P_2–c^2D_2				
22.50	1	2 IV?	095.9	a^2G_4–z^2F_3				
36.48	2	2 IV?	064.1	$z^4G'_4$–$e^4F'_3$				
50.60	2	8 IV	032.1	$a^2P'_2$–$z^2S'_1$	(0.20) 1.04	(0.33) **1.00**, 1.67		
64.38	2	3 IV?	15,001.0	$z^4G'_5$–$e^4F'_4$				
87.57	25	80 I	14,949.0	a^2D_2–z^4F_2	(0.52) 0.63 B	(0.20, **0.60**) 0.20, **0.60**, 1.00	−	0
91.82	2	2 V	939.5	$z^4G'_6$–$e^4F'_5$				
6,694.75	1	1 V	933.0	a^2G_5–$z^2G'_4$				
6,700.71	15	20 III	919.7	a^2G_4–$z^2G'_4$	(0.00) 0.89	(0.00) 0.89		
13.20	4	6 III	891.9	z^2F_3–d^2D_3				
35.98	5	7 III	841.6	$a^2P'_2$–$z^2D'_3$				
6,793.71	25	80 I	715.4	a^2D_3–z^4F_3	(−) 1.10 B	(0.34) 1.11 B ur	0N?	1
6,803.14	1	1 V	695.0	z^4P_2–$b^4P'_2$				
15.16	2	5 IV	669.1	$a^2P'_1$–$z^2D'_2$				
45.24	5	10 III	604.7	z^4P_2–a^4D_4	(−) 1.18	(0.18) 1.22 A^1 ur		
6,887.23	2	8 IV	515.6	z^4F_4–d^2D_3	(−) 0.99	(0.06) 1.07 A^1 ur	−2?	
6,908.26	2	2 III	471.3	z^4F_3–$b^4F'_3$				
33.55	2	6 II A	418.7	a^2D_3–z^4F_2				
41.79	1		401.5	$z^4G'_3$–$d^4F'_2$				
50.32	4	8 IV	383.9	z^4P_2–a^4D_3				
58.08	2	4 I A	367.8	z^4F_2–$b^4F'_4$				
6,979.88	4	8 V ?	323.0	z^4F_3–$b^4F'_2$				
7,008.97	3	5 V	263.5	z^4P_2–a^4D_2				
09.93	2	4 V	261.6	z^4P_1–a^4D_2				
35.18	3	5 IV	210.3	z^4P_2–a^4D_2				
52.94	4	10 III	174.6	z^4F_2–$b^4F'_3$				
54.28	3	4 V	171.9	z^4P_1–a^4D_1				
7,075.17	2		130.0	z^4F_4–$b^4F'_5$				
7,127.92	3 h ?	2 III ?	14,025.5	z^4F_3–$b^4F'_2$?				
91.66	5	10 III	13,901.2	z^4F_4–$b^4F'_4$				
7,195.95	2		892.9	$z^4D'_4$–$e^4P'_3$				
7,295.10	2		707.8	z^4F_4–$b^4F'_3$				
7,303.2	1		688.9	a^2G_5–y^4F_5				
46.47	10	10 III	608.2	z^4F_5–$b^4F'_5$				
7,398.80	4		512.0	$a^4P'_2$–$z^4G'_4$				
7,455.20	2		409.8	a^2G_5–y^4F_4				
72.2	2		379.3	z^4F_5–$b^4F'_4$				
78.8	2		367.5	$a^2F'_3$–$z^4G'_3$; $a^4F'_3$–y^2F_4				
86.4	1		353.9	$z^2D'_3$–$b^4F'_3$?				
7,494.90	5		338.7	z^4P_2–$b^4P'_2$				
7,563.13	10	5 V	218.4	z^4P_2–$b^4P'_1$				
7,622.94	5		114.7	z^4P_1–$b^4P'_2$				
52.89	3		063.4	z^4P_2–$b^4P'_2$				
7,689.49	2		13,001.2	z^4P_1–$b^4P'_1$				
7,719.89	6	2 V	12,950.0	z^4P_2–$b^4P'_1$				
24.08	5	2 IV	943.0	z^4P_2–$b^4P'_2$				
88.42	3		836.1	$z^4D'_1$–$b^4F'_2$				
7,796.32	4		823.1	$z^4D'_2$–$b^4F'_3$				
7,802.52	2		812.9	$a^2F'_3$–z^2P_2				
12.16	5		797.0	$z^4D'_3$–$b^4F'_4$				
23.94	1		777.8	y^4P_2–$e^4P'_3$				
55.52	7		726.4	$z^4D'_4$–$b^4F'_5$				
7,870.04	2		12,702.9	z^2F_3–c^2D_2				

TABLE 6.—*Classified lines of Yt I*—Continued

λ	Intensity M	Intensity Class K	ν	Terms	Zeeman effect		Solar intensity	
					Observed	Calculated	Disk	Spot
7,887.51	2		12,675.0	$z^4D'_2$–$b^4F'_2$				
7,999.33	3		497.6	$z^4D'_4$–$b^4F'_4$				
8,025.60	3		456.7	y^4F_4–$c^4F'_4$				
8,134.9	3		289.3	$y^2D'_2$–d^2D_2				
8,211.71	4		174.4	y^2F_4–(1₂)				
8,231.23	2		145.5	b^2D_2–x^2P_2				
8,329.61	5		12,002.1	y^4F_3–$d^4F'_3$				
8,344.43	10		11,980.8	b^2D_3–x^2P_2				
8,365.64	4		950.4	y^2P_2–d^2D_3				
8,450.36	8		830.6	b^2D_2–x^2P_1				
8,475.64	3		795.3	y^4F_4–$d^4F'_4$				
8,528.94	4		721.6	y^2P_1–d^2D_2				
8,556.04	2 d ?		684.4	$y^2D'_2$–d^2D_3				
8,575.77	2		657.6	y^4F_3–$d^4F'_3$				
8,627.9	1		587.2	y^4F_2–$d^4F'_2$				
8,800.62	10		11,359.7	a^2D_2–z^2P_2				
9,231.58	8		10,829.4	a^2D_2–z^2P_2				
9,494.81	2		10,529.2	a^2D_2–z^2P_1				

TABLE 7.—*Unclassified lines of Yt I*

λ	Intensity	Temp. class	ν	λ	Intensity	Temp. class	ν
2,826.29		1 IV A	35,371.7	4,300.34	2	2 III	23,247.1
2,835.78		1 IV	35,253.3	15.48	2	2 III	165.9
3,044.84	(2 E)	5 III	32,832.9	22.30	2	2 III	129.3
47.11	(1 E)	3 III	808.5	29.89	1	1 III	23,088.8
47.41	(1 E)	3 III	805.2	4,387.74	4	8 III	22,784.4
56.33	(1 E)	2? III ?	709.5	4,465.27	3	1 IV	388.8
59.50	(2 E)	4 III	675.6	72.78	2	2 n IV	351.2
72.32	(2 E)	5 III	539.3	4,473.88	5	7 III	22,345.7
76.49	(2 E)	5 III	495.2	4,564.37	2	4 III	21,902.7
3,091.70	(3 E)	15 III	335.3	4,590.77	(3 E)	1 V	21,776.8
3,103.69	(2 E)	4 IV	210.4	4,658.88	3	6 III	458.4
14.27	(3 E)	2 III	32,101.0	4,670.82	2	4 III A	21,403.5
3,171.69	(2 E)	4 III A	31,519.8	4,863.11	(2 E)	1 III	20,557.2
3,252.28	1	8 III	30,738.8	4,912.05	1	tr III A ?	332.4
75.56	(2 E)	2 IV	520.4	4,950.64	3	2 III	20,193.8
78.43	(2 E)	5 III A	493.6	5,072.19	3	5 IV	19,709.9
3,287.21	(3 E)	4 III	30,412.2	5,686.62	(1 E)	1 IV ?	17,580.3
3,335.20	(2 E)	8 n V	29,974.6	5,713.81	1 h	3 n IV	17,496.6
44.53	(2 E)	4 n V	891.0	6,251.05	3		15,992.9
82.83	(½ E)	5 V	552.6	6,338.14	3	5 I	773.1
83.06	(1 E)	7 V	550.6	6,462.59	2	8 III	15,469.4
3,394.97	(2 E & H)	4 III	446.9	7,536.73	3		13,264.2
3,414.5	(2 E & H)	8 n III	278.5	7,698.00	4		12,986.8
24.16		7 III A	195.9	8,165.5	2		243.2
31.67	(2 E & H)	5 III	132.0	8,258.5	2		105.4
33.79	(2 E & H)	6 n IV	114.0	8,297.07	2		049.2
37.95	1	8 n IV	29,078.8	8,326.40	1		000.7
71.7	1	10 n V ?	28,796.1	8,330.92	1		12,000.2
3,473.18	(2 E & H)	5 III	783.8	8,443.28	1		11,840.5
3,500.60	1	7 III	558.4	8,552.42	1		689.4
00.47	(2 E & H)	6 III	28,510.6	8,658.4	1		546.3
3,587.75	5	20 III	27,864.7	8,759.24	1		413.4
3,904.59	2	5 III	25,603.7	8,831.2	1		11,320.4
3,955.08	3	5 III	25,276.8	9,392.7	1		10,643.6
4,224.25	3	4 III	23,666.2				

V. THEORETICAL INTERPRETATION OF THE SPARK SPECTRA AND COMPARISON WITH SCANDIUM

In our paper on scandium spectra we gave a summary of the theoretical advances which correlate the observed spectral terms with the electron configurations in the atoms producing them. There is no necessity for repeating this, especially since the subject has since been discussed in detail in Hund's notable monograph.

A. Yt III. The relatively simple spectrum of doubly ionized yttrium has already been discussed; there is only one valency electron, and its various orbits are responsible for the doublet terms as in the arc spectrum of an alkali. Analysis of the Yt III spectrum shows that the $4d$ orbit is most firmly bound, $5s$, $5p$, and $4f$ being next in order.

A comparison of Yt III and Sc III [20] is given in Table 8.

TABLE 8.—*Comparison of Yt III and Sc III*

Electron configuration	Predicted term	Observed term	Main level	Separation	Yt III–Sc III	Separation ratio, Yt III/Sc III
$4d$	^1D	4^1D_2	724.8	724.8	+527	3.67
$5s$	^1S	5^1S_1	7,466.2		−18,077	
$5p$	^1P	5^1P_1	42,954.7	1,553.5	−19,621	3.28
$6s$	^1S	6^1S_1	86,713.9		−28,150	
$5d$	^1D	5^1D_2	88,577.1	198.3	−23,677	4.41

The corresponding terms in scandium have total quantum numbers smaller by one unit. The difference of binding for the lowest d and s electrons is less for Yt III than for Sc III. The higher s-electron is more firmly bound than the d in both cases.

B. Yt II. The singly ionized yttrium atom has two valency electrons, and the spectral terms (atomic energy states) corresponding to their various configurations are readily obtained by adding an electron to the lower electron configurations of Yt^{++}. The addition of a $5s$ electron to the normal $4d$ state should give the terms ^3D and ^1D; that of a $4d$ electron to the same state produces $^3F'$, $^3P'$, ^1G, ^1D, ^1S, while adding a $5s$ electron to one already present gives ^1S alone. These terms account completely for the observed terms of the low set (leaving one ^1S term to be discovered). Since their configurations contain no p or f electrons, these terms are all "even" and do not combine among themselves. The addition of a $5p$ electron to the $4d$ and $5s$ states of Yt^{++} gives the middle set of terms, exactly as observed, which are "odd" and combine with the lowest terms and also with the higher "even" terms arising from several configurations.

[20] Russell and Lang, Astrophys J., **66**, p. 20; 1927.

Table 9 gives the predicted terms corresponding to each configuration and the observed terms with which they have been identified, and also a comparison with Sc II similar to that made for Sc III. The identification of the lower and middle levels is obvious—the wide separation of z^3P showing that it belongs to the *sp* configuration. Among the higher terms the pentads coming from $4d.5d$ are recognizable by the strength of their combinations and the relative intensities of the different multiplets. The terms b^3D, c^1D, and c^1S are determined by the series relations discussed below; a^3S and d^3D are placed because of the strength of their combinations with z^3P (*sp*) and also by the narrow separation of the latter which belongs to a series converging toward the single limit 5^2S of Yt III. The wide separation of b^3P', as well as its high level, assigns it to $(5p)^2$, and the term f^1D is too high to belong to any but this configuration. The assignment of e^1D is uncertain, but it fits in well where it is placed.

TABLE 9.—*Predicted and observed terms in the Yt II spectrum*

Electron configuration	Predicted term	Observed term	Main level	Level separations	Yt II–Sc II	Ratio of separation Yt II/Sc II
$(5s)^2$	$^1S_0$	a^1S_0	0.0		−11, 736	
$5s\cdot4d$	^3D	a^3D_3	1, 449. 9	404. 8; 204. 9	+1, 272	3. 42
	^1D	a^1D_2	3, 296. 3		+755	
$(4d)^2$	$^3F'$	$a^3F'_4$	8, 743. 4	415. 4; 324. 9	+3, 756	4. 00
	$^3P'$	$a^3P'_2$	14, 098. 2	79. 8; 134. 9	+1, 944	2. 66
	^1G	a^1G_4	15, 683. 0		+1, 422	
	^1D	b^1D_2	14, 832. 9		+3, 888	
	^1S	?				
$5s\cdot5p$	^3P	z^3P_2	24, 647. 2	870. 9; 331. 2	−14, 698	3. 50
	^1P	y^1P_1	44, 568. 2		−11, 148	
$4d\cdot5p$	^3P	y^3P_2	32, 283. 6	159. 5; 75. 3	+2, 460	2. 79
	$^3D'$	$z^3D'_3$	29, 214. 1	484. 0; 134. 8	+1, 053	2. 54
	^3F	z^3F_4	28, 394. 3	862. 1; 305. 3	+553	2. 94
	^1P	z^1P_1	27, 516. 7		−3, 299	
	$^1D'$	$z^1D'_2$	26, 147. 2		+66	
	^1F	z^1F_3	33, 336. 7		+987	
$5s\cdot6s$	^3S	a^3S_1	58, 261. 7			
	^1S	c^1S_0	61, 367. 3			
$4d\cdot6s$	^3D	b^3D_3	55, 645. 4	613. 4; 76. 4	−2, 098	3. 59
	^1D	c^1D_2	55, 724. 9		−2, 527	
$5s\cdot5d$	^3D	d^3D_3	65, 275. 0	86. 3; 57. 2		
	^1D	e^1D_2	62, 495. 2			
$4d\cdot5d$	^3G	a^3G_5	59, 900. 4	428. 6; 292. 9	−557	3. 81
	$^3F'$	$b^3F'_4$	61, 934. 1	283. 6; 313. 8	−1, 593	3. 88
	^3D	c^3D_3	59, 327. 1	380. 5; 226. 9	−674	4. 79
	$^3P'$	$c^3P'_2$	64, 597. 1	334. 4; 159. 8	−108	5. 50
	^3S	b^3S_1	61, 200. 2		+129	
	^1G	b^1G_4	63, 350. 0		−1, 886	
	$^1F'$	$a^1F'_3$	58, 533. 0		−995	
	^1D	d^1D_2	60, 535. 1		−3, 831	
	$^1P'$	$a^1P'_1$	59, 715. 4		−685	
	$^1S_0$	b^1S_0	59, 615. 8?		−5, 328?	
$(5p)^2$	$^3P'$	$b^3P'_2$	59, 669. 6	522. 4; 371. 5	−16, 919	2. 58
	^1D	f^1D_2	70, 223. 2			
	^1S	?				

The comparison of the levels and separations with those in Sc II is of much interest. The separations are always much wider in Yt II, the mean of 13 ratios being 3.54 as against 3.78 for Yt III

compared with Sc III. In comparing the levels it should be remembered that they are measured from different origins $^1S_0$ for Yt II and $^3D_1$ for Sc II. In discussing them it will be well to use similar origins, which may be done by subtracting 1,272 from the tabular values, so that the $^3D_3$ levels agree. The mean differences in level for the various electron configurations are then found to be:

Configuration	Difference Yt II–Sc II	Number of cases	Configuration	Difference Yt II–Sc II	Number of cases
s^2	−13,008	1	d^2	−1,480	4
sp	−14,195	2	dp	−969	6
p^2	−18,191	1	$d \cdot s$	−3,584	[1] 2
ds	−259	2	$d \cdot d$	−2,411	[2] 9

[1] The symbols $d \cdot s$ and $d \cdot d$ denote configurations with one electron excited to a higher quantum state.
[2] The term b^1S in Yt II has been omitted from the last mean. It gives such a discordant difference as to make its reality very doubtful.

For the configurations which contain a d-electron the relative levels are much the same in Sc^+ and Yt^+ except that those involving an excited electron are a little lower in the latter because of the greater ease of ionization. Those configurations which do not contain a d-electron are very much lower in Yt^+. This is obviously a consequence of the fact that the s and p states of Yt^{++}, from which these configurations are derived, are lower compared with the d state than in Sc^{++}. The differences in the two first spark spectra, which involves a change in the nature of the normal terms or states of the ions, could, therefore, have been predicted from the second spark spectra.

VI. A NOTE ON Sc II

The considerations just developed have led to a change in one of the conclusions expressed in our previous paper regarding the interpretation of the terms of Sc II. The term a^1S_0 at the level 11,736.35 was then attributed to the configuration $(3d)^2$, while the similar term arising from $(4s)^2$ was not found. The ^1P term from $4s4p$ was also missing. Comparison with yttrium suggests that the observed ^1S term belongs to the s^2 configuration and is homologous with the lowest energy level of Yt II. If so, it should give a strong combination with the term ^1P (sp). This term has now been identified at the level 55,715.52; it combines with a^1S_0 and b^1D to give the one remaining strong spark line (2273 A) and a faint one recorded by Exner and Haschek, as follows:

Terms		ν calculated	ν observed	λ observed	Intensity
b^1P_1	55,715.52				
a^1S_0	11,736.35	43,979.17	43,979.17	2,273.10	3
b^1D_2	10,944.51	44,771.0	44,769.7	2,232.96	1

For the stronger line Exner and Haschek's wave length is 0.08 A greater than Meggers's. If a corresponding correction is applied to the fainter line, the agreement with the computed position is exact. These terms have been used in calculating the differences entered in the appropriate places in Table 9.

It is now clear that the Sc II and Yt II spectra are exactly analogous; every line in the first has its correlative in the second. The only difference in the observed spectra is found in the apparent absence in Sc II of the terms coming from the configuration $s \cdot s$ and $s \cdot d$. These terms are already high in Yt II, and should be fully 12,000 frequency units higher in Sc II; their combinations will be faint and far in the ultra-violet.

VII. INTERPRETATION OF THE TERMS OF Yt I

The presence of three electrons in neutral yttrium atoms greatly increases the number of possible terms and thus accounts for the greater complexity of this spectrum. The possible electron configurations and corresponding terms are tabulated in Table 10, where a summary of the observed terms, their main levels and level separations, are also given. In cases where the assignment is uncertain the observed term is preceded by a question mark. The comparison with the levels and separations in Sc I is made as before. A few terms which were not found in the Sc I spectrum have been identified in the Yt I spectrum, and vice versa, but in general there is a remarkably close correspondence of the terms of the two spectra.

The interpretation of the low even levels is simple. The ds^2 configuration gives the normal state, a^2D_1, while d^2s gives $^4F'$, $^4P'$, ^2D, $^2F'$, $^2P'$ and a higher ^2D. The ^2S term which should be produced by this configuration has not been identified. The same is true for Sc I.

The middle terms are also easy to classify. Most of them should be arranged in triads, combining strongly with one of the low terms, and all these triads are clearly present, except for the ^2P term combining with a^2P'. The configuration s^2p should give an isolated ^2P term, which we may expect to be low (since no d electron is involved) and of wide separation. This is evidently z^2P. All the odd terms are now accounted for.

TABLE 10.—*Predicted and observed terms in the Yt I spectrum*

Electron configuration	Predicted terms	Observed terms	Main level	Level separations	Yt I–Sc I	Ratio of separations Yt I/Sc I
$(5s)^2.4d$	^2D	a^2D_3	530.5	530.5	+362	3.16
$5s(4d)^2$	$^4F'$	$a^4F'_3$	11,532.1	254.1, 199.4, 141.2	−145	3.78
	$^4P'$	$a^4P'_3$	15,476.7	147.7, 107.3		
	^2G	a^2G_3	18,499.2	−13.2	−1,738	4.68
	$^2F'$	$a^2F'_4$	15,864.4	537.6	+822	2.75
	^2D	b^2D_3	16,158.8	164.8	−854	(−13.3)
	$^2P'$	a^2P'	19,406.1	168.4		(2.10?)
	^2S					
$(4d)^3$	$^4F'$	$b^4F'_3$	29,842.6	229.0, 193.3, 148.3	−4,064	4.00
	$^4P'$	$b^4P'_3$	32,366.3	275.3, 113.5	−4,206	4.86
	$^2H'$					
	^2G					
	$^2F'$					
	^2D					
	$^2P'$					
$(5s)^2.5p$	^2P	z^2P_2	11,359.7	830.5	−7,495	5.76
$5s.4d.5p.$	^4F	z^4F_3	16,234.5	522.1, 466.6, 296.8	+208	3.63
	$^4D'$	$z^4D'_4$	17,116.3	299.7, 219.3, 161.5	+906	3.39
	^4P	z^4P_3	19,148.0	120.5, 51.2	+577	2.55
	^2F	z^2F_4	21,915.4	386.8	+830	(7.28)
	$^2D'$	$z^2D'_3$	16,066.0	−80.1	+43	(1.07)
	^2P	y^2P_2	24,480.6	−218.2	−176	(∞)
	^2F	y^2F_4	24,899.5	380.7	+2,315	2.72
	$^2D'$	$y^2D'_3$	24,746.6	615.4	−268	4.16
	^2P	z^2P_2	28,139.6	315.1	−2,567	2.36
$(4d)^2.5p$	$^4G'$	$z^4G'_5$	29,820.4	456.2, 375.3, 294.9	+517	4.00
	^4F	y^4F_3	32,188.1	278.9, 229.2, 171.6	+837	4.37
	$^4D'$	$y^4D'_4$	33,614.5	256.9, 92.3, 49.9	+863	3.50
	$^4D'$	$x^4D'_4$	36,361.3	300.3, −74.7, 319.0	(?)	
	^4P	y^4P_3	37,476.0	327.5, 109.0	(?)	(?)
	$^4S'$	$z^4S'_2$	36,750.8		(?)	
	^2H	z^2H_4	37,967.2	379.0	−1,282	3.95
	$^2G'$	$y^2G'_5$	38,596.7	117.7	−827	3.83
	^2F	z^2F_4	42,994.8	136.9	+3,106	(17.3)
	$^2G'$	$z^2G'_5$	33,788.8	356.5	+637	3.74
	^2F	x^2F_4	34,029.8	421.6	+751	3.38
	$^2D'$	$x^2D'_3$	34,247.7	340.9	+540	3.70
	^2F	w^2F_4	37,619.8	206.9	(?)	(?)
	$^2D'$	$w^2D'_3$	36,618.5	166.2	−421	(1.57)
	^2P	w^2P_2	37,243.7	−35.6	+157	(0.91)
	$^2D'$	$v^2D'_3$	40,672.4	36.1		
	^2P					
	$^2S'$	$z^2S'_1$	34,438.2			
	^2P					
$(5s)^2.6s$	$^2S_1$	a^2S_1	31,671.6			
$(5s)^2.7s$	$^2S_1$	c^2S_1	43,643.9			
$(5s)^2.5d$	^2D	c^2D_2	43,069.8	414.0		
$(5s)^2.6d$	^2D					
$5s.4d.6s$	^4D	a^4D_4	33,752.7	341.2, 173.7, 89.5	−815	3.42
	^2D	d^2D_3	36,431.0	10.5	+703	(0.14)
$5s.4d.7s$	^4D	c^4D_4	44,922.1	267.1		

Electron configuration	Predicted terms	Observed terms	Main level	Level separations	Yt I–Sc I	Ratio of separations Yt I/Sc I
$(4d)^2.6s$	$^4F'$	$c^4F'_{\frac{5}{2}}$	44,759.6	393.9, 312.77 ?	+2,675	
	$^4P'$	?$e^4P'_{\frac{3}{2}}$	50,254.0	?, ?		
	^2G					
	$^2F'$					
	^2D					
	$^2P'$					
	^2S					
$5s.4d.5d$	^4G	$a^4G_{\frac{5}{2}}$	39,233.0	283.7, 187.3, 126.4	−795	3.58
	$^4F'$	$c^4F'_{\frac{5}{2}}$	39,963.8	206.0, 192.8, 118.7	−707	3.46
	^4D	$b^4D_{\frac{1}{2}}$	38,865.6	190.2, 131.7, 73.8	−924	4.01
	$^4P'$	$d^4P'_{\frac{1}{2}}$	40,517.1	62.0, ?		
	^4S					
	^2G					
	$^2F'$					
	^2D					
	$^2P'$					
	^2S					
	^2G					
	$^2F'$					
	^2D					
	$^2P'$					
	^2S					
$5s.(5p)^3$	$^4P'$	$c^4P'_{\frac{3}{2}}$	34,521.2	365.4, 244.3		
	^2D	?$c^2D_{\frac{3}{2}}$	34,257.4	26.2		
	$^2P'$	?$b^2P'_{\frac{3}{2}}$	33,842.3	229.1		
	^2S	?$b^2S_{\frac{1}{2}}$	42,685.5			
$4d.(5p)^3$	$^4F'$	$f^4F'_{\frac{5}{2}}$	45,796.5	408.0, 319.2, 326.7?	+673	3.48
	^4D	$d^4D_{\frac{1}{2}}$	45,204.0	195.7, 260.0, 88.1		
	$^4P'$					
	^2D					
	$^2P'$, ^2D, $^2F'$	?$c^2P'_{\frac{3}{2}}$	45,994.0	46.5		
	^2S, $^2P'$, ^2D					
	$^2F'$, $^2G'$					
$(4d)^2.5d$	$^4P'$, ^4D, $^4F'$	?$d^4F'_{\frac{5}{2}}$	44,190.5	486.1, 366.9, 241.8		
	^4G, $^4H'$, $^4P'$					
	^4D, $^4F'$					
	^2D, $^2F'$, ^2G					
	$^2H'$, ^2I, $^2P'$					
	^2D, $^2F'$, ^2G					
	$^2H'$, ^2S, $^2P'$					
	^2D, $^2F'$, ^2G					
	$^2P'$, ^2D, $^2F'$					
	^2D					

Among the high quartet terms those from the configurations $ds.6s$ and $ds.5d$ are clearly recognizable by their strong combinations with the dsp triad. The terms arising from $ds.7s$ and $d^2.6s$ have been identified by series relations; they give very faint lines, and some of the component levels have not been detected. The high term d^2F', which combines with the d^2p terms to give fairly strong lines in the deep red may be assigned to $d^2.5d$, though it lies lower than might have been expected. The other terms of this pentad probably give lines in the infra-red. The only other configurations which can give terms near the observed level are sp^2 and dp^2. The former gives $^4P'$ which should be relatively low since the configuration contains no d electron. This fits c^4P'. The latter gives $^4F'$, ^4D, $^4P'$, and f^4F' and d^4D may be placed here. All the quartet terms are now identified.

The higher terms of the doublet system are much less fully developed (as usually happens with the lower multiplicity). The term d^2D, which combines with the *dsp* triad, may be assigned to *ds*.6*s;* its separation is much smaller than should be expected, but the combinations appear to assure this interpretation. The configuration *ds*.5*d* probably gives lines just outside the limit of observation in the red. The remaining terms combine most strongly with z^2P; three of them, a^2S, b^2P′, c^2D, are confirmed by Zeeman patterns. The high term c^2P′ combines strongly with z^2D′ (*dsp*). The remaining levels, though undoubtedly real, are close enough together to make it difficult to arrange them into terms. The isolated lines 3252.28 A, 3152.67 A and 3091.70 A give evidence by their behavior in the furnace that they originate from the z^2P level, but, in the absence of Zeeman effects, they can not be certainly classified.

The configurations which should combine strongly with s^2p are s^2s, giving ^{2}S, s^2d (^{2}D), and sp^2 (^{2}P′, ^{2}D, ^{2}S). The term a^2S may be assigned with confidence to s^2·6*s*. The level here called c^2S may be in series with it though the corresponding lines are stronger than might be anticipated, and are inverted in intensity.

The assignment of the remaining levels is not so easy. There are two ^{2}P′ terms where only one is to be anticipated. The second must come from dp^2. A "double jump" is involved, but this sometimes gives strong lines. The dp^2 and sp^2 configurations should give stronger combinations with *dsp* than s^2s or s^2d, thus indicating that c^2D and c^2P′ come from these configurations. The latter lies surprisingly high, but the ^{1}P (*sp*) term in Yt II is also high. On the other hand, one would not expect a term from dp^2 to lie nearly as low as b^2P′. The lower term has, therefore, been provisionally assigned to sp^2, and the higher to dp^2. The other levels have been tentatively arranged into the terms e^2D, b^2S, and c^2S, and assigned to s^2d, sp^2, and s^2.7*s;* but these assignments are subject to correction when Zeeman data for the particular lines in question become available.

The intensities of the various combinations are shown in summary fashion in Table 11, which gives the values on Meggers's scale (except those in parenthesis) for the strongest line in each multiplet. The letter *a* denotes that the multiplet is absent, *i*, that it lies in the infra-red, and *u* that it is in the ultra-violet. The large number of predicted infra-red lines is noteworthy; some of them should be very strong.

TABLE 11.—*Intensities of strongest lines in Yt I multiplets*

QUARTET SYSTEM

		ds^2p			d^3p					
		z^4F	z^4D'	z^4P	z^4G'	y^4F	y^4D'	x^4D'	y^4P	z^4S'
d^2s	a^4F_1	1	1	1	50	60	40	a		
	a^4P'						2	10	6	2
d^3	b^4F'	10	7		1	1	1	1		
	b^4P'		a	10			1	1	1	1
$ds.6s$	a^4D	15	8	5			1	1	1	
$ds.7s$	c^4D	2	1	a			a	a	a	
$ds.5d$	a^4G	25	1		1	1				
	c^4F'	5	6		1	1	1	1		
	b^4D	2	10	2		1	1	1	1	
	d^4P'		2	2			1	1	1	1
$d^3.6s$	c^4F'	a	a		2	3	a	a		
	c^4P'		a	a			a	2	1	a
$d^3.5d$	d^4F'	5	3		1	5	1	a		
sp^3	c^4P'		6	0			1	1	1	1
dp^3	f^4F'	a	4		u	u	u	a		
	d^4D	2	a	(2)		u	u	a	u	

DOUBLET SYSTEM

		ds^2	d^3s				$ds.6s$	$s^2.6s$	$s^2.7s$	$s^2.5d$	sp^3			dp^3
		a^2D	a^2G	a^2F'	b^2D	a^2P'	d^2D	a^2S	c^2S	$c^2D?$	b^2P'	c^2D	$b^2S?$	c^2P'
s^2p	z^2P	10			1	1	2	10	2	(2)	8	5	2	2
	z^2F	50	1	1	1	1	4					2		
	z^2D'	100		1	1	1	3				2	2		3
	y^2P	40			1	1	4	1			1	1	1	a
dsp	y^2F	150	1	1	1	1	1					1		
	y^2D'	150		1	1	1	3				1	1		a
	x^2P	50			10	1	1	1			1	1	a	a
	z^2H		4											
	y^2G'		6	(2)										
	v^2F	3	3	a	3?									
d^3p	z^2G'	1	15	10	1									
	x^2F	10	3	10	2									
	x^2D'	5		20	2	5								
	w^2F	(1)	2	2	10									
	w^2D'	3		3	3									
	w^2P	(3)			6									
	z^2S'					5								
	??P													
	v^2D'	(1)		2	a	1								

Table 10 shows the predicted and observed terms and a comparison with the levels and separations of the corresponding terms in scandium. The arc spectra of the two elements are almost as much alike as the others. The levels are nearly the same except that the d^3 and sp configurations lie lower in yttrium. The ratio of the separations is less regular than in the spark spectra, especially for some of the terms which go to singlet terms in the spark as limits.

If the ratios given in parenthesis in Table 10 are excluded, the mean for the rest is 3.74—nearly the same as for the higher states of ionization.

VIII. IONIZATION POTENTIALS OF YTTRIUM ATOMS

The first two members of series have been identified in the spectrum of yttrium in all three degrees of ionization, and the ionization potentials for three different yttrium atoms, Yt, Yt^+, Yt^{++}, may thus be determined.

1. For Yt III the application of a simple Rydberg formula to the 5^2S and 6^2S terms gives an ionization potential of 20.79 volts for the normal state 4^2D_2. Bowen and Millikan's value of 20.41 volts, which is derived from the value of the 4F term estimated by comparison with Rb I and Sr II, should be much more accurate. If the result of the Rydberg formula is corrected by the empirical method suggested by one of us,[21] it becomes 20.63 volts—still too high. There is other evidence that this correction which holds good for the first long period of elements should roughly be doubled for the second. A Rydberg formula applied to the ^4D and ^5D terms gives 21.79 volts—much too high, as usual.

2. In Yt II, according to the analysis already made, the terms b^3D, c^1D, and c^1S are in series with the low terms a^3D, a^1D, and a^1S, respectively, since they result from the latter when an electron is shifted from a $5s$ to a $6s$ state. Applying the Rydberg formula to the various components of these terms, we find the term values given below. These represent the interval between the term component in question and the limit of the series to which each belongs. In order to find the position of the series limit relative to the lowest energy state of Yt^+, the observed term values relative to this state must be added. According to Hund's theory, $^3D_3$ and $^1D_2$ converge to $^2D_3$ in Yt III as a limit, and $^3D_2$ and $^3D_1$ to $^2D_2$. To find the difference between the lowest energy levels of the singly and doubly ionized atom, we must, therefore, subtract the difference $^2D_3 - {}^2D_2 = 725$, from the sum found in the first two cases and $^2S_1 - {}^2D_2 = 7{,}466$ from the limit of the ^1S series.

	$^3D_3$	$^3D_2$	$^3D_1$	$^1D_2$	$^1S_0$
Levels above $^1S_0$ (Yt II) $(5s)$	1,450	1,045	840	3,296	0
Levels above $^1S_0$ (Yt II) $(6s)$	55,645	55,032	54,956	55,725	61,367
Distance to series limit $(5s)$	100,015	99,711	99,902	97,443	110,300
Distance to series limit $(6s)$	45,820	45,724	55,786	45,014	48,933
Limit above $^1S_0$	101,465	100,756	100,742	100,739	110,300
Limit above $^2D_2$ (Yt III)	725	0	0	725	7,466
$^2D_2 - {}^1S_0$	100,740	100,756	100,742	100,014	102,833

[21] Russell and Lang, Astrophys. J., **66**, p. 247; 1927.

The five determinations agree excellently. In particular, the distribution of the components of the ^3D term between the limits evidently agrees with Hund's predictions. The mean of the five determinations is 101,017, corresponding to an ionization potential of 12.47 volts. Applying the doubled empirical correction mentioned above, this is reduced to 98,720 (12.11 volts). The round number 100,000, or an ionization potential of 12.3 volts, is probably very near the truth.

3. In Yt I, d^2D is in series with a^2D and d^4D with a^4D (both converging to a^3D in Yt II); e^4F' with a^4F' (limit a^3F'); e^4P' with a^4P' (limit a^3P'); and c^2S with a^2S (limit a^1S). Treating the components of these terms as before, we find—

	$^2D_3$	$^2D_2$	$^4D_4$	$^4D_3$	$^4F'_4$	$^4F'_3$	$^4F'_2$	$^4P'_2$	$^2S_1$
Levels above $^2D_2$ (Yt I)	530 36,431	0 36,421	33,752 44,922	33,411 44,655	11,532 44,760	11,278 44,366	11,079 44,053	15,477 50,254	31,672 43,662
Distances to limit	54,690 18,789	55,340 18,929	21,498 10,328	21,610 10,366	51,325 18,097	51,148 18,060	51,079 18,045	53,278 18,501	22,668 10,721
Limit above $^2D_2$	55,220 1,450	55,340 1,045	55,250 1,450	55,021 1,045	62,857 8,743	62,426 8,328	62,158 8,003	68,755 14,098	54,304 0
a^1S_0—a^2D_2	53,770	54,295	53,800	53,976	54,114	54,098	54,155	54,657	54,304

The general agreement is again good, though the two components of the ^2D term are rather discordant. The mean of the nine values is 54,127, corresponding to an ionization potential of 6.68 volts. Applying the appropriate correction reduces this to 6.5 volts, and this is probably very close to the actual ionization potential of neutral yttrium atoms.

IX. YTTRIUM IN THE SUN

The evidence for the existence of both neutral and ionized yttrium in the sun's atmosphere is conclusive, but the two sets of lines behave very differently.

The enhanced lines are well represented. Of those which arise (in absorption) from the low levels, a^1S, a^3D, a^1D, all but the faintest, including many intercombinations, are present or else masked by lines of other elements. The strongest lines reach the intensity 3 on Rowland's scale. The next level a^3F' gives lines of maximum intensity 2; the higher levels a^3P', b^1D, a^1G, none exceeding intensity 0, but all except the fainter lines are either present in the sun or masked. The lines which arise from transitions between the middle and higher terms and are faint in the arc are almost absent from the solar spectrum; the strongest of all, z^3F_4–a^3G_5 (3173.07 A), shows no trace, but z^3F_4–b^3D_3 (3668.50 A) is faintly present.

In the spot spectrum the lines arising from the three lowest levels are very little affected, being, perhaps, slightly weakened. Those

coming from a^3F' are decidedly weakened by a unit of Rowland's scale, and the faint lines from a^3P' and b^1D are practically obliterated.

The arc lines are at best very faint in the spectrum of the sun's disk, but are strengthened to a remarkable degree in the spots. Of the multiplets arising from the low term a^2D the stronger lines are present or masked in the Fraunhofer spectrum, but the strongest of all, a^2D_3–y^2F_4 (4102.38 A), is only of intensity 0. In the spot spectrum these lines are greatly strengthened, the change increasing from two of Rowland's units in the violet to about five in the red. Many of the fainter satellites and intercombinations which are absent from the ordinary solar spectrum appear in that of the spots.

For the next level a^4F' the strong "diagonal" lines of the two principal multiplets, when not masked by other lines, are very feebly present (with maximum intensity − 2) and are moderately strengthened in the spots by about one unit. The weaker lines are absent, even in the spots. About 20 other lines arising from this and from higher levels are attributed to yttrium in the solar spectrum tables. The low-temperature line 5556.43 A is strengthened in the spots, and may really belong to Yt I. Not one of the others is strengthened, and it is therefore practically certain that the solar lines are of other origin and the agreement in wave length with yttrium lines is accidental.

The data on yttrium lines identified with solar spectrum lines may be summarized as follows:

	Yt I	Yt II		Yt I	Yt II
Present in spots only	10		Doubtful	4	5
Unblended	10	42	Total	37	72
Blended with weaker lines		7	Not due to yttrium	22	
Masked by other lines	13	18			

This behavior is exactly what should be expected of an element of moderate abundance and easy ionization. Over the disk almost all the atoms are ionized, and the arc lines are very faint. Over the spots the percentage of ionization, though diminished, is still large, so that the arc lines gain much more in proportion than the enhanced lines lose. The lowered temperature diminishes the relative number of atoms in excited states of higher energy, so that the lines absorbed by such atoms weaken, relatively to those arising from the normal state, for both the neutral and ionized atoms.

WASHINGTON AND PRINCETON, October 25. 1928.

THE PRECISE MEASUREMENT OF X-RAY DOSAGE [1]

By Lauriston S. Taylor

ABSTRACT

A comparison of the unit of X-ray dosage was made by Behnken and showed a variation of 4 per cent between various laboratories. For the purpose of definition and constancy a well controlled direct-current voltage source is provided for the X-ray tube. Using this, a comparison was made between the various methods using the same equipment for all. A large parallel plate ionization chamber was used to measure the *r* unit as defined by international agreement. The discrepancies were found to be due to the electrostatic field distortion introduced by the various ionization current measuring devices. For the purpose of measuring *r* precisely a null method is used and described. Sources of error are discussed and their probable magnitude indicated in certain cases. Under known conditions the difference between Behnken's and Glasser's determination has been duplicated in order of magnitude and in direction. A complete description of the Bureau of Standards equipment for the standard measurement of Röntgen dosage is given.

CONTENTS

	Page
I. Introduction	771
II. X-ray generating equipment	772
III. Ionization measuring system	774
IV. Results	779
V. Accuracy of measurements	784

I. INTRODUCTION

With the increase in the use of X radiation in medical therapy it has become more important to be able to express with some exactitude the actual amount of radiation being received by a patient. It is also necessary that this quantity be expressed in a common unit which is readily reproduced and in which there is no ambiguity.

In practice there are three distinct operations necessary in order to describe the radiation at a given location. (1) The measurement of the radiation intensity by means of a dosage meter. (2) the calibration of the dosage meter against a standard which measures the unit of X radiation exactly. (3) A determination of the wave-length

[1] Read before the Radiological Society of North America, Dec. 5, 1928.

distribution of the total radiation. It is with the second part that the Bureau of Standards is particularly interested and more especially with the exact measurement of the unit which was defined at the Second International Congress of Radiology at Stockholm, July, 1928, as follows: * * * "the quantity of radiation which, when the secondary electrons are fully utilized and the wall effect of the chamber is avoided, produces in one cubic centimeter of atmospheric air at 0° C. and 76 cm mercury pressure such a degree of conductivity that one electrostatic unit of charge is measured at saturation current." This unit is called the "Röntgen" and is designated by small "*r*."

In a recent paper Behnken [2] gives the results of his comparison of the unit between the laboratories of Grebe, Küstner, Holthusen, Duane, Glasser, and the Physikalisch Technischen-Reichsanstalt. According to his measurements there is a discrepancy of about 4 per cent between various laboratories. No explanation for these differences has been given, and it is assumed that they are traceable to experimental error. However, as a result of some preliminary measurements made at the Bureau of Standards with the cooperation of Doctor Behnken, it was evident that improper electrostatic field conditions within the ionization chamber could account for at least some of the variation. To test this, a single ionization chamber was used under the same X-ray conditions but with various combinations of potentials applied to the plates as shown below.

II. X-RAY GENERATING EQUIPMENT

During the above-mentioned comparisons of Behnken it was demonstrated very clearly at the Bureau of Standards that, from the point of view of regularity of action, a mechanically rectified system was unsuited to precise X-ray measurements.

The wave-length energy distribution in the X-ray continuous spectrum excited by constant voltage can be expressed mathematically [3] and can be determined experimentally with fair precision [4] as a function of the X-ray tube voltage and other factors, such as target material, etc. The total energy varies approximately as the square of the voltage. Consequently, with a tube potential fluctuating in an uncertain manner—as the mechanical rectified case—the energy distribution with time becomes uncertain; and, due to the shifting of the short wave length cut-off voltage, the quality is uncertain, since the spectral range is constantly shifting. As a result it was decided to use a kenetron rectified direct current source of high potential in which the voltage fluctuation or ripple was a minimum.

[2] H. Behnken, Strahlentherapie, **29**, p. 192; 1928.
[3] H. Behnken, Zeit. fur Phys., **4**, p. 241; 1921.
[4] T. Ulrey, Phys. Rev., **11**, p. 401; 1918

Thus there is a constant energy distribution and constant quantum cut-off within narrow limits.

This must not be confused with the medical application, for Coolidge has shown [5] that for the requirements of medical treatment the direct and alternating high voltage source are about equally effective.

The circuit used is of the Hull [6] and Webster and Henning [7] type shown in Figure 1. The main transformer T_1 has one end of the secondary S grounded. The other end goes to the cathode and anode, respectively, of two 250,000-volt kenetrons of the newest type. The filament current for these is supplied by separate insulation transformers T_2. The condensers C_1 and C_2 are of the Meirowsky Pertinax type in single units of 0.05 μf each, thus avoiding the difficulty of series condensers. The two chokes L_1 L_2 have 12,000 henrys induc-

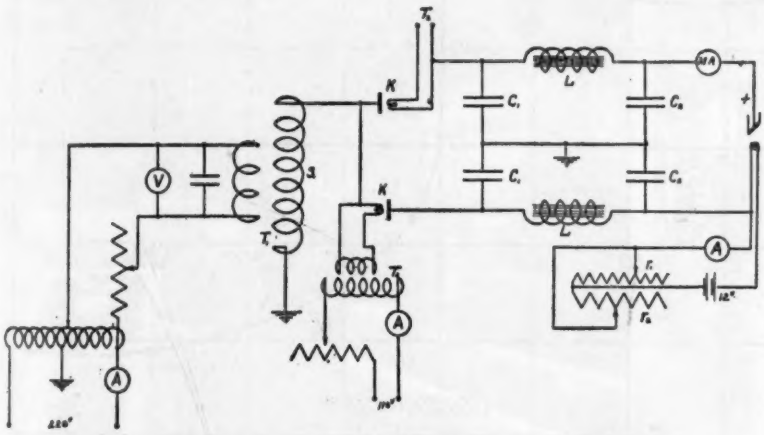

FIG. 1.—*Diagram of X-ray generating system showing controls*

tance and are wound on closed iron cores immersed in oil. Protective sphere spark gaps are placed across the kenetrons K, condensers and X-ray tube.

The voltage is measured ordinarily by means of a large sphere gap, but an electrostatic voltmeter is available for control. An X-ray tube of the Coolidge 200 k. v. deep therapy type has its filament current supplied from storage batteries placed in a coronaless copper case and in which the current is adjusted by remote control. The high-tension system is of three-fourths-inch tubing carefully installed to eliminate any corona discharge with consequent unsteadiness. It was found unnecessary to have any corona to act as a "safety valve," since the circuit design eliminated the likelihood of severe surges. A

[5] Am. J. Röent., **9**, p. 77; 1922.
[6] A. W. Hull, Am. J. Röent., **2**, p. 153; 1915.
[7] P. L. Webster and A. E. Henning, Phys. Rev., **21**, p. 301; 1923.

60-cycle 25 K. V. A. synchronous motor generator supplies all of the transformers in order to obtain best control. A carefully adjusted overload circuit breaker in the main transformer primary prevents the possibility of damage from any heavy current discharges in the system. It has not been found necessary to use any protective resistances next to the X-ray tube, as no evidence of gas has been shown with the tubes used.

When making precise measurements a second operator controls the filament current and primary voltage. Under good conditions a precision of observation of 0.2 to 0.3 per cent can readily be obtained

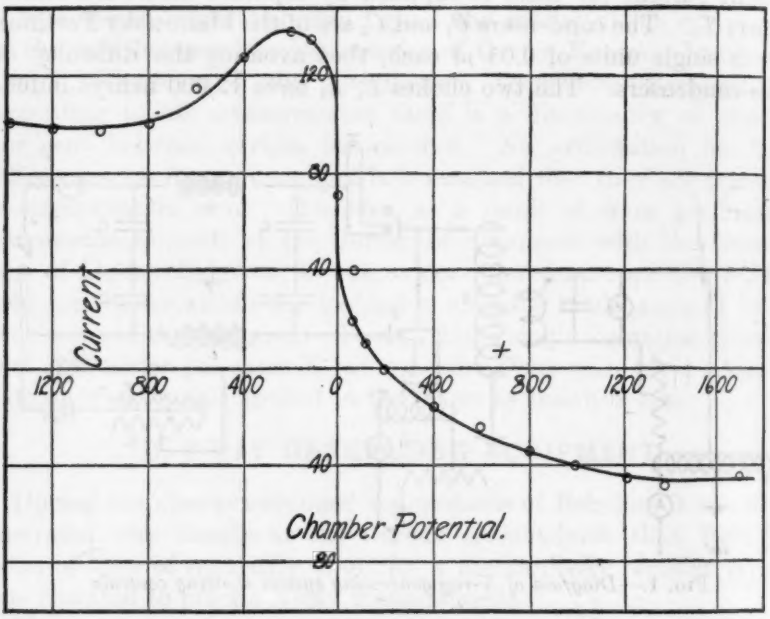

FIG. 3.—*Curve showing ionization current as a function of the chamber potential, using early model Duane chamber and Victoreen electroscope*

over a period of several hours. The variation from day to day, however, is frequently found to be double this amount.

III. IONIZATION MEASURING SYSTEM

It was decided from the start to use a large parallel plate ionization chamber as suggested by Duane [8] in his early work. The first form of Duane's chamber was not of sufficient size, and the guards were not properly placed. Using such a chamber at the bureau with the cooperation of Doctor Behnken, mentioned above, the ionization current curve shown in Figure 3 was obtained where the current is

[8] Wm. Duane, Am. J. Röent., **9**, p. 467; 1922.

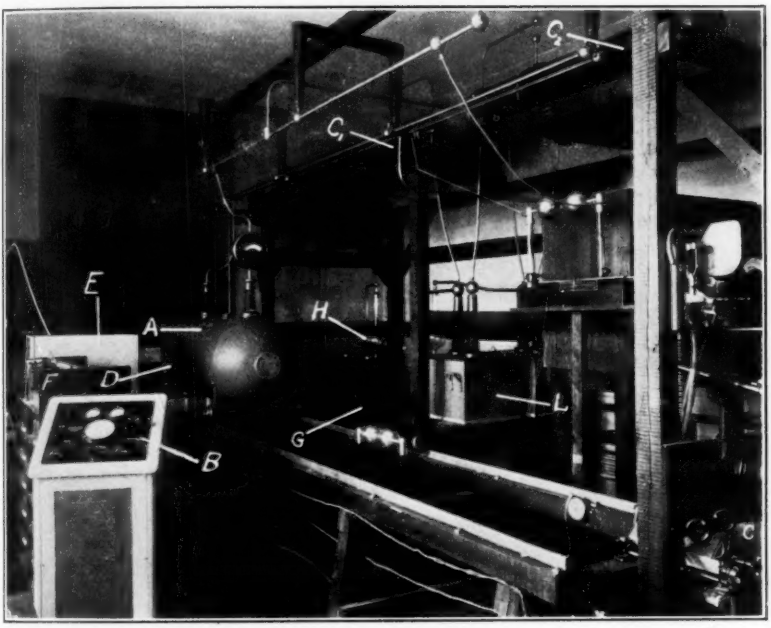

FIGURE 2.—*General assembly of constant potential generator*

L, Choke coils; C_1, C_2, condensers; *A*, one-quarter inch lead tube shield; *B*, control panel; *D*, magnetic shutter; *E*, ionization chamber; *F*, 1,500-volt battery; *G*, main transformer; *H*, kenetrons.

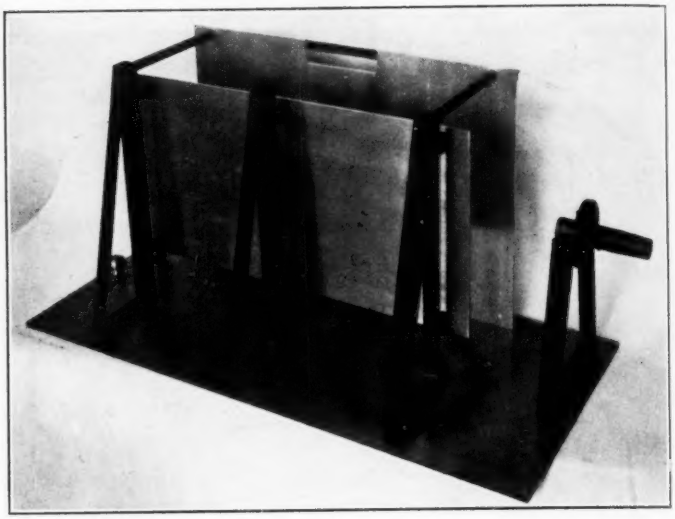

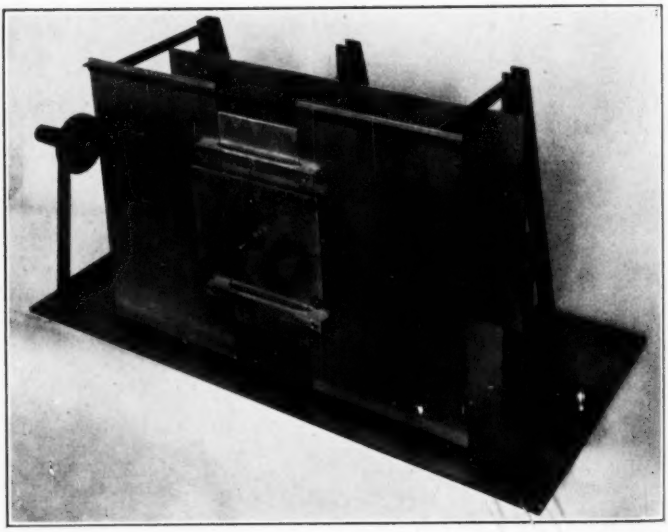

FIGURE 5.—*Photographs of condenser plates composing the standard ionization chamber*

plotted as a function of the chamber voltage. By analysis of this curve some approximate idea can be obtained of the field conditions within the chamber. This curve is shown because it is quite typical for a faulty system where the electrode potentials differ and was present in an early type of chamber when used with an idiostatic electrometer in place of a galvanometer.

To avoid this difficulty, a null electrostatic measuring method is used. This has the advantage of being quite sensitive and being applicable to studying the field distortion as shown below. The galvanometer gives equally reliable results but does not have a sufficient range of sensitivity in the particular system.

The final form of standard chamber is shown in Figures 4 and 5. The plate spacing is 10 cm. The measuring electrode is 10 cm

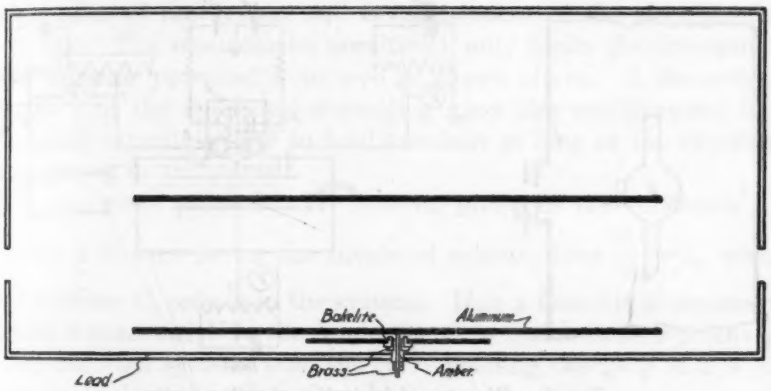

FIG. 4.—*Cross section of ionization chamber*

wide and the guards 20 cm wide with a 0.5 mm spacing between. The collector electrode is supported from the back by four amber posts bearing an aluminum yoke spread between the guards. All of the electrodes are mounted on a brass plate as shown in the photograph (fig. 5). The guard plates are ordinarily earthed. The entire electrode system is placed in a one-eighth inch lead box with a one-fourth inch lead front. The spacing between the high-voltage electrode and the case was never less than the distance across the condenser normal to the beam (10 cm). In the present chamber it is about 15 cm. Since the assembled unit is very large and heavy, it is mounted on an adjustable track so as to be readily aligned. Behind the ionization chamber is a lead chamber for preventing as much radiation as possible from escaping into the room. There is no measurable back scattering from this chamber.

The diaphragm system is arbitrary, being approximately the same as used by Behnken[9] and Glasser.[10] More recent work by Failla[11] has indicated that these diaphragm systems are perhaps not exactly correct. In any case it was not altered throughout the entire experiments. About ½ cm from the X-ray tube wall is placed a disk of 55 per cent lead glass 2 cm thick and having in the center a 12 mm hole. The position of this diaphragm is adjustable in all directions.

The tube is contained in a one-fourth inch lead cylinder lined with steel for rigidity. This is mounted on a 16-foot track so as to move into several positions.

An electrically operated lead shutter is mounted on the tube shield and controlled from the observer's position. The shutter system is similar to that used by Webster[12] and others, and the timing is

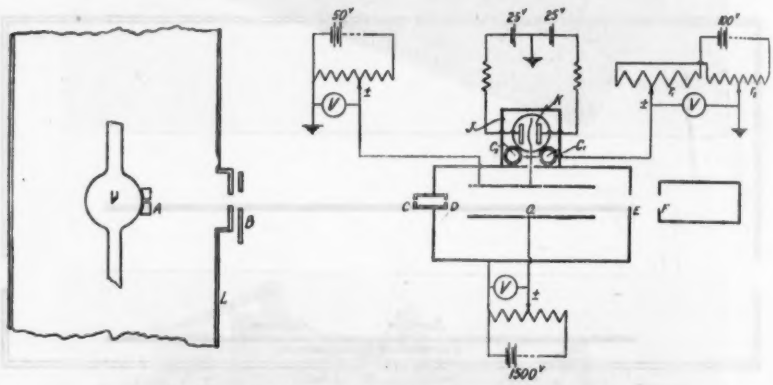

FIG. 6.—*Diagram of ionization chamber system*

A, lead glass diaphragm. *B*, diaphragm and shutter on tube shield. *C*, diaphragm for defining the standard beam. *D*, diaphragm to reduce scattering of radiation within the chamber. *E*, diaphragm at back of lead box. *F*, lead box to stop radiation from entering the room. *G*, ionization chamber. *J*, one-eighth inch lead box surrounding electroscope system. *K*, Lutz-Edelmann Wollaston fiber electrometer. *L*, cylindrical X-ray tube shield

independent of any uncertain electrical contacts. The shutter can be opened for any multiple of 7.5 seconds to within at least 1/1,000 second and avoids the use of a stop watch.

Figure 6 shows the electrostatic measuring system. The electrometer and condensers are in a one-eighth inch lead box fastened to the chamber box. This provides electrostatic and X-ray protection. The system was carefully tested and all measurable leakage eliminated. K is a Lutz-Edelmann fiber electrometer, which for the null readings was connected as shown with ±25 volts on each knife-edge. C_1 and C_2 are amber insulated concentric cylinder condensers, and

[9] H. Behnken, Strahlentherapie, **26**, p. 79; 1927.
[10] O. Glasser, Am. J. Röent., **19**, p. 47; 1928.
[11] G. Failla (seen in manuscript form).
[12] D. L. Webster and A. E. Henning, Phys. Rev., **21**, p. 301; 1923.

C_2 (140 $\mu\mu$f) can be cut in and out of the system from outside the shield. For the purpose of null reading, on one side of C_1 a variable potential is applied by means of the coarse and fine rheostats r_1 and r_2. This is read on a precision voltmeter.

In making observations the electrode is first ungrounded and the shutter then opened. An observer maintains the cross hairs on the zero potential mark by continuously adjusting the rheostats r_1 and r_2 during the entire exposure. Thus, the potential of the collector electrode never differs from that of the guards by more than a small amount, which is determined by the sensitivity of the electrometer and the capacity of the system. In the particular case it was ± 0.3 volt.

In such a method the potential necessary to counteract a given potential increase of the system depends solely upon the geometrical configuration of the system and is independent of the electrometer sensitivity. The electrometer sensitivity only limits the divergence of the collector potential from zero as shown above. A theoretical constant k of the apparatus depending upon this configuration has been found experimentally to hold constant as long as the capacity of the system is unchanged.

If a change of potential ΔV between plates of the condenser C_1 produces a change Δv on the insulated system, then $\frac{\Delta V}{\Delta v} = k_c$ when the condenser C_1 only is in the system. If in a time t it is necessary to apply a potential V to the condenser C_1 to maintain zero potential on the insulated system, then the corresponding charge Q in e. s. u. due to the ionization is then given by

$$Q = \frac{C\,V}{k_c} \quad (V \text{ in e. s. u.}) \tag{1}$$

$$= 0.9\,\frac{C\,V}{300\,k_c} \quad (V \text{ in volts and } C \text{ in } \mu\mu\text{f}) \tag{2}$$

where C is the total capacity of the system. Thus, under standard conditions of temperature and pressure, the dose in r per minute is given by

$$r/\text{min} = \frac{0.9 \times C\,V \times 60}{300 \times t\,k_c\,W} \tag{3}$$

where W is the effective volume of ionized air and C is measured in micromicro farads. Including next, the approximate correction for temperature T (degrees absolute) and pressure P (mm)

$$r/\text{min} = \frac{0.9\;\;C\;\;V \times 60 \times 273 \times \text{P}}{300 \times t\,k_c\;W\;T \times 760} \tag{4}$$

The constant k_e was determined carefully by charging the electroscope first directly from a potentiostat and then to the same scale points by means of the compensating potential applied to the condenser C_1. The curves in Figure 7 give the experimental relation between V, the compensating potential, and v, where k is given by

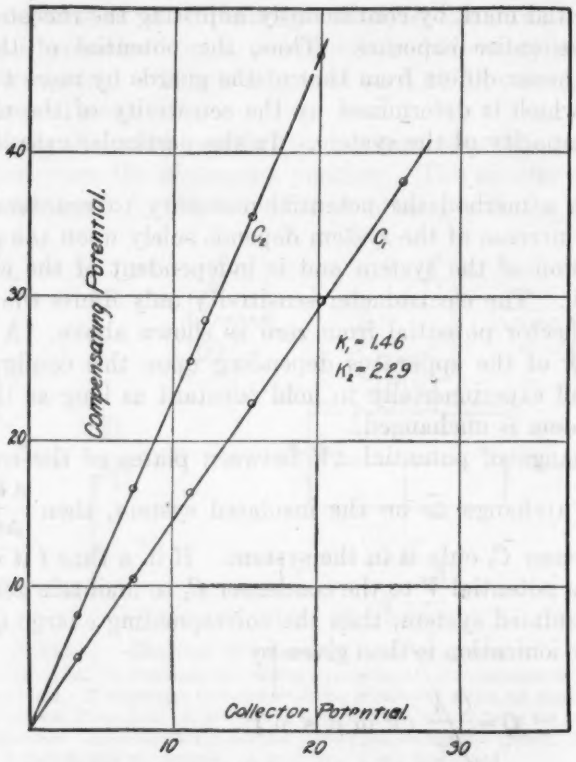

FIG. 7.—*Curves used for the determination of the apparatus constant "k"*

the slope. In the particular case only two capacities were used, but it is noticed that the relation is closely linear, and by taking the best line through the points a very accurate determination of k is possible. In addition, this was tested, using a standardized variable condenser outside the case and the same accuracy was found. In the expression (4) above the ratio $\frac{C}{k_e}$ should be a constant for all capacities. This was found to be true over a wide range of electrometer sensitivities and from day to day. Thus the error introduced in r by certain other measuring methods due to the measurement of the volt sensitivity of the electrometer is eliminated.

IV. RESULTS

The discrepancies between the various measuring methods is at once apparent from the saturation curves obtained by the same chamber under constant X-ray conditions. Four such curves are shown in Figure 8. In all cases the chamber potential was positive. (*a*) The electroscope was charged negatively and the discharge time from −50 to −32 volts measured. The saturation value was 3.55 *r*/min. (*b*) The electroscope was charged positively and the charge time from +32 to +50 volts measured. The saturation value was 2.77 *r*/min. (*c*), the electroscope was again charged positively and charging time from +50 to −50 measured. (This can be considered

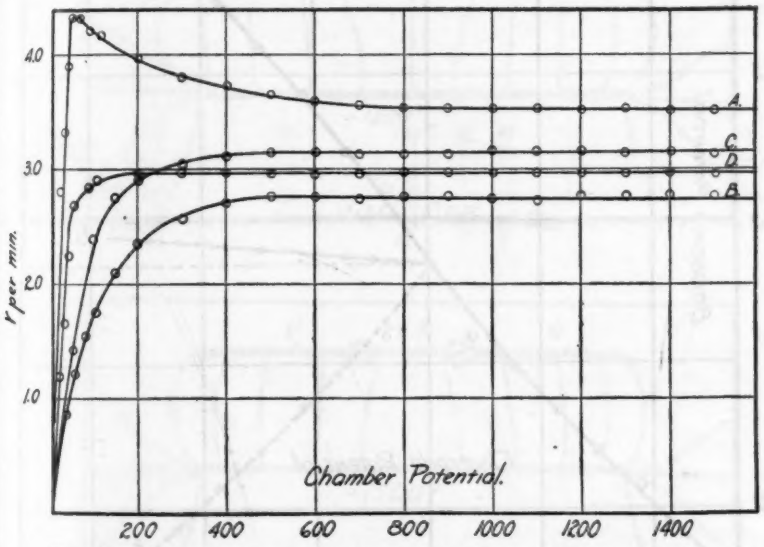

FIG. 8.—*Saturation curves for standard ionization chamber using different measuring methods*

A, using a discharging, fiber electrometer. *B*, using a charging, fiber electrometer. *C*, using an idiostatic fiber electrometer. *D*, using a null reading fiber electrometer

as an average of *a* and *b*.) The saturation value was 3.15 *r*/min. (*d*) The null reading method gave a saturation value of 2.93 *r*/min. (*e*) Galvanometer method. (For the low energies used it was not practicable to determine the whole curve with the galvanometer, but above saturation it agreed within the experimental error with the null method.)

Field distortion (to be described later) in the first two methods can account for the peculiar form of the curves. Glasser apparently recognizes this and then assumes that the distortion shown by curves *A* and *B* is equal and opposite, since he essentially uses method C. Since, however, method C produced a higher saturation value than

D and E, the actual field distortion was carefully determined in the present case by experiment.

To study this two methods were used which agreed within experimental error. With the chamber potential positive and well above saturation, the guard plates were set at zero potential and the electrometer system charged to various potentials from -45 to $+45$ volts. At each voltage value r was measured by the null method, maintaining the potential difference between guards and collector constant to within ± 0.3 volts. Since $r = \text{const} \times V$ (equation (4)), a curve

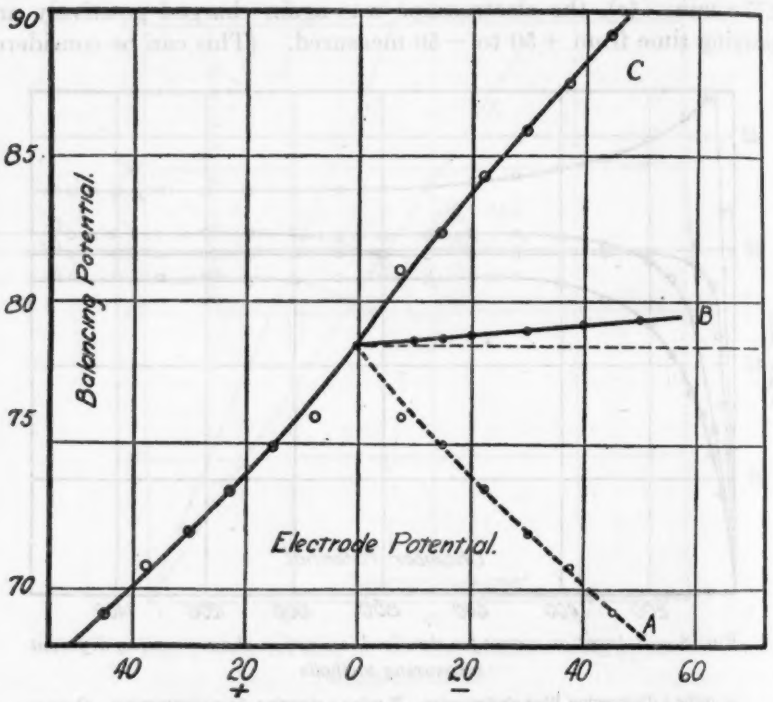

FIG. 9.—*Saturation current in the standard ionization chamber as a function of the potential difference between the guard plates and collector plate*

Curve *B* shows the average saturation current for corresponding positive and negative potential differences. (Balancing potential is proportional to the saturation current)

showing V plotted against the potential difference between plates will give the difference in r according as the potential of the collector is above or below the guard. This is given by C in Figure 9. The value of r by the null method is that where the curve crosses the axis (78.4 volts in the particular case). The broken line A is simply the positive portion of the curve swung under the negative portion for more obvious comparison. Averaging these values it is seen at once from curve B that the mean falls consistently *above* the value determined by the null method. In other words, the distortion pro-

duced when the collector is negative is greater than that when the collector is positive with respect to the guard potential. A picture of the field is given in Figure 10 for each case.

Exactly the same result was obtained when the collector was maintained at zero potential and the guards are set at the same potentials as above.

It may be said that the irradiated volume is determined by the cross section of the beam and the bounding lines of force that just reach the collector at the edges. Thus it has been shown that due

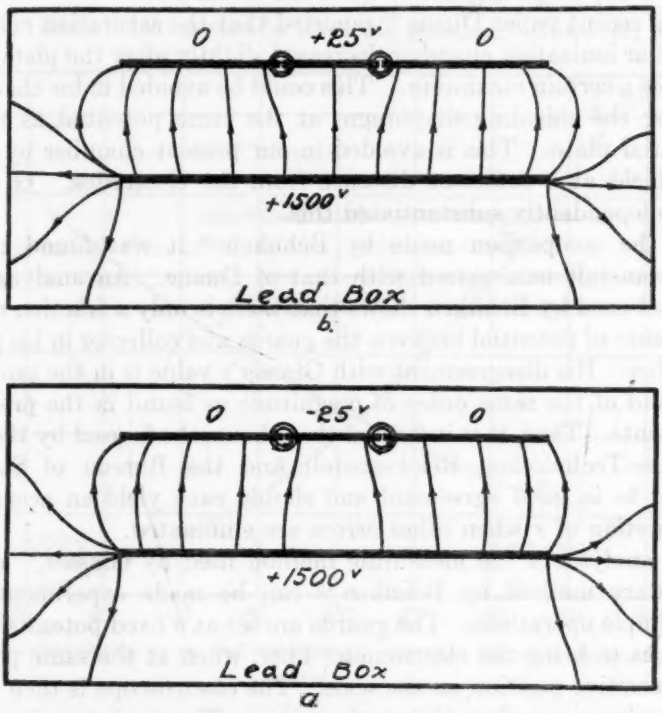

FIG. 10.—*Probable electrostatic field diagram in the standard chamber*

A, when using a discharging electrometer. *B*, when using a charging electrometer

to controlled field distortion the length of irradiated volume varies in an unsymmetrical manner, the degree of dissymmetry depending upon the geometrical configuration of the system. This effect should be symmetrical when the width of the collector and the width of the guards are both very great with respect to the spacing of the condenser plates.

Referring again to Figure 9 we may regard the curves *A* and *C* as defining the irradiated volume limits for different potential differences between guard and collector. The average curve *B* then indicates

the change in length of the irradiated volume and the corresponding error introduced by a potential difference between the guard and collector, such as caused by the use of an idiostatic electrometer.

Rosa and Dorsey,[13] in their work with precision guard plate condensers, have calculated the error due to a very small displacement between the guards and collectors if their potential differs. A measurable error of this kind was found by displacing the collector plate in the present ionization chamber when using the deflection method of measurement. It is not likely, however, that this error has been of any large amount in the work of others.

In a recent paper Duane [14] reported that the saturation current for a similar ionization chamber decreased slightly after the plate spacing reaches a certain maximum. This could be avoided in his chamber by placing the shielding diaphragm at the same potential as the high potential plate. This is avoided in our present chamber by spacing the shield at a sufficient distance from the electrodes. G. Failla[15] has independently substantiated this.

In the comparison made by Behnken [16] it was found that the Reichsanstalt unit agreed with that of Duane. An analysis of the method used by Behnken shows that there is only a fraction of a volt difference of potential between the guards and collector in his pressure chamber. His disagreement with Glasser's value is in the same direction and of the same order of magnitude as found in the present experiments. Thus, it is indicated that the methods used by the Physikalische-Technischen Reichsanstalt and the Bureau of Standards should be in good agreement and should each yield an accurate determination of r when other errors are eliminated.

An analysis of the measuring method used by Glasser,[17] and as a secondary method by Behnken,[18] can be made experimentally by two simple operations. The guards are set at a fixed potential of such value as to bring the electrometer fiber, when at the same potential, to a sensitive position on the scale. The electroscope is then charged to a value somewhat higher than this. Times of transit are then measured with a split second stop watch between every five divisions on the scale. The voltage sensitivity curve of the electrometer is shown in A (fig. 11) and is seen to be continuously changing. The point a on the sensitivity curve corresponds to the guard plate potential (147 volts). Points b and c correspond to equal voltage steps above and below a, through which range the electrometer was discharged; b' and c' are the corresponding time points. The corre-

[13] E. B. Rosa and N. E. Dorsey, B. S. Bull., **3**, p. 433.
[14] Wm. Duane, Am. J. Röent., **19**, p. 461; 1928.
[15] See footnote 11, p. 776.
[16] See footnote 1, p. 771.
[17] O. Glasser, Am. J. Röent., **19**, p. 47; 1928.
[18] H. Behnken, Strahlentherapie, **26**, p. 79; 1927.

sponding transit time curve B for the electrometer discharging is given below and is also seen to be continuously varying. The formula used in calculating (4) from this data is given by

$$r/\text{min} = \frac{C \times V \times 60}{300 \times W \times t}$$

where V in this case is the volt sensitivity. From the curves above the ratio $\frac{V}{t}$ can be obtained in any suitably small increments. Thus, in order to determine r/min accurately the ratio $\frac{\Delta V}{\Delta t}$ should be either constant or linear with respect to the scale position. However, in the

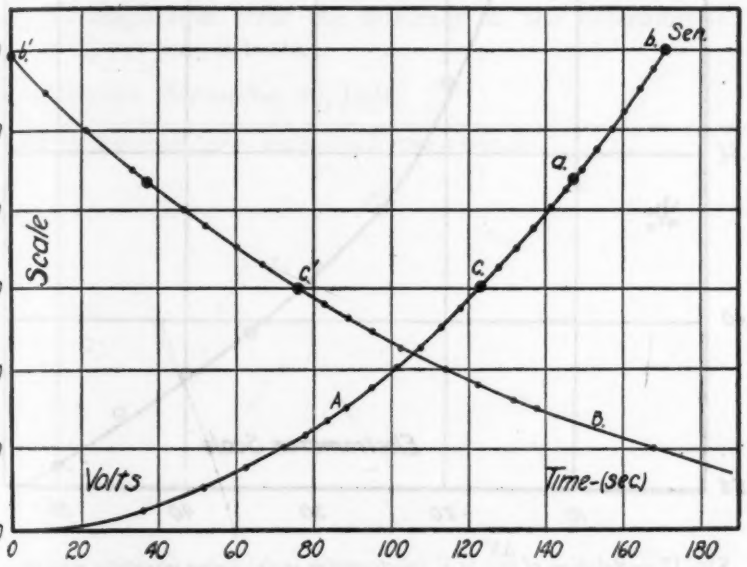

FIG. 11.—*Sensitivity curve and time-transit curve for idiostatic measuring method*

particular case the ratios obtained from the curves in Figure 11 when plotted against scale position gave a nonlinear relation as indicated in Figure 12. It is thus clear that under ordinary circumstances the above method will not yield an accurate determination of r/min. It must be pointed out, however, that if a sufficiently small voltage range is used the error will not be large, since the relation is nearly linear for short ranges of voltage.

Also, it is probable that by varying the gap between collector and guards this nonlinearity may be increased or diminished, thus changing the error introduced. When the above method of measurement is used, the error should be carefully studied and proper precautions be taken to eliminate it or reduce it to a minimum.

There is yet another source of error detectable when using a comparatively highly charged collector or guard plates. A small amount of secondary radiation scattered by the air may actually pass between the guards and collector producing ionization both between the guards and collector and in the space behind them. In the first case the ionization current changes direction as the collector potential passes that of the guards. The error introduced is thus additive in one case and subtractive in the other. In the second case the ionization will be constant provided saturation exists behind the plates.

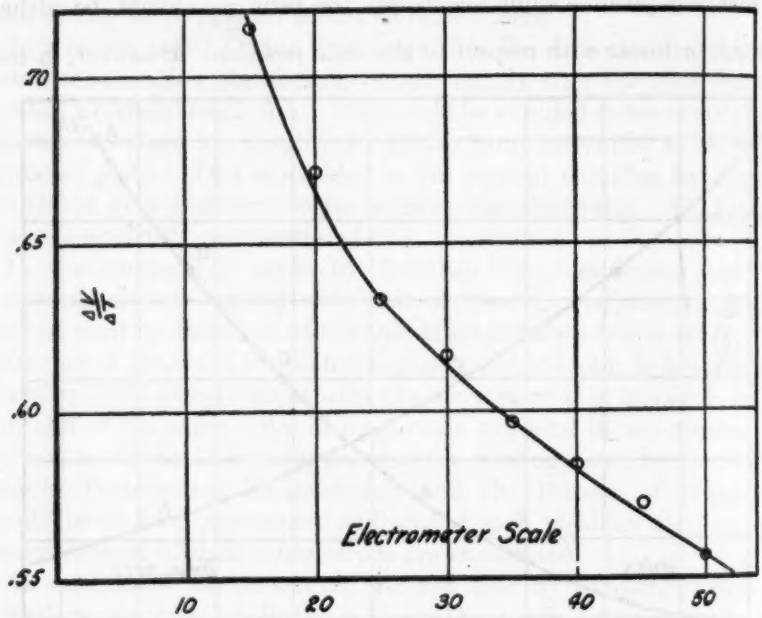

FIG. 12.—*Relation of* $\frac{\Delta V}{\Delta t}$ *to V (electrometer scale) using idiostatic measuring method*

When employing a null method in which the collector, guards, and box are all at zero potential, these errors will be absent.

V. ACCURACY OF MEASUREMENTS

The actual error in the present measuring system can be approximately determined. It must be emphasized, however, that an arbitrary diaphragm system has been used thus far and the error in determining the volume W of air ionized has been omitted. For an accurate measurement of r/min this should, of course, be known.

The primary voltage on the high tension and filament transformers is measured to within ± 0.1 volt. The ripple or fluctuation in the

rectified voltage was calculated with sufficient accuracy [19] and found to be approximately 0.2 per cent when a current of 1.0 m. a. is being drawn. The X-ray tube current is controlled to within ± 0.005 m. a.

When using the compensating potential the mean deviation of a number of readings is usually found to be 0.2 to 0.3 per cent. The voltage can be read to ± 0.1 volt out of 100 volts, and the meter is accurate to 0.25 per cent. The capacity of the system is measured by means of a bridge calibrated at the Bureau of Standards. The capacitance can be determined with an accuracy of 0.5 per cent or better. By referring to the curves in Figure 6 for the determination of k, it was shown that the ratio $\frac{C}{k}$ = const. This also serves as a check on the capacitance measurements. It is thus seen that aside from the diaphragm error the accuracy in the determination of r/min. is 1.0 per cent or better.

WASHINGTON, September 30, 1928.

[19] L. B. Jolley, Alternating Current Rectification, J. Wiley & Sons; 1924.

NOTE ON AN ELECTRICAL CONDUCTANCE METHOD FOR DETERMINING LIQUEFACTION TEMPERATURES OF SOLIDS

By Edward W. Washburn and Edgar R. Smith

ABSTRACT

A conductance method for measuring liquefaction temperatures, which requires only a few milligrams of the substance investigated, is described. The method has been applied to the determination of eutectic temperatures of water-salt systems and to the determination of transition temperatures of salt hydrates. The method is applicable to any system which is practically a nonconductor of electricity below the liquefaction temperature and which abruptly exhibits an appreciable conductance at this temperature.

CONTENTS

	Page
I. Introduction	787
II. Experimental procedure	788
III. Apparatus and method	788
IV. Experimental results	789
1. Eutectic temperatures	789
2. Incongruent melting points	790

I. INTRODUCTION

When a solid or a mixture of solids behaves as an electrical insulator below its liquefaction temperature but becomes a conductor as soon as the liquid phase appears, the temperature at which the system acquires this electrical conductance will be the liquefaction temperature of the system. This paper describes an apparatus for determining this temperature and gives some experimental results obtained in applying the method to the determination of eutectic temperatures and of incongruous melting points of salt hydrates.

The method will be found especially convenient where only small quantities of material are available. It has the additional advantage, in comparison with other methods, of being unaffected by the presence of any impurity which does not lower the initial liquefaction temperature. It will give reliable results in many cases in which the customary methods fail for any of the following reasons:

1. Because of the presence of impurities soluble in the liquid phase.
2. Because of a small latent heat of liquefaction which renders the equilibrium method, the calorimetric method, or the method of thermal analysis unreliable.

3. Because of the acuteness of the angle of intersection of the solubility curves in the case of the solubility method.

4. Because of a small volume change on liquefaction in the case of the dilatometer method.

II. EXPERIMENTAL PROCEDURE

For the determination of eutectic temperatures of aqueous systems containing at least one electrolyte the method consists essentially in applying a voltage across the electrodes of a cell filled with ice in contact with the solid electrolyte or mixture in question. The cell is immersed in a well-stirred bath below the eutectic temperature and is connected with a galvanometer. The temperature of the bath is allowed to rise slowly. When the eutectic temperature is reached, solution forms in equilibrium with the solid mixture and causes a marked increase in conductance. At this point the galvanometer deflects and the corresponding temperature is measured by means of a thermometer immersed in the bath. For the measurement of a melting point a similar procedure is followed.

FIG. 1

III. APPARATUS AND METHOD

After experimenting with several arrangements, the apparatus (fig. 1) finally adopted consists of an iron cell, shown to scale in the figure, containing a platinum-wire electrode sealed in the glass tube which projects through the bottom of the cell. The cell serves as the other electrode. During the measurement it is immersed in a well-stirred bath of mercury precooled below the temperature to be measured and contained in a Dewar tube. If a eutectic temperature is to be measured, the cell is first partly filled with water, which is then frozen so that the end of the platinum wire extends through the surface of the ice. A few milligrams of the powdered electrolyte are placed on the ice surface around the electrode,[1] the cap is screwed into place, and the cell is completely immersed in the bath close to the bulb of a thermometer. The cell is connected in series with the heating element of a vacuum thermocouple and with the 6-volt

[1] A little melting and immediate refreezing might occur when the warmer particles first touch the ice surface. The result would be a thin surface layer of frozen eutectic mixture which would do no harm and might even be an advantage.

terminals of a small transformer operated on the 60-cycle 110-volt line. The thermocouple leads are connected to the terminals of a galvanometer. The galvanometer used had a voltage sensitivity of 0.3 mm per microvolt and was suitably damped when connected to the thermocouple. The temperature of the bath is allowed to rise slowly, and when the galvanometer shows a deflection the reading of the thermometer is taken as the eutectic temperature. It is worth noting that the galvanometer deflection is proportional to the square of the conductance, since the heat developed at the thermocouple junction is proportional to the square of the current. The successful use of the thermocouple and galvanometer arrangement depends largely on this second power proportionality.

It was found best, in order to obtain results reproducible to about 0.02 to 0.03°, to keep the circuit open until the temperature is within 0.1 to 0.2° of the eutectic point; otherwise the small current across the solid mixture may cause a cumulative heat effect within the cell resulting in the formation of solution and a marked increase in conductance before the outside bath has reached the eutectic temperature. The experimental fact that, with the circuit continuously closed, larger impressed voltages may result in deflections at lower temperatures seems to bear out this conclusion. For this reason, the circuit is closed only momentarily every 0.02°, starting 0.1 to 0.2° below the eutectic temperature and continuing until slightly above. A preliminary experiment may be necessary in some cases to establish the approximate location of the eutectic point.

If a melting point is to be measured, the cell is filled with the dry salt below the desired temperature and the same procedure is followed.

TABLE 1.—*Temperature galvanometer readings for the system K_2SO_4–H_2O*

Temperature	Galvanometer deflection	Galvanometer deflection
°C.	mm	mm
−1.61	0	0
.59	0	0
.57	0	0
.55	0	0.5
.53	1	2
.51	6	8
.49	20	35

Average eutectic temperature, 1.54°.

IV. EXPERIMENTAL RESULTS

1. EUTECTIC TEMPERATURES

Typical temperature and galvanometer readings obtained by the method outlined are shown in Table 1 for two experiments with potassium sulphate and water. In order to give the method a further test, the eutectic temperatures of several salts and of a salt mixture were

measured and compared with the values obtained by investigators using the equilibrium method with large quantities of the salts. These results are summarized in Table 2. Each result given in the table is the average of two or three determinations agreeing to within 0.02 to 0.03°. The known values were taken from Landolt-Börnstein Tabellen, fifth edition, and International Critical Tables. It is evident, from the comparison of the known eutectic temperatures with the measured values for the salts given in the table, that the method gives results which are correct within its own degree of precision. Temperature lag between the bulb of the Beckmann thermometer and the contents of the cell and, perhaps, the time required for the spreading of a finite film of solution over the surface of the ice may account for the variability observed. The use of a small thermocouple placed within the cell instead of the thermometer in the bath would probably reduce the temperature lag and eliminate the variability due to this cause.

TABLE 2.—*Eutectic temperatures measured by the conductance method compared with their known values*

Electrolyte	Eutectic temperature by conductance	Known eutectic temperature
	°C.	°C.
K_2SO_4	−1.54	−1.55
$FeSO_4.7H_2O$	−1.80	−1.821
KNO_3	−2.84	−2.9
Mixture of K_2SO_4-KNO_3	−3.27	−3.3
$Na_2CrO_4.10H_2O$	−4.92	−4.9

2. INCONGRUENT MELTING POINTS

The temperature at which the dekahydrate of sodium sulphate is in equilibrium with the anhydrous salt and solution and the temperature at which the dekahydrate of sodium chromate is in equilibrium with the hexahydrate and solution are known to an accuracy of about 0.001° and are used as fixed points in thermometry.[2] These transition temperatures were measured by the conductance method and furnish a reliable test of the method for such systems. The thermometer used for this purpose was graduated in 0.2° divisions and had a Bureau of Standards calibration certificate. It was further standardized at the transition temperature of the dekahydrate of sodium sulphate (32.384°) by immersing it in a Dewar tube filled with the equilibrium mixture at this temperature. The temperatures found by the conductance method are compared with the known values in Table 3. Corrections were applied for the emergent stem.

[2] Richards and Wells, Proc. Am. Acad., **38**, p. 431; 1902. Dickinson and Mueller, B. S. Bull. **3**, p. 641; 1907. Richards and Kelly, Proc. Am. Acad., **47**, p. 171; 1911.

TABLE 3.—*Transition temperatures determined by the conductance method compared with those determined by the equilibrium method*

Mixture	Transition temperature by conductance	True transition temperature
	° *C.*	° *C.*
$Na_2SO_4.10H_2O+Na_2SO_4$	32.33	32.384
$Na_2CrO_4.10H_2O+Na_2CrO_4.6H_2O$	19.51	19.525

WASHINGTON, November 21, 1928.

CALIBRATION OF SIXTY-FIVE 35-YELLOW LOVIBOND GLASSES [1]

By Irwin G. Priest, Deane B. Judd, K. S. Gibson, and Geraldine K. Walker [2]

ABSTRACT

This report deals with 65 nominally 35-yellow Lovibond glasses collected from members of the American Oil Chemists' Society, submitted to the Bureau of Standards in August, 1927, by H. P. Trevithick, and identified by AOCS numbers engraved on the glasses. It is understood that Mr. Trevithick has a key to these numbers showing the ownership of each glass.

The fundamental standard to which the values here reported are referred is contained implicitly in a particular set of glasses obtained directly from the Lovibond establishment (The Tintometer (Ltd.)) in 1912, kept at the Bureau of Standards, and designated as B. S. 9940 for purposes of identification. The units of the red and yellow scales effective in the present calibration are as derived from this set of glasses by Priest and Gibson in 1927 after adjusting the inconsistencies among the different glasses in the set.

The data reported include, for each glass: (1) The equivalent in terms of standard Lovibond yellow and red; (2) the sunlight transmission.

Explicit directions are given for using the equivalents in practice. Special comments are made on seven glasses having strikingly abnormal transmissions or badly marred surfaces. Also, to aid in the possible identification of the origin of the glasses, detailed information is given as to engraved marks found on the glasses, thickness of the glasses, and character of the edges.

The average equivalent for all of these glasses is 32.3 yellow 0.17 red. The average sunlight transmission is 3.5 per cent higher than the transmission adopted as standard for 35 yellow. It is, however, only 0.6 per cent higher than the standard transmission proper to the average yellow numeral (32.3) found for these glasses, which shows that, in the average, the data for sunlight transmissions

---

[1] This is one of a series of papers dealing with standardization of Lovibond glasses by the Bureau of Standards. Previous publications have been:

1. Gibson, Harris, and Priest, A Spectrophotometric Analysis of the Lovibond Glasses, B. S. Sci. Paper No. 547; February, 1927.
2. Judd and Walker, A Study of 129 Lovibond Red Glasses with Respect to the Reliability of Their Nominal Grades, Oil and Fat Industries, **5**, pp. 16-26; January, 1928.
3. Priest and Gibson, Standardizing the Red and Yellow Lovibond Glasses, J. Opt. Soc. Am. and Rev. Sci. Inst., **16**, p. 116; February, 1928.
4. Priest, Tests of Color Sense of A. O. C. S. Members and Data on Sensibility to Change in Lovibond Red, Oil and Fat Industries, **5**, pp. 63-73; March, 1928.
5. Judd, Effect of Temperature Change on the Color of Red and Yellow Lovibond Glasses, B. S. Jour. Research, **1** (RP31), pp. 859-866; November, 1928.

The present paper is one of the results of a cooperative investigation by the bureau and the American Oil Chemists' Society, one of the authors (Walker) being an employee of that society detailed to the bureau as a research associate, September 12, 1927, to July 2, 1928. Monthly reports of progress on this cooperative work have been published in Oil and Fat Industries as follows: December, 1927, pp. 433-435; January, 1928, pp. 27-29; February, 1928, pp. 58-59; March, 1928, pp. 92-94; April, 1928, pp. 114-117; May, 1928, pp. 152-156; June, 1928, pp. 184-188 (there are many misprints in this report); July, 1928, pp. 220-221; August, 1928, pp. 247-250; and September, 1928, p. 278.

[2] The authors have had the assistance of Mabel E. Brown and J. O. Riley in observing and computing.

30442°—29——1

and yellow-scale numerals are in accord. The maximum errors found in the collection are:

Yellow numeral	About 7
Red numeral	About 0.3
Sunlight transmission	About 14 per cent

The sunlight transmission of one of the glasses (AOCS No. 125) is quite remarkably higher (12 per cent) than the standard transmission for 35 yellow. The sunlight transmissions of six glasses (AOCS Nos. 27, 31, 41, 97, 125, and 131) depart notably (9 to 14 per cent) from the transmissions proper to the yellow numerals assigned to them in this calibration.

It is clear that the average equivalent of these 65 glasses is not in precise accord with the standard 35 yellow derived by Priest and Gibson from the Bureau of Standards set (B. S. 9940) obtained from the Lovibond establishment. On the other hand, the discrepancy is certainly not more than two or three times the least difference perceptible with certainty by the best observers under the most favorable conditions of observation. The idea occurs that it might seem reasonable to adopt the average as standard instead of the standard which has been adopted. There are, however, grave objections to this proposal, as explained in the report.

Of course, if their own average were taken as standard instead of the standard arbitrarily adopted, the "errors" for most of the glasses would be notably decreased. With a very few possible exceptions, the *uniformity* of these glasses is quite as good as could be required or expected in order to comport with the purposes and methods of use for which they were intended by the makers. The irregularities found and reported here have only been discovered by methods of observation greatly exceeding in sensibility and accuracy the methods of color matching contemplated by the makers, and the methods actually used by the oil chemists in grading oils.

The surfaces of three glasses (AOCS Nos. 41, 97, and 119) were so badly marred that it might seem advisable to discard them. With the possible exception of these badly marred glasses, all of the glasses are considered fit to be regarded as equivalent to standard 35 yellow under the present customary conditions of grading oils. The point to this recommendation is not that the glasses are perfect from the point of view of precision calibration, but that the errors found are negligible in comparison with the uncertainties inherent in the customary methods of using the glasses. When more reliable and precise methods of grading are adopted, it will be in order to consider using the precise equivalents which are given for each glass. Of course, even under present conditions, the glasses which approach more nearly standard 35 yellow may perhaps be regarded with somewhat greater satisfaction and respect by those who use them. The detailed data given in Table 1 of the report will enable such glasses to be identified.

An outstanding result of this investigation is the conclusion that the discrepancies of color grading which have troubled the oil trade can not be charged to lack of uniformity among the 35-yellow glasses. The sources of these troubles are rather to be sought in the following factors:

1. Unstandardized, nonuniform, and insensitive methods of comparing the oil samples with the glasses.

2. Grading of oil by observers having abnormal color sense or low power of hue discrimination.

3. Errors in the red glasses.

It seems just to assume that this rather large collection of glasses constitutes a fair sample of 35-yellow glasses issued by the Lovibond establishment and in use in the oil trade in the United States. If this be admitted, it seems superfluous to

test individual 35-yellow glasses further under present conditions. The chance of finding one with an error great enough to be of consequence in comparison with the other uncertainties just mentioned is very small. After the above-mentioned sources of error have been eliminated in practice, it will be due season to reconsider the calibration of 35-yellow glasses if it then appears necessary. In the meantime it may well be considered legitimate to accept on faith the 35-yellow glasses as issued by the Lovibond establishment.

CONTENTS

	Page
I. Description of glasses	795
II. Relation of character of the glasses to accuracy of calibration	798
III. Standards and units	798
1. Standard glasses and derivation of units	798
2. Colorimetric specification of standard 35 yellow	801
3. Physical specification of standard 35 yellow	801
4. Actual glass standard for 35 yellow	802
IV. Fundamental principles and methods of calibration	802
V. Special methods of calibration used in the present case	803
1. Empiric formula for sunlight transmission	804
2. Empiric formula for yellow-scale numeral	805
3. Apparatus and methods for the direct comparison of the colors of the standard and the glasses being tested	807
4. Determination of red correction	807
VI. Synopsis of results of calibration	812
1. Sunlight transmission	812
2. Red and yellow equivalents	814
3. Application to the color grading of oil	815
VII. General conclusions	818

I. DESCRIPTION OF GLASSES

These glasses were submitted by H. P. Trevithick, president of the American Oil Chemists' Society, in August, 1927. They are to be identified by the engraved initials, AOCS, followed by a number which refers to the individual glass, as shown in Column I of Table 1. It is understood that nearly all of these glasses were collected from members of the A. O. C. S., and that Mr. Trevithick has preserved a key by which the ownership of each glass can be found from its identification number. Nearly all of these glasses had been in use for some time. Very few new glasses were included. Engraved marks found on the glasses have been carefully noted and are cited as precisely as possible in Column IX of Table 1. It will be noticed that there are four distinctly different styles of labels and many minor variations. As further information, which might be of interest and possible service in resolving questions as to the origin, age, and history of the individual glasses, we give also in Table 1 the thicknesses of the glasses (Column X) and notes on the character of the edges (Column XI).

TABLE 1.—*Summary*

NBS No.	Color Quality Equivalents: Rigorous Equivalent N* D_T	Color Quality Equivalents: Usual Equivalent R_q	Sunlight Transmission: τ_U	τ_D	$\frac{\tau_U - \tau_D}{\tau_U}$ per cent	$\frac{\tau_U - \tau_{Std35}}{\tau_{Std35}}$ per cent	$\frac{\tau_U - \tau_{N^*}}{\tau_U}$ per cent	Engraved Marks (Refer to next page)	Thickness in millimeters	Character of Edges: Smooth	Matte	Rough	Chipped	Sharp	Remarks (See notes below)
I	II	III	IV	V	VI	VII	VIII	IX	X		XI				III
5	31.8T+0.13R	35T+0.05R	0.636	0.6331	+0.6	+6.4	+1.4	A	2.18	x					
8	30.8 + .18	+ .08	.643	.6300	+2.1	+2.6	+1.7	A	3.00		x				
12	30.0 + .26	+ .16	.615	.6183	-0.5	+1.9	-3.2	A_1	2.92	x			x		
13	31.8 + .14	+ .06	.637	.6288	+1.5	+5.6	+1.8	A	2.13	x					
14	33.4 + .19	+ .15	.607	.6146	-1.2	+0.6	-1.0	A_2	3.08	x					
15	31.0 + .22	+ .14	.609	.6344	-4.1	+0.9	-3.1	A_1 a	2.99	x			x		
16	31.5 + .10	+ .04	.642	.6362	+0.9	+6.4	+2.7	A	2.17	x					
22	33.6 + .15	+ .13	.629	.6257	+0.5	+4.3	+2.7	A_1	2.99		x				
24	33.2 + .09	+ .05	.645	.6362	+1.4	+6.3	+4.9	A_1	3.99	x			x		
27	29.2 + .06	+ .14	.649	.6505	-0.2	+7.6	+11.4	B	2.85		x				f
31	37.4 + .04	+ .08	.663	.6628	0.0	+9.9	+11.9	B b	2.82			x	x		f
32	31.5 + .11	+ .09	.629	.6307	-0.3	+4.3	+2.6	A_1	2.84	x					
37	28.9 + .22	+ .10	.613	.6313	-2.9	+1.6	-5.7	A_2	2.76	x					
41	32.8 + .12	+ .08	.557	.6449	-14.1	-7.7	-9.6	A_1	2.80	x					«β f
42	29.6 + .19	+ .09	.629	.6270	+0.3	+4.3	-1.4	A	1.96	x					
43	30.0 + .22	+ .12	.624	.6245	-0.1	+3.4	-1.8	A_1	2.64		x				
46	31.9 + .27	+ .21	.607	.6028	+0.7	+0.6	-2.5	A_1	2.28			x	x		
50	30.8 + .22	+ .14	.598	.6202	-3.6	-0.9	-5.1	C	2.11		x				
61	32.7 + .25	+ .21	.607	.6267	+1.7	+0.6	-2.7	D	2.92	x					
56	30.2 + .27	+ .17	.605	.6103	-0.8	+0.3	-2.6	A_1	3.03				x		
57	30.3 + .20	+ .10	.637	.6286	+2.3	+5.6	+0.6	A	2.83	x					
61	30.6 + .14	+ .04	.637	.6300	+1.1	+5.6	+0.8	A	2.79			x			
62	32.4 + .08	+ .04	.644	.6214	+4.5	+7.4	+4.8	A	1.90			x			
67	29.2 + .18	+ .02	.644	.6294	+2.5	+6.7	+0.6	A	3.21		x				
71	34.3 + .13	+ .11	.648	.6266	+3.4	+7.4	+6.5	A_2 c	3.12	x			x		
75	35.1 + .08	+ .08	.633	.6263	+1.1	+4.9	+4.9	A_1 d	3.02			x	x	x	
76	34.3 + .24	+ .28	.960	.9923	-0.4	-2.2	-2.8	A_1	3.20		x				
77	31.2 + .21	+ .18	.609	.6078	+0.2	+0.9	-2.9	A_1	3.07		x				
78	32.2 + .25	+ .20	.594	.6078	-2.2	-1.5	-4.3	A_1	2.80		x				
83	30.5 + .24	+ .14	.615	.6214	-1.0	+1.9	-2.7	D_1	2.41		x				
84	30.0 + .25	+ .14	.633	.6189	+2.3	+4.9	-0.3	A_1	2.87			x			
91	31.1 + .26	+ .18	.620	.6047	+2.5	+2.8	-1.3	A_2	2.79			x			
97	32.4 + .02	+ .04	.555	.6406	-13.7	-8.0	-10.5	A_1	2.13		x				
98	32.6 + .11	+ .07	.648	.6366	+1.8	+7.4	+4.8	A_1	2.66		x				
99	33.8 + .11	+ .09	.641	.6304	+1.7	+6.2	+4.9	B_1	2.85				x	x	«G f
100	29.8 + .23	+ .13	.622	.6078	+2.3	+3.1	-2.3	A_1	2.58				x		
101	34.5 + .11	+ .09	.631	.6282	+0.4	+4.6	+4.0	A_2	2.84	x				x	
102	33.5 + .26	+ .22	.605	.5892	+2.5	+0.3	-1.4	C_1	3.04	x				x	
103	36.7 + .12	+ .16	.612	.6127	-0.1	+1.4	+3.1	B_2	3.11	x				x	
109	28.8 + .20	+ .08	.635	.6270	+1.3	+5.3	-1.3	D_2	2.85		x				
110	31.5 + .19	+ .13	.632	.6164	+2.5	+4.8	+1.1	D	2.56		x				
114	34.8 + .15	+ .13	.612	.6164	-0.7	+1.4	+1.0	A_1	3.99	x			x		
115	29.2 + .20	+ .08	.635	.6294	+0.5	+5.3	-0.9	A_2	2.45		x				
116	30.0 + .23	+ .13	.608	.6214	-0.8	+2.1	-2.5	A_1	2.56			x			
119	33.9 + .11	+ .09	.617	.6276	-1.7	+2.3	+1.1	B	3.35	x					β
126	37.4 + .01	+ .03	.676	.6573	+3.0	+12.1	+13.0	B	3.02		x				f
127	29.9 + .15	+ .06	.647	.6270	+2.2	+7.3	+1.8	A_2	2.85		x				
130	30.1 + .20	+ .10	.617	.6189	-0.3	+2.3	-2.8	A_1	2.80			x		x	
131	27.9 + .18	+ .04	.592	.6270	-5.6	-1.9	-5.2	A_{10}	2.55			x			f
135	35.2 + .18	+ .18	.640	.6300	+1.6	+6.1	+6.1	D_2	2.98	x					
137	34.1 + .11	+ .09	.645	.6300	+2.4	+6.9	+5.8	B	2.91			x		x	
140	31.4 + .21	+ .15	.604	.6103	-1.0	+0.1	-3.5	C_2 e	2.86	x				x	
141	34.0 + .19	+ .17	.636	.6263	+1.6	+5.4	+4.5	A_1	2.86			x		x	
145	33.0 + .19	+ .15	.619	.6115	+1.2	+2.6	+0.5	A	4.27	x					
148	33.5 + .08	+ .06	.638	.6351	+0.8	+5.8	+4.1	B_1	3.35			x		x	
150	31.1 + .05	- .03	.651	.6361	+2.1	+7.9	+3.7	A_2	1.64		x				
152B	33.4 + .20	+ .16	.608	.6084	-0.1	+0.8	-0.8	A f	2.77	x				x	
153	28.6 + .07	+ .05	.657	.6299	+2.7	+8.9	+6.2	A_{11}	2.69			x		x	
156	29.9 + .25	+ .15	.607	.6158	-1.4	+0.6	-0.6	A_1	2.89		x				
157	33.6 + .10	+ .08	.632	.6257	+1.0	+4.8	+3.2	B_1	3.37		x		x		
158	31.2 + .30	+ .22	.619	.6022	+2.7	+2.6	-1.3	A_2	2.64		x				
162	33.9 + .18	+ .16	.635	.6282	+1.1	+5.3	+4.0	D_2	2.96	x					
165	36.7 + .12	+ .16	.608	.6171	-1.5	+0.8	+2.4	A_{12}	2.92	x			x		
166	30.6 + .23	+ .15	.616	.6134	+0.4	+2.1	-2.4	A_1	2.93		x				
191	32.2 + .15	+ .09	.639	.6257	+2.1	+5.9	+2.9	A	1.87		x				
Alg. Mean	32.26 +.167	+ .112			+0.13	+3.5	+0.62		2.77						

a Reject in critical work on account of large difference between τ_U and τ_D.
b Reject in critical work on account of badly scratched, hazy surface.
f Reject in critical work on account of large departure from normal transmission for given value of N*.

Notes referred to in Column IX of Table 1

ENGRAVED MARKS ON THE GLASSES

(Presumably Engraved by the Maker)

A	Lovibond	Colour Scale	510 NT	350	
A_1	Lovibond's	Colour Scale	510 NT	350	
A_2	Lovibond's	Colour Scale	510 NT	350	England
A_3	Lovibond's	Colour Scale	510 NT	Δ350	
A_4	Lovibond's	Colour Scale	510 NT	350F	
A_5	Lovibond's	Colour Scale	510 NT	λ350	
A_6	Lovibond's	Colour Scale	510 NT	350G	
A_7	Lovibond's	Colour Scale	510 NT	G350	
A_8	Lovibond	Colour Scale	510 NT	350	England
A_9	Lovibond	Colour Scale	510 NT	P350	
A_{10}	Lovibond's	Colour Scale	510 NT	350	England 35
A_{11}	Lovibond's	Colour Scale	510 NT	P350	
A_{12}	Lovibond's	Colour Scale	510 NT	35[illegible]	

B	510 NT	350			
B_1	510 NT	350	+		
B_2	510 NT	350	Y Lovibond's	Colour Scale	
B_3	510 NT	Δ350			
B_4	510 NT	350	Z		

C	Lovibond's	Colour Scale	510 NT	350G	
C_1	Lovibond's	Colour Scale	510 NT	350F	
C_2	Lovibond's	Colour Scale	510 NT	350	

D	6	Reg'd No.	410631	510 NT	350	
D_1	6	Reg'd No.	410631	510 NT	350P	
D_2	6	Reg'd No.	410631	510 NT	350	England.

Notes

a "L" in "Lovibond" and "C" in "Colour" chipped off.
b "5" in "510" chipped off.
c "e" in "Scale" chipped off.
d Additional mark (over "Lovibond's"): 3h0
e "e" in "Scale" and "T" in "NT" chipped off.
f Part of "T" chipped off.

All of these glasses depart, many quite markedly, from one or more of the following ideal conditions which are highly desirable for precision color standards: (1) Planeness of surfaces; (2) parallelism of surfaces; (3) freedom from haze, pits, and scratches on the surfaces; and (4) freedom from striæ and bubbles.

The following glasses were particularly bad in the respects noted: (1) Haze, AOCS Nos. 41, 97, 119; (2) scratches, AOCS Nos. 15, 41, 97, 98, 103, 116, 119; (3) striæ, AOCS Nos. 27, 31, 43, 98; and (4) waviness of surface, AOCS No. 114.

The type of spectral transmission with which we are dealing and the extent of its variation among the present lot of glasses are shown in Figure 1. The much-confused and widely divergent continuous curves were plotted from the data on spectral transmission of 23 individual glasses, about half of which are included in the present lot. The circles and × marks indicate, respectively, the maximum and minimum transmissions found among the present lot of 65 glasses.

II. RELATION OF CHARACTER OF THE GLASSES TO ACCURACY OF CALIBRATION

With glasses having such imperfections as these, the highest degree of precision and reliability in calibration is out of the question. An analogous situation would arise if we should attempt a precision calibration of an ordinary wooden foot rule with its crudely marked divisions. No amount of tedious scientific measurement could make of the wooden rule a length standard comparable with a finely ruled steel, quartz, or platinum-iridium precision standard. In the present instance we have done our best to calibrate the glasses submitted, but in considering this report one must not lose sight of the character of the material concerned. The uncertainties remaining in the present results are largely inherent in the nature of the glasses themselves; to attempt to reduce them by further measurements or observations would be quite futile.[3]

III. STANDARDS AND UNITS

1. STANDARD GLASSES AND DERIVATION OF UNITS

The fundamental standard to which the values here reported are referred is contained implicitly in a particular set of glasses obtained in 1912 directly from the Lovibond establishment (The Tintometer (Ltd.)), now kept at the Bureau of Standards, and designated as B. S. 9940 (Bureau of Standards inventory number).[4] The units

[3] These remarks are not to be interpreted as an unqualified condemnation of the Lovibond glasses. The scratches, pits, and haze have probably resulted from careless usage. As supplied by the Lovibond establishment, these glasses serve a useful purpose to the extent that their characteristics permit; but, as implied above, they are comparable to the common weights and measures of trade rather than to the precision weights and measures of the scientific laboratory.

[4] See B. S. Sci. Paper No. 547.

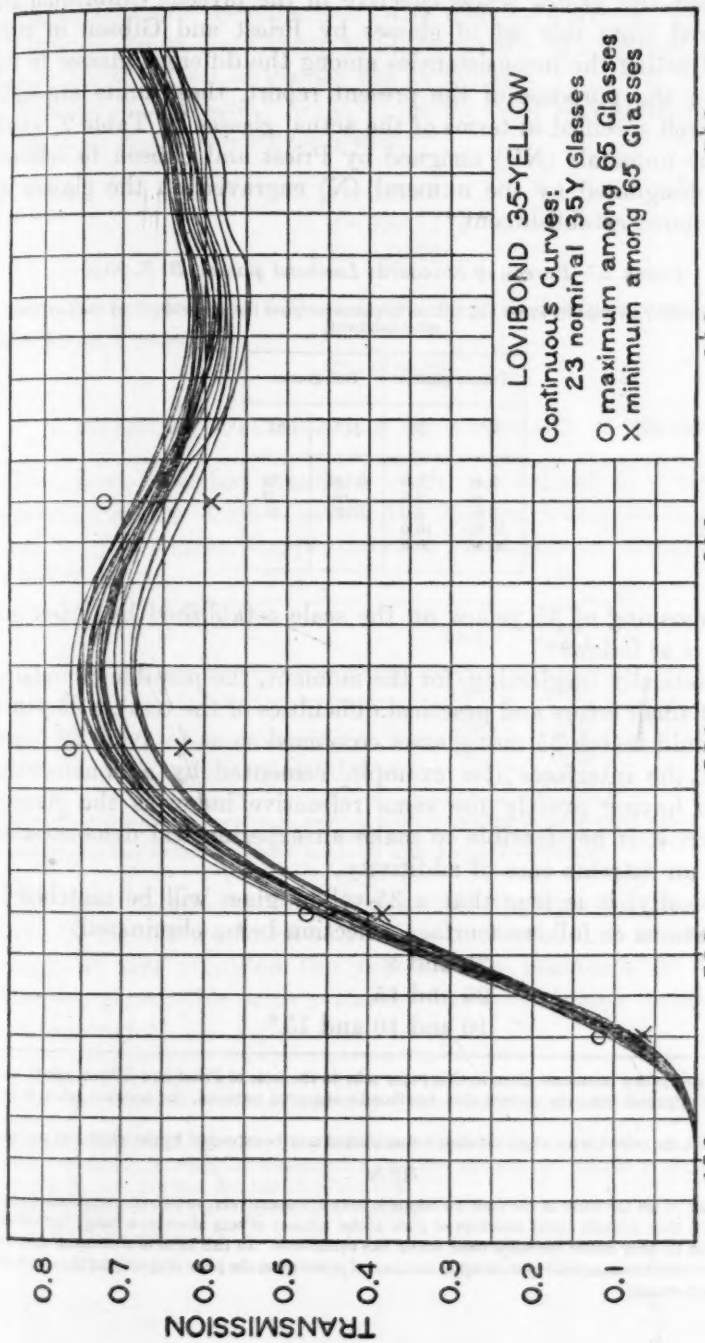

FIG. 1.—*Typical spectral transmission curves of nominal 35-yellow Lovibond glasses*

of the red and yellow scales effective in the present calibration are as derived from this set of glasses by Priest and Gibson in 1927 after adjusting the inconsistencies among the different glasses in the set. For the purposes of the present report, these units are sufficiently well specified in terms of the actual glasses by Table 2, which gives the numerals (N″) assigned by Priest and Gibson to selected glasses designated by the numeral (N) engraved on the glasses by the Lovibond establishment.[5]

TABLE 2.—*Bureau of Standards Lovibond glasses, B. S. 994O*

[Numerals (N″) assigned by Priest and Gibson to glasses assigned the numeral (N) by the Lovibond establishment]

Yellow glasses		Red glasses	
N″	N	N″	N
1.19	1.0	0.104	0.02
2.07	2.0	.199	.13
5.07	5.0	1.17	1.0
10.05	10.0		
20.86	20.0		

The meaning of 35 yellow on the scale established by Priest and Gibson is as follows:

Theoretically (neglecting, for the moment, the possible cumulative effect of small errors and practical difficulties of the test), a 35-yellow glass would match 35 unit glasses combined so as to avoid all loss of light at the interfaces (for example, cemented by a nonabsorbing medium having exactly the same refractive index as the glasses). However, it is not feasible to make an experimental demonstration of such an extreme case of additivity.

Practically, it is true that a 35-yellow glass will be matched by combinations as follows (surface reflection being eliminated):

30 and 5
20 and 15
10 and 10 and 15.[6]

[5] All red and yellow numerals given in this paper refer to the scale of Priest and Gibson, except where it is clearly apparent from the context that Lovibond's engraved numeral, the nominal grade, is being referred to.

[6] In general, the principle on which the scale is constructed may be expressed by the additivity condition,

$$S_1 = S_2$$

where S_1 and S_2 are the sums of the scale numerals attached, respectively, to two combinations of glasses such that (1) they contain equal numbers of glass plates (glasses of zero absorption being introduced if needed), and (2) they evoke the same color under like conditions. In this form of statement, specifying that the two combinations shall contain equal numbers of plates takes the place of specifying the elimination of surface reflections.

2. COLORIMETRIC SPECIFICATION OF STANDARD 35 YELLOW

The colorimetric specifications (with Abbot-Priest sun [7] as neutral) adopted by Priest and Gibson to represent the 35Y derived from the above-mentioned set of glasses are as follows:

Trilinear Coordinates [8] *(r, g, b) on the basis of excitations* [9] *given by the O. S. A. colorimetry committee:* [10]

$$r = 0.5017$$
$$g = 0.4611$$
$$b = 0.0372$$

Sunlight transmission (T) on the basis of visibility recommended by Gibson and Tyndall: [11]

$$T = 0.6033$$

3. PHYSICAL SPECIFICATION OF STANDARD 35 YELLOW

The above-described standard would be realized to a very close approximation by a glass having the spectral transmission given in Table 3. The degree of approximation in colorimetric terms is shown as follows:

	Ideal	From Table 3
r	0.5017	0.5018
g	.4611	.4611
b	.0372	.0371
Transmission for sunlight	.6033	.6033
Purity	.931	.9315
Dominant wave length [1] mμ	575.66	575.66

[1] These values of dominant wave length are given to the nearest hundredth of a millimicron, not because they may be computed via the O. S. A. excitations with this absolute accuracy (which is not possible), but because they may be (and have been) computed with this relative accuracy.

The scale numeral of the glass having the spectral transmission shown in Table 3 would be 35.1. One-tenth of a unit is a negligible amount at this point on the yellow scale, inasmuch as the least difference perceptible with certainty has been found to be greater than one unit.

---

[7] Phys. Rev. (2), **11**, p. 502; 1918. J. Opt. Soc. Am. and Rev. Sci. Inst., **12**, p. 479; 1926.

[8] J. Opt. Soc. Am. and Rev. Sci. Inst., **9**, pp. 506-508; 1924. This paper gives the definition of "trilinear coordinates."

[9] The excitations used are essentially those referred to in the following footnote. The actual values used are those extrapolated by Priest and Gibson (J. Opt. Soc. Am. and Rev. Sci. Inst., **10**, p. 230; 1925).

[10] J. Opt. Soc. Am. and Rev. Sci. Inst., **6**, p. 549; 1922.

[11] B. S. Sci. Paper No. 475, p. 174, Table 3, last column.

TABLE 3.—*Spectral transmission of hypothetical glass approximating closely to standard Lovibond 35Y adopted by Priest and Gibson*

Wave length	Transmission	Wave length	Transmission
$m\mu$		$m\mu$	
450	0.0001	600	0.6618
460	.0016	610	.6294
470	.0202	620	.6018
480	.0795	630	.5777
490	.1786	640	.5610
500	.2958	650	.5490
510	.4215	660	.5471
520	.5219	670	.5598
530	.5998	680	.5769
540	.6535	690	.5810
550	.6882	700	.5924
560	.7075	710	.6135
570	.7110	720	.6391
580	.7036		
590	.6869		

4. ACTUAL GLASS STANDARD FOR 35 YELLOW

We have not been able to find a glass fulfilling the ideal specifications for standard 35Y. We have, however, a two-glass combination, the spectral transmission of which is given by multiplying each transmission in Table 3 by the constant 0.93386. The trilinear coordinates, dominant wave length, and purity are consequently the same as computed from this table; and the sunlight transmission is $0.93386 \times 0.6033 = 0.5634$. This combination consists of the two glasses, $35Y_{B.\ S.\ 10289C}$ and $1Y_{B.\ S.\ test\ 41960}$.

IV. FUNDAMENTAL PRINCIPLES AND METHODS OF CALIBRATION

The results to be given must be considered in terms of certain fundamental ideas which will now be presented.

A complete description of the color evoked by one of these glasses must comprehend three items (or their equivalents)—hue, saturation, and brilliance.[12] A perfect standard 35Y would be correct in all three of these attributes of color and would be characterized by certain values of—

Trilinear coordinates	(r, g, b)
Dominant wave length	(λ)
Purity	(P)
Sunlight transmission	(T) [13]

[12] Report of the Colorimetry Committee, Optical Society of America, J. Opt. Soc. Am. and Rev. Sci. Inst., **6**, pp. 534–535; August, 1922. Separate copies of this report may be purchased at 50 cents per copy of Prof. F. K. Richtmyer, business manager, J. Opt. Soc. Am. and Rev. Sci. Inst., Cornell University, Ithaca, N. Y.

[13] For definitions of these terms, see following papers by Priest: Apparatus for Determination of Color * * * J. Opt. Soc. Am. and Rev. Sci. Inst., **8**, pp. 174–176; January, 1924. Computation of Colorimetric Purity, J. Opt. Soc. Am. and Rev. Sci. Inst., **9**, pp. 503–505; November, 1924.

However, the Lovibond yellow scale is primarily a saturation scale, running from neutral to a very saturated yellow. The outstanding colorimetric variable is purity. The preeminent significance of the yellow numeral is that greater numerals indicate greater saturation determined chiefly by colorimetric purity. Nevertheless, it is also true that dominant wave length and sunlight transmission both change with the yellow numeral. On the scale established by Priest and Gibson certain values of purity, dominant wave length, and sunlight transmission appertain to each value of the yellow numeral.

The fundamental method [14] of calibrating a yellow Lovibond glass consists essentially of the following steps:

1. The trilinear coordinates (r, g, b), the dominant wave length (λ), the purity (P), and the sunlight transmission (T) are computed from the spectral transmission of the glass.

2. The glass is assigned a yellow-scale numeral proper to its colorimetric purity.[15]

3. The difference between the actual dominant wave length of the glass and the dominant wave length proper to the numeral which has been assigned it is then considered. If this difference is zero, the glass may be regarded as standard in hue. If the difference does not exceed a certain tolerance, the glass may be regarded as practically standard in hue. If the difference is very small but not negligible, it may sometimes be advantageously stated in terms of Lovibond red, as described later.

4. The difference between the actual sunlight transmission of the glass and the transmission proper to the numeral which has been assigned it is then considered. If this difference is zero, the glass is standard in transmission and brilliance. If this difference is not zero, due account may be taken of it in using the glass.

V. SPECIAL METHODS OF CALIBRATION USED IN THE PRESENT CASE

As has been pointed out in the preceding section, the fundamental method of calibration requires the complete determination of spectral transmission throughout the visible spectrum followed by elaborate computations. For a large number of glasses (as in the present case), this would be a very laborious and time-consuming task; therefore, certain short-cut methods have been used. These short cuts are based on certain empiric formulas and methods which will now be described briefly.

[14] As developed by Priest and Gibson.

[15] The parameter actually used by Priest and Gibson for finding the correct numeral was $1/b$. The procedure, however, is equivalent to assigning the glass a numeral in accord with its colorimetric purity.

1. EMPIRIC FORMULA FOR SUNLIGHT TRANSMISSION

Adopt symbols as follows:

T is transmission for Abbot-Priest sunlight computed from complete spectral transmission on basis of visibility recommended by Gibson and Tyndall;

T_{510} is transmission for wave length 510 mμ (millimicrons);

T_{550} is transmission for 550 mμ; and

T_{610} is transmission for 610 mμ.

The following formula [16] has been shown to hold to a close approximation for 15 nominal [17] 35Y glasses previously investigated:

$$T=0.0070+0.2456(T_{510}+2T_{550}+T_{610}) \quad (1)$$

Considering all of the data for the 15 glasses from which it was derived (by least-square adjustment), the average error of this formula is $0.0012T$, and the maximum error in the 15 cases is $0.0029T$.

As a further check on this formula we have determined the complete spectral transmission for eight glasses in the present lot and have computed the values shown in the following table:

AOCS No.	T from complete spectral transmission data	$0.0070+0.2456(T_{510}+2T_{550}+T_{610})$	
		For T_{510}, T_{550}, and T_{610} from complete spectral transmission data	For preliminary values of T_{510}, T_{550}, and T_{610}
71	0.6442	0.644	0.648
75	.6355	.635	.633
76	.6005	.600	.590
101	.6268	.628	.631
103	.6190	.618	.612
114	.6159	.617	.612
135	.6419	.641	.640
165	.6168	.616	.608

The second column of the above table gives the sunlight transmission as computed by rigorous methods from the complete data on spectral transmission. The two results by the formula (third and fourth columns of above table) are derived from two sets of values for T_{510}, T_{550}, and T_{610}, namely:

1. Preliminary isolated measurements of T at wave lengths 510, 550, and 610 made before the complete spectral transmission data were obtained (fourth column). These results have the same status as all of the values given in Column IV of Table 1.

[16] Derived and verified by Priest and Judd, July–August, 1927.

[17] That is, 35 according to engraved marks.

2. Final values as read from the final curve for spectral transmission (third column).

It happens that 3 of the glasses in the present lot of 65 were also included in the lot of 15 previously investigated, and data on their spectral transmission obtained about January, 1927, are thus available. Using these data and the present independent values for T_{510}, T_{550}, and T_{610}, the values given in the following table have been computed:

AOCS No.	T from complete spectral transmission data	$0.0070+0.2456(T_{510}+2T_{550}+T_{610})$	
		For T_{510}, T_{550}, and T_{610} from complete spectral transmission data	For independent values of T_{510}, T_{550}, and T_{610} found in present investigation
156	0.6114	0.611	0.607
157	.6346	.634	.632
158	.6224	.621	.619

In either of the two tables just preceding, the differences between the second and third columns show merely specimen errors of the formula itself when using only one set of data. The average error is less than $0.0013T$. The differences between the second and fourth columns show the magnitude of errors which may be expected in the values of T given in Column IV of Table 1. The average error is about $0.0078T$.

From the foregoing presentation it is evident that the error of this empiric formula for sunlight transmission (equation (1)) is negligible.

2. EMPIRIC FORMULA FOR THE YELLOW-SCALE NUMERAL

Adopt symbols as follows:

N'' is the yellow-scale numeral as found (via $1/b$) by the fundamental method;

T_{480} is the transmission for wave length 480 mμ; and

T_{550} is the transmission for wave length 550 mμ.

The following empiric formula was derived[18] from a study of the 15 above-mentioned nominal 35Y glasses previously investigated:

$$N'' = -37.04 \log_{10}(T_{480}/T_{550}) \qquad (2)$$

Considering all of the data for the 15 glasses from which it was derived (by least-square adjustment), the average error of the formula is 0.23; and the maximum error in the 15 cases is 0.83.

[18] By Priest and Judd; August–September, 1927.

As a further check on this formula we have also made computations from the complete spectral transmission data for eight glasses from the present lot (the same eight as mentioned in the preceding section). In the following table the results are shown in a manner analogous to the results for transmission in the preceding section (V, 1):

AOCS No.	N'' from complete spectral transmission data via $1/b$	$-37.04 \log_{10}(T_{480}/T_{550})$	
		For T_{480} and T_{550} from complete spectral transmission data	For preliminary values of T_{480} and T_{550}
71	34.3	34.4	34.3
75	35.4	35.3	35.1
76	34.2	33.5	34.3
101	33.8	34.1	34.5
103	35.9	36.5	36.7
114	33.9	34.4	34.6
135	34.3	34.9	35.2
165	36.4	36.6	36.7

Here again the numerals in the second column are those obtained by the more rigorous computation; the third column gives numerals computed by equation (2) taking values of T_{480} and T_{550} from the final complete spectral transmission data; and the numerals in the fourth column (from preliminary values of T_{480} and T_{550}) have the same status as all values of N'' in Column II of Table 1.

Likewise, the 3 glasses in the present lot of 65, also included in the lot of 15 previously investigated, afford spectral transmission data from which the values given in the following table have been computed:

AOCS No.	N'' from complete spectral transmission data via $1/b$	$-37.04 \log_{10}(T_{480}/T_{550})$	
		For T_{480} and T_{550} from complete spectral transmission data	For independent values of T_{480} and T_{550} found in the present investigation
156	30.0	29.8	29.9
157	33.1	33.3	33.6
158	31.6	31.4	31.2

In either of the two tables just preceding the differences between the second and third columns show merely specimen errors of the formula itself when using only one set of data. The average error is 0.34. The differences between the second and fourth columns show the magnitude of errors which may be expected in the values

of the yellow numerals (N'') reported in Column II of Table 1. The average error is 0.44; the maximum error is 0.9.

Since the least difference in yellow perceptible with certainty on the $35Y+nR$ scale has been found to be greater than one unit, it appears, from the foregoing presentation of data, that this empiric formula is sufficiently accurate for determining the yellow numeral for all practical purposes.

3. APPARATUS AND METHODS FOR DIRECT COMPARISON OF THE COLORS OF THE STANDARD AND THE GLASSES BEING TESTED

The findings which are of chief interest in the present report are derived from the immediate visual comparison of the test glasses with standard glasses. The essential features of the apparatus and method used in this comparison are as follows:

1. The observer conducting the calibration sees, by looking into the Martens photometer,[19] an illuminated circular field subtending an angle of about 6° and divided by a vertical diameter.

2. The illumination of both halves of the field is produced by natural north skylight which has been diffused by transmission through a plate of milk glass.

3. Lovibond glasses can be inserted so as to color either half of the field. By placing one glass in the path of the light illuminating one half and another glass in the path of light illuminating the other half, the colors of the two glasses may be compared in immediate juxtaposition.

4. The two halves may be matched in brightness at the will of the observer. If the two glasses are alike in dominant wave length and purity, the adjustment of the brightnesses of the two halves to equality will cause the dividing line to vanish. If, by matching the brightness, by making first one side and then the other brighter, by looking back and forth from one side to the other, and by reversing the positions of the glasses, the observer can perceive no difference in saturation or hue, he concludes that the glasses may be accepted as duplicates in color except that they may have different transmissions.

4. DETERMINATION OF RED CORRECTION

As pointed out above, one of the ways in which a 35Y glass may depart from normal is in regard to its hue. Experience has, indeed, shown that this is the most important error from the practical point of view. The practical import of this circumstance is that the equivalent of a nominal 35Y glass must usually be given in terms of yellow and red. Thus, of a nominal 35Y which does not have the

[19] The apparatus and methods used have been described in a previous paper, Oil and Fat Industries, 5, pp. 16-18; January, 1928. Naturally, the yellow glass used over the ocular in the previous calibration of red glasses was not used in the present case.

standard hue for 35Y, but is otherwise normal, we may say that it is equivalent in hue and saturation to $35Y+nR$ or $35Y-nR$, where n is some fraction usually less than 0.3. The meaning of the first equivalent would be that the glass in question was matched (brightness being independently equated) by a standard 35Y combined with a red glass of numeral n. The meaning of the second equivalent would be that the standard 35Y was matched (brightness being independently equated) by the glass in question combined with a red glass of numeral n. In the first case, the error of the glass in question consists in its being reddish relative to the standard. In the second case, the error consists in its being greenish relative to the standard.

The determination of equivalents in this form is, however, complicated by the approximate empiric equivalence of small amounts of red and yellow at 35Y. This equivalence will be discussed later (Section VI, 2).

Let us now consider more closely the problem of finding the yellow and red equivalent of an unknown nominal 35Y which is not exactly a true 35Y. Let it be assumed that we have a standard 35Y with which to compare it. The problem will then consist of finding the yellow and red which must be added to (or subtracted from) the standard in order to match the unknown. The following cases may be distinguished:

1. It will be necessary to add only yellow.
2. It will be necessary to add only red.
3. It will be necessary to add both yellow and red.

In the present lot of glasses approximate matches could be found in all cases by adding only red [20] ("Quasi equivalents," n_q, Column III, Table 1).[21] It was realized, however, that in some cases we were dealing only with quasi ("make-believe") matches forced by the imposed condition that only red glasses were being added, with the object of obtaining the best practical match that could be obtained subject to this condition. It was apparent that, in these cases, a more satisfactory match would have been obtained by adding yellow (in

[20] The striking differences among these glasses appeared to be hue differences.

[21] The quasi equivalents were determined by direct comparison, as just described, independently by two observers (DBJ and GKW), and all glasses for which these two values differed by more than 0.05R (11 out of the 65) were retested. Then the quasi equivalents were checked independently by a different observer (IGP) using a different method and different apparatus. (For a description of this apparatus, see J. Opt. Soc. Am. and Rev. Sci. Inst., **8**, pp. 178-200; January, 1924.) In this method the dominant-wave-length difference between the standard 35Y glass and each test glass was determined and then converted into Lovibond red difference by multiplying by the proper factor (0.5) as determined by previous investigation. Although each final dominant-wave-length difference was the average of 20 independent settings of the difference, which is about as many settings as entered into the direct determination (by DBJ and GKW) of the quasi equivalents, it was found that the values of quasi equivalent obtained via dominant wave length were not as reliable as those determined directly, due to uncertainties inherent in the method. Hence, in combining the two sets of data, the values of quasi equivalent from direct comparison were given three times the weight of those obtained via dominant wave length. The resulting average values, influenced slightly by the values of rigorous equivalent (to be discussed presently), are recorded in Column III, Table 1.

addition to the red) either to the standard or to the glass being tested; and these cases were recorded as observations were being made.[22] However, to have selected by trial and error both the yellow and red requisite to obtain the best match would have been an exceedingly laborious and time-consuming task, almost impossible of accurate execution because of the approximate empiric equivalence of small differences in yellow and small differences in red (Section VI, 2).

This difficulty was circumvented by use of the above-mentioned empiric formula (2) for finding the yellow-scale numeral (Section V, 2). The yellow components (N'') in the "rigorous equivalents" (N''Y n_rR) given in Column II of Table 1 were obtained by this formula from measured values of T_{480} and T_{550}.[23] The red components, n_r, in the "rigorous equivalents" (N''Y n_rR) are to be understood in experimental terms as follows:

1. Direct comparison of glasses is made by means of the Martens photometer as before.

2. The standard 35Y is placed to cover one half of the field and the glass being calibrated to cover the other half.

3. On the basis of the yellow-scale numeral already computed for the glass being calibrated (N'' of equation (2)), standard yellow glasses[24] are combined with the standard or with the glass being tested so that the sums of the yellow-scale numerals pertaining, respectively, to the two halves of the field are equal.

4. The field is then scrutinized (brightness being independently adjusted by the observer).

5. If the two halves of the field should seem perfectly matched in all respects, this direct comparison of colors would merely serve as a check on the computed value of N'', and no red correction would be required. (No such glass was found, however.)

6. If red glasses are required to complete the match, they are added, by trial and error, to one side or the other until a match is found. This correction in Lovibond red units is the red component (n_r) of the rigorous equivalent (N''Y n_rR) recorded in Column II of Table 1.

---

[22] In most of these cases (34 out of 38) it seemed that more yellow should be added to the glass being tested.

[23] In finding the quasi equivalents, notes were made concerning the saturation equivalence (the necessity of adding yellow as mentioned before) of the standard 35Y and the glass combination being tested. Subsequent analysis of these notes showed them to be in close agreement with the values of N'' from formula (2); that is, whenever the note was to the effect that the test combination was more saturated than the standard 35Y, it was also true that N'' was considerably greater (greater by at least three units) than 35; and whenever the note was to the effect that the test combination was less saturated than the standard 35Y, it was also true with but two exceptions that N'' was smaller (by at least three units) than 35. Furthermore, in obtaining (by the method about to be described) the rigorous red equivalent, n_r, no saturation differences could be detected in any case. Hence, it may be said that, although N'' was not determined by direct experimentation, the formula from which it was determined has been verified by extensive direct comparison.

[24] Carefully selected to have practically a zero hue error.

The foregoing six steps constitute an idealized description of the procedure leading up to the rigorous red equivalent (n_r). The values which appear in Column II of Table 1 are not quite the same as those obtained experimentally by this procedure but have been influenced by the experimental values of the quasi red equivalents (n_q), thus:

In comparing the experimental values of n_r (designated n'_r) with the experimental values of n_q (designated n'_q) it was found that n'_r could be computed from n'_q with good approximation according to the relation:

$$n'_r = n'_q + (35 - N'')/50 - 0.06$$

where N'' is the yellow component of the rigorous equivalent. It was also found true (though not with such good approximation) that

$$n'_r = \Delta\Lambda/2 + (35 - N'')/50 - 0.13$$

where $\Delta\Lambda$ is the difference in dominant wave length in millimicrons between each test glass and the standard 35Y glass.

It is apparent that neither of these two relations which hold approximately for the experimental values (n'_r, n'_q, and $\Delta\Lambda/2$) can apply at all closely to the adopted values (n_r and n_q), because, from its definition, the quasi equivalent (n_q) is equal to the rigorous red equivalent (n_r) when the yellow component of the rigorous equivalent (N'') is equal to 35. We attribute the constants, -0.06 and -0.13, which should be zero if the true standard 35Y had been available for all three comparisons, largely to the fact that the standard 35Y was in these three cases evaluated via three different working standards.[25] If these three working standards had been correctly evaluated, the constants which actually turned out to be -0.06 and -0.13 would have been nearly zero; hence, it seems reasonable to conclude that the grades of these working standards found by computation from their spectral transmissions are relatively somewhat in error.[26] This conclusion has been verified independently as follows:

[25] To obtain the values of n'_r, 35Y B. S. 12288C 1Y B. S. test 41962 was used; for n'_q, 35Y Trevithick B, Gibson No. 5; and for $\Delta\Lambda/2$, 35Y B. S. test 41960.

[26] The extent of the error is not greater than might be accounted for by (1) the measurement of the working standards at different times at unnoted room temperatures, and (2) their imperfect optical nature.

1. A 25° C. change in temperature has been shown (Judd, B. S. Jour. Research, 1 (RP31), p. 855; November, 1928) to change the color of 35 yellow by an amount equal to 0.2R+3Y. The three glasses were measured spectrophotometrically at different times, and experience has shown that a 5° C. change in the room where the measurements were made often occurs from one day or week to another.

2. Only by repeated extensive measurements can a perfect optical sample be guaranteed correct in spectral transmission to better than 1 per cent throughout. The spectral transmissions of any of these three 35-yellow glasses (except possibly B. S. test 41960, which has been more carefully measured than the other two) may well be uncertain by 1 or 2 per cent. The total selectivity in a 0.13R glass (that is, the difference between maximum and minimum transmission) is but 3 per cent. Furthermore, the spectrophotometric data refer to unidirectional illumination of a small area near the centers of the glasses, while the illumination under which these glasses were used as working standards was diffuse and affected a somewhat different area.

1. Direct comparison of $35Y_{\text{B. S. test 41960}}$ with $35Y_{\text{B. S. 10289C}}\,1Y_{\text{B. S. test 41960}}$ by two observers gave an average value of -0.12 as the error in the red correction of the latter relative to the former.

2. A somewhat more indirect comparison of these two standards was afforded by some previous experimental measurements of dominant wave length. By this method the corresponding relative error in the red corrections was obtained as -0.175.

Although both of these independent determinations (-0.12R and -0.175R) of the relative error are in good agreement with the error (-0.13) determined indirectly from the grading of these 65 test glasses, neither one is comparable to it in reliability, because neither involves nearly so many readings. The less reliable independent determinations are of value, however, as a closing check.

The relation which the adopted values of n_r and n_q should follow is, therefore—

$$n_r = n_q + (35 - N'')/50 \qquad (3)$$

We have, then, three experimental evaluations of the red component of the rigorous equivalent:

(*a*) n'_r

(*b*) $n'_q + (35 - N'')/50$, and

(*c*) $\Delta\Lambda/2 + (35 - N'')/50$.

However, from the relations already given, we know that the average value from (*a*) for the 65 glasses is lower than the average value from (*b*) by 0.06, which, in turn, is lower by 0.07 than the average value from (*c*), these differences being ascribable mostly to uncertainty in the evaluation of the working standards. Accordingly, the (*a*) values (n'_r) were all raised, for the purpose of averaging, by 0.06, while the (*c*) values (via $\Delta\Lambda$) were lowered by 0.07.

As to the question of weights in taking this average, the (*a*) values were taken as of two-thirds the importance of the (*b*) values, because, while the (*a*) values resulted from an experimental method roughly twice as reliable (due to absence of saturation difference) as that resulting in the (*b*) values, only about one-third as many readings were involved. The (*b*) values were taken as of three times the importance of the (*c*) values for reasons previously discussed. (See footnote 21, p. 808.) The value of n_r (Column II, Table 1) for each glass was, therefore, computed as—

$$n_r = 1/3\,[n'_r + 0.06] + 1/2\,[n'_q + (35 - N'')/50] + 1/6\,[\Delta\Lambda/2 + (35 - N'')/50 - 0.07].$$

The value of n_q for each glass was then computed from equation (3), but the experimental data were so congruent that in no case did the

value of n_q so computed differ from n'_q (experimentally determined) by more than 0.04. The average absolute value of $(n_q - n'_q)$ was found to be 0.01_2.

VI. SYNOPSIS OF RESULTS OF CALIBRATION

The essential results of the measurements made on the glasses are shown in Columns II, III, IV, and V of Table 1. Columns VI, VII, and VIII show certain ratios of transmissions (computed from Columns IV and V) which are of interest as criteria of the imperfections of the glasses in their present condition. The remainder of this report will be devoted to explaining these data and pointing out their significance.

1. SUNLIGHT TRANSMISSION

Columns IV and V give the sunlight transmission for two different conditions of illumination. T_U (Column IV) is the sunlight transmission for an approximately unidirectional beam incident normal to the face of the glass.[27] T_D (Column V) is the transmission for diffuse illumination, literally, the ratio of the brightness of a diffusing surface (milk glass) viewed through the glass to the brightness of the same surface viewed directly.[28] If the glasses were optically clear[29] plates bounded by perfectly polished plane and parallel surfaces, and if the photometric measurements were free from error, the difference $T_U - T_D$ (and, consequently, the ratio $(T_U - T_D)/T_U$), would be zero. Column VI shows the difference, $T_U - T_D$, in parts per hundred of T_U. The departures from zero (plus or minus) are probably due largely to the imperfections of the glasses themselves (scratches, haze, departures of the surfaces from planeness and parallelism), although they may be, in part, due to the unavoidable uncertainties of photometric measurement. The following comments are in order:

1. The very small algebraic average value of $(T_U - T_D)/T_U$ (+0.13 per cent) shows that there is no significant systematic difference between T_U and T_D.

2. Values of $(T_U - T_D)/T_U$ less than 1 per cent may be dismissed without further notice.

3. If the glasses were to be used (in connection with precise photometric measurements) in grading oils by transmission as well as by hue and saturation, it would be advisable to calibrate more carefully all glasses for which $(T_U - T_D)/T_U$ is greater than 1 per cent.

4. Under the present customary conditions of using the glasses, no attention need be paid to values of $(T_U - T_D)/T_U$ less than 10 per cent.

---

[27] The given values of T_U were computed by formula (1) given in Section V, 1 above.

[28] The given values of T_D were obtained by measuring the transmission of each glass relative to a glass of known transmission. These measurements were made by means of the Martens photometer. The known glass was B. S. 10289B, and its sunlight transmission was taken as 0.6183.

[29] Free from scratches, haze, and all imperfections causing diffusion of light.

5. In the two cases (AOCS Nos. 41 and 97) in which $(T_U - T_D)/T_U$ is greater than 10 per cent it is recommended that the glasses be discarded. These large negative values of $(T_U - T_D)/T_U$ are readily explained by the fact that these glasses are very badly scratched. They are obviously unfit to be used in color grading to which any importance is attached.

Column VII gives the percentage difference between the sunlight transmission of each glass and the sunlight transmission for the standard 35Y. Column VIII gives the percentage difference between the sunlight transmission of each glass and the sunlight transmission proper to the yellow numeral given in Column II. If these glasses are used (in connection with suitable photometric apparatus) to grade oils in terms of transmission as well as hue and saturation, due account should be taken of the data given in Columns VII and VIII. It is noted that the following glasses have strikingly abnormal transmissions: AOCS Nos. 27, 31, 41, 97, 125, 131 (Column VIII). Under the present customary conditions of using the glasses, no attention need be paid to these data.

Incidentally, the algebraic mean of the differences given in Column VIII affords a kind of check on the values of N'' given in Column II. The argument is as follows: In the average the actual sunlight transmission of these glasses (T_U) is 0.6 per cent (foot of Column VIII) higher than the transmission proper to the values of N'' given in Column II. Referring to Figure 15, page 46, Bureau of Standards Scientific Paper No. 547, we readily see that a 10 per cent difference in transmission (that is, a difference of 0.06 at a value of transmission equal to 0.6) corresponds to a difference of about 12 in N'' at this point (32) on the yellow scale. Hence, a difference of 0.6 per cent corresponds to a difference of about 0.7 in N''. In other words, in the average, the sunlight transmissions found for the glasses check the given values of N'' to within less than one unit on the yellow scale. At this point on the yellow scale one unit is less than the least perceptible difference. It appears then that if we had obtained N'' by calibration in terms of sunlight transmission, we would have obtained for all practical purposes the same average value of N'' as has been obtained by the method actually used to obtain N'' (equation (2) above).[30]

[30] It may be noted that one item of experimental data (T_{550}) is common to the formula for transmission (equation (1)) and the formula for N'' (equation (2)). It is therefore in order to inquire whether this circumstance may in itself account for the good agreement just mentioned and render it of no real significance. Assume a positive error in T_{550}. Examination of equations (1) and (2) shows that this would result in *positive* errors in *both* T_U and N''. But, we know that the sunlight transmission *decreases* as the scale numeral *increases*. It is therefore apparent that an error in T_{550} would *prevent* the obtaining of concordant results in the computed values of T_U and N''. Hence, it follows that the concordant results obtained are *not* a mere mathematical necessity due to entering the *same* item of data (T_{550}) in the two formulas; on the contrary, concordant results in T_U and N'' can only be obtained when that item of data is *correct*.

2. RED AND YELLOW EQUIVALENTS

The data in Columns II and III are to be understood as follows:

Brightness being independently equated, the glass designated by AOCS No. in Column I would be accurately matched by the combination of standard yellow and red given in Column II, and approximately matched by the quasi equivalent given in Column III.[31]

These yellow and red equivalents are connected (as stated before) by relation (3) which may be rewritten:

$$n_q - n_r = (N'' - 35)/50$$

or, stated in words, the difference between the red equivalents is equal to one-fiftieth the difference between the yellow equivalents. From this relation it is apparent that 5 yellow may be, in a sense, substituted for 0.1 red. What is meant by this may be most clearly explained by an experiment. Let the two halves of a photometric field (for example, the Martens photometer field) be perfectly matched at 35Y. Add 0.1R to one side and match the brightness; there will be a very small but perceptible difference in color. It will be seen that the addition of 0.1R has made the field redder and more saturated. Remove the red and let the two halves again be perfectly matched at 35Y. Add 5Y to one side and match the brightness again; there will again be a very small but perceptible difference in color, apparently of much the same nature as before; that is, the addition of 5Y also makes the field redder and more saturated. In a certain limited sense, then, there is an equivalence between red and yellow. This quasi equivalence is, however, a thing to be warned against rather than a thing to be used. The true meaning of this approximate equivalence may be stated as follows:

Consider a two-part photometric field of which the two halves are, respectively, 35Y and 40Y. A perfect match would be obtained by adding 5Y to the first half. Let it be required, however, just as in grading oils on the 35Y+nR scale, to obtain the closest approximation to a match possible by adding red and only red. It will be found that adding about 0.1R gives the best practical approximation to a match. It will readily be admitted that 35Y+0.2R is redder than 40Y and that 35Y alone is less red than 40Y. It must also be admitted, however, that 35Y+0.1R does not match 40Y exactly.

[31] A minus sign preceding the red component indicates that it is to be combined with the test glass (Column I) to match the yellow glass designated in Column II or Column III. The condition of equal brightness may be approximated by combining a plate of clear nonabsorbing glass with the single yellow glass which is being compared with the two-glass combination of yellow and red.

As stated before, the addition of 5Y to 35Y increases both the redness and the saturation just as the addition of 0.1R does; but the whole truth includes the statement that the redness increment produced by 5Y is smaller than that produced by 0.1R, while the saturation increment is larger. Hence, when 40Y is compared to 35Y + 0.1R it seems less red (that is, greener) and more saturated. Moreover, if 7.6R be now added to both sides, the relative greenness of 40Y+7.6R becomes more obvious. In fact, 35Y+7.7R is not the best practical approximation to a match for 40Y+7.6R; indeed the latter is more nearly matched by 35Y+7.5R. In other words, the addition of 5Y, which, at 35Y, is the practical equivalent of adding 0.1R, is, on the contrary, at 35Y+7.6R the practical equivalent of subtracting about 0.1R. The fallacy of using, without reservation, the "quasi equivalent," n_q, (Column III) for color grading oils should be quite apparent. A true 40Y glass would have a quasi equivalent of 35Y+0.1R for grading an oil of color about 35Y; but for the purpose of grading an oil of color about 35Y+7.6R, the true 40Y glass would have to be given a quasi equivalent of 35Y minus an amount (perhaps about 0.1 unit) of red. Thus, the added yellow strength (5Y) which adds to the red strength at 35Y subtracts from it at 35Y+7.6R; furthermore, the amount of this addition or subtraction is not constant but varies along the whole 35Y+nR scale. The quasi equivalents, therefore, can not be used for color grading unless N'' (in the rigorous equivalent) is nearly equal to 35, and, in this case, the rigorous equivalent may about as well be used, because the two are nearly the same. The values of the quasi equivalents (35Y n_qR, Column III) are included only because they are satisfactory for use in grading oils between 35Y and 35Y+1R. Even for these oils the quasi equivalents become unsatisfactory when N'' departs too much from 35, their applicability being questionable when N'' differs from 35 by more than about three units.

The rigorous equivalent is the strictly correct one; it is applicable to all cases.

3. APPLICATION TO THE COLOR GRADING OF OIL

The application of the results here given to the practical problem of color grading oil must be considered under two separate headings, viz:

A. Use of glasses under conditions which permit of the highest attainable accuracy.

B. Use of glasses under the present conditions customary in the oil trade.

These two sets of conditions may be contrasted as follows:

A	B
Conditions permitting of highest attainable accuracy	*Present customary conditions*
1. Use of a color comparator in which the two fields showing, respectively, the color of the oil and the color of the glasses are viewed in close juxtaposition so that when the fields are matched there is no visible line separating them.	1. Use of a color comparator ("tintometer") in which the two fields are separated by a considerable distance or, at least, by a visible coarse line which does not disappear.
2. Use of a comparator which permits of matching the brightnesses of the two fields by an adjustment independent of the oil and glasses (for example, the Martens photometer).	2. Use of a color comparator without any device for matching brightness.
3. Rules which permit of varying yellow as well as red so as to make it possible to obtain a match in saturation as well as hue; that is, a complete color match.	3. Arbitrary selection of yellow glass, obtaining closest approximation to match, subject to condition of varying only red.
4. Illumination by standard artificial sunlight, with most favorable field brightness.	4. Illumination not standardized with regard to either quality or field brightness.
5. Grading by observers who have been proven normal in their color sense and particularly in their ability to perceive small differences in color.	5. Grading by untested observers.

We now proceed to the discussion of the use of the glasses and the equivalents here given under these two sets of conditions.

A. Conditions of Observation Permitting of Highest Obtainable Accuracy.

To give a definite example, we will assume an oil sample which may be perfectly matched by yellow between 25 and 45 with the addition of red between 0 and 20. To obtain the Lovibond equivalent of this oil in red and yellow, proceed as follows:

1. Have at hand the following Lovibond glasses:

One of these standardized yellow glasses (nominally 35 and really not much different from 35).

A group of yellow glasses ranging from 0 to 10 (such as 2, 4, 6, 8, and 10).

A group of red glasses ranging from 0 to 20 (such as 0.1, 0.2, 0.3, 0.4, 0.5, 0.6, 0.7, 0.8, 0.9, 1.0, 2.0, 3.0, 4.0, 7.0, 12.0, and 17.0).

Five zero glasses.

2. Match the oil with red and yellow glasses by trial and error, subject to the following conditions:

(*a*) The added red must consist of a combination of not more than three red glasses.

(*b*) The added yellow (that is, in addition to the nominal 35Y glass) must consist of one glass only, this glass being added either to the oil or to the other glasses, whichever is needed to give a perfect match (that is, a saturation match as well as a hue match).

(*c*) The number of glass plates in each path should be constant during all observations,[32] zero glasses being substituted for either red or yellow when they are removed.[33]

(*d*) All judgments of match are to be made at (or near) a brightness match to be obtained by suitable instrumental adjustment.

3. Specify the quality of the color of the oil[34] by (*a*) the equivalent shown in yellow and red in Column II of Table 1 for the calibrated glass in question; (*b*) plus the added red; (*c*) plus or minus the added yellow, the plus sign applying if this yellow was added to the other glasses, and the minus sign applying if it was added to the oil.

Or, in symbols, the result will be—

$$(N'' + N)\mathrm{Y} + (n_r + n)\mathrm{R}$$

where

N'' and n_r are taken from Column II of Table 1; and

N is the numeral of the added yellow glass (assuming it has no sensible "red correction"), N being positive if added to the other glasses and negative if added to the oil sample; and

n is the sum of the numerals of the added red glasses.

The above procedure takes care of specifying the quality of color (involving hue and saturation) but gives no information concerning brilliance, which depends upon the transmission of the oil. If it is desired to report the transmission of the oil, in addition to its color quality on the Lovibond scale, this may be computed by taking account of (*a*) the transmission of the glasses, and (*b*) the photometer (Martens) scale reading for brightness match.[35]

[32] It may not be obvious, either in the standardization of Lovibond glasses or in the grading of oils as here outlined, why there is need for the use of zero glasses when a photometer is available for equating brightnesses. The purpose is to avoid the possibility of error, even though slight, introduced as a result of the multiple reflections that take place between the various surfaces. Any such error is avoided in the standardization of Lovibond glasses by keeping the number of glass plates combined with the standard equal to the number combined with the test glass.

However, in the grading of oils in terms of Lovibond glasses the experimental conditions under which the match is obtained must of necessity be somewhat arbitrary, and there would be no point in specifying that the numbers of surfaces in the sample path and the glass path be equal. The scheme outlined keeps the number of reflecting surfaces constant in each beam for all oil samples and thus avoids any possibility of this error entering into the grading of one oil relative to another.

[33] This will mean that at the start there will be (1) on the oil side, one zero glass (to be replaced by yellow later if found necessary); and (2), on the glass side, the approximate 35Y glass with four zero glasses (one of which is to be replaced by yellow later if found necessary and three of which may be replaced by red).

[34] Quality takes account of both hue and saturation but not brilliance.

[35] To discuss this in detail would take us beyond the scope of the present paper, and the discussion would not be seasonable until the interested parties demand a report on transmission. We merely point out the possibility here.

B. Under Present Customary Conditions of Using the Glasses.

Under these conditions it is to be expected that an observer who can detect a difference of 0.2R under favorable conditions will often make errors as large as 0.5R even with glasses accurately specified by their attached numerals.[36] With the frequent occurrence of errors as large as 0.5R due to the method of using the glasses, it is plainly useless to apply corrections of only 0.1R and 0.2R. Perhaps it would be advisable to use glasses having n_r (Column II, Table 1) greater than 0.2 (about 25 glasses of the 65) with some caution in critical cases where some refinement of the customary methods is used. Seven glasses (AOCS Nos. 27, 31, 41, 97, 119, 125, and 131) should likewise be regarded with suspicion under similar circumstances for reasons cited in detail in Column XII of Table 1 (see notes at foot of the table).[37] But, under the present customary conditions of grading oils, all of the glasses, with the possible exception of three (AOCS Nos. 41, 97, and 119) whose surfaces are badly marred, may be regarded as practically equivalent to standard 35 yellow.

VII. GENERAL CONCLUSIONS

1. It is clear (from the algebraic mean, foot of Column II, Table 1) that the average equivalent of these 65 glasses is not in precise accord with the standard 35 yellow derived by Priest and Gibson from the Bureau of Standards set (B. S. 9940) obtained from the Lovibond establishment. On the other hand, the discrepancy is certainly not more than two or three times the least difference perceptible with certainty by the best observers under the most favorable conditions of observation.[38]

2. Of course, if their own average were taken as standard instead of the standard arbitrarily adopted, the "errors" for most of the glasses would be notably decreased. With a very few possible exceptions, the uniformity of these glasses is quite as good as could be required or expected in order to comport with the purposes and methods of use for which they were intended by the makers. The

[36] Actual tests carried out in May, 1928, in connection with the convention of the A. O. C. S. at New Orleans disclosed many such errors. A report on these tests is in preparation.

[37] The glasses having notably abnormal transmissions may be troublesome in instruments in which the fields are close together.

[38] The idea occurs that it might seem reasonable to adopt the average as standard instead of the standard which has been adopted. It must be remembered, however, that the present standard 35Y is only one of a series of standard yellow glasses (varying from 0 to 40 in Lovibond numeral) specified indirectly by the set of glasses (B. S. 9940) possessed by the Bureau of Standards. If the present standard 35Y be rejected in favor of a new standard, we must reject also the entire series of old standards; hence, there would be available no specifications by which departures from the new standard 35Y could be expressed. The logical way to use the average value of the present lot of nominal 35Y glasses as a factor in the specification of a new standard 35Y would be to investigate equally large numbers of yellow glasses of other grades and to redetermine standard specifications of the entire yellow scale. Such a plan is plainly unfeasible. Furthermore, the present standards undoubtedly approximate closely to those which would result from carrying out such a plan.

irregularities found and reported here have only been discovered by methods of observation greatly exceeding in sensibility and accuracy the methods of color matching contemplated by the makers and the methods actually used by the oil chemists in grading oils.

3. With the possible exception of three badly marred glasses, all of the glasses are considered fit to be regarded as equivalent to standard 35 yellow under the present customary conditions of grading oils.[39]

4. An outstanding result of this investigation is the conclusion that the discrepancies of color grading which have troubled the oil trade can not be charged to lack of uniformity among the 35-yellow glasses. The sources of these troubles are rather to be sought in the following factors:

(*a*) Unstandardized, nonuniform, and insensitive methods of comparing the oil samples with the glasses.

(*b*) Grading of oil by observers having abnormal color sense or low power of hue discrimination.

(*c*) Errors in the red glasses.

It seems just to assume that this rather large collection of glasses constitutes a fair sample of 35-yellow glasses issued by the Lovibond establishment and in use in the oil trade in the United States. If this be admitted, it seems superfluous to test individual 35-yellow glasses further under present conditions. The chance of finding one with an error great enough to be of consequence in comparison with the other uncertainties just mentioned is very small. After the above-mentioned sources of error have been eliminated in practice, it will be due season to reconsider the calibration of 35-yellow glasses if it then appears necessary. In the meantime, it may well be considered legitimate to accept on faith the 35-yellow glasses as issued by the Lovibond establishment.

WASHINGTON, August, 1927, to November, 1928.

[39] The point to this recommendation is not that the glasses are perfect from the point of view of precision calibration, but that the errors found are negligible in comparison with the uncertainties inherent in the customary methods of using the glasses. When more reliable and precise methods of grading are adopted, it will be in order to consider using the precise equivalents which are given for each glass. Of course, even under present conditions, the glasses which approach more nearly standard 35 yellow may, perhaps, be regarded with somewhat greater satisfaction and respect by those who use them. The detailed data given in Table 1 of the report will enable such glasses to be identified.

THE COMPRESSIVE AND TRANSVERSE STRENGTH OF BRICK

By J. W. McBurney

ABSTRACT

This paper reports the compressive strength flat and on edge and the transverse strength of 27 makes of bricks covering a range of conditions in method of manufacture and degree of burning. The attempt is made to correlate the variation in ratios of these different measures of strength with the various structural features of the brick.

CONTENTS

	Page
I. Introduction	822
II. Review of literature	822
III. Source of samples	823
IV. Methods of testing	824
V. Description of test specimens	824
1. Dry press bricks	824
2. Semidry press bricks	825
3. Soft-mud brick	825
4. Stiff mud, end cut	826
5. Stiff mud, side cut	826
VI. Discussion of results	827
1. Relation of compressive strength flatwise to compressive strength edgewise	827
(*a*) Effect of method of forming	828
(*b*) Effect of kind of raw material	829
(*c*) Presence and character of laminations and cracks	829
(*d*) Effect of nodules	830
(*e*) Character of texture	830
(*f*) Degree of burning	830
(*g*) The character of the fracture in compressive tests edgewise	831
2. Relation of transverse to compressive strength	832
(*a*) Effect of method of manufacture	832
(*b*) Effect of type of raw material	832
(*c*) Effect of lamination and cracks	832
(*d*) Effect of nodules	833
(*e*) Effect of variation in burning	833
VII. Specification requirements	833
VIII. Summary	834
IX. Acknowledgments	835

I. INTRODUCTION

In a previous paper [1] the author makes the following statement: "The various measures of the strength of brick, compressive flatwise and on edge, transverse, tensile, and shearing vary in their relation one to another for different makes of brick." This statement was based upon the consideration of but five makes of bricks. The purpose of the present paper is to present data representing a range of conditions and determine if possible what are the factors influencing variation in relation of certain strength measures. A secondary purpose is that of determining the degree of justification for the practice followed in certain specifications where but one of these strength measures (usually the transverse strength) is used. Apparently it is assumed either that the various strength measures are so related that one can serve as a measure of the others or that the one selected has a sufficiently close relation to the strength of the masonry to justify the omission of the other strength tests.

II. REVIEW OF LITERATURE

Confining consideration to tests reported for the United States and Canada and taking them in chronological order the more important contributions where two or more strength tests of brick are compared are as follows:

Bleininger [2] reports 176 tests on brick collected in a district covering a radius of 150 miles from Washington, D. C. His values represent half bricks tested in compression flatwise and edgewise. He states that "the bricks tested were of the harder grade, and practically all of them were made by the stiff-mud process. * * * Both shale and clay bricks are represented." No information was provided as to whether given specimens were side cut or end cut, nor was information provided as to laminar structure. On the basis of these 176 tests, the average ratio of compressive strength flat to compressive strength on edge is given as 1.153, and "individual tests vary widely from the average ratio." From an inspection of Bleininger's graph it is evident that there is much less scattering of ratios for the clay bricks than for the shale bricks. He stated in the discussion "some of the end-cut bricks were stronger when tested on edge than when subjected to the load in the flat condition. Most of the side-cut bricks showed the opposite to be the case." Ries [3] reports results of compressive flat and on edge and transverse tests on 16 makes of bricks. These bricks are classified as dry-press, soft-mud, and stiff-mud manufacture.

---

[1] The Effect of Strength of Brick on Compressive Strength of Brick Masonry, Proc. Am. Soc. for Test. Materials, pt. 2, pp. 605–625; 1928.

[2] A. V. Bleininger, The Relation Between the Porosity and Crushing Strength of Clay Products, Trans. Am. Cer. Soc., 12, pp. 564–584; 1910.

[3] H. Ries, Results of Tests on Some Bricks from the Province of Western Canada, Trans. Am. Cer. Soc., 14, pp. 82–86; 1912.

Committee C-3 on Brick of the American Society for Testing Materials[4] in its report for 1915 presents results of compression tests flatwise and transverse tests of brick. Unfortunately the data as to method of manufacture are incomplete. Williams[5] reports 14 sets of tests on soft-mud and 20 sets of tests on stiff-mud bricks. These test values are for compressive strength on edge and transverse strength.

Orton[6] reports an elaborate series of comparisons between the compressive strength of half bricks tested flatwise and edgewise.

III. SOURCE OF SAMPLES

Table 1 gives values for the transverse strength, compressive flatwise strength, and compressive edgewise strength of 27 makes of bricks, arranged according to method of manufacture.

Samples Nos. 2A, 6, 13A, and 14A represent random samplings from large shipments. It will be noted that for these the number of specimens tested are 50 or more. The values for samples 7 and 17A are the averages from tests of 50 specimens selected from shipments of 300 bricks of each type. The rest of the specimens represent samples of a few bricks each supplied by the manufacturer. In all cases, however, each sample number is confined to a single grade of a given manufacturer. None of the samples represent "run of kiln."

The data of Table 1 represent tests made by the author at the National Bureau of Standards.

TABLE 1.—*Transverse and compressive strengths of bricks*

Sample No.	Number of tests	Method of manufacture	Modulus of rupture	Compressive strength, half bricks		Ratios		
				Flat	Edge	Modulus of rupture to compressive flat	Modulus of rupture to compressive edge	Compressive flat to compressive edge
			Lbs./in.²	*Lbs./in.²*	*Lbs./in.²*			
1	3	D. P.	1,126	5,760	5,413	0.195	0.218	1.06
2A	98	D. P.	800	3,520	3,630	.227	.220	.97
3B	5	D. P.	141	1,860	1,142	.070	.123	1.62
5	4	D. P.	2,020	18,980	11,700	.106	.173	1.62
14A	3	S. D. P.	852	7,710	7,220	.111	.118	1.07
13B	3	S. D. P.	887	7,300	7,300	.121	.121	1.00
14C	3	S. D. P.	293	2,430	2,470	.120	.119	.985
4	5	S. M.	515	2,720	3,032	.189	.170	.900
6	50	S. M.	670	3,320	3,360	.201	.200	.990
7	50	S. M.	489	3,110	3,169	.157	.155	.982

[4] Proc. Am. Soc. for Test. Mats., **15**, Pt. I, pp. 150–162; 1915.

[5] Ira A. Williams, Strength Tests of Oregon Building Brick, Trans. Am. Cer. Soc., **17**, pp. 660–666; 1915.

[6] Edward Orton, jr., A Comparison Between the Absorption, Crushing Strength, and Resistance to Freezing of Some Ohio Building Bricks, Trans. Am. Cer. Soc., **18**, pp. 686–760; 1916.

TABLE 1.—*Transverse and compressive strengths of bricks*—Continued

Sample No.	Number of tests	Method of manufacture	Modulus of rupture	Compressive strength, half bricks		Ratios		
				Flat	Edge	Modulus of rupture to compressive flat	Modulus of rupture to compressive edge	Compressive flat to compressive edge
			*Lbs./in.*²	*Lbs./in.*²	*Lbs./in.*²			
8	3	S. M.	765	3,270	3,630	0.234	0.211	0.900
9	3	S. M.	730	4,215	3,730	.173	.196	1.13
10	1	S. M.	1,170	7,000	7,450	.168	.157	.940
11	1	S. M.	510	3,850	4,520	.132	.113	.853
12	1	S. M.	500	1,990	2,280	.251	.219	.877
13A	100	S. M.	1,550	8,610	11,600	.180	.134	.742
13B	6	S. M.	349	1,917	2,240	.182	.160	.856
14A	94	S. M. E. C.	1,320	3,370	3,780	.392	.349	.891
14B	7	S. M. E. C.	685	2,710	2,040	.251	.336	1.33
15	5	S. M. E. C.	1,295	3,040	3,190	.426	.406	.953
16A	5	S. M. E. C.	947	6,910	7,200	.160	.131	.969
16B	5	S. M. E. C.	1,250	6,550	6,780	.191	.184	.965
16C	4	S. M. E. C.	418	2,350	2,100	.178	.199	1.12
17A	50	S. M. S. C.	1,573	10,170	9,104	.154	.173	1.12
17B	11	S. M. S. C.	776	6,093	5,380	.127	.144	1.13
18	6	S. M. S. C.	2,130	14,100	10,750	.151	.198	1.32
19A	5	S. M. S. C.	2,834	11,260	10,340	.151	.175	1.09
19B	5	S. M. S. C.	1,234	13,780	10,440	.090	.117	1.33
20	2	S. M. S. C.	1,477	8,085	7,415	.183	.200	1.09
21	25	S. M. S. C.	2,890	22,600	18,950	.128	.153	1.19
22A	5	S. M. S. C.	1,864	5,950	5,560	.314	.335	1.07
22B	5	S. M. S. C.	1,170	4,040	4,070	.290	.288	.944
23A	2	S. M. S. C.	603	8,100	3,585	.074	.168	2.26
23B	3	S. M. S. C.	721	5,990	3,816	.120	.189	1.57
23C	3	S. M. S. C.	307	3,546	2,030	.087	.151	1.75
24A	3	S. M. S. C.	3,230	21,200	14,200	.152	.227	1.49
24B	4	S. M. S. C.	987	6,250	5,890	.158	.168	1.06
25	1	S. M. S. C.	1,320	7,940	9,500	.166	.139	.835
26	1	S. M. S. C.	1,020	6,570	5,750	.155	.177	1.14
27	1	S. M. S. C.	790	3,270	3,470	.242	.228	.942

D. P.=Dry press.
S. D. P.=Semidry press.
S. M.=Soft mud.
S. M. E. C.=Stiff mud, end cut.
S. M. S. C.=Stiff mud, side cut.

IV. METHODS OF TESTING

The tentative methods of testing brick (C67–27T) of the American Society for Testing Materials were followed. The half bricks from the transverse test were used in the compressive tests, one of the two halves from each brick being tested flatwise and the other on edge. Where the transverse tests gave a break which was oblique or otherwise irregular, the halves were trimmed by cutting or grinding.

V. DESCRIPTION OF TEST SPECIMENS

1. DRY PRESS BRICKS

1. Well made and free from lamination. Sample supplied by manufacturer and represented " well-burned " color range, dark to light.

2A. Random samples from shipment of 52,000 "commons." Granular texture, no laminations. Color reddish brown, surface clay.

2B. Samples supplied by the manufacturer of 2A, but quite underburned salmons. Weak and friable. Color pink to orange.

3. This sample represents an experimental dry press brick formed and burned at the plant of a brick-machinery manufacturer. Nos. 19A and 19B represent the same shale and, in the opinion of the plant superintendent, 19A represents the same degree of vitrification as No. 3.

2. SEMIDRY PRESS BRICKS

4A. "Arch," or "clinker." Very considerably cracked and crazed. The cracks were apparently kiln cracks, since samples 4B and 4C were comparatively free from them. Some warpage.

4B. "Body" brick corresponding to 4A. Much less evidence of kiln cracking. Good red in color.

4C. The salmon of this manufacture. Orange in color.

3. SOFT-MUD BRICK

5. Manufacturer's sample representing a considerable range of color. Some kiln cracking and warping.

6. Random sample representing 18,000 "select common"; occasional nodules. The harder burned bricks (as judged by color) frequently showed kiln cracks normal to the long axis of the brick.

7. Sample represents random sampling of shipment of 300 "select common." Brick characterized by a sandy core and numerous lime nodules in size up to three-quarters inch in diameter. It may be of interest to note that salmons corresponding to No. 7 were provided, but expansion of the nodules disrupted the specimens during drying. About one-third of specimens tested showed cracks.

8. "Typical common brick of district" in judgment of building inspector. Resembles No. 6 in appearance. Some irregular laminar structure.

9. Also considered "typical common brick." Very fine grained. Some small nodules. No noticeable laminar structure.

10. One specimen. Nodules and cavities evident on examining cross section.

11. One specimen. Gave a very oblique break when tested transversely.

12. One specimen. Nothing noted in way of lamination, nodules, or cavities.

13A. Sample from shipment of 52,000 brick. It was impossible to distinguish any granular or laminated structure. Appearance as

of a fused body. Core colors different from outer portion of brick were quite common. Colors dark.

13B. Salmons of 13A light orange. Weak. Original clay grains easily distinguishable.

4. STIFF MUD, END CUT

14A. Double column. Due to lamination gave the appearance of being made of bundles of fibers running parallel to long axis of brick. Frequently on compression a circular core extending the length of the brick would result from spalling of the sides. Black cores were common. The brick itself, aside from its structure, gave some evidence of being rather hard. Large lime nodules were common.

14B. The "unmarketable salmon" of 14A. There was very little to distinguish it in appearance from 14A. Noticeably weaker.

15. A manufacturer's sample. Sample 15 is indistinguishable in appearance and properties from 14A. It, however, comes from a different district.

16A. "Rough hard," which is the local name for "the arch" or "clinker" bricks of other districts. This brick showed much cracking, crazing, and warping, probably due to overburning. Little evidence of lamination. Such lamination as existed gave planes parallel to the broad face of the brick.

16B. The "straight hard" or "body" brick corresponding to 16A. Good red and free from cracking and crazing characterizing 16A. Slight lamination as in 16A.

16C. The salmon of the two preceding samples. Color was characteristic of that which gave the name salmon. No cracking or crazing and otherwise resembled 16B.

5. STIFF MUD, SIDE CUT

17A. Random sample of 50 from manufacturer's sample of 300. Well-made shale. Granular structure, no evidence of lamination. The entire sample was remarkably uniform in all its properties.

17B. The salmon of 17A. Resembles 17A except for color and strength.

18. Well-made characteristic shale. No evidence of lamination.

19A. Manufacturer's sample. Same shale and, in opinion of manufacturer, same burning history as sample No. 3. No evidence of lamination.

19B. Another sample from maker of 19A. From evidences of color and comparative water absorption 19B was not as hard burned as 19A.

20. Manufacturer's sample "common." No lamination evident. Shale brick, but from color and water absorption apparently not very hard burned

21. Manufacturer's sample of "hard shale commons." No laminations. Degree of burning such that granular structure was practically suppressed.

22A and 22B. Together represent a vertical section of a down-draft kiln; 22A is the top half, 22B the lower half. From color and water absorption the grading is obvious. The structure is granular, with an appearance of what might be called internal crazing; small short cracks at irregular intervals and direction. Shale.

23A. Manufacturer's sample of "clinker." Black glazed exterior, red interior. This and samples 23B and 23C were outstanding examples of die lamination. Apparently an imperfect mixture of two clays existed, and the laminar structure was very noticeable. Aside from lamination, sample 23A showed the cracking, crazing, and warping usually associated with clinker bricks.

23B. The body brick corresponding to 23A. Highly die laminated, not so irregular as 23A.

23C. The salmon corresponding to the two preceding samples. Also laminated but little cracked.

24A. Manufacturer's sample offered as "face." These represent the top portion of the kiln. Hard burned, unlaminated shale.

24B. Lower portion of kiln. Marked "fillers" by manufacturer. Salmon color; otherwise description of 24A applies.

25. One speciment side-cut clay. Some nodules, no lamination evident.

26. One specimen. Some irregular lamination (auger), clay.

27. One specimen. Clay, sandy texture, no lamination.

VI. DISCUSSION OF RESULTS

1. RELATION OF COMPRESSIVE STRENGTH FLATWISE TO COMPRESSIVE STRENGTH EDGEWISE

Assuming that brick behaves like the Swiss sandstone tested by Bauschinger,[7] the ratio of compressive strength flatwise to compressive strength edgewise would be 1.26. Actually, the data here presented show a wide variation. The two extremes for this ratio are 0.74 for sample No. 13A and 2.26 for sample No. 23A. It is obvious that the structure of the brick is responsible for this variation, hence it is in order to examine these data for the purpose of seeing if there is any correlation between the structure of the brick and the ratio of compressive strength flatwise to compressive strength edgewise.

[7] Johnson's Materials of Construction, 6th ed., pp. 113–114.

Referring to the descriptions of the samples, it will be observed that the following data have been recorded:

(*a*) Method of manufacture.

(*b*) Kind of raw materials, clay or shale.

(*c*) Presence or absence and character of laminations and cracks.

(*d*) Presence or absence and character of nodules or other inclusions.

(*e*) Character of texture; that is, granular, glassy, etc.

(*f*) In some cases degree of burning is noted.

In the opinion of the writer too much weight should not be given to differences within 10 per cent where the samples are small, due to the large variation in results due to sampling.

(*a*) Effect of Method of Forming.—Considering the effect of method of forming on the ratio compressive strength flatwise to edgewise, it would appear on the basis of the very limited series of dry-press specimens that the range for this ratio is from unity up to 1.6. Increase in the ratio appears to be produced by pronounced underburning (note sample 2B in comparison with 2A). No obvious explanation is noted for the high ratio of No. 3. It has been observed that excessive pressure in forming a dry-press brick will produce laminations or planes of weakness normal to the direction of the pressure. The results of Ries[8] give a range of from 1.06 to 1.72 for five samples of dry-press bricks.

The semidry press samples are close to unity for their ratio. The fact that the arch brick (4A) is somewhat stronger flat than on edge would seem explainable by its cracked and crazed structure.

The soft-mud samples, with one exception (No. 9), were all stronger on edge than flat.

The eight samples of soft-mud bricks reported on by Ries[8] were stronger on edge than flatwise. The five samples reported by Orton[9] gave ratios varying from 0.93 to 1.18 for the hard and medium burns. It is evident from the data here presented that soft-mud bricks tend toward a lower ratio than characterizes the other methods of manufacture. Why this should be is not apparent. Soft-mud bricks are formed by light pressure in a mold at semiliquid consistency. No laminar structure or planes of weakness should be formed. They should show the effect of change in ratio of cross section to a height to give greater strength flatwise than edgewise. The only explanation that comes to mind is that these bricks are burned on edge and the pressure of the bricks may produce a consolidation in the line of the applied forces giving greater strength on edge than on flat. This possibility will be mentioned again in connection with the discussion of effect of degree of burning on the compressive-strength

[8] See footnote 3, p. 822.

[9] See footnote 7, p. 827.

ratio. Like the soft-mud bricks, the well-burned stiff-mud end-cut bricks were generally stronger on edge than on flat. The salmon stiff-mud end-cut show the reverse of this.

The characteristic of side-cut bricks is that of being stronger flat than on edge. In general, the data of Orton and Ries confirm this.

(*b*) EFFECT OF KIND OF RAW MATERIAL.—It is not considered that these data are sufficient to warrant any conclusions as to differences between clays and shales which may affect the ratio of compressive strengths flat to compressive strength on edge. It should be remembered that the type of raw material is usually the consideration that determines the method of forming.

(*c*) PRESENCE AND CHARACTER OF LAMINATIONS AND CRACKS.—Considering the same clay molded by different processes, the presence or absence of laminations in its various degrees is largely a result of

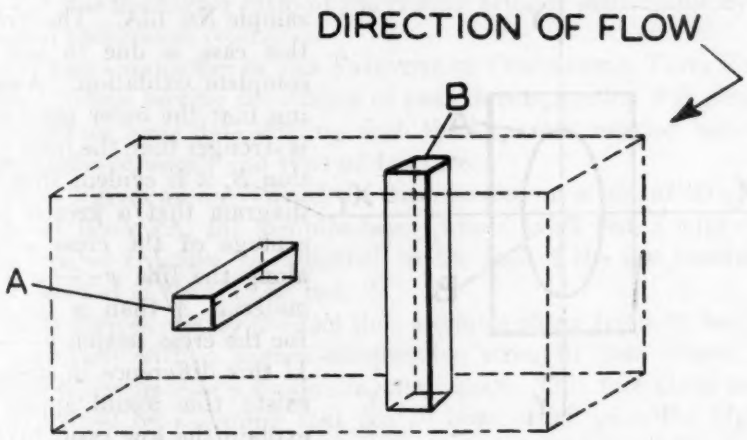

FIG. 1

the methods of manufacture. Soft-mud bricks should be practically free from lamination. Stiff-mud bricks may be substantially free from laminations or may have a highly laminar structure. Dry-press bricks may develop planes of weakness normal to the direction of the applied pressure, when improperly pressed.

Considering a laminated side-cut brick, the flow of material in the die is normal to the large face. Hence, the planes of lamination would, in general, be normal to the large face. It would appear reasonable to expect that a small prism, such as *A* in Figure 1, would have a greater strength than *B*, due to the compacting of the grains in the case of prism *A* and their separation due to differential flow in the case of prism *B*. It is conceived that burning on edge may have an effect toward overcoming this tendency, which may explain the occasional reversal of the ratio. The presence of irregular cracking and crazing, such as frequently characterize clinker bricks, would

seem to offer an explanation of high ratios of flat to edge compressive strength. Surface cracks would be expected to have a greater effect on the compressive strength when the bricks were tested on edge, because the portions cracked would occupy a greater percentage of the sectional area than when the bricks were tested flatwise.

(*d*) Effect of Nodules.—Presence or absence of nodules does not appear to have any definite effect on the relation between the two compressive strengths. However, it is possible that if a nodule, inclusion, or core were of a size such that it represented a considerable portion of the cross section of the brick and were of a different strength, then an effect would be produced on the relative compressive strength flatwise to edgewise by the difference in percentage of the two materials effective for the two cross sections. Figure 2 shows schematically a cross section normal to the long axis of sample No. 13A. The core in this case is due to lack of complete oxidation. Assuming that the outer portion *A* is stronger than the inner portion *B*, it is evident from the diagram that a greater percentage of the cross section along the line $x---x$ is of material *A* than is the case for the cross section $y---y$. If this difference in strength exists, this would appear to explain the low ratio (0.742) for sample 13A.

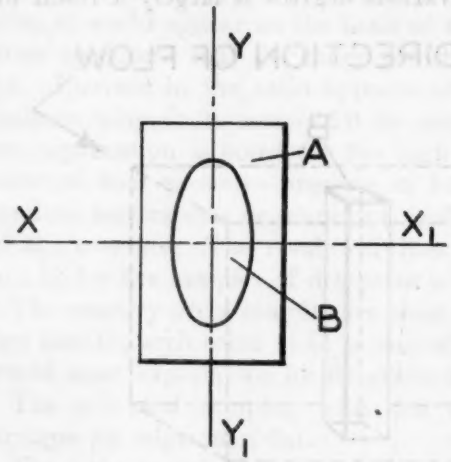

Fig. 2

(*e*) Character of Texture.—The character of the texture does not appear to be related to variation in the ratio of the two compressive strengths. In general, a vitreous structure is associated with high compressive strength and an open, granular, poorly bonded structure has low strength. But extremes of ratios are associated with both types of structures.

(*f*) Degree of Burning.—A casual inspection of the data where the product of the kiln is classified into arch, body, and salmon, or where the sample represents a vertical section of the kiln and classification was made by position, seemed to indicate a very marked effect on ratios of compressive strength by degree of burning. However, in some cases (2A and 2B, 13A and 13B, 14A and 14B, 16A, 16B and 16C) the effect was for the underburned brick to have higher ratios of compressive strength flat to edge. In other cases (22A and 22B, 24A and 24B) the direction of change was reversed. In yet other

cases there was no significant difference in the ratios (4A, 4B, and 4C, 17A and 17B) or the order was mixed (23A, 23B, and 23C).

However, the suggestion that the burning of bricks on edge might add to their apparent compressive strength on edge by the effect of the weight of the superimposed bricks during burning does much to explain these data. Samples 2, 13, 14, and 16 represent bricks from scove kilns. The salmons from scove kilns come from the top and outer portions of the kilns. They represent specimens that have been subjected to relatively little pressure in burning. Samples 22 and 24 are from down-draft kilns. Here the salmons are from the bottom of the setting. Samples 4 and 16 are from small scove kilns, and the clinker specimens are both quite cracked and crazed. No. 17 was burned in a down-draft kiln, but the location of the specimens is unknown. The type of kiln used for No. 23 is also unknown. In any case the higher ratio of the clinker brick is explainable by its cracked and crazed condition.

(*g*) THE CHARACTER OF THE FRACTURE IN COMPRESSIVE TESTS EDGEWISE.—Before leaving the subject of tests in compression it is desired to introduce some data dealing with the apparent relation between compressive strength and type of fracture.

Table 2 gives an analysis of the data secured on a test of 50 specimens of brick 2A, the samples being whole brick tested edgewise. The type of fracture, as indicated on the end of the test specimen, was recorded at the time of test.

Table 2 gives clearly the fact that a double shear (cone or wedge) is associated with a higher compressive strength than where the failure takes place in a single diagonal shear. This fact alone could be explained by assuming that the 10 tests which gave the higher strength and double shear were concentrically loaded, while the 13 tests which failed in single diagonal shear with low strength were eccentrically loaded. However, the fact that the difference in strength is actual and not due to difference in loading is vouched for by the inverse relation of the water absorption. The possibility exists that eccentric loading was present for both types of fractures, but the stronger bricks were better able to resist the effect of eccentricity.

TABLE 2.—*Brick 2A*

[Total number of specimens, 50]

Number of tests	Compressive strength, whole brick on edge	Water absorption, five-hour boil	Type of break (see fig. 3)
	Lbs. /in.²	*Per cent*	
50	3,300	22.26	All types.
10	4,100	21.29	A.
13	2,470	23.96	B.
27	3,400	21.80	C, D, E, F.

2. RELATION OF TRANSVERSE TO COMPRESSIVE STRENGTH

The ratios of modulus of rupture to compressive strength flat given in Table 1 range from 0.426 to 0.070. The transverse strength is notably quite sensitive to imperfections in the brick. Usually it will be found that where a series of bricks are tested the percentage deviation from the mean of the modulus of rupture will exceed the percentage deviation from the mean of the compressive strength. In other words, nodules, slight laminations, or other planes of weakness will very noticeably reduce the transverse strength.

(*a*) EFFECT OF METHOD OF MANUFACTURE.—As would be expected, soft-mud bricks were the most constant in this ratio. Nodules are the principal interfering factor likely to be present. The 10 ratios

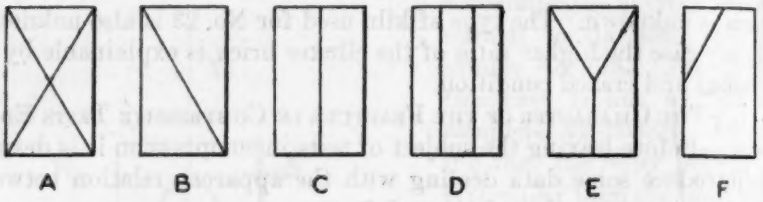

FIG. 3

given in Table 1 range between 0.132 and 0.251. Fourteen values given by Williams [10] range from 0.171 to 0.256.

The ratios for dry-press bricks range from medium values, 0.227, down to 0.070.

The ratios for stiff-mud end-cut bricks range from medium values to 0.426.

For stiff-mud side-cut bricks the ratios differ rather widely, going from 0.074 to 0.314.

(*b*) EFFECT OF TYPE OF RAW MATERIAL.—If there is any consistent effect on the relations between transverse and compressive strength due to the use of shale or clay, it is obscured by the variation in other factors.

(*c*) EFFECT OF LAMINATIONS AND CRACKS.—Not only do laminations exercise the obvious effect of lowering the ratio modulus of rupture to compressive strength, but in certain cases they are believed to be responsible for raising the ratio. Samples 14A and 15 are considered examples of this effect. They are both double-column, end-cut bricks and were auger laminated to a very considerable degree. The net result was to produce a tubular structure. From analogy to the strength of a metal tube acting as a beam and the strength of a metal tube in compression normal to its axis as compared to the corresponding strengths of a solid shaft of the same diameter, this explanation of the high ratio of transverse to com-

[10] See footnote 5, p. 826.

pressive strength for these bricks seems warranted. Samples 23A, 23B, and 23C are illustrations of laminar structure acting to lower this ratio.

Kiln cracking normal to the long axis of the brick is, of course, a sure way to lower the transverse strength.

(*d*) Effect of Nodules.—From observations of the tests of soft-mud bricks it is believed that a heterogeneous section, the visible evidences of which are nodules, has much to do with moderate variation in the ratio nodulus of rupture to compressive strengths. The effect of texture is uncertain.

(*e*) Effect of Variation in Burning.—No definite effect on modulus of rupture—compressive-strength ratio seems to be produced by variation in burning. The salmon bricks are usually not far from the well-burned bricks in ratio. Samples 2A and 2B provide a notable exception. The clinker bricks are usually low in ratio, probably explainable by their cracking and crazing.

VII. SPECIFICATION REQUIREMENTS

In the words of Orton, "We can not safely translate data made by crushing on the flat into terms of crushing on the edge, except in large masses or averages, and here with many reservations."

These data, in the writer's opinion, give no justification for the belief held in some quarters that the B grade of the Tentative Specification for Building Brick (C62–27T) of the American Society for Testing Materials is necessarily the equivalent of the medium grade of the former Standard Specification for Building Brick (C21–20) of the same society. Grade B (C62–27T) gives compressive strength flatwise as 2,500 to 4,500 lbs./in.^{2} Grade medium (C21–20) gives compressive strength edgewise as 2,000 to 3,500 lbs./in.^{2} The equivalence of these two grades is certainly not true for soft-mud brick and only occasionally fit certain kinds of stiff-mud bricks.

The data on transverse strength compared with compressive strength likewise gives no warrant for assuming any general relation between the measures of strength such as would be expected for isotropic and homogenous material. The fact that a given ratio may be the average for a very large number of tests does not increase the probability that the average ratio will represent the actual ratio for a particular kind of brick. As an extreme illustration, consider a field occupied by an equal number of cattle and horses. The statement that the animals in that field have on an average one horn apiece illustrates the fallacy of attempting to average separate categories. The practice of plotting one measure of strength against another measure of strength where a wide scattering exists, as in the

present data, and then drawing a line by least squares to represent the "most probable" relation would be valid if the scattering of the points represented "error." To illustrate: Sample 14A is typical of that clay and method of manufacture. Repeated tests confirm its high ratio (0.392) quite closely. The fact that brick 14A has a high modulus of rupture along with a comparatively low compressive strength is not chance. It is the nature of that brick. Hence, taking a ratio based on averages of all bricks does not represent the truth concerning this particular kind of brick.

The application of this to specification writing is that brick is purchased as the product of a given manufacturer. If a given property (say a certain flat compressive strength) is desired, that property should be asked for, not another property assumed to be related to the wanted property by a presumably fixed ratio.

VIII. SUMMARY

From the data and discussion here given the following conclusions are believed warranted in so far as they are limited to bricks made of shale or clay.

1. The ratio compressive strength of brick flat to compressive strength of brick on edge ranges from 0.74 to 2.3.

2. The tendency of soft-mud brick is to give higher unit strengths tested on edge than when tested flat.

3. The "compacting effect" on the structure of the edge-set brick by the superimposed weight of the other bricks in the kiln is offered as a tentative explanation of the tendency toward higher strength on edge.

4. This tendency toward higher strength on edge is overcome by laminar and cracking structure in the case of certain bricks.

5. The ratio of modulus of rupture to flat compressive strength ranged from 0.426 to 0.070.

6. Soft-mud bricks tend to display less deviation in the ratio modulus of rupture to flat compressive strength than any of the other methods of manufacture, but even with these the ratio ranged between 0.13 and 0.26.

7. Auger lamination in end-cut brick appears to be associated with high ratios for modulus of rupture to flat compressive strength.

8. Die lamination in side-cut brick appears to be associated with low ratios for modulus of rupture to flat compressive strength.

9. In view of the variation in the ratio compressive strength flat to compressive strength on edge, there exists no general rule for converting values from one kind of test to the other kind.

10. In view of the variation in the ratio modulus of rupture to compressive strength flat, the possibility of inferring a compressive strength from a transverse test or vice versa is open to very large errors for any given make of brick.

IX. ACKNOWLEDGMENTS

The author acknowledges his indebtedness to the various members of the staff of the National Bureau of Standards who gave assistance and counsel in the preparation of this paper. Particular thanks are due to R. T. Stull for his suggestions drawn from his plant experience.

Acknowledgment is made of the assistance rendered by the various manufacturers who generously provided samples and information.

WASHINGTON, November 23, 1928.